Organizers:

IBIB PAN

IFMBE

PTIB

MCB

PAN Committee of Biocybernetics and Biomedical Engineering

Doskonała Nauka

Minister of Science Republic of Poland

The conference is co-financed from the state budget, allocated by the Minister of Science under the Excellent Science II Programme Contract No. KONF/SP/0624/2024/02

Sponsors:

LABSOFT

Endorsing Organizations:

European Alliance for EAMBES Medical and Biological Engineering & Science

Engineering the Future of Health

BOOK OF ABSTRACTS

NBC 2025 & PCBBE 2025

June 16-18, 2025, Warsaw, Poland

Joint
20th Nordic-Baltic Conference
on Biomedical Engineering
&
24th Polish Conference on Biocybernetics
and Biomedical Engineering

https://www.nbc2025.ibib.waw.pl

Joint 20th Nordic-Baltic Conference on Biomedical Engineering and the 24th Polish Conference on Biocybernetics and Biomedical Engineering (NBC 2025 & PCBBE 2025)

June 16 - 18, Warsaw, Poland

BOOK OF ABSTRACTS

ORAL PRESENTATIONS

Oral Session OS01
Artificial Intelligence in Healthcare: Cardiovascular Applications
Chairs: Virginia Ballarin(Argentina), Piotr Foltynski (Poland)
OP001–OP004

OP001

Automatic Text Classification in Cardiac Risk Management: A Pilot Study

Jacopo VITALE[1], Mark C.H. de GROOT[2], Imo HÖFER[2], Leandro PECCHIA[1], Saskia HAITJEMA[2], Bram VAN ES[2]

1 Research Unit of Intelligent Technology for Health and Wellbeing, Research Unit of

Intelligent Technology for Health and Wellbeing, Department of Engineering,

Universit`a Campus Bio-Medico di Roma, Rome, Italy

3acopo.vitale@unicampus.it,

2 Central Diagnostic Laboratory, Universitair Medisch Centrum Utrecht,

Heidelberglaan 100, 3584 CX, Utrecht, Netherlands

Keywords: EHR, NLP, Cardiovascular Risk

Abstract. This pilot study explores the feasibility of using text from Electronic Health Record (EHR) at the University Medical Center Utrecht to classify patient eligibility for cardiovascular risk management. The primary goal is to improve the identification of at-risk patients and facilitate timely, personalized interventions. Through a ResNet architecture, which is used as a feature extractor, the outputs are then passed into a neural network classifier to predict patient eligibility for cardiovascular risk management. Despite excluding numerical data from EHR during model training and inference, and the imbalanced nature of the dataset, the model achieved promising results with an accuracy of 85% and an F1-score of 0.85. This preliminary analysis demonstrates the feasibility of the approach and establishes a solid foundation for further improvements. Future research directions include integrating Explainable AI techniques to enhance model transparency, expanding the dataset, and addressing class imbalance through data augmentation or resampling techniques.

OP002

Echocardiographic Image-Based Classification of Cardiac Amyloidosis: A Proof of Concept

Maria Elisabetta PAGNANO[1], Martina SASSI[1], Jacopo VI-TALE[1], Margherita A.G. MATARRESE[1], Chiara CIRILLO[2], Filippo CRISPINO[1], Giuseppe LIMONGELLI[2], Leandro PECCHIA[1]

1 Research Unit of Intelligent Technology for Health and Wellbeing, Department of Engineering, Università Campus Bio-Medico di Roma, Rome, Italy

2 Inherited and Rare Cardiovascular Diseases Unit, Department of Translational Medical Sciences, University of Campania "Luigi Vanvitelli", Naples, Italy

m.matarrese@unicampus.it

Abstract. Cardiac amyloidosis is a major cause of left ventricular hypertrophy, characterized by thickening of the left ventricular walls due to amyloid fibril dep- osition. Early diagnosis is crucial for optimizing patient management and reduc- ing morbidity. This study proposes an approach based on automated echocardio- graphic image analysis for cardiac amyloidosis classification. A total of 21 sub- jects were included in this study. The A4-chamber view was selected from all cardiac chambers, and an automated pipeline was developed for field-of-view recognition. Machine and deep learning models were implemented to differenti- ate cardiac amyloidosis from healthy conditions using echocardiographic images. Preliminary results show high classification accuracy of 92% using Gradient Boosting, suggesting a potential improvement in differential diagnosis. This study highlights the growing role of artificial intelligence in cardiac imaging and paves the way for more efficient and precise diagnostic tools.

Keywords: Cardiac amyloidosis, artificial intelligence, classification, echocardiographic images.

OP003

Custom Attention in Transformer Architectures for Multiclass ECG Beat Classification

Elia PATTACINI[1,2], Vaidotas MAROZAS[2]

1 Polytechnic University of Milan, Milan, Italy

2 Kaunas University of Technology, Kaunas, Lithuania

elia.pattacini@mail.polimi.it

Abstract. Electrocardiogram (ECG) beat classification plays an important role in diagnosing and managing cardiovascular conditions. This study introduces a method for classifying ECG beats into normal, supraventricular, and ventricular types using a transformer-based architecture with a custom attention mechanism. The preprocessing steps include filtering, resampling, normalization, and seg- mentation of ECG signals. Two classification approaches are proposed: (a) a cas- cade method employing sequential binary classifications, and (b) a multiclass method for direct classification. Synthetic data simulating supraventricular and ventricular arrhythmia is generated to address data imbalance and enhance model performance. The training and testing processes leveraged various datasets, in- cluding the MIT-BIH Arrhythmia, Supraventricular Arrhythmia, European ST, and Long-Term ST databases. The results highlight the superior performance of the cascade model, achieving a macro-average F1 score of 0.92 and a precision score of 0.90 on the Long-Term ST database. These findings show the importance of dataset selection and enhancement, demonstrating the model's potential for clinical applications.

Keywords: Electrocardiogram, Arrhythmias, ECG beat classification, synthetic data; RR interval normalization

OP004

The influence of color on semantic ulcer segmentation using deep learning models

Muhammad USMAN, Jacek RUMIŃSKI

Gdansk University of Technology, FETI, Department of Biomedical Engineering,

Gdansk, 80-233, Poland

muhammad.usman1@pg.edu.pl

Abstract. Accurate and early image analysis is crucial for proper diagnosis and treatment. Convolutional neural networks (CNNs) have the ability to precisely classify and segment the affected wound areas, which has revolutionized biomedical imaging for automatic detection and diagnosis. However, CNN models often face challenges like generalization and overfitting issues due to limited wound image data. In addition, RGB images are computationally intensive. They may prompt the model to focus on irrelevant features, such as color variations, instead of the most important ones, like silhouettes, ultimately leading the model to the over- fitting problem. This study investigates the influence of color on ulcer semantic segmentation. We explore different color-to-grayscale conver- sion techniques to study the learning behavior of the CNN model. Tra- ditionally, image conversion from an RGB color space to grayscale uses fixed transformation parameters, e.g., YUV color model weights, which are standardized for human observers. The YUV color model separates luminance (Y) from chrominance (U and V), allowing efficient brightness and color information representation. However, machine-based process- ing does not require 'seeing' the content but focuses on extracting the essential features for model training, data augmentation, or future design of task-specific sensors. We designed a universal model architecture to analyze the learning procedure's ability to learn task-specific weights for color-to-grayscale conversion. The experiment results show how grayscale images based on learned weights could be used in task-specific semantic segmentation compared to color images and grayscale images obtained using traditional conversion techniques. The grayscale images based on learned weights are computationally efficient, and simplified feature representation helps the model emphasize the most relevant attributes while suppressing irrelevant ones.

Keywords: Convolution neural network, Foot ulcer segmentation, Image Modalities, learned grayscale, RGB and grayscale images

Oral Session OS02
Nanotechnology and Molecular Engineering
Chairs: Marta Kopaczyńska (Poland), Kamila Sadowska (Poland)
OP005–OP008

OP005

Zinc phosphate-protein hybrid nanoflowers as new local drug delivery systems

Kornelia BOBROWSKA[1], Elżbieta REMISZEWSKA[1], Aleksandra GŁOWACKA[2], Piotr GOLEC[2], Kamila SADOWSKA[1*]

1 Nalecz Institute of Biocybernetics and Biomedical Engineering, Polish Academy of Sciences, Ks. Trojdena 4, 02-109 Warsaw, Poland

2 Department of Molecular Virology, Institute of Microbiology, Faculty of Biology, University of Warsaw, Warsaw, Poland

* ***Corresponding author***. *E-mail address*: ksadowska@ibib.waw.pl

Keywords: hybrid nanoflowers, local drug delivery, osteomyelitis

Motivation and Aim: Osteomyelitis is an inflammation of bone tissue and bone marrow, mainly caused by *Staphylococcus aureus* and *Pseudomonas aeruginosa* [1]. The primary challenge in infection treatment today is bacterial resistance to antimicrobial agents, largely driven by inappropriate, insufficient, or excessive use of antibiotics. Local antibiotic delivery has emerged as a promising therapeutic approach to address the limitations of conventional treatments and manage osteomyelitis effectively [2]. The aim of this study is to manufacture local drug delivery systems composed of organic and inorganic component, which mimics composition of bones.

Novelty: Zn-protein nanostructures as drug carriers for local delivery of antibiotics used in the osteomyelitis treatment was studied for the first time.

Methods: Manufactured Zn-BSA nanostructures were characterized by Fourier-transform infrared spectroscopy (FTIR), X-ray diffraction (XRD) and scanning electron microscopy (SEM). Drug release kinetics were evaluated by ultraviolet-visual spectroscopy (UV-vis) and the antibacterial activity against *Pseudomonas aeruginosa* and *Staphylococcus aureus* were studied by optical density and disc diffusion methods. Toxicity studies are being conducted both *in vitro* and *in vivo* using zebrafish models.

Main results: Although, metal-protein nanoflowers are known for years, synthesis of Zn-based nanoflowers has not been studied in details. Therefore, in the first step the parameters of synthesis, as time, concentration and volume of PBS and ratio of reagents were studied. The optimal parameters were found to obtain Zn-BSA nanoflower-like structures with high content of protein, which was proved by FTIR spectroscopy (see Figure 1 A). X-ray diffraction analysis showed, that the inorganic phase was a hydrated zinc phosphate (see Figure 1 B). The content

of inorganic phase in Zn-BSA samples increased with time and PBS concentration. Two antibiotics, namely ciprofloxacin (CF) and vancomycin (VN), used in osteomyelitis treatment were successfully embedded in Zn-BSA nanostructures. The antibacterial activity of the synthesized nanoflowers was demonstrated against *S. aureus* and *P. aeruginosa*, two main pathogens found in osteomyelitis and the results are presented in Figure 2.

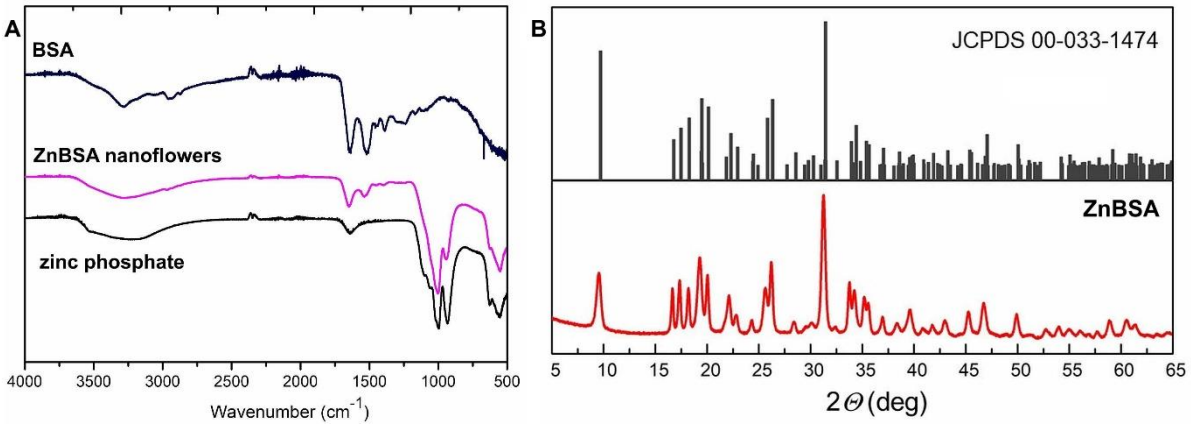

Figure 1. A) FTIR spectra of ZnBSA nanoflowers in comparison to BSA and zinc phosphate; B) X-ray diffractograms of ZnBSA and $Zn_2(PO_4)_3 \cdot 4H_2O$ (JCPDS 00-033-1474).

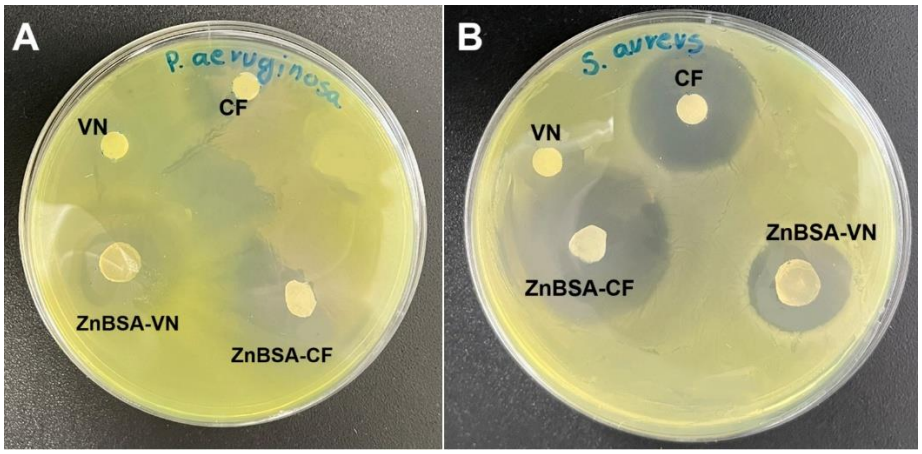

Figure 2. Susceptibility testing of *P. aeruginosa* (A) and *S. aureus* (B) using the disk diffusion method.

Conclusion: The designed nanoflowers have the potential to serve as an effective local antibiotic delivery system. With their non-toxic, biodegradable components and eco-friendly synthesis, hybrid nanoflowers show great promise as drug delivery systems for treating infections in the skeletal system.

Acknowledgements: Project financed by Polish Ministry of Science and Higher Education, Program Science for the Society NdS-II/SP/0335/2023/01.

References:

[1] García Del Pozo E, Collazos J, Cartón JA, Camporro D, Asensi V. Bacterial osteomyelitis: microbiological, clinical, therapeutic, and evolutive characteristics of 344 episodes. Rev Esp Quimioter. 2018;31(3):217–225.

[2] Jain KK. An Overview of Drug Delivery Systems. Drug Delivery Sys. 2020:1–54. doi:10.1007/978-1-4939-9798-5_1.

OP006

Nanolayer of monocrystalline Si towards nanodosimetry of electron radiation

Galina BOKA[1], Yuri DEKHTYAR[2], Mirko ROCCA[2], Elizabete SKREBELE[2], Hermanis SOROKINS[2]

1 Oncology Center of Latvia, 4 Hipokrata street, Riga LV-1038, Latvia

2 Riga Technical University, 6A Kipsalas Street, Riga LV-1048, Latvia

Hermanis.Sorokins@rtu.lv

Abstract. Nanodosimetry aims to measure the ionizing radiation dose absorbed in nanosized volumes. For that, photothermostimulated exoelectron emission (PTSE) of monocrystalline silicon (Si) nanolayer might be used to detect weak electrons, because their mean free path in the solid is around 100 nm. The current work aims to explore the possibility of using monocrystalline Si for nanodosimetry of high energy electron radiation. It is demonstrated that the PTSE of monocrystalline Si can be used for the identification of 6 MeV electron radiation doses 35-60 Gy. The total emitted charge of PTSE is connected with the delivered dose. The near-threshold photoelectric emission spectroscopy and Fourier-transform infrared spectroscopy (FTIR) indicate that PTSE is influenced by radiation-induced reconstructions.

Keywords: High energy electron radiation. Exoelectron emission. Monocrystalline silicon. Nanodosimetry.

OP007

The role of sphingosine kinase 1 pharmacological modulation on crucial pro/anti-apoptotic proteins in alpha-synuclein-transduced cells: The promising role of siponimod and ponesimod

Joanna Agata MOTYL[1*], Agnieszka WENCEL[1], Kinga CZUBOWICZ[2], Robert Piotr STROSZNAJDER[2]

1 Laboratory of Tissue Engineering, Hybrid and Analytical Microbiosystems Department, Nalecz Institute of Biocybernetics and Biomedical Engineering, Polish Academy of Sciences, Ks. Trojdena 4 St., 02-109 Warsaw, Poland

2 Laboratory of Preclinical Research and Environmental Agents, Mossakowski Medical Research Institute, Polish Academy of Sciences, 5 Pawińskiego St., 02-106 Warsaw, Poland

* ***Corresponding author***. *E-mail address*: jmotyl@ibib.waw.pl

Keywords: alpha-synuclein, sphingosine kinase 1, Parkinson's disease, siponimod, ponesimod

Motivation and Aim: Alpha-synuclein (α-syn) is a presynaptic protein highly abundant in the brain, where it plays a crucial role, particularly in regulating synaptic plasticity and neurotransmitter turnover. Nonetheless, the exact mechanisms remain unclear, but α-synuclein is capable of undergoing conformational alterations and progressively aggregating, ultimately leading to the formation of filamentous structures known as Lewy bodies (LBs), which are a hallmark of Parkinson's disease (PD). Moreover, growing evidence suggests that the altered expression or activity of sphingosine kinase 1 (Sphk1), which synthesizes sphingosine-1-phosphate (S1P), is implicated in PD and other neurodegenerative diseases.

Novelty: This underscores the importance of investigating the interaction between α-syn and Sphk1, an area that remains poorly understood in the pathomechanism of PD. Moreover, the other aim was to analyze the potential protective mechanism of S1P modulators, such as siponimod and ponesimod, in a PD cellular model.

Methods: In the genetic context of familial PD, evidence for the critical role of the α-syn gene (SNCA) comes from dominantly inherited gene duplications and several missense mutations. Therefore, SH-SY5Y cells, transduced with a lentivirus carrying the human α-syn gene (SH-SNCA), along with control cells transduced with an empty vector, were used to model PD *in vitro*. The mRNA and protein levels of key pro- and anti-apoptotic proteins were analyzed using RT-PCR, Western blotting, and Fluorescence-Activated Cell Sorting (FACS).

Main results: First, overexpression of α-syn in SH-SY5Y cells resulted in a reduction of brain-derived neurotrophic factor (BDNF) mRNA levels and an increase in the pro-apoptotic/anti-apoptotic Bax/Bcl-2 ratio. Furthermore, treatment with the Sphk1 inhibitor (SK1-I) significantly elevated α-syn expression in SH-SNCA cells. On the other hand, pharmacological activation of Sphk1 led to an increase in BDNF mRNA levels. In contrast, the expression of neurotrophic tyrosine kinase receptor 2 (NTRK2), a receptor for BDNF, was decreased by the Sphk1 activator and upregulated by SK1-I treatment. Notably, the administration of the Sphk1 activator/inhibitor had opposite effects on the Bax/Bcl-2 ratio, inducing its reduction and elevation, respectively. Finally, administration of S1P receptor modulators, such

as siponimod and ponesimod, increased BDNF levels, which were reduced by the pro-apoptotic agent, cell-permeable C2-ceramide. Moreover, siponimod and ponesimod enhanced the phosphorylation of key pro-survival kinases AKT and ERK1/2, which was diminished by C2-ceramide. Both compounds notably protected cells from C2-ceramide-induced toxicity.

Conclusion: Our results suggest that both α-syn overexpression and the imbalance in Sphk1 activity may be linked to an elevation in the Bax/Bcl-2 ratio, a reduction in BDNF levels, and inhibition of AKT/ERK1/2 kinases. Moreover, siponimod and ponesimod provide protection against these alterations, positioning them as promising candidates for future PD studies.

Acknowledgements: This research was funded by the National Science Centre, Poland, under grant No. 2019/32/C/NZ4/00455.

OP008

The insight into the distinct molecular changes induced by methylation inhibitors in leukemia cells in relation to so far well-defined mechanism of action

Przemysław SAREŁO[1,2*], Aleksandra KACZOROWSKA[1], Marlena GĄSIOR-GŁOGOWSKA[1], Anna LICZNERSKA[1], Kinga GODKOWICZ[3], Ewa ZIOŁO[3], Wojciech KAŁAS[3], Halina PODBIELSKA[1], Marta KOPACZYŃSKA[1]

1 Department of Biomedical Engineering, Faculty of Fundamental Problems of Technology, Wrocław University of Science and Technology, Wybrzeże Stanisława Wyspiańskiego 27, 50-370 Wrocław, Poland

2 Pre-clinical Research Center, Wrocław Medical University, Karola Marcinkowskiego 1, 50-368 Wrocław, Poland

3 Department of Experimental Oncology, Ludwik Hirszfeld Institute of Immunology and Experimental Therapy, Polish Academy of Sciences, Rudolfa Weigla 12, 53-114 Wrocław, Poland

* ***Corresponding author***. *E-mail address*: przemyslaw.sarelo@pwr.edu.pl

Keywords: DNA methylation inhibitors, azacitidine, decitabine, haematological malignancies, chromatin remodeling

Motivation and Aim: Nowadays, there is a growing recognition of DNA methylation as a pivotal role in cancer development. Thus, the potential of hypomethylating agents like azacitidine (AZA) and decitabine (DEC) as therapeutic tools for myelodysplastic syndromes (MDS) and acute myeloid leukaemia (AML) is emerging. Despite their established clinical use in cancer treatment, the precise molecular mechanisms through which these drugs influence DNA and chromatin structure remain inadequately understood. While the primary mechanism of action for AZA and DEC involves the modification of DNA methylation patterns via the inhibition of DNA methyltransferase (DNMT) activity, their broader, multi-layered effects on chromatin structure and DNA mechanics have yet to be fully explored. Furthermore, the differences between AZA and DEC in terms of their incorporation into DNA and RNA, as well as their potential effects on chromatin modifications and nuclear architecture, suggest that these drugs may have more complex and far-reaching impacts than currently recognized. Therefore, the use of advanced measurement methods has allowed to shed new light on the molecular and cellular processes that accompany the previously defined mechanism of action of the indicated agents.

Novelty: By means of innovative tools and methodologies provided by biomedical engineering, the effects of DNA methylation inhibitors on chromatin organization in leukemia cells could be explored.

Methods: All the experiments were performed on the newly-established primary leukaemia cell line AML-007 (consent of the Bioethics Committee at the Medical University of Wrocław no. 593/2012). The research aimed to elucidate the cellular and molecular effects of AZA and DEC on cancer cells, with particular emphasis on their influence on cell viability and proliferation, nuclear morphology, its refractive index and stiffness as well as chromatin

accessibility and structure. The advanced techniques such as atomic force microscopy (AFM), optical tweezers (OT), Fourier-transform infrared microscopy (μFTIR), digital holographic microscopy (DHM) were employed and accompanied by well-known confocal laser scanning microscopy (CLSM), flow cytometry and cell-based assays.

Main results: The CLSM revealed significant changes in cell nucleus size and actin fiber structure following treatment with both drugs. As the concentration of the methylation inhibitor was higher, the area of the cell nucleus increased. The OT experiments showed that both AZA and DEC decreased cell nucleus stiffness, with DEC having a more significant effect. The changes in the refractive index of cell nuclei, which were examined by DHM, indicated chromatin loosening, what was also confirmed by chromatin condensation analysis by means of flow cytometry. It demonstrated that DEC increased chromatin accessibility in a concentration-dependent manner, while the effects of AZA were less pronounced. AFM studies have shown that both AZA and DEC induced chromatin decondensation and disrupt its proper structure. This softening effect is likely a result of DNA hypomethylation, which promotes a more open chromatin configuration. It was proven that the above-mentioned changes were not caused by cell death, however the tested cells were characterized by reduced metabolic activity in cell-based assays. Moreover, the spectroscopic analysis by means of μFTIR confirmed differences in DNA methylation and chromatin structure between control and drug-treated cells.

Conclusion: All the obtain results suggest that while both drugs affect chromatin structure, they do so via different mechanisms, what is followed by distinct molecular and cellular changes, and though despite so far well-defined mechanism of action. Moreover, the study clearly demonstrates that chromatin structure alterations can be observed not only through biological methods but are also reflected in biophysical parameters, such as refractive index and nuclear stiffness.

Acknowledgements: The study was supported by the statutory funds of the Department of Biomedical Engineering, Faculty of Fundamental Problems of Technology, Wroclaw University of Science and Technology and statutory funds of the Wrocław Medical University subsidy with internal number of SUBK.Z516.24.068.

Oral Session OS03
Medical Image Processing
Chairs:
Zhivko Bliznakov (Bulgaria), Lukasz Roszkowiak (Poland)
OP009–OP012

OP009

An Approach to Create a Computational Model of a Trabecular Bone

Kristina BLIZNAKOVA[1], Dimitar TRIZLOV[1], Nikolay DUKOV[1], Stoyan IVANOV[1], Zhivko BLIZNAKOV[1]

1 Medical University of Varna, Varna, Bulgaria

kristina.bliznakova@mu-varna.bg

Abstract. Spheres are simple 3D geometrical primitives, which when arranged in specific patterns, can form structures exhibiting fractal characteristics. Consequently, spheres are used to construct breast phantoms for x-ray imaging. This study aims to apply this approach of creating complex breast phantoms to bone applications. For this purpose, we utilized realistic tibia outlines based on Computed Tomography patient data and a 3D texture derived from spherical geometrical primitives. Then, these were combined to generate a trabecular bone model. Three bone models were created, and x-ray planar images of these models were produced using a dedicated x-ray imaging simulator. The models were evaluated by orthopedic physicians, who confirmed the realistic appearance of the trabecular structures. The bone model is intended for use in osteoporosis research studies and 3D printing techniques.

Keywords: spherical geometrical primitives, bone model, x-ray images, model- ling and simulation

OP010

Assessment of quality of colorectal endoscopic images

Damian PAWŁOWSKI[1*], Andrzej ŻELOWSKI[2], Klaudia KOZŁOWSKA[1], Mirosław ŁĄTKA[1*].

1 Wroclaw University of Science and Technology, Wrocław, Poland

2 Krapkowickie Centrum Zdrowia Sp. z o.o., Krapkowice, Poland

* ***Corresponding author***. *E-mail address*: *damian.pawlowski@pwr.edu.pl, miroslaw.latka@pwr.edu.pl*

Keywords: colon cancer, colon polyps, image quality, classification, colonoscopy

Motivation and Aim: According to the World Health Organization (WHO), colorectal cancer (CRC) is the third most common cancer worldwide and accounts for approximately 10% of cancer-related deaths. Colon polyps are defined as abnormal tissue growth that projects from the mucous layer. They are histologically classified into non-neoplastic and neoplastic (adenomatous) polyps. The latter gives rise to 95% of CRC cases. Such polyps must be removed during colonoscopy. Many classification algorithms have been developed based on texture analysis or neural networks to minimize the risk of medical errors. However, the low quality of the endoscopic images can deteriorate the performance of classifiers trained on carefully selected datasets.

Novelty: We employed a reference-free Naturalness Image Quality Evaluator[1] (NIQE) to investigate how endoscopic image quality affects the detection rate of adenomatous polyps.

Methods: We analyzed 2,439 unique colorectal polyp images (547 non-neoplastic and 1892 neoplastic) obtained through narrow-band imaging. Dual-tree complex wavelet transform (DT-CWT), Gray Level Co-occurrence Matrix (GLCM), Local Binary Pattern (LBP), and Multi-Fractal Spectrum with Local Fractal Dimension[2] (MFS-LFD) were used to extract features. Then, the corresponding binary classifiers were created through supervised learning. We downsampled the neoplastic images to obtain balanced datasets. We repeated the ten-fold cross-validation ten times and averaged the classification metrics such as accuracy (ACC), true positive rate (TPR), true negative rate (TNR), Matthews correlation coefficient (MCC). For each texture algorithm, we tested several classifiers and reported the results only for the best one. We repeated the process after filtering out all pictures with NIQE greater than the chosen threshold (8.5). There were 199 and 580 images of non-neoplastic and neoplastic polyps, respectively. Again, we used balanced datasets.

Main results:

Fig. 1 and Table 1 show that regardless of the feature extraction algorithm, the classifiers' performance on the unfiltered dataset was inferior but markedly improved for the images with the best quality. For the DT-CWT, the accuracy increased from 66% to 78%, and MCC increased from 32% to 56%.

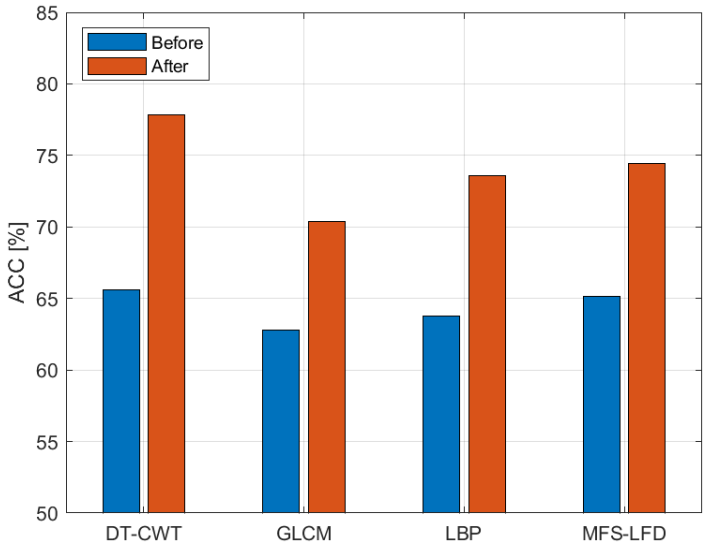

Fig. 1. Accuracy of the polyp classification for the four different feature extraction algorithms before and after filtering the low-quality images (with a high value of the NIQE index).

Table 1. The performance metrics of four classifiers before and after filtering the low-quality images (with a high value of the NIQE index).

Method	Classifier	Before NIQE filtration					After NIQE filtration				
		Polyps	ACC [%]	TPR [%]	TNR [%]	MCC [%]	Polyps	ACC [%]	TPR [%]	TNR [%]	MCC [%]
DT-CWT	SVM	2439	65.6	63.0	68.2	31.5	779	77.8	74.4	81.3	56.3
GLCM	SVM		62.8	51.6	73.9	26.4		70.4	60.5	80.6	42.0
LBP	Random forest (bagging)		63.8	65.9	61.6	27.7		73.6	73.4	73.7	47.6
MFS-LFD	Random forest (bagging)		65.1	63.1	67.2	30.4		74.4	72.5	76.4	49.4

Conclusion: The application of NIQE enabled the filtering of images whose quality may limit the classifiers' applicability for clinical deployment. Further studies are required to establish how the endoscopists' experience determines image quality.

References:

[1] Mittal A, Soundararajan R, Bovik AC. Making a “Completely Blind” Image Quality Analyzer. *IEEE Signal Processing Letters*. 2013;20(3):209-212. doi:https://doi.org/10.1109/lsp.2012.2227726.

[2] Häfner M, Tamaki T, Tanaka S, Uhl A, Wimmer G, Yoshida S. Local fractal dimension based approaches for colonic polyp classification. *Medical image analysis*. 2015;26(1):92-107. doi:https://doi.org/10.1016/j.media.2015.08.

OP011

Does Semi-Automatic Segmentation-Based Classification Enable AI-Assisted Detection of Sinusitis in an Equine Model?

Marta BOROWSKA[1*], Paweł LIPOWICZ[1], Hubert ASZTEBORSKI[2], Tomasz JASIŃSKI[2], Bernard TUREK[2], Małgorzata DOMINO[2*]

1 Institute of Biomedical Engineering, Faculty of Mechanical Engineering, Białystok University of Technology, Bialystok, Poland

2 Department of Large Animal Diseases and Clinic, Institute of Veterinary Medicine, Warsaw University of Life Sciences, Warsaw, Poland

* ***Corresponding author***. *E-mail address*: m.borowska@pb.edu.pl; malgorzata_domino@sggw.edu.pl

Keywords: horse, computed tomography, 3D segmentation, K-means clustering

Motivation and Aim: Diagnostic imaging in both human and veterinary medicine is rapidly evolving, with significant advancements in artificial intelligence (AI) applications, including i.a. automated disease detection and assisted clinical decision-making. In equine practice, computed tomography (CT) is the preferred method for imaging the head and diagnosing paranasal sinus diseases due to the anatomical complexity and superimposition of osseous, dental, and soft tissue structures [1]. CT imaging aids in diagnosing the causes of paranasal sinus diseases and identifying the affected compartments, allowing for more targeted surgical treatment [2]. Therefore, this study aims to semi-automatically segment the paranasal sinuses of healthy and diseased horses and demonstrate the feasibility of AI-assisted sinusitis detection using the K-means clustering algorithm.

Novelty: To date, equine sinuses have been semi-automatically segmented on CT images in only a few studies [3-6], focusing on volume measurements of paranasal sinuses [3], their communication [4], anatomical relationships with maxillary cheek teeth [5], and volumetric changes with age [6]. However, all these studies examined only healthy adult horses. To the best of our knowledge, this study is the first attempt at AI-assisted identification of diseased paranasal sinuses on CT images of equine heads, which may advance veterinary practice.

Methods: The study was conducted on CT scans of the heads of 30 horses, aged 2 to 25 years, acquired using a 64-slice CT scanner (GE Healthcare, USA). The study focused on the rostral maxillary sinus (RMS), caudal maxillary sinus (CMS), and frontal sinus (FS). In 15 horses (control group), no radiological signs of sinusitis were observed, while in 15 horses, at least one sinus on at least one side exhibited a hyperdense area indicative of inflammation (disease group). The RMS, CMS, and FS were semi-automatically segmented using 3D Slicer ver. 5.6.0 following a previously described protocol [6], and morphometric measurements (volume [mm^3] and surface area [mm^2]) were extracted. Since both RMS and CMS volume and surface area increase with age [6] due to dental eruption [5], volume, surface area, and horses' age

represented an input data for clustering. Clustering was performed using the unsupervised K-Means machine learning method [7] implemented in the Scikit-Learn module in Python ver. 3.11. Clustering considered three classes: healthy sinus/control group (0), sinusitis/diseased group (1), and healthy sinus/diseased group (2). To assess how the K-Means predicted clusters aligned with clinical classifications, classification metrics (accuracy, precision, recall, and F1-score) were calculated using a confusion matrix.

Main results: RMS, CMS, and FS were successfully segmented using a semi-automatic protocol in both healthy horses and horses diagnosed with sinusitis. Since not all sinuses were inflamed in the diseased horses, classification was assessed by comparing healthy horses [0,1] and distinguishing between inflamed and healthy sinuses within diseased group [1,2].

Table 1. Classification metrics of sinuses into healthy sinus (0, 2) and sinusitis (1) classes.

	RMS [0, 1]	RMS [1, 2]	CMS [0, 1]	CMS [1, 2]	FS [0, 1]	FS [1, 2]
Accuracy	0.73	0.80	0.58	0.77	0.73	0.60
Precision	0.71	0.81	0.56	0.84	0.70	0.78
Recall	0.73	0.80	0.57	0.77	0.70	0.60
F1-score	0.72	0.80	0.56	0.75	0.70	0.52

The K-means clustering algorithm achieved the highest classification metrics for distinguishing between healthy and inflamed RMS within the diseased group and the lowest metrics for classifying inflamed CMS when compared to healthy horses (Table 1). However, in all cases considered, the classification metrics exceeded 0.50, indicating a level of accuracy that may be valuable for further clinical applications in equine veterinary practice.

Conclusion: Semi-automatic segmentation of head CT images is effective for identifying both healthy and inflamed sinuses. The K-means clustering algorithm demonstrated high accuracy and precision in classifying healthy and inflamed sinuses in comparison to healthy horses and within diseased horses, thus may be implemented into equine clinical practice.

Acknowledgements: Project no WZ/WM-IIB/2/2024 partially financed by the PMSHE (MNiSW).

References:

[1] Manso-Díaz G, García-López JM, Maranda L, Taeymans O. The role of head computed tomography in equine practice. Equine Vet Educ. 2015; 27(3): 136-145. doi: 10.1111/eve.12275.

[2] Dixon PM, Barnett TP, Morgan RE, Reardon RJ. Computed tomographic assessment of individual paranasal sinus compartment and nasal conchal bulla involvement in 300 cases of equine sinonasal disease. Front Vet Sci. 2020; 7, 580356. doi: 10.3389/fvets.2020.580356.

[3] Brinkschulte M, Bienert-Zeit A, Lüpke M, et al. Using semi-automated segmentation of computed tomography datasets for three-dimensional visualization and volume measurements of equine paranasal sinuses. Vet Radiol Ultrasound. 2013; 54(6), 582-590. doi: 10.1111/vru.12080.

[4] Köhler L, Schulz-Kornas E, Vervuert I, et al. Volumetric measurements of paranasal sinuses and examination of sinonasal communication in healthy Shetland ponies: Anatomical and morphometric characteristics using computed tomography. BMC Vet Res. 2021; 17, 41. doi: 10.1186/s12917-021-02748-6.

[5] Liuti T, Reardon R, Dixon PM. Computed tomographic assessment of equine maxillary cheek teeth anatomical relationships, and paranasal sinus volumes. Vet Rec. 2017; 181(17), 452 doi: 10.1136/vr.104185.

[6] Borowska M, Lipowicz P, Daunoravičienė K, et al. Three-Dimensional Segmentation of Equine Paranasal Sinuses in Multidetector Computed Tomography Datasets: Preliminary Morphometric Assessment Assisted with Clustering Analysis. Sensors. 2024; 24(11), 3538. doi: 10.3390/s24113538.

[7] Sinaga KP, Yang MS. Unsupervised K-means clustering algorithm. IEEE Access. 2020; 8, 80716-80727. doi: 10.1109/ACCESS.2020.2988796.

OP012

Surface-area-to-volume ratio as a diagnostic indicator in the assessment of avascular necrosis of femoral head

Adam PATALAS[*1], Patryk ZYCH[1], Kacper FILIPEK [1], Paweł ZAWADZKI[1]

1 Poznan University of Technology, Poznan, Poland

* ***Corresponding author***. *E-mail address*: adam.patalas@put.poznan.pl

Keywords: bone morphometry, microCT, hip head

Motivation and Aim: The aim of this study was to evaluate the surface-area-to-volume ratio (BS/BV) as a potential diagnostic indicator for the assessment of femoral head morphology in avascular necrosis (AVN), with the goal of identifying distinct structural differences that could aid in the early detection and understanding of AVN progression. BS/BV representing Bone Surface normalized by Bone Volume, was calculated to assess the structural characteristics of femoral heads affected by AVN compared to healthy specimens.

Novelty: Unlike traditional methods, the use of micro-CT-based morphometric analysis allows for precise quantification of bone structural alterations. The findings provide a new perspective on the diagnostic potential of the BS/BV ratio in AVN, offering a more objective and quantifiable measure of bone changes associated with this condition.

Methods: The study was approved by the Institutional Review Board of Poznan University of Medical Science, approved by the Bioethics Committee (Approval No. 777/2022, 15 November 2022). Fourteen femoral heads were collected(7 from patients with diagnosed avascular necrosis undergoing total hip arthroplasty (THA) and 7 from cadavers without diagnosed diseases of the musculoskeletal system). Patients with known history of hip trauma, infection, and rheumatoid arthritis were excluded. Inclusion criteria also involved a macroscopic inspection of specimens. The micro-CT evaluation was conducted using a GE phoenix v|tome|x s240 system (Waygate Technologies, Wunstorf, Germany). The microCT reconstruction of femoral head specimens and the datasets were analyzed usingsoftware (Volume Graphics 2.2, Heidelberg, Germany). Following the approach used in the pilot study [6,7]. The bonemorphometric parameters were computed with using open-source software, which was created in project R01EB021391 (Textural Biomarkers of Arthritis for the Subchondral Bone in the Temporomandibular Joint) supported by the National Institutes of Health (NIH in the USA).

Main results: The average BS/BV mm-1 was found to be 1.45 ± 0.39 for femoral heads with AVN and 1.69 ± 0.26 for healthy femoral heads. This indicates that femoral heads affected by AVN exhibit a lower surface-area-to-volume ratio compared to healthy specimens. Furthermore, the minimum observed BS/BV mm-1 values were notably different between AVN-affected (minimum: 0.65) and healthy specimens (minimum: 1.15), highlighting distinct structural variations associated with the presence of AVN.

Conclusion: These findings underscore the potential diagnostic utility of surface-area-to-volume ratio in distinguishing between femoral heads affected by AVN and those from healthy

subjects. The results align with the hypothesis that AVN leads to alterations in bone morphology, reflected in lower BS/BV values compared to healthy counterparts

Acknowledgements: The study was conducted according to the guidelines of the Declaration of Helsinki, and approved by the Institutional Review Board of Poznan University of Medical Science, approved by the Bioethics Committee (Approval No. 777/2022, 15 November 2022).

References:

[1] Wang C, Gou W, Xu X, Yuan X, Peng J, Lu S. Microstructure features and pathology of trabecula in different regions of femoral head necrosis. Acad J Chin PLA Med Sch. 2014;35(5):463-465,469. doi:10.3969/j.issn.2095-5227.2014.05.018.

[2] Toussirot É, Jeunet L, Michel F, Kantelip B, Wendling D. Avascular necrosis of the hallucal sesamoids update with reference to two case-reports. Joint Bone Spine. 2003;70(4):307-309.

[3] Yao X, Wang P, Dai R, et al. Microstructures and properties of cancellous bone of avascular necrosis of femoral heads. Acta Mech Sin. 2010;26:13-19. doi:10.1007/s10409-009-0309-8.

[4] Handa A, Xu L, Machado-Rivas F, et al. Magnetic resonance imaging in neonates: a practical approach to optimize image quality and increase diagnostic yield. Pediatr Radiol. 2023;53:1300-1313. doi:10.1007/s00247-022-05550-0.

[5] Gao R, Xia X, Liu J, et al. Study on bone microstructure and pathology of type L2 and L3 osteonecrosis of the femoral head specimens classified by China-Japan Friendship Hospital classification based on "three-columns structure". Zhongguo Xiu Fu Chong Jian Wai Ke Za Zhi. 2022;36(8):1003-1010. doi:10.7507/1002-1892.202203108.

[6] Uklejewski R, Winiecki M, Patalas A, Mietliński P, Zawadzki P, Dąbrowski M. Micro-CT Assessment During Embedding of Prototype Ti Alloy Multi-Spiked Connecting Scaffold in Subchondral Trabecular Bone of Osteoarthritic Femoral Heads, Depending on Host BMI. Journal of Functional Biomaterials. 2024; 15(12):387. https://doi.org/10.3390/jfb15120387

[7] Dąbrowski M, Rogala P, Uklejewski R, Patalas A, Winiecki M, Gapiński B. Subchondral Bone Relative Area and Density in Human Osteoarthritic Femoral Heads Assessed with Micro-CT before and after Mechanical Embedding of the Innovative Multi-Spiked Connecting Scaffold for Resurfacing THA Endoprostheses: A Pilot Study. J. Clin. Med. 2021, 10, 2937.

Special Symposium SE01
Integrating Artificial Intelligence in Clinical Engineering: Perspectives For the Future
Chair: Fabiola Martinez-Licona (Mexico)
OP013–OP016

OP013

The impact of Artificial Intelligence in predictive maintenance

Fabiola MARTINEZ-LICONA[1]

1 Universidad Autonoma Metropolitan, Mexico City, Mexico

* ***Corresponding author***. *E-mail address*: fmml@xanum.uam.mx

Keywords: Predictive Maintenance, Industry 5.0, Clinical Engineering

Motivation and Aim: The growing complexity of medical equipment and the limitations of traditional maintenance strategies highlight the need to explore alternative maintenance techniques. The aim would be to explore how integrating AI can significantly improve healthcare services by enhancing equipment data collection and employing sophisticated data analytics.

Novelty: The emphasis in the alignment of AI-driven predictive maintenance with the core principles of Industry 5.0, such as human-centricity, sustainability, and resilience. This involves showing how AI not only improves maintenance but also enhances the roles of human workers, promotes sustainable practices by reducing waste and resource consumption, and ensures operational resilience

Methods: A systematic literature review was performed, and an analysis of current trends, challenges and future directions is presented. The focus was on articles, reports and other types of resources from the last 10 years (2015-2025) in English specifically addressing AI applications in medical device maintenance. The relevant information from the included resources, for example AI techniques used, types of medical devices, reported benefits, challenges, and key findings. Finally, the alignment of the results found with the core principles of Industry 5.0, human-centricity, sustainability and resilience, was analyzed.

Main results: A detailed categorization of AI and machine learning algorithms applied to predictive maintenance and articulation of their benefits in terms of time, costs, and safety were found. Also, the challenges arising from using AI in data quality, human resources, and ethical concerns, were defined. The alignment to Industry 5.0 principles was analyzed and found in

specific cases where the role of human workers, sustainable practices, and ethical considerations regarding the use of AI are highlighted. Future trends like more sophisticated AI models, integration with telemedicine platforms, and enhanced data analytics for comprehensive system oversight are presented.

Conclusion: AI on predictive maintenance presents a paradigm shift in healthcare, offering significant improvements in operational efficiency, cost savings, and patient care. The medical device sector can harness the transformative power of AI to ensure the reliability, safety, and sustainability of its equipment.

References:

[1] Murtaza AA, Saher A, Zafar MH, Syed, Aftab MF, Sanfilippo F. Paradigm Shift for Predictive Maintenance and Condition Monitoring from Industry 4.0 to Industry 5.0: A Systematic Review, Challenges and Case Study. Results in Engineering. Published online September 1, 2024:102935-102935. doi:https://doi.org/10.1016/j.rineng.2024.102935

[2] Coandă P, Avram M, Constantin V. A state of the art of predictive maintenance techniques. *IOP Conference Series: Materials Science and Engineering*. 2020;997:012039. doi:https://doi.org/10.1088/1757-899x/997/1/012039

OP014

Artificial Intelligence for the diagnosis and treatment of otosclerosis

Virginia L. BALLARIN[12]*, Gustavo J. MESCHINO[2], Nicolas NIETO ARIAS [3], Carlos CAPIEL Jr.[3]

1 School of Medicine, Universidad FASTA, Mar del Plata, Argentina

2 School of Engineering, Universidad FASTA, Mar del Plata, Argentina

3 Radiological Institute of Mar del Plata, Mar del Plata, Argentina

* ***Corresponding author***. *E-mail address*: vballari@gmail.com

Keywords: Otosclerosis Diagnosis, Artificial Intelligence, Healthcare, Deep Learning, Medical Imaging

Motivation and Aim: Otosclerosis is a middle ear disease that can lead to hearing loss if not detected early. Early detection of otosclerosis is critical to enable timely intervention, thereby limiting disease advancement and improving the likelihood of hearing preservation. However, the complexity of ear anatomy and the subtle radiological alterations associated with otosclerosis make diagnosis challenging, especially for non-specialist medical professionals. This study aims to develop an artificial intelligence (AI)-based diagnostic tool to assist in otosclerosis detection.

Novelty: This research explores the application of deep neural networks, particularly convolutional architectures, to the automated analysis of computed tomography (CT) scans for the identification of otosclerosis-associated morphological alterations. Unlike traditional methods, this AI-driven system enhances diagnostic accuracy and accessibility, particularly in settings with limited otology expertise.

Methods: A dataset of 120 CT images from patients with confirmed otosclerosis was compiled for AI model training. Different architectures of convolutional neural networks (CNNs) were tested to internally recognize the radiological patterns that allow the otosclerosis diagnosis. Model performance was evaluated using Accuracy computed by 10 cycles hold-out estimation, considering random 30 images for testing in each cycle.

Main results: Preliminary results indicate that the AI model achieves 81% accuracy in detecting otosclerosis-related features in CT images. The model demonstrated effective discrimination between pathological and normal cases, supporting its potential utility as a reliable diagnostic support tool. Expert radiologist review confirmed the accuracy of the AI model's findings.

Conclusion: The developed AI-based tool will provide an efficient and accurate method for otosclerosis detection, supporting clinicians in early diagnosis and treatment planning. Other architectures will be tested to improve the Accuracy. This advancement could lead to improved patient outcomes by enabling timely intervention and management of the disease.

Acknowledgements: The authors would like to express their gratitude to FASTA University for its valuable support in funding this research.

References:

[[1] Abouzari M, Gopen Q, Finnell JE, et al. Prediction of vestibular schwannoma recurrence using artificial neural network. *Laryngoscope Investig Otolaryngol.* 2020;5(2):278. doi:10.1002/LIO2.362.

[2] Ayral M, Kıyak E, Ekşi M, et al. How advantageous is it to use computed tomography image-based artificial intelligence modelling in the differential diagnosis of chronic otitis media with and without cholesteatoma? *Eur Rev Med Pharmacol Sci.* 2023;27(1):215-223. doi:10.26355/EURREV_202301_30874.

[3] Comas DS, Meschino GJ, Ballarin VL. Framework de segmentación y análisis de imágenes mediante reconocimiento de texturas. In: *Argentinian Symposium of Technology (AST).* Buenos Aires, Argentina; 2010:1529-1541.

[4] Duan B, Guo X, Fan Y, et al. An in-depth discussion of cholesteatoma, middle ear inflammation, and Langerhans cell histiocytosis of the temporal bone, based on diagnostic results. *Front Pediatr.* 2022;10. doi:10.3389/FPED.2022.809523.

[5] Eroğlu O, Ayral M, Kıyak E, et al. Is it useful to use computerized tomography imagebased artificial intelligence modelling in the differential diagnosis of chronic otitis media with and without cholesteatoma? *Am J Otolaryngol.* 2022;43(3):103395. doi:10.1016/J.AMJOTO.2022.103395.

[6] Fujima N, Yoshida D, Kwee TC, et al. Utility of deep learning for the diagnosis of otosclerosis on temporal bone CT. *Eur Radiol.* 2021;31(7):5206-5211. doi:10.1007/S00330-020-07568-0.

[7] Ke J, Chen X, Shen Y, et al. Deep learning-based approach for the automatic segmentation of adult and pediatric temporal bone computed tomography images. *Quant Imaging Med Surg.* 2023;13(3):1577-1591. doi:10.21037/QIMS-22-658.

[8] Meschino GJ, Andrade RE, Ballarin VL. A framework for tissue discrimination in magnetic resonance brain images based on predicates analysis and compensatory fuzzy logic. *Int J Intell Comput Med Sci Image Process.* 2008;2(3):209-224.

OP015

Early prediction of ICU readmissions using Machine Learning in a Colombian university hospital

Joel Andrés LERMA PAZOS[1], J.E Camacho COGOLLO[2], Jose Leonardo MOJICA PEÑARANDA[3]

1 EIA University, Envigado, Colombia

2 EIA University, Envigado, Colombia

3 Pablo Tobón Uribe Hospital, Medellín, Colombia

javier.camacho@eia.edu.co

Abstract. Hospital readmissions are common, unplanned, and potentially avoidable occurrences linked to elevated morbidity and mortality rates. In Colombia, the primary concerns regarding ICU readmissions involve the significant expenses associated with treating patients readmitted due to deteriorating circumstances or heightened illness severity, alongside inadequate discharge decisions made by certain physicians or experts, which decrease the efficacy of healthcare facilities. This study aims to develop a predictive model that provides an early warning for the readmission of adult patients to the intensive care unit. In order to accomplish this, a variety of database administration and data analysis technologies were employed, alongside with machine learning models referenced in the literature. These models were trained and validated using data provided by the Hospital Pablo Tobón Uribe (HPTU) in Medellín. As a result of this project, a predictive model was developed with an accuracy score of 0.74 and an AUC value of 0.74, providing valuable information to physicians and specialists when making ICU discharge decisions. This model generates alerts for patients at risk of readmission if discharged, improving decision-making in intensive care settings.

Keywords: ICU Readmission; Machine Learning, Classification algorithms

OP016

Artificial Intelligence challenges for medical device regulation

Fabiola MARTINEZ-LICONA[1]

1 Universidad Autonoma Metropolitan, Mexico City, Mexico

* ***Corresponding author***. *E-mail address*: fmml@xanum.uam.mx

Keywords: Regulatory Affairs, Smart Medical Devices, Clinical Engineering

Motivation and Aim: Incorporating artificial intelligence into medical device design is transforming healthcare through advanced diagnostics, personalized treatment, and improved patient outcomes. However, the dynamic nature of AI presents unique challenges for regulatory bodies responsible for market approval, as they must ensure the safety, efficacy, and performance of these devices. Unlike traditional devices, AI systems are iterative and constantly learning from new data, making them less predictable. This unprecedented challenge requires regulatory agencies to adapt their frameworks to accommodate the unique characteristics of AI.

Novelty: Artificial Intelligence's challenges are unique and unprecedented in medical device regulations. Intelligent systems are dynamic in nature and have an increasing learning rate from new data, making it difficult to track their safety and efficacy. This requires regulatory bodies to adapt existing frameworks designed for static devices to accommodate the evolving nature of AI technologies.

Methods: Based on a search of bibliographic resources and official documents from different regions, proposing how to address the challenges that AI has imposed in other areas, we will establish a reference framework to address the most relevant aspects of medical devices. In particular, it will address the AI algorithm´s assessment, which often makes outcomes interpretation difficult, the software´s update and modification management, specifically the post-market long-term performance tracking, the ethical considerations, and global access to AI developments.

Main results: Among the most relevant findings are regulatory gaps in specific risk addressing with a higher necessity for handle the safety and efficacy along their lifecycle, issues regarding data bias and quality where the guaranty of diverse and high quality datasets is a priority, a problem with the harmonization of AI-driven standards in different regions, and the difficulty of monitoring AI-based systems in the post-market phase. Discussion on these topics will be encouraged.

Conclusion: The rapid advancement of AI in medical devices demands a paradigm shift in regulatory frameworks. Regulatory bodies can foster innovation while safeguarding public health by addressing challenges related to transparency, adaptability, ethics, and global harmonization.

References:

[1] Onitiu, D., Wachter, S., & Mittelstadt, B. (2024). How AI challenges the medical device regulation: patient safety, benefits, and intended uses. Journal of Law and the Biosciences, lsae007. https://doi.org/10.1093/jlb/lsae007.

[2] Palaniappan, K., Lin, E. Y. T., & Vogel, S. (2024). Global Regulatory Frameworks for the Use of Artificial Intelligence (AI) in the Healthcare Services Sector. Healthcare (Basel, Switzerland), 12(5), 562. https://doi.org/10.3390/healthcare12050562.

Oral Session OS04
Artificial and Bioartificial Organs
Chairs:
Loredana De Bartolo (Italy), Dorota D. Pijanowska (Poland)
OP017–OP020

OP017

Advance in Skin and Liver Tissue Engineering by using Organotypic Membrane Systems and Mesenchymal Stem Cells

Simona SALERNO[1*], Loredana DE BARTOLO[1]

1 Institute on Membrane Technology, National Research Council of Italy (CNR-ITM), Via P. Bucci 17/c, 87036 Rende (CS), Italy

* ***Corresponding author***. *E-mail address*: s.salerno@itm.cnr.it

Keywords: Tissue Engineering, Membranes, Organotypic Models

Motivation and Aim: Advanced organotypic tissues made of polymeric membranes and human cells, in both homotypic and heterotypic co-culture systems with mesenchymal stem cells (MSCs), were developed as an ambitious attempt for the bio-fabrication of self-renewing human tissue models. Polymeric membranes mimic the *in-vivo* 3D microenvironment, recapitulating the natural niches for hosting cells and promoting cell-cell and cell-matrix interactions.

Novelty: Through the modulation of the preparation process parameters, membranes with specific functionalities and structural features can be designed, representing a challenging strategy for the control of the cellular fate. Specific membranes properties provide the biochemical stimuli and mechanical support able to boost cellular adhesion, proliferation and differentiation, and thus the overall morpho-functional behavior [1-3]. Porous semipermeable membranes enable the compartmentalization and the physical separation of cells allowing in the meantime their crosstalk by the selective mass transfer of the secreted paracrine factors and therefore mimicking the *in-vivo* physiological cell niches [3-5]. Moreover, the membrane loading with a bioactive molecule constantly released in the time, represents a further strategy to trigger or modulate biological processes needed for tissue regeneration and therapy.

Methods: Biodegradable membranes were prepared by phase inversion method. Nanoporous and microporous chitosan membranes were developed optimizing the polymer solution, by the addition of polyethylene glycol as porogen at different ratio, by blending with poly(ε-caprolactone), or by adding drug-loaded inclusion complexes or mesoporous nanoparticles. The developed membranes were characterized and utilized for the creation of partial or complete skin layers using human keratinocytes and MSCs isolated from human dermis. Porous semipermeable membranes were used for membrane bioreactors design and optimization, as bioartificial liver engineering. Specific configurations and fluid dynamics were tested for human liver cell compartmentalization and dynamic direct and connected co-cultures with endothelial cells and MSCs.

Main results: Engineered microenvironments made by the combination of polymeric membranes with human cells were created as tissue models. Specific or complete epidermal strata and partial or complete skin layers were engineered by using biodegradable membranes, that through specifically tuned structural and physico-chemical surface properties, triggered proper cell responses modulating the stratification and terminal differentiation of human keratinocytes, and the epidermal and dermal differentiation of MSCs. The membrane loading with active compounds allowed cellular protection and repair in induced skin damages.

Dynamic organotypic membrane bioreactors offered interesting opportunities for the design of bioartificial livers with high morpho-functional performance, simulating the high perfusion and the sinusoidal organization of the in vivo hepatic microenvironment. Cell compartmentalization allowed the physical separation of MSCs and the selective mass transfer of their secreted factors. A stable hepatic human phenotype was maintained for a prolonged time, which is strictly required for therapeutic purpose and for drug testing assessment in preclinical pharmacological research.

Conclusion: Innovative culture strategies, by using engineered membrane biohybrid systems have been developed and presented in this work as interesting approach for skin and liver reconstruction, providing valid tools for therapeutic and drug-screening applications.

References:

1. Salerno S, Morelli S, Giordano F, Gordano A, De Bartolo L. Polymeric membranes modulate human keratinocyte differentiation in specific epidermal layers. *Colloids Surf. B Biointerfaces* 2016; 146:352-362.

2. Salerno S, Messina A, Giordano F, Bader A, Drioli E, De Bartolo L. Dermal-epidermal membrane systems by using human keratinocytes and mesenchymal stem cells isolated from dermis. *Mat Sci Eng C-Mater* 2017; 71:943-953.

3. Salerno S, Tasselli F, Drioli E, De Bartolo L. Poly(ε-caprolactone) hollow fiber membranes for the biofabrication of a vascularized human liver tissue. *Membranes* 2020; 10(6): 112.

4. Salerno S, Curcio E, Bader A, Giorno L, Drioli E, De Bartolo L. Gas permeable membrane bioreactor for the co-culture of human skin derived mesenchymal stem cells with hepatocytes and endothelial cells. *J Membr Sci* 2018*;* 563:694–707.

5. Salerno S, Piscioneri A, Morelli S, Gori A, Provasi E, Gagni P, Barile L, Cretich M, Chiari M, De Bartolo L. Extracellular vesicles selective capture by peptide-functionalized hollow fiber membranes. *J Colloid Interf Sci* 2024; 667:338-349.

OP018

Characteristics of dedifferentiated human hepatocytes isolated from liver tissues

Monika Joanna WIŚNIEWSKA[1*], Małgorzata JAKUBOWSKA[1], Agnieszka WENCEL[1], Dorota Genowefa PIJANOWSKA[1], Krzysztof Dariusz PLUTA[1]

1 Nalecz Institute of Biocybernetics and Biomedical Engineering Polish Academy of Sciences, Department 1, Laboratory of Tissue Engineering, Ks. Trojdena 4 st. 02-109 Warsaw, POLAND

* ***Corresponding author.*** *E-mail address:* mwisniewska@ibib.waw.pl

Keywords: Human hepatocytes, dedifferentiation, fibroblast-like cells, BAL, hepatocyte isolation

Motivation and aim: Currently, liver transplantation is the only method used to cure patients with liver failure. Because of the donor shortage, approximately 10% of patients on the transplantation waiting list die. Scientists have searched for alternative methods that prolong patients' lives until liver transplantation. One of the most promising techniques seems to be devices called bioartificial liver (BAL) support systems, which include biological material. The best source of cells for these devices is human hepatocytes. Unluckily, hepatocytes after isolation dedifferentiate very quickly and lose their ability to perform their functions. The aim of this research was to characterize our newly obtained cell type (liver-derived fibroblasts (LDFs)), which is derived from a liver isolate. Moreover, we want to use them as a potentially new source of cells in BAL devices.

Novelty: Our newly obtained cell type, LDFs, dedifferentiated from isolated liver cells, can divide and partially retain hepatocyte functions such as albumin production.

Methods: In our laboratory, we established a new method of human hepatocyte isolation on the basis of mechanical defragmentation and enzymatic digestion of liver tissue. This method allows the isolation of the whole range of liver cells, including hepatocytes. Isolated hepatocytes are cultured with a dedicated commercial medium kit, which enables the dedifferentiation of hepatocytes into fibroblast-like cells. Using flow cytometry, immunostaining, and western blot techniques, we investigated whether LDFs can produce proteins specific for hepatocytes.

Main results: The results confirmed that LDFs can produce markers specific for hepatocytes even after dedifferentiation. However, the protein level during cell passages changed, which suggests the progression of cell dedifferentiation.

Conclusion: Liver-derived fibroblasts (LDFs), which are dedifferentiated from isolated liver cells, seem to constitute promising biological material for use in BAL systems.

OP019

Tunable Isotropic TPMS-based 3D-Architected Scaffolds for Diabetic Bone Regeneration

Fátima MORALES-GÓMEZ[1], Fabiola HERNÁNDEZ-ROSAS [1,2], Araceli ZAPATERO-GUTIÉRREZ[2,3], Erick RAMÍREZ-CEDILLO[4], Josué GARCÍA-ÁVILA[3,5]

1 Ingeniería Biomédica, División de Ingenierías, Universidad Anáhuac Querétaro. Santiago de Querétaro, 76246, México

2 Centro de Investigación, Universidad Anáhuac Querétaro. Santiago de Querétaro, 76246, México

3 Ingeniería Mecánica para la Innovación, División de Ingenierías, Universidad Anáhuac Querétaro. Santiago de Querétaro, 76246, México

4 School of Engineering and Sciences, Tecnológico de Monterrey, Monterrey, 64700, Nuevo León, México

5 Department of Mechanical Engineering, Stanford University, Stanford, 94305, California, USA

josue.garciaavila@anahuac.mx

Abstract. Diabetes mellitus significantly compromises bone health, increasing the risk of fractures, osteoporosis, and limb amputations due to metabolic dys- functions. Effective bone regeneration is critical for managing complex fractures and bone-related complications, with over two million bone grafts performed an- nually. This research focuses on designing and developing personalized 3D-ar- chitected scaffolds to enhance bone regeneration in patients with diabetes using computational simulation techniques. These scaffolds are tailored to replicate the mechanical and structural properties of natural bone by optimizing key features such as anisotropy, porosity, and nutrient mass flow. The study highlights the transformative potential of personalized 3D-architected scaffolds in addressing critical challenges associated with diabetic bone health. Customizing scaffold de- signs to meet the specific needs of patients with diabetes aims to reduce postop- erative complications, improve healing outcomes, and enhance overall patient quality of life. Future work will refine scaffold designs and validate their perfor- mance in diabetes-specific clinical in vitro and in vivo models.

Keywords: Scaffold, Bone Regeneration, Diabetes Mellitus

OP020

Patterns of relative blood volume changes during hemodialysis

Leszek PSTRAS*, Mauro PIETRIBIASI

Nalecz Institute of Biocybernetics and Biomedical Engineering, Polish Academy of Sciences, Warsaw, Poland

* ***Corresponding author***. *E-mail address*: lpstras@ibib.waw.pl

Keywords: Hemodialysis, Blood volume, Ultrafiltration, Mathematical Modeling

Motivation and Aim: During hemodialysis (HD), a few liters of excess fluid are removed from the body in the process called ultrafiltration (UF). This typically results in a decrease in blood volume, which in turn can lead to hemodynamic instability [1]. However, neither too much nor too little reduction in blood volume (BV) during HD is good for the patient, as it has been shown that there are specific ranges of relative blood volume (RBV) during HD that are associated with reduced all-cause mortality [2]. Intradialytic RBV changes are largely dependent on UF but can also be affected by various patient parameters. A few characteristic patterns of RBV changes during HD have been identified, including an exponential or a linear decrease. However, patients can exhibit a wide range of RBV patterns during HD, including a paradoxical increase in BV during the treatment. The aim of this study was to investigate possible patterns of RBV changes during HD using synthetic data generated with a mathematical model of cardiovascular response to HD.

Novelty: We proposed a method for normalizing intradialytic RBV curves to reduce the influence of UF and thus enable the identification of patterns of RBV changes during HD regardless of the magnitude of RBV changes.

Methods: We studied a publicly available synthetic dataset of BV changes during a standard 4-hour HD simulated using a lumped-parameter model of the cardiovascular response to HD [3]. This dataset includes intradialytic BV curves simulated in a diverse cohort of 5,000 virtual patients with randomly assigned values of 90 physiological parameters and UF. We normalized all RBV curves to values in the range [-1 1], with 0 representing the initial (baseline) BV level and individual curves normalized to values [0 1], [-1 0], (-1 1], or [-1 1), depending on the direction of BV changes during HD and the maximum and minimum RBV levels during HD. We then applied various rules on the values and derivatives of such normalized RBV curves at specific time points during HD (at 10, 30, 60, 120, 180, and 240 min) to identify 12 patterns of RBV changes during HD. All computations were performed in MATLAB® (The Mathworks Inc.).

Main results: Fig. 1A shows the averaged normalized RBV curves corresponding to the 12 considered patterns of intradialytic RBV changes (i.e. averaged curves from all virtual patients exhibiting a given pattern), whereas Fig. 1B shows the associated averaged original (non-normalized) RBV curves for the same groups of virtual patients. We found that patients with relatively similar patterns in normalized RBV (e.g. patterns no. 7, 8, and 9) may show substantially different RBV changes during HD, which may be at least partly explained by different levels of UF. On the other hand, patients with similar overall RBV reduction during

HD may have significantly different patterns of intradialytic RBV changes (e.g. patterns no. 8 and 12).

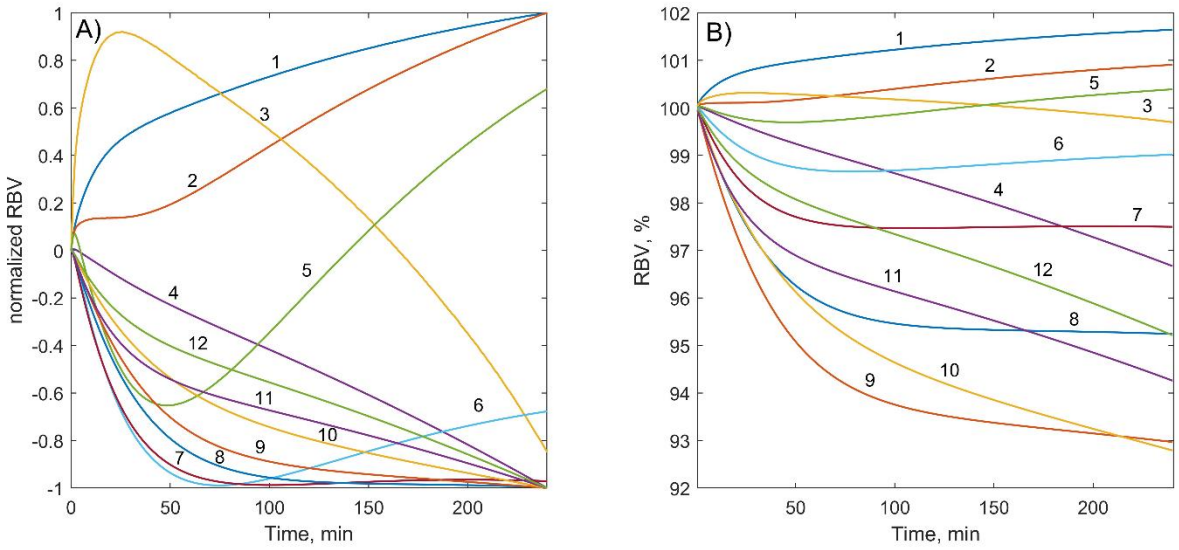

Fig. 1. Averaged intradialytic RBV curves in 12 groups of virtual patients exhibiting the considered RBV patterns. **A)** normalized RBV curves, **B)** original (non-normalized) RBV curves.

Conclusion: The proposed normalization of intradialytic RBV curves may help identify specific patterns of RBV changes during HD and may help assign individual patients to such patterns, even if their RBV curves differ in the magnitude of RBV changes during HD (the latter being strongly associated with UF). The ability to classify patients according to the pattern of normalized RBV changes during HD could potentially be used in the future to introduce some modifications to dialysis treatment that would be beneficial to a given type of patient, especially for patients suffering from intradialytic hypotension. Further research is needed to enable automatic clustering of patients exhibiting similar intradialytic RBV patterns (e.g. using machine learning clustering methods) and to investigate parameters influencing those patterns as well as possible treatment modifications that could improve hemodynamic stability in patients with specific RBV patterns.

Acknowledgements: This study was supported by the National Science Centre, Poland (grant no. 2021/43/D/NZ5/01887).

References:

[1] Reeves PB, Mc Causland FR. Mechanisms, Clinical Implications, and Treatment of Intradialytic Hypotension. *Clin J Am Soc Nephrol*. 2018;13:1297-303.

[2] Preciado P, Zhang H, Thijssen S, Kooman JP, van der Sande FM, Kotanko P. All-cause mortality in relation to changes in relative blood volume during hemodialysis. *Nephrol Dial Transplant*. 2019;34:1401-8.

[3] Pstras L, Waniewski J. A Model-Based Dataset for In-Silico Exploration of the Patterns of Relative Blood Volume Changes During Hemodialysis. 2023 IEEE EMBS Special Topic Conference on Data Science and Engineering in Healthcare, Medicine and Biology. 2023:149-50.

Special Symposium SE02
EAMBES and IEEE EMBS Symposium
Chairs: Giuseppe Fico (Spain)

- **EAMBES: State of the Alliance and Plan for 2025-2026**

  Giuseppe Fico

- **EAMBES Public Affair Working Group**

  Leandro Pecchia

- **EAMBES Outreach and Actions toward Diversity, Inclusiveness and Equity TBA**

- **Poland Section IEEE EMBS**

  Antoni Grzanka, Paweł Strumiłło

PLENARY LECTURE 1

PL1

Using Light Absorption and Laser Speckle Dynamics to Measure Human Brain Function

Prof. David A. Boas, PhD (USA)

David Boas, Ph.D. (Professor, Biomedical Engineering) is Director of the Neurophotonics Center at Boston University. He received his BS in Physics at Rensselear Polytechnic Institute and PhD in Physics at the University of Pennsylvania. During his academic career, he has supervised more than 50 students and post-doctoral fellows, and he has published over 300 papers that have received over 46,000 citations and an h-index of 117. He is the founding President of the Society for Functional Near Infrared Spectroscopy and founding Editor-in-Chief of the journal Neurophotonics published by SPIE. Dr. Boas was awarded the Britton Chance Award in Biomedical Optics in 2016 for his development of several novel, high-impact biomedical optical technologies in the neurosciences, as well as following through with impactful application studies, and fostering the widespread adoption of these technologies. He was elected a Fellow of AIMBE, SPIE, and OSA in 2017.

As Director of the Neurophotonics Center, he facilitates the development and application of novel optical methods to address a broad range of neuroscience questions from basic science to clinical translation. His own research efforts focus on neurovascular coupling, cerebral oxygen delivery and consumption, functional near infrared spectroscopy (fNIRS), and physiological modeling. Studies are done in rodents and humans, invasively and non-invasively, microscopically and macroscopically, providing a powerful ability to translate findings from animals to humans, and conversely to address in animals questions raised during human studies. One example of this that will tie together many of Dr. Boas' activities is studying functional brain recovery in survivors of stroke. Human neuroimaging by fMRI and fNIRS measures hemodynamic functional recovery but it is not known if neuro-vascular coupling differs in these patients compared to healthy subjects. Animal studies will answer this question enabling more quantitative interpretation of the human neuroimaging studies.

Professor (BME, ECE)

Neurophotonics Center

Boston University College of Engineering, USA

PLENARY LECTURE 2

PL2

AI-powered MRI: Towards an Omni Imaging Technology for Brain Mapping

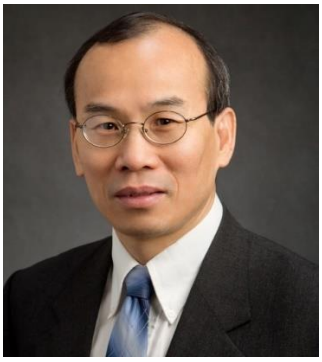

Prof. Zhi-Pei Liang, PhD (USA)

Zhi-Pei Liang received his Ph.D. degree from Case Western Reserve University in 1989. He subsequently joined the University of Illinois at Urbana-Champaign (UIUC) first as a postdoctoral fellow (supervised by Nobel Laureate Paul Lauterbur) and then as a faculty member. Dr. Liang is currently the Franklin W. Woeltge Professor of Electrical and Computer Engineering; he also chairs the Computational Imaging Group in the Beckman Institute for Advanced Science and Technology. Dr. Liang's research is in the general area of magnetic resonance imaging, signal processing and machine learning. His work has been recognized by a number of awards, including the Sylvia Sorkin Greenfield Award (Medical Physics, 1990), the Whitaker Biomedical Engineering Research Award (1991), the NSF CAREER Award (1995), the University Scholar Award (UIUC, 2001), the Isidor I. Rabi Award (ISMRM, 2009), the Otto Schmitt Award (IFMBE, 2012), IEEE-EMBC Best Paper Awards (2010, 2011, 2021), IEEE-ISBI Best Paper Awards (2010, 2015), the Technical Achievement Award (IEEE-EMBS, 2014), and the Gold Medal (ISMRM, 2022). Dr. Liang was selected as the Paul C. Lauterbur Lecturer for the 2016 ISMRM meeting and as the Savio L. Woo Distinguished Lecturer for the 2017 WACBE World Congress on Bioengineering. He is a Fellow of IEEE, ISMRM and AIMBE. He was elected to the International Academy of Medical and Biological Engineering in 2012 and to the US National Academy of Inventors in 2021. Dr. Liang served as President of the IEEE-EMBS from 2011-2012 and received its Distinguished Service Award in 2015. He has been serving as Chair-elect (2022-2024) and Chair (2025-2027) of the International Academy of Medical and Biological Engineering.

Franklin W. Woeltge Professor

Department of Electrical and Computer Engineering, and

Beckman Institute for Advanced Science and Technology

University of Illinois at Urbana-Champaign

USA

Special Symposium SE03
AI and Deep Learning in Medicine and Biology
Chair: Domènec Savi Puig Valls (Spain), Anna Korzyńska (Poland)
OP021–OP024

OP021

Deep Learning for Centroblast Detection in H&E-Stained Whole Slide Images

Zaneta SWIDERSKA-CHADAJ[1,2,*] ,Adam KRAWCZYK [2,3], Aleksandra OSOWSKA-KURCZAB[2], Sławomir PAKUŁO[4], Wojciech KOTŁOWSKI[3]

1 Warsaw University of Technology, Faculty of Electrical Engineering, Pl. Politechniki 1, Warsaw, 00-661, Poland
2 IDEAS NCBR, Chmielna 69, Warsaw, 00-801, Poland
3 Poznan University of Technology, Faculty of Computing and Telecommunications, Piotrowo 2, Poznan, 60-965, Poland
4 Maria Sklodowska-Curie National Research Institute of Oncology, Tumor Pathology Department, Wybrzeze Armii Krajowej 15, Gliwice, 44-102, Poland

* ***Corresponding author***. *E-mail address*: zaneta.swiderska@pw.edu.pl

Keywords: cell classification, deep learning, digital pathology, follicular lymphoma

Motivation and Aim: AI is playing an increasingly pivotal role in the field of medicine. Novel Computer Aided Diagnosis methods offer promising avenues to assist pathologists, alleviating their workload and reducing associated costs. However, the development of specialized solutions tailored to specific tasks, such as support of the Follicular Lymphoma (FL) diagnosing, is impeded by various challenges, including multistage data collection and inconclusive annotation.

To address the intricacies of pathologists' tasks, we propose an AI-based method for detecting centrocytes (CCs) and centroblasts (CBs) in FL cases. This is particularly challenging because, identifying CBs presents a formidable challenge, even for experts, given their potential confusion with centrocytes. Our method is designed to detect cells and classify them into one of three categories: CBs, CCs, or other. Using input data at x20 resolution, our proposed approach diverges from methods outlined in existing literature and comprises two distinct phases: detection and classification.

Novelty: In this paper, we proposed a novel method to assist in the detection of centroblasts for the assessment of FL. The method operates effectively using lower-resolution input data compared to existing approaches in the literature[1,2,3]. CBs detection poses a significant challenge even for experts, as CBs can easily be misclassified as CCs, and classification is not always feasible. To address these challenges, we introduced a three-class schema wherein we

distinguish between centroblasts, non-centroblasts (centocytes and other cells), and an "unknown" class comprising ambiguous cells.

Methods: For research purposes, we collected a dataset comprising 41 routinely stained hematoxylin and eosin glass slides depicting cases of FL across a range of grades. These slides were collected from the Maria Sklodowska-Curie National Research Institute of Oncology in Gliwice, Poland, and digitized using a 3DHISTECH PANNORAMIC 250 Flash II scanner. All experiments were conducted in strict adherence to the Declaration of Helsinki guidelines for responsible research practices.

The collected dataset was annotated by trained pathologists employing a two-step annotation method and the active learning pipeline. In total, 12,704 cells were annotated, comprising 1,406 CBs, 9,514 CCs, and 1,784 other cell types, subsequently partitioned into distinct train, validation, and test sets.

Both the detection and classification steps were executed utilizing deep learning models, with YOLOv8 employed for cell detection and a shallow CNN model utilized for cell classification.

Main results: While the majority of studies predominantly focus on CBs detection, we extended our investigation to assess its efficacy in classifying centroblasts against non-centroblast cells, encompassing centrocytes and other classes, to mirror setups outlined in existing literature. In this particular configuration, we attained a precision of 58% and a recall of 57% for CBs classification.

Pathologists also noted uncertainty in discerning particular cells, given the visual similarities between CBs and CCs. To mitigate this challenge, we introduced an artificial class 'unknown', designated for cells with a classification confidence score below 0.5 as determined by our softmax classifier. In this refined setup, with a focus on select cells, we achieved a precision of 62% and a recall of 57%.

Conclusion: The relatively modest performance of centroblast (CB) detection models, observed in both our proposed method and prior studies, suggests that this task poses challenges not only for seasoned pathologists but also for training highly effective machine learning systems.

Our findings on CBs detection using the proposed method underscore the viability of detecting CBs within whole slide images scanned at x20 resolution. Despite utilizing images with lower resolution, we have demonstrated the capability to achieve results in CB classification that are comparable to state-of-the-art approaches.

References:

[1] Yuenyong, S., Boonsakan, P., Sripodok, S., Thuwajit, P., Charngkaew, K., Pongpaibul, A., et al. (2024). Detection of centroblast cells in H&E stained whole slide image based on object detection. Frontiers in Medicine, 11, 1303982.

[2] Dimitropoulos, K., Barmpoutis, P., Koletsa, T., Kostopoulos, I., & Grammalidis, N. (2017). Automated detection and classification of nuclei in pax5 and H&E-stained tissue sections of follicular lymphoma. Signal, Image and Video Processing, 11, 145-153.

[3] Fauzi, M. F. A., Pennell, M., Sahiner, B., Chen, W., Shana'ah, A., Hemminger, J., et al. (2015). Classification of follicular lymphoma: the effect of computer aid on pathologists grading. BMC medical informatics and decision making, 15, 1-10.

OP022

Tumor Morphological and Texture Feature Analysis to Classifying the Breast Cancer Molecular Subtypes in Digital Mammograms

Adnan KHALID[1], Hatem A. RASHWAN[1], Domenec PUIG[1]*

1 Universitat Rovira i Virgili, Department of Computer Engineering and Mathematics, Tarragona, Spain

* ***Corresponding author***. *E-mail address: domenec.puig@urv.cat*

Keywords: Breast Cancer, Molecular Subtypes, Radiological Imaging, Texture Analysis,

Deep Learning

Motivation and Aim: Breast Cancer (BC) remains an immense global health concern, recognized as a leading cause of cancer-related death among women, requiring accurate and effective diagnostic methods. The widespread influence of this issue requires efficient screening and diagnostic methods to address its high recurrence and death rates. Mammography is considered a fundamental method in the detection of breast cancer. It is widely acknowledged for its effectiveness in reducing mortality rates by enabling the early identification of the illness by 42% since 1989 [1]. BC is a heterogeneous disease that consists of different molecular subtypes. The presence of both intra and inter-tumor heterogeneity plays a significant role in drug resistance and treatment effectiveness. The molecular subtypes are categorized into four classes based on the expression of immunohistochemical markers: Luminal A, Luminal B, HER2, and Triple-Negative [2]. In addition to facilitating tailored treatment methods, having an understanding of the molecular subtype of breast cancer helps with risk assessment and prognostication, which ultimately leads to improved patient outcomes.

Novelty: This work aims to automate the process of classifying the molecular subtypes of BC using Artificial Intelligence (AI), leveraging advanced Deep Learning algorithms in multi-modal radiological imaging, mainly mammography, to provide a non-invasive, efficient, and cost-effective alternative to biopsies [3].

Methods: Our research includes an end-to-end framework for classifying BC molecular subtypes from radiological images (e.g., mammograms), structured into three key stages.

- Tumor Detection and Segmentation Based on Deep Learning: In the first stage, a deep learning-based segmentation model is employed to detect and precisely segment the tumor region. The model ensures accurate delineation of tumor boundaries, enhancing the reliability of subsequent feature extraction.

- Feature Extraction via Image Processing & Radiomics: The second stage focuses on extracting key morphological and radiomic (texture-based) features from the segmented tumor region. Advanced image processing techniques are applied to quantify tumor shape and margin characteristics, which are crucial for distinguishing molecular subtypes.

- Molecular Subtype Classification Based on Machine Learning: In the final stage, the extracted morphological and radiomic features are fed into machine learning models— such as Random Forest (RF), CatBoost, and Support Vector Machine (SVM)—to classify tumors into molecular subtypes (Luminal A, Luminal B, HER2+, and Triple- Negative).

The proposed framework enhances subtype classification accuracy, providing a more precise approach to BC diagnosis from mammography.

Main results: We employed quantitative and qualitative measures to compare the proposed framework to determine its effectiveness. We conducted an in-depth analysis of the relationship between tumor shape, margin, radiomics features, and BC molecular subtypes. This analysis identified novel correlations that are strongly supported by clinical data, offering new insights into the biological behavior of different subtypes. Based on the results we got from our private in-house dataset using this framework for subtype classification, we present a more accurate and efficient approach to classifying breast cancer molecular subtypes compared to existing methods.

Conclusion: Our framework consistently outperforms other approaches in distinguishing subtypes such as Luminal, HER2-positive, and Triple-negative, highlighting its potential for use in clinical and research settings, contributing to more precise and personalized breast cancer treatment strategies. Future work will focus on expanding this framework to incorporate additional imaging modalities, such as MRI and ultrasound, to enhance the model's diagnostic accuracy and generalizability across different clinical settings. **Acknowledgements:** This work was supported by the BosomShield Project, a grant from Marie Sklodowska-Curie Doctoral Networks Actions (HORIZON-MSCA-2021-DN-01-1- 101073222).

References:

[1] J. Ferlay, M. Ervik, F. Lam, M. Colombet, L. Mery, M. Piñeros, A. Znaor, I.Soerjomataram, and F. Bray. Global Cancer Observatory: Cancer Today. Lyon, France: International Agency for Research on Cancer. [Internet]. 2018.

[2] Ana M. Mota, Joao Mendes, and Nuno Matela. Breast Cancer Molecular Subtype Prediction: A Mammography-Based AI Approach. Biomedicines, 12(6):1371, 2024.

[3] Nariya Cho. Molecular subtypes and imaging phenotypes of breast cancer. Ultrasonography, 35(4):281, 2016.

OP023

EGGS: Efficient Gathering and Structuring of Avian Egg Datasets

Lukasz ROSZKOWIAK[1]⋆, Pawel PSTROKONSKI[2]⋆, Wojciech WOJCIK[2], Krzysztof DAMAZIAK[2], Anna KORZYNSKA[1]

1 Nalecz Institute of Biocybernetics and Biomedical Engineering Polish Academy of Sciences

lroszkowiak@ibib.waw.pl,

2 Warsaw University of Life Sciences, Poland

Abstract. This paper presents EGGS, a novel and purpose-driven image processing ap- proach designed specifically for creating a standardized and comprehensive dataset of avian egg images. The proposed approach integrates advanced techniques for image preprocessing, orientation detection, and the removal of damaged specimens, addressing key challenges in oological data analysis. With a primary focus on enhancing the quality of avian egg datasets, this study highlight the potential for combining advanced image processing techniques with deep learning models to address challenges in ecological data analysis. Beyond basic preprocessing, EGGS incorporates a robust orientation detection component and precise contour analysis, offering a focused and efficient framework for egg annotation. This innovative solution is tailored to support targeted ecological and heritage research, providing a unique tool for advancing ornithological studies. The resulting dataset not only enables downstream analyses but also serves as a critical resource for ornithological research, opening pathways for deeper insights into avian reproductive strategies, evolutionary adaptations, and environmental resilience.

OP024

Reinforcement Learning with Graph Neural Networks for Gene Regulatory Network Control

Andrzej MIZERA[1,2*], Jakub ZARZYCKI[1,2*]

1 University of Warsaw, Warsaw, Poland
2 IDEAS NCBR, Warsaw, Poland

* ***Corresponding author***. *E-mail address*: amizera@mimuw.edu.pl, jakub.zarzycki@ideas-ncbr.pl

Keywords: Gene Regulatory Network, Cellular Reprogramming, Boolean Network, Network Control, Graph Convolution Network, Deep Reinforcement Learning

Motivation and Aim: Cellular reprogramming, the artificial transformation of one cell type into another, has been attracting increasing research attention due to its therapeutic potential for complex diseases. However, discovering cellular reprogramming strategies solely through wet-lab experimentation is hindered by long timeframes and high costs. This strongly motivates us to explore *in-silico* methods for identifying viable reprogramming targets and intervention strategies to achieve efficacious cellular reprogramming.

The formal computational framework of Boolean Networks (BNs), introduced by S. Kauffman[1], has recently acquired significant interest in studying gene regulatory networks (GRNs) in the context of cellular reprogramming, where the goal is to control gene expression dynamics. Our work builds on previous research that applies Deep Reinforcement Learning (DRL) techniques to control BN models of GRNs[2-3]. In this study, we evaluate our approach using several BN models of real-life biological processes taken from the literature, whose properties have been experimentally validated.

Novelty: We propose a novel control framework that leverages our concept of pseudo-attractors and reinforcement learning to efficiently navigate BN state transitions. Since finding optimal control strategies is generally an NP-hard problem, our approach enhances the computational feasibility of identifying minimal target control strategies for cellular reprogramming applications.

Methods: A BN is a discrete dynamical system represented as a directed graph, where nodes correspond to genes and edges represent their interactions. Since finding attractors of large BNs is often computationally intractable, we define pseudo-attractor states as states where the BN dynamics spends a significant amount of time. To identify these states, we propose the Pseudo-Attractor States Identification Procedure (PASIP).

We define the attractor-target control problem, where the goal is to drive a BN toward one of its (pseudo-)attractor states that aligns with a specified target configuration for a subset of genes. We formulate this control problem as a Markov Decision Process and solve it using a DRL algorithm that optimises the length of control sequences while limiting the number of perturbed genes per intervention. To incorporate prior knowledge of the BN structure, we use a Graph Convolutional Network[4] as part of the artificial neural network approximator for the action-value function learned by the DRL agent.

We evaluate our method on four real-world biological networks from the literature: the bladder tumorigenesis network (35 genes)[5], the CD4+ T-lymphocyte network (188 genes)[6], the bortezomib-induced apoptosis network (67 genes)[7], and the T-leukocyte differentiation network (68 genes)[8].

Main results: We demonstrate that our DRL-based approach effectively identifies optimal or near-optimal attractor-target control strategies across various cellular reprogramming case studies. On average, the length of the control strategies found is typically within one intervention of the optimal solutions obtained by an exact algorithm (see Tab. 1). Importantly, our approach can handle larger and more complex networks than state-of-the-art exact algorithmic methods (data not shown).

Table 1: Comparison of the average number of steps required to control the network from the source state to the target configuration using GraphBDQ and an exact approach implemented in CABEAN[9]. The PASIP method correctly identifies all attractor states within the found pseudo-attractor states, with the numbers of each given in the '#Attr. states' and '#PA states' columns, respectively.

Model	Model size	#PA states	#Attr. states	#Steps (GraphBDQ)	#Steps (CABEAN)
bladder	35	34	4	1.0	1.0
t-diff	68	12	12	2.55	1.18
bortezomib	67	5	5	1.99	1.05
CD4+	188	16	6	1.16	1.03

Conclusion: The proposed framework offers a scalable and effective solution for BN control problems in the context of cellular reprogramming. By integrating graph-based models and reinforcement learning, we introduce a novel approach to solving the attractor-target control problem in large-scale BNs. Our PASIP method provides a strong alternative to traditional methods for finding BN attractor states, delivering results in a reasonable amount of time.

Acknowledgements: Funded by the National Science Centre, Poland under the OPUS call in the Weave programme, project nr 2023/51/I/ST6/02864.

References:

1. S.A. Kauffman. Metabolic stability and epigenesis in randomly constructed genetic nets. *Journal of Theoretical Biology*, 22(3):437-467, 1969.
2. G. Papagiannis and S. Moschoyiannis. Deep Reinforcement Learning for Control of Probabilistic Boolean Networks. In R.M. Benito, C. Cherifi, et al. (eds), Proc. Complex Networks & Their Applications IX, pp. 361-371. Springer, Cham, 2021.
3. A. Mizera and J. Zarzycki. Deep Reinforcement Learning for Controlled Traversing of the Attractor Landscape of Boolean Models in the Context of Cellular Reprogramming. *arXiv*. Published 20-02-2024. Accessed 18-02-2025. https://arxiv.org/abs/2402.08491.
4. T.N. Kipf and M. Welling. Semi-Supervised Classification with Graph Convolutional Networks. In Proc. 5th International Conference on Learning Representations (ICLR 2017), OpenReview.net, 2017.
5. E. Remy, S. Rebouissou, et al. A Modeling Approach to Explain Mutually Exclusive and Co-Occurring Genetic Alterations in Bladder Tumorigenesis. *Cancer Research,* 75(19):4042-4052, 2015.
6. B. Conroy, T. Herek, et al. Design, Assessment, and *in vivo* Evaluation of a Computational Model Illustrating the Role of CAV1 in $CD4^+$ T-lymphocytes. *Frontiers in Immunology*, 5:599, 2014.
7. V.L. Chudasama, M.A. Ovacik, et al. Logic-Based and Cellular Pharmacodynamic Modeling of Bortezomib Responses in U266 Human Myeloma Cells. *J Pharmacol Exp Ther.,* 354(3):448-58, 2015.
8. A. Naldi, J. Carneiro, et al. Diversity and Plasticity of Th Cell Types Predicted from Regulatory Network Modelling. *PLOS Computational Biology*, 6(9):e1000912, 2010.
9. C. Su and J. Pang. CABEAN: A software for the control of asynchronous Boolean networks. *Bioinformatics*, 37(6):879–881, 2021.

Special Symposium SE04

Modern Therapeutic Technologies in Medicine

Chair: Zbigniew Paszenda (Poland)

OP025–OP028

OP025

Strategies for Surface Coating of Implants in the Cardiovascular System

Anna TARATUTA[*1], Zbigniew PASZENDA[1], Marcin BASIAGA[1]

[1] Silesian University of Technology, Faculty of Biomedical Engineering, Zabrze, Poland

* ***Corresponding author***. *E-mail address*: anna.taratuta@polsl.pl

Keywords: Coatings, Stents, Titanium Alloys, Hemocompatibility

Motivation and Aim: The surface properties of cardiovascular implants play a key role in their biocompatibility and interaction with blood and surrounding tissues. However, standard surface treatments do not prevent the release of harmful nickel ions into the body or improve the corrosion resistance of NiTi alloy. Advanced coating techniques, particularly Atomic Layer Deposition (ALD), enable the creation of thin, uniform coatings even on implants with complex geometries, improving their functionality and safety.

Novelty: Recent studies related to implant coatings focus on developing ultrathin, bioactive layers that promote cell adhesion while minimizing thrombosis risk. This research shows the potential of thin coatings obtained by Atomic Layer Deposition Method, emphasizing the advantages of improving hemocompatibility and mechanical stability. The findings contribute to the continuous development of next-generation cardiovascular implants with optimized surface properties.

Methods: The tested material was a NiTi alloy designed for use in implants coated with different coatings at various ALD process parameters. The surface properties were analyzed using transmission electron microscopy (TEM) and scratch test was used to assess coating adhesion. Biocompatibility was evaluated through corrosion resistance tests and endothelial cell proliferation assays. Hemocompatibility was assessed by measuring platelet adhesion and coagulation activity, ensuring the coatings effectively reduce thrombogenic potential.

Main results: The ALD process parameters have a strong influence on the surface properties of the material. The obtained coatings showed good adhesion to NiTi alloys. Preliminary results indicate that thin coatings enhance endothelial cell proliferation, supporting faster healing and reducing the risk of clot formation. These improvements suggest that advanced coating strategies may lead to safer and more durable cardiovascular implants.

Conclusion: Surface modification of cardiovascular implants using advanced coating technologies presents a promising approach to improving their clinical performance. By enhancing endothelialization and reducing thrombogenicity, these coatings could help extend implant lifespan and lower the risk of postoperative complications.

Acknowledgements: The research was funded by the National Science Centre, Poland, allocated based on decision No. 2023/49/B/ST11/03301.

OP026

Modification of titanium surfaces with circular and hexagonal TiO_2 nanotubes

Katarzyna ARKUSZ[1*], Aleksandra JĘDRZEJEWSKA[1], Ewa PARADOWSKA[1,], Mieczysław JURCZYK[1]

[1] Department of Biomedical Engineering, Faculty of Engineering and Technical Sciences, University of Zielona Gora, Zielona Gora, Poland

* ***Corresponding author***. *E-mail address*: k.arkusz@iimb.uz.zgora.pl

Keywords: titanium, nanotubes, anodization, surface modification, electrochemical properties

Motivation and Aim: Titanium dioxide (TiO_2) nanotubes have gained significant attention for biosensing applications due to their high surface area and electrochemical properties. The objective of this study is to modify titanium surface with both conventional circular and novel hexagonal TiO_2 nanotubes and to comparatively evaluate their electrochemical properties to assess their potential for biosensing applications.

Novelty: While the electrochemical behavior of circular TiO_2 nanotubes has been extensively investigated, hexagonal TiO_2 nanotubes represent a novel morphological variation that may offer superior electrochemical performance. This study introduces a systematic comparison between these two nanostructures, contributing to a deeper understanding of the impact of nanotube geometry on electrochemical properties.

Methods: Titanium foil was anodized to fabricate both circular and hexagonal TiO_2 nanotubes. The electrochemical properties of these nanostructures were characterized in phosphate-buffered saline (PBS) solution using open-circuit potential (OCP) measurements, electrochemical impedance spectroscopy (EIS), and Tafel analysis. To ensure a direct and meaningful comparison, the characteristic diameter of both nanotube morphologies was maintained at 50 nm, where the diameter of the hexagonal nanotubes was defined as the circumscribed circle around their hexagonal cross-section.

Main results: Electrochemical impedance spectroscopy (EIS) measurements revealed that before thermal treatment, the impedance modulus (|Z|) at 0.1 Hz was approximately 1.2×10^4 $\Omega\cdot cm^2$, which was about 25% lower than that of circular TiO_2 nanotubes. After thermal annealing at 550°C, the impedance modulus further decreased to approximately 9.0×10^3 $\Omega\cdot cm^2$. These findings confirm that the hexagonal morphology and subsequent annealing process promote improved charge transfer properties, suggesting a clear advantage for advanced electrochemical applications where high ionic conductivity is essential..

Conclusion: The results of this study demonstrate that the modification of titanium surfaces with hexagonal TiO_2 nanotubes leads to a substantial improvement in electrochemical properties compared to circular nanotubes. After thermal treatment, further enhancement of conductivity parameters was observed. The observed improvements highlight the potential of hexagonal nanotubes for advanced electrochemical applications, particularly where high ionic conductivity is critical. Further research should focus on optimizing the fabrication parameters and exploring functionalization strategies to fully exploit their potential in engineering and sensor technologies.

OP027

Analysis of the Possibility of Using the UR10e Cobot in Neurological Treatment

Sławomir SUCHOŃ[1,*], Wojciech WOLAŃSKI[1], Robert MICHNIK[1], Michał BURKACKI[1], Miłosz CHRZAN[1], Hanna ZADOŃ[1], Piotr SZAFLIK[1], Justyna SZEFLER-DERELA[2], Dagmara WASIUK-ZOWADA[2]

1 Department of Biomechatronics, Faculty of Biomedical Engineering, Silesian University of Technology, 41-800 Zabrze, Poland

2 Department of Physiotherapy, Faculty of Health Sciences in Katowice, Medical University of Silesia, 40-754 Katowice, Poland

* ***Corresponding author***. *E-mail address*: ssuchon@polsl.pl

Keywords: rehabilitation; cobot UR10e; kinematic; Noraxon; proprioception neuromuscular facilitation

Motivation and Aim: Due to the increasing number of people requiring rehabilitation and an aging society, the need to streamline, improve, and increase the availability of rehabilitation has been identified. In the present study, research was conducted to evaluate the feasibility of adapting an industrial-grade cobot to assist in the rehabilitation process.

Novelty: This study is among the first to compare the kinematics of movements performed by a physiotherapist with those replicated by a UR10 cobot in neurological rehabilitation of lower leg.

Methods: The study included four measurement series, which consisted of ten repetitions of Proprioception Neuromuscular Facilitation (PNF) movements. The first two series were performed with the assistance of a physiotherapist, the next two with the support of the Cobot UR10e. The lower limb movement was analyzed using the Noraxon Ultium Motion system using inertial sensors (IMU). The study analyzed the following parameters: hip flexion and abduction angles; knee flexion and rotation angles; ankle dorsiflexion angle; and motion cycle..

Main results: Based on the results, it can be seen that the cobot reproduces physiotherapeutic movements more precisely and with greater repeatability. The cobot reproduced the movements in the hip and knee joints very well with exception of the hip abduction and ankle dorsiflexion movements, where a weak similarity was obtained.

Conclusion: From the analysis, it can be concluded that with proper adaptation, the robot could be used in the rehabilitation process.

Acknowledgements: This research was conducted with support from the Silesian University of Technology and the Medical University of Silesia

OP028

Mental workload and the task allocation for collaborative robot systems with an Industry 5.0 human-centered perspective - an experimental study

Anita POLLAK[1], Sławomir SUCHOŃ[2], Miłosz CHRZAN[2], Michał BURKACKI[2], Marek PLES[2] Patrycja ROMANISZYN-KANIA[2] i Małgorzata KOZUSZNIK[3]

1 University of Silesia in Katowice, Katowice, Poland

2 Silesian University of Technology, Zabrze, Poland

3 Ghent University, Gent, Belgium

* ***Corresponding author***: slawomir.suchon@polsl.pl

Keywords: cobot, mental workload, fatigue, safety, human-centred perspective

Motivation and Aim: Despite the increasing use of robots in industry, assembly and manufacturing processes in small and medium-sized enterprises are still performed manually [1]. Integrating cobots (collaborative robot - is specifically designed to work safely alongside humans in a shared workspace). with manual assembly combines human dexterity and perceptual abilities with the precision and strength of robots [2]. In repetitive tasks, unlike humans, robots do not experience fatigue or fluctuations in work performance [3]. Their implementation reduces physical strain and lowers the risk of injuries, which are significant factors contributing to decreased productivity and absenteeism [4]. This study focused on designing human-robot interactions that enhance job satisfaction and performance. It examined the relationship between mental workload and task allocation and considered the role of feedback on safety and work outcomes.

Novelty: Efforts are ongoing to identify the human requirements and expectations that are essential for effective collaboration and stable employment in this field [5]. It is crucial to understand which support systems enhance job satisfaction and performance when working with robots. To the authors' knowledge, the impact of positive and negative feedback (such as approval versus disapproval, critique) in human-robot collaboration has not yet been studied.

Methods: The experiment followed a 2 (feedback type: positive vs. negative; between-subjects) × 4 (measurement time points; within-subjects) mixed-design. 53 participants were randomly assigned to one of the feedback conditions. The UR10e cobot was equipped with an RG2 OnRobot gripper, enabling precise gripping of boxes and their handoff to participants. The cobot was positioned in front of a rack containing the boxes designated for the study. During each cycle, the robot delivered six boxes. Participants completed four task blocks with the robot. After each block, a 20-second feedback session was provided. First, the participant received the box from the cobot. Then, they assembled the components inside the box according to a detailed pattern provided on an instruction sheet inside. These components consisted of LEGO bricks, simulating parts of a printed circuit board. After completing the assembly, the participant evaluated the quality of their work by comparing the placement and color of the components

against a reference circuit board. Finally, they placed the completed product back into the box and handed it over to the experimenter.

Task completion time was measured from the moment the robot handed over the box to the participant until its return to the experimenter. Electrodermal activity (EDA), heart rate (HR), and heart rate variability (HRV) were recorded using the Empatica 4 device. Single-item scales were used to assess the intensity of stress, tension, fatigue, and happiness before and after working with the robot. After the study, participants provided information on their experienced pleasure and boredom during the experiment.

Main results: Lack of prior experience working with a robot contributed to perceived stress and tension before the experiment while simultaneously evoking happiness due to the novelty of using the cobot. The task allocation used in the study reduced negative emotions and increased happiness. The highest HRV values were observed in the second block of the experiment. The type of feedback provided influenced participants' behavior. Participants who received approval for their work were less likely to modify their task execution strategy, which leading to longer task duration. In contrast, negative feedback shortened the time required to complete the task but also reduced enjoyment and increased boredom experienced during the work with cobot.

Conclusion: The study shows that a lack of prior experience with a cobot triggered mixed emotions: participants reported stress and tension before the interaction, but also happiness due to the novelty of the situation. This highlights the need to address both stress-inducing and motivational factors when introducing cobots.The task allocation used in the study reduced negative emotions and increased positive affect over time, suggesting that structured task design can facilitate emotional adaptation in human–robot collaboration. HRV data showed lower physiological arousal in the second phase of the experiment, indicating growing comfort and task familiarity. This supports the role of adaptive task progression in reducing stress. Cobot feedback significantly shaped participant behavior. Positive feedback enhanced satisfaction but reduced behavioral flexibility, resulting in longer task durations. Negative feedback shortened completion time but lowered enjoyment and increased boredom. These findings reflect a trade-off between affective experience and efficiency, depending on feedback type. Overall, the results point to the importance of feedback strategies that balance performance and emotional well-being. In small and medium-sized enterprises, where employees may lack prior technological exposure, carefully designed onboarding and supportive communication may foster sustainable engagement and effective collaboration with cobots.

References:

[1] Petzoldt C, Harms M, Freitag M. Review of task allocation for human-robot collaboration in assembly. Int J Comput Integr Manuf. 2023;36(11):1675-1715. doi:10.1080/0951192X.2023.2204467

[2] Fast-Berglund Å, Palmkvist F, Nyqvist P, Ekered S, Åkerman M. Evaluating cobots for final assembly. Procedia CIRP. 2016;44:175-180. doi:10.1016/j.procir.2016.02.114

[3] Bauer W, Bender M, Braun M, Rally P, Scholtz O. Lightweight robots in manual assembly – best to start simply! Examining companies' initial experiences with lightweight robots. Fraunhofer Publica; 2016. Available at: http://publica.fraunhofer.de/dokumente/N-415111.html

[4] Makrini IE, Merckaert K, De Winter J, Lefebre D, Vanderborght B. Task allocation for improved ergonomics in human-robot collaborative assembly. Interact Stud Soc Behav Commun Biol Artif Syst. 2019;20(1):102-133. doi:10.1075/is.18018.mak

[5] Sonal G, Mohammad Israrul H, Ganesh S. Human skills in the era of Industry 4.0 in the Indian automotive industry. *Abhigyan.* 2024;42(2):123-144.

PLENARY LECTURE 3

PL3

European Medical Device CE Mark – Current Challenges and Future Opportunities

Dr. Bassil Akra (Germany)

Dr. Bassil Akra is CEO and President of AKRA TEAM in Germany (GmbH) and the USA (Inc), a globally acting consultancy company. Dr. Akra was the Vice President of Strategic Business Development at the Global Medical Health Services of TÜV SÜD Product Service GmbH. He has vast experience in leadership, business management, research, development, quality management, and regulatory approval of medical devices, combination devices, and ATMP Products. Dr. Akra played an essential role during the implementation of the medical device regulation in Europe. He was also involved in the drafting of several European guidance documents (e.g. MEDDEV, MDCG, etc.) and International Standards. He spent the last years of his career at TÜV SÜD training and educating various stakeholders on EU Legislations. Dr. Akra is also member of the Board of the EU Association TEAM PRRC. He is also member of the MDR EY Survey Advisory Group.

CEO, AKRA TEAM GmbH

Special Symposium SE05
Diverse Biomaterials, Unified Impact: Biomedical Progress Driven by Innovation
Chairs:
Elżbieta Pamuła (Poland), Patrycja Domalik-Pyzik (Poland)
KL01, OP029–OP032

KL01

Lipid nanoparticles as carriers for antibacterial peptides

Katarzyna RECZYŃSKA-KOLMAN

Department of Biomaterials and Composites, Faculty of Materials Science and Ceramics, AGH University of Krakow, al. Mickiewicza 30, 30-059 Kraków, Poland

E-mail: kmr@agh.edu.pl

Keywords: lipid nanoparticles, antibacterial peptides, nisin, LL-37, wound healing, pulmonary delivery

Motivation and Aim: Conventional treatment of bacterial infections is based on the systemic administration of antibiotics (oral or intravenous). However, due to growing bacterial resistance to antibiotics, novel antibacterial therapies are being investigated extensively.

Novelty: Antibacterial peptides (ABPs) are cationic molecules consisting of 12-45 amino acids that can hamper bacterial proliferation as effectively as antibiotics, whereby bacteria are not able to develop resistance for ABPs. ABPs are prone to inactivation by various proteolytic enzymes present in the human body. Thus, the aim of this study was to fabricate lipid nanoparticles as carriers of ABPs, protecting them from degradation and allowing their direct delivery to infected sites, particularly infected wounds and respiratory tract.

Methods: Solid lipid nanoparticles were fabricated using the oil-in-water emulsification/solvent evaporation method. In brief, lipids were dissolved in organic solvent and homogenized with an internal aqueous phase containing selected APBs (bacitracin, nisin, or LL-37). As obtained primary emulsion was then poured into external aqueous phase containing surfactant and emulsified using ultrasound probe. After solvent evaporation, the nanoparticles were purified via centrifugation and repeated rinsing with Milli-Q water or diafiltration method, and freeze-dried. Physicochemical properties of the nanoparticles were evaluated using different methods, including atomic force microscopy (AFM), dynamic light scattering (DLS), zeta potential measurements; APBs encapsulation efficacy was also assessed. Antibacterial activity of the nanoparticles against both Gram+ and Gram- bacteria was determined. Cytotoxicity of the nanoparticles was assessed *in vitro* using either fibroblasts (L929) or lung epithelial cells (BEAS-2B, Calu-3).

Main results: The properties of the nanoparticles varied depending on the type of lipid. The nanoparticles based on saturated fatty acid – stearic acid were significantly larger than the nanoparticles based on wax – cetyl palmitate (average diameters of approximately 340 nm and 40 nm, respectively). APBs encapsulation efficacy (EE) was related to the type of lipid used, and the properties of ABP itself. Highly water soluble bacitracin (BCT) was poorly loaded into the nanoparticles (EE = 15%), while less

soluble peptide LL-37 was successfully encapsulated in stearic acid nanoparticles (EE = 71%), but not as effectively in cetyl palmitate nanoparticles (EE = 34%) [1]. The least water-soluble peptide, nisin, achieved the highest EE = 82% in stearic acid [2].

Nisin-loaded stearic acid-based nanoparticles (NP_NSN) were spherical with an average particle size of around 300 nm and were cytocompatible with L929 fibroblasts for up to a concentration of 500 μg/ml. The nanoparticles were later embedded in hydrogel wound dressings based on gellan gum (GG) and a mixture of gellan gum and sodium alginate (GG/Alg). GG and GG/Alg sponges containing either free nisin (GG+NSN and GG/Alg+NSN) or nisin-loaded nanoparticles (GG+NP_NSN and GG/Alg+NP_NSN) were highly porous with a high swelling capacity (swelling ratio above 2000%). The most effective antimicrobial activity against Gram-positive *Streptococcus pyogenes* was observed for GG+NP_NSN, whereas in GG/Alg it was decreased by interactions between NSN and Alg leading to NSN retention within the hydrogel matrix. All materials, except GG/Alg+NP_NSN, were cytocompatible with L929 fibroblasts and did not cause an observable delay in wound healing. The materials developed are promising for wound healing application and the treatment of bacterial infections in the wounds.

Since cetyl palmitate-based nanoparticles were significantly smaller, with average diameters below 50 nm, they were suitable for direct pulmonary delivery via nebulization. Nanoparticles fabricated using different lipid to LL-37 ratios, were spherical with median diameters of 35 – 42 nm, with a maximal LL-37 loading of 6.1%. Unloaded nanoparticles were negatively charged (-15.5 mV), while those loaded with LL-37 were neutral or positively charged (the more LL-37 encapsulated, the more positive charge of the nanoparticles). Increased zeta potential allowed more effective adsorption of mucins on the surface of nanoparticles, leading to enhanced penetration through artificial mucus. Unloaded nanoparticles were non-cytotoxic towards lung epithelial cells (BEAS-2B), on the contrary to LL-37 alone (LD_{50}: 157 μg/ml). Encapsulation of LL-37 protected the cells from the negative impact of the peptide. In the presence of the nanoparticles and LL-37, the cells were able to maintain their barrier properties in the air-liquid interface model (Calu-3). LL-37 as well as unloaded and LL-37 loaded nanoparticles, prevented the formation of *Pseudomonas aeruginosa* biofilm and were able to disrupt existing early biofilm. The dose of LL-37 required to decrease biofilm viability by 50% was lower in the case of loaded nanoparticles, than for LL-37 alone (LD_{50}: 103 μg/ml and 310 μg/ml, respectively). The developed nanoparticles exhibited suitable properties for inhalation, the ability to migrate through mucus, cytocompatibility with lung epithelial cells, and antibiofilm properties against *P. aeruginosa*.

Conclusion: This study proved that solid lipid nanoparticles are suitable carriers for ABPs, however, the selection of lipid and APBs must be done carefully to ensure successful encapsulation of peptides. Depending on the properties of the nanoparticles, they can be used in different applications, including antibacterial wound healing dressings and pulmonary delivery via nebulization.

Acknowledgments: The study was supported by Polish National Science Centre (project no. 2018/29/N/ST5/01543) and by the Program ”Excellence Initiative – Research University” for the AGH University of Krakow.

References:

1. Reczyńska-Kolman K, Ochońska D, Brzychczy-Włoch M, Pamuła E. Stearic acid-based nanoparticles loaded with antibacterial peptides – Bacitracin and LL-37: Selection of manufacturing parameters, cytocompatibility, and antibacterial efficacy. *International Journal of Pharmaceutics*. 2024;667:124876.
2. Reczyńska-Kolman K, Hartman K, Kwiecień K, Brzychczy-Włoch M, Pamuła E. Composites based on gellan gum, alginate and nisin-enriched lipid nanoparticles for the treatment of infected wounds. *International Journal of Molecular Sciences*. 2021;23(1):321.

OP029

Biomedical Potential of the Methanolic Leaf Extract of Verbesina persicifolia: Antimicrobial Properties and Applications in Wound Healing

Carlos Alberto LÓPEZ-ROSAS[1], Seojin HAN[2 ŧ], Margarita V. SAAVEDRA VÉLEZ[1], José Rafael ALANIS GÓMEZ[2], Fabiola HERNÁNDEZ-ROSAS[2,3]

1 Facultad de Química Farmacéutica Biológica, Universidad Veracruzana, 91090, Xalapa-Enríquez, Veracruz, México

2 Escuela de Ingeniería Biomédica, Universidad Anáhuac Querétaro, 76246 Zibatá, Querétaro, México

3Centro de Investigación, Universidad Anáhuac Querétaro, 76246 Zibatá, Querétaro, México.

ŧThe authors contributed equally to this work

Correspondence: fabiola.hernandezro@anahuac.mx

Abstract. Extracts from the leaves of plants of the genus Verbesina have shown promising biomedical potential, especially for their antimicrobial and anti- inflammatory properties and their application in wound healing. In this study, we analyzed the biological properties of the methanolic extract of Verbesina persicifolia using the minimum inhibitory concentration (MIC) assay to determine its antimicrobial activity against various pathogenic bacteria. In addition, cell viability was evaluated using the Alamar Blue assay to determine the effect of plant extracts on bacterial viability and the cytotoxicity of the extracts in murine fibroblasts in culture. The results demonstrated significant antimicrobial activity, making the extract a potential candidate for the development of new antimicrobial agents. Furthermore, the non-toxic effects on fibroblasts highlight its potential to promote wound healing, suggesting that Verbesina persicifolia could serve as a natural alternative for therapeutic applications in wound management.

Keywords: Verbesina persicifolia, methanolic extract, antimicrobial properties, cytotoxicity, medicinal plants

OP030

Synergy between antibiotics and α-linolenic acid as an promising cure for biofilm bacterial infections

Konrad KWIECIEŃ[1*], Karolina KNAP[1], Dorota OCHOŃSKA[2], Katarzyna RECZYŃSKA-KOLMAN[1], Monika BRZYCHCZY-WŁOCH[2], Elżbieta PAMUŁA[1]

1 Faculty of Materials Science and Ceramics, Department of Biomaterials and Composites, AGH University of Krakow, Al. Mickiewicza 30, Kraków, 30-059, Poland

2 Faculty of Medicine, Chair of Microbiology, Department of Molecular Medical Microbiology, Jagiellonian University Medical College, ul. Św. Anny 12, Kraków, 31-121, Poland

* ***Corresponding author***. *E-mail address*: kkwiecien@agh.edu.pl

Keywords: Synergy, antibiotics, biofilm, *Staphylococcus aureus*

Motivation and Aim: *Staphylococcus aureus* is a common pathogen responsible for various infections, often forming biofilm which decreases the efficacy of antimicrobial treatment leading to permanent colonization and significantly enhanced risk of developing antibiotic resistance. Biofilm formation involves extracellular polymeric substances (EPS), acting as a protective barrier. A promising strategy for combating biofilm-associated infections involves quorum sensing inhibitors (QSIs), which disrupt bacterial communication and virulence[1,2]. Among the potential QSIs, linolenic acid (LNA), a natural compound, has demonstrated antimicrobial activity against *S. aureus*, primarily by disrupting cell membranes, and also enhanced the activity of tobramycin against *Pseudomonas aeruginosa*[3,4]. Our study evaluated the antibacterial effects of gentamicin (GEN), tobramycin (TOB), azithromycin (AZM), and LNA on *S. aureus* in planktonic and early biofilm states. It assessed LNA's role in biofilm inhibition and its synergistic effects with antibiotics[5].

Novelty: The novelty of this study lies in its investigation of the synergistic effects of linolenic acid (LNA) with antibiotics (gentamicin, tobramycin, and azithromycin) against *S. aureus* in both planktonic and early biofilm states. While LNA has been recognized for its antimicrobial properties, its impact on biofilm inhibition in combination with antibiotics remains underexplored. By evaluating the potential of LNA as a quorum sensing inhibitor (QSI) and its role in enhancing bacterial susceptibility to antibiotics, the study provides new insights into alternative strategies for combating biofilm-related infections and overcoming antibiotic resistance.

Methods: The study examined *S. aureus* (ATCC 25923), cultured on Mueller-Hinton agar. Susceptibility testing was performed using the E-test for GEN, TOB, and AZM. Antibiotics and LNA were dissolved according to standard protocols and UV-disinfected. Minimum inhibitory concentrations (MICs) and minimum bactericidal concentrations (MBCs) were determined using broth microdilution and plating methods. Biofilm inhibition (MBIC) was assessed with a resazurin-based metabolic assay (AlamarBlue), while biofilm mass reduction was evaluated using a crystal violet assay (CV). Synergistic effects between antibiotics and LNA were 57nalysed via a checkerboard assay. Statistical analysis was performed using one-way ANOVA with Tukey's post hoc test, with significance set at $p < 0.0001$.

Main results: The MIC values of antibiotics against *S. aureus* ATCC 25923 were determined using E-tests and EUCAST guidelines. E-test results showed MICs of 0.125 μg/ml (GEN), 0.38 μg/ml (TOB), and 0.19 μg/ml (AZM), while EUCAST values were 0.125 μg/ml (GEN, TOB) and 0.5 μg/ml (AZM). MBCs were 1 μg/ml (AZM, GEN) and 0.5 μg/ml (TOB). LNA's MIC was not determined due to turbidity, but its MBC was 1024 μg/ml.

For GEN and LNA, synergy was observed in six combinations allowing GEN dose reductions of 4 to 32 times while maintaining effectiveness. For TOB and LNA, synergy was found in five combinations enabling similar dose reductions. AZM and LNA showed synergy in two combinations, reducing AZM dose fourfold. Biofilm viability at MBIC90 remained comparable across synergistic treatments.

Conclusion: LNA has the potential to prevent *S. aureus* biofilm formation as a QSI and affects planktonic bacteria, though only at high concentrations. Combining antibiotics with LNA enhances their effectiveness, reducing the required dose due to their synergistic effect. This strategy holds promise for treating *S. aureus* infections and combating antibiotic resistance in biofilms. However, further testing on various reference and clinical strains is needed to confirm its efficacy.

Acknowledgements: This study was supported by the National Science Centre, Poland (project no 2019/35/B/ST5/01103) and by the Program „Excellence initiative – research university" for the AGH University of Krakow, grant ID: 9786. The purchase of the equipment used in this study has been supported by a grant from the Priority Research Area Qlife under the Strategic Programme Excellence Initiative at Jagiellonian University.

References:

1. da Silva RAG, Afonina I, Kline KA. Eradicating biofilm infections: an update on current and prospective approaches. *Current Opinion in Microbiology*. 2021;63:117-125.

2. Idrees M, Sawant S, Karodia N, Rahman A. Staphylococcus aureus Biofilm: Morphology, Genetics, Pathogenesis and Treatment Strategies. *International Journal of Environmental Research and Public Health*. 2021;18(14):7602.

3. Chanda W, Joseph TP, Padhiar AA, et al. Combined effect of linolenic acid and tobramycin on Pseudomonas aeruginosa biofilm formation and quorum sensing. *Experimental and Therapeutic Medicine*. 2017;14(5):4328-4338.

4. Kusumah D, Wakui M, Murakami M, Xie X, Yukihito K, Maeda I. Linoleic acid, α-linolenic acid, and monolinolenins as antibacterial substances in the heat-processed soybean fermented with Rhizopus oligosporus. *Bioscience, Biotechnology, and Biochemistry*. 2020;84(6):1285-1290.

5. Knap K, Kwiecień K, Ochońska D, Reczyńska-Kolman K, Pamuła E, Brzychczy-Włoch M. Synergistic effect of antibiotics, α-linolenic acid and solvent type against Staphylococcus aureus biofilm formation. *Pharmacol Rep*. 2024;76(6):1456-1469.

OP031

Silver and Copper Nanoparticles Combined with Alginates for Ovarian Cancer Theranostics

Patrycja DOMALIK-PYZIK[1*]

1 AGH University of Krakow, Faculty of Materials Science and Ceramics, Department of Biomaterials and Composites, Krakow, Poland

* ***Corresponding author***. *E-mail address*: pdomalik@agh.edu.pl

Keywords: silver nanoparticles, copper nanoparticles, theranostics, ovarian cancer, SERS

Motivation and Aim: Ovarian cancer remains one of the most lethal gynecological malignancies due to late-stage diagnosis and resistance to platin therapy developed with time. Hence, there is an urgent need for novel strategies that combine early detection with effective treatment. Surface-enhanced Raman spectroscopy (SERS) allows for highly sensitive molecular detection, but it requires optimized nanomaterials. The study aimed to design, fabricate, and characterize systems based on silver and copper nanoparticles (NPs) combined with alginate hydrogels for theranostic applications in ovarian cancer.

Novelty: Multifunctional hybrid system that combines early cancer detection with targeted therapy, addressing key challenges in ovarian cancer management.

Methods: Hollow alginate capsules were decorated with silver or copper nanoparticles. Prepared systems were evaluated in terms of physicochemical properties. Also, initial biological characterization was performed.

Main results: SEM analysis confirmed successful decoration of hollow alginate capsules with silver and copper nanoparticles. Quantitative microstructural analysis of silver alginate particles indicated that the hydrogel capsules had a mean diameter of 1.11 ± 0.26 μm, and the average size of Ag NPs was below 100 nm. Raman spectroscopy demonstrated enhancement in signal intensity for silver and copper modified capsules.

Conclusion: The designed nanoparticles have the potential to enhance SERS detection of ovarian cancer biomarkers. The alginate hydrogel acts as a biocompatible carrier of carboplatin. The whole systems presents a promising solution for theranostics of ovarian cancer.

Acknowledgements: This study was funded by the National Science Centre in Poland under the project „Theranostic nanoplatforms for therapy and diagnostics of ovarian cancer - preliminary studies”, no 2024/08/X/ST11/01187.

OP032

PEDOT:PSS Composite Integration with PDMS Substrate for Flexible Bioelectronics Applications

Natalia ZALEWSKA[1], Izabela LEWANDOWSKA[1], Karolina CYSEWSKA[1*]

1 Faculty of Electronics, Telecommunications and Informatics, Advanced Materials Centre, Gdańsk University of Technology, Poland

* ***Corresponding author***. *E-mail address*: karolina.cysewska@pg.edu.pl

Keywords: flexible electronics, PEDOT:PSS, sensors, neural electrodes

Motivation and Aim: The increasing demand for flexible and biocompatible electronic materials has generated significant interest in conductive polymers, especially poly(3,4-ethylenedioxythiophene):polystyrene sulfonate (PEDOT:PSS)[1]. While PEDOT:PSS alone exhibits poor adhesion to elastic substrates such as polydimethylsiloxane (PDMS), incorporating silane crosslinkers and adhesion enhancers enables the formation of stable composites. Unlike traditional metallic conductive layers, which suffer from mechanical mismatch and cracking on soft substrates, PEDOT:PSS-based composites offer a flexible and biocompatible alternative for biomedical applications. However, the synthesis of such composites involves trade-offs, as increasing the crosslinking density or using stronger crosslinkers can improve stability and mechanical integrity but may concurrently diminish the conductivity and overall biocompatibility of the final layer. These limitations pose challenges for their biomedical applications, including neural interfaces, sensors, and wearable devices. This research is driven by the need to identify the optimal formulation to enhance the functional performance of PEDOT:PSS-based composites for biomedical uses.

Novelty: This study investigates the use of various silane crosslinkers and solvents to enhance the stability, conductivity, and biocompatibility of PEDOT:PSS films on a flexible PDMS substrate, specifically targeting neural electrode applications. A significant innovation is the introduction of (3-mercaptopropyl)trimethoxysilane (MPTMS) crosslinker as an alternative to the commonly employed (3-glycidyloxypropyl)trimethoxysilane (GPTMS)[2] to improve biocompatibility. Furthermore, this research systematically examines the role of solvents in boosting conductivity while assessing their effects on the adhesion and biocompatibility of the composite. By evaluating the impact of silane crosslinkers and their concentrations on adhesion to PDMS, this study offers new insights into optimizing PEDOT:PSS composites for cutting-edge flexible bioelectronic devices.

Methods: The composites were prepared by dissolving ethylene glycol (EG), dodecylbenzenesulfonic acid (DBSA), and a silane crosslinker (MPTMS or GPTMS) in a 1.3% PEDOT:PSS solution. The resulting liquid composite was then drop-casted onto an oxygen plasma-treated PDMS surface and subjected to an annealing process to enhance film stability. To evaluate the performance of PEDOT:PSS composites on PDMS substrates, a series of adhesion, electrical, and electrochemical tests were conducted. Adhesion strength was assessed under both dry and wet conditions to examine the effects of different silane crosslinkers and solvent concentrations on composite bonding and their stability in different environments. Electrical properties were characterized through sheet resistance measurements, providing

insights into how crosslinker type, as well as solvent selection and concentration, influence conductivity. Electrical interface parameters such as interfacial impedance, redox activity, double-layer capacitance and charge storage capacity were evaluated based on the electrochemical studies carried out under simulated body conditions.

Main results: In the investigated composite, a 1.3% PEDOT:PSS solution serves as the base, requiring the mandatory addition of dodecylbenzenesulfonic acid (DBSA) and a silane crosslinker (MPTMS or GPTMS) to induce crosslinking. While ethylene glycol (EG) addition is optional, it significantly enhances conductivity[3]. The optimal balance of adhesion and electrical performance was achieved with a 2 $wt\%_{PEDOT:PSS}$ concentration of the silane crosslinker. However, exceeding 3 $wt\%_{PEDOT:PSS}$ led to excessive shrinkage and a decline in conductivity. Notably, increasing the concentration of the EG did not compromise adhesion to the PDMS substrate. These findings provide valuable insights into how different crosslinkers and solvents influence stability, biocompatibility and electrical properties of the PEDOT:PSS composites on elastic PDMS surfaces, paving the way for the development of more tailored flexible electronics for biomedical applications.

Conclusion: This study demonstrates the potential to develop and optimize PEDOT:PSS conductive layers on elastic PDMS substrates, emphasizing their applicability in flexible bioelectronic applications. However, challenges related to long-term stability and biocompatibility must be addressed to fully enable their use in biomedical devices such as implantable sensors, neural interfaces, and wearable electronics. The findings provide valuable insights into optimizing material composition to enhance adhesion, conductivity, and electrochemical performance. By refining crosslinking strategies and solvent selection, this research lays the groundwork for the design of flexible bioelectronic devices with custom electrochemical parameters, improved durability and functionality in physiological environments.

Acknowledgements: The work was supported by National Science Centre (NCN), Poland: Sonata grant based on the decision 2021/43/D/ST7/01362.

References:

[1] Tourchi Moghadam MT, Cysewska K. Electrical Interface Parameters of PEDOT:PSS: Effect of Electrodeposition Charge Evaluated Under Body Conditions for Neural Electrode Applications. J Electrochem Soc. 2024;171(7):075502. doi:10.1149/1945-7111/ad6074

[2] Tang K, Miao W, Guo S. Crosslinked PEDOT:PSS Organic Electrochemical Transistors on Interdigitated Electrodes with Improved Stability. ACS Appl Polym Mater. 2021;3(3):1436-1444. doi:10.1021/acsapm.0c01292

[3] Khodagholy D, Curto VF, Fraser KJ, et al. Organic electrochemical transistor incorporating an ionogel as a solid state electrolyte for lactate sensing. J Mater Chem. 2012;22(10):4440-4443. doi:10.1039/c2jm15716k

Special Symposium SE06a
IFMBE, Biomedical Engineering Education: Challenges, Digital Health Technology and Learning Methodology
Chairs:
Nicolas Pallikarakis (Greece), Martha Zequera (Colombia)
KL02, IP01, OP033–OP035

KL02

Biomedical Engineering Education – Challenges, Digital Health Technology and Learning Methodology

Krunoslav JURČIĆ[1], Tamara ĆORIĆ[1], Nicolas PALLIKARAKIS[2], Martha ZEQUERA DIAZ[3], Ratko MAGJAREVIĆ[1]

1 University of Zagreb Faculty of Electrical Engineering and Computing Zagreb, Croatia

2 University of Patras, INBIT - Institute of Biomedical Technology, Patras, Greece

3 Pontificia Universidad Javeriana, Bogota, Colombia

Digital health technologies have significantly improved processes in healthcare, enabled personalized patient treatment and care and also increased prevention in medicine. Extended usage of digital technologies was accelerated by appearance of COVID-19 pandemics. During the pandemic, interest for fast and reliable engineering solutions like digital health records, telemedicine, integration of wearables and small medical devices in the service of public health and preventing the spread of the epidemic emphasized the role of biomedical engineers in health care worldwide. Numerous challenges arose also in biomedical engineering education during and after the coronavirus pandemic: for a long time, the students were separated from their teachers and fellow students, from medical instrumentation and laboratories and from clinical practice. Willingly and not-willingly, distance learning methodologies were implemented in BME teaching, which resulted in an increased number of on-line BME courses. The other change arising recently is extensive use of big data analytics and artificial intelligence in health care not only in research but also in clinical settings. In this paper, we want to tackle those issues and discuss the solutions educators found. An overview of biomedical engineering programs in sample countries from Europe is presented as a part of the survey conducted by the International Federation for Medical and Biological Engineering (IFMBE). The survey is intended to support future generations of BME engineers and explore new demands for their employability.

OP033

Introduction of artificial intelligence, big data and data science in biomedical engineering and biomedical informatics

Lenka LHOTSKA

Czech Technical University in Prague, Czech Republic

Development in interdisciplinary areas has become faster in recent decades and encompasses many fields. Specialists in individual fields naturally regard their own area for the most important one. This brings quite frequently tension to discussions about new curricula development or restructuring existing curricula. keep in mind different levels of education in Bachelor, Master and PhD study. Here we can mention the metaphor of the cone we use in discussion about the ratio between deep and broad knowledge in a discipline. Bachelor study should lead to broader fundament that allows for successive deepening in Master study even when changing the topic. Master study goes deeper but still keeps certain breadth. And finally the PhD study focuses on a certain specialization. It is expected that a PhD student is able to orientate himself/herself in neighbouring disciplines and identify mutual relations with the specialization.

At the Czech Technical University in Prague there were developed during last two decades several interdisciplinary study programs. The author has personal experience with the design of curricula in biomedical engineering and biomedical informatics. The Faculty of Biomedical Engineering (FBME) and Faculty of Electrical Engineering (FEE) chose different approaches to design of structure of courses in the study programs that will be put into contrast in the presentation. The main difference is due to the character of the Biomedical Technology (Bc.) and Biomedical Engineering (MSc.) study programs at FBME. They have accreditation from the Ministry of Health Care as health care study programes giving the graduates label of health care professionals. That is definitely an advantage. However, the main disadvantage is that the curricula are rather fixed with limited space for innovation or even introduction of new courses. At FBME there is the study program Biomedical and Clinical Informatics which is more flexible and offers up-to-date courses on AI, big data, ethical and regulatory issues of AI in medicine etc. Similar philosophy for development of study programs was chosen at FEE where study program Medical Electronics and Bioinformatics is offered. It has several specializations: Bioinformatics, Medical Electronics, Image Processing, and Signal Processing. In all of them, there is enough space for optional courses, which opens the possibility to introduce up-to-date topics in the education.

OP034

Convergence in Science and Education: Enhancing Biomedical Research and Teaching Through Digital Innovations

Anna KORZYNSKA

Laboratory of Analysis and Processing of Microscopic Image, Nalecz Institute of Biocybernetics and Biomedical Engineering Polish Academy of Sciences, Ks. Trojdena 4, 02-109 Warsaw, Poland

* ***Corresponding author***. *E-mail address*: akorzynska@ibib.waw.pl

Keywords: Education for Biomedical Engineering, Digital technologists in education, Convergence in sciences, AI – support, distance learning

Motivation and Aim: Digital technologies such as learning and teaching software with the personalized speed of learning, virtual reality tools, AI-driven educational platforms stimulate the need for the development and employment of new methodologies for education. It imposes the need for special skills by educators and researchers to encourage students and young researchers to lead investigations more effectively. These methods are particularly convenient for the education of young researchers giving them a wide overview of sciences. It concerns biomedical engineering (BE) as well as other science domains. AI-driven education also implicates new ethical problems.

Novelty: Convergence approach in sciences emphasizes the importance of matching balance and synergy between theory and practice, specifically in the interdisciplinary fields such as biomedical engineering, biomedicine and bioengineering. It involves collaboration across various disciplines and technologies, and crossing of ideas to tackle complex challenges, generate new knowledge, and develop innovative solutions in healthcare and medicine.

Methods: The analysis focused on the educational methods employed at the Nalecz Institute of Biocybernetics and Biomedical Engineering, Polish Academy of Sciences (IBBE PAS), which aim to provide students with a comprehensive understanding of various science domains and their applications. Our educational methods are based on the concept of convergence in the research.

In our experience, interdisciplinary collaboration among biomedical engineering researchers, technologists, and end-user groups — such as physicians, nurses, and other healthcare professionals — enhances outcomes that enable to gain unique and deep insights into BE. This develops multidirectional understanding of research problems and encourage students to interactions, e.g. asking questions, discussions, brain storming while solving problems, team working and compromising.

At IBBE PAS, workshops for young researchers and Ph.D. students provided by clinicians in healthcare units are organized. For instance, during a workshop at the Gdansk Medical University clinics, young researchers have the opportunity to observe daily hospital practices and identify needs for improvements in diagnostics and treatment processes. Other Ph.D. students involved in the European Maria Skłodowska-Curie Doctoral Network project they do internships in project partner institutions, that are universities, collaborating vendors and healthcare units to observe and participate in their daily activities and discuss scientific,

practical/technological problem and clinical needs. Our teaching approach is based on interdisciplinary collaboration, personal observation of students, and building relationships with members of end-user groups. Direct communication with physicians is also facilitated through joint projects. For example, close cooperation between scientists from IBBE PAN and the Medical University of Białystok resulted in a joint doctoral dissertation written by a doctor employed at IBBE PAN who graduated from the Doctoral School of the Medical University of Białystok. Based on his research concerning digital pathology, it was proved that results of AI based tool prepared in IBBE PAS for histopathological evaluation of ISCL patients tissue samples compared to classical methods used by pathologists (morphometry and microscopic inspection), reveal prognostic and predictive potential.

IBBE PAS introduces to Ph.D. students not only AI-based software useful for scientists but mainly the ethical problems related to AI utilization, such AI hallucination and confabulations, publishing papers based on analysis done by AI tools, and text generated using LLM tools. Moreover, the knowledge about plagiarism is introduced.

As digital ethics, data privacy is important in biomedical engineering, Ph.D. students and young researchers practice a data management system, which is a technology used to organize and store various types of data with special regards to anonymized data from hospitals.

Personalized, interactive, and engaging learning methods are employed in both online and blended learning environments, under the condition that educators receive ongoing training and practice in new educational methodology.

Main results:

In general, recommended strategies for transforming research and education highlight the institutional support in gathering necessary infrastructure and software, as well as providing continuous professional development for educators and researchers through appropriate courses on new tools and teaching methodologies. This increase in the teachers' and supervisors' skills indicates that the curriculum is continuously redesigned to incorporate the process of student and researcher education in not only knowledge of AI-based tools but also their ethical considerations. At IBBE PAS, we focus on the selection open-minded and creative candidates for Ph.D. study. Than the convergence approach in education through involvement of Ph.D. students into ongoing projects as well as end-users communications is successfully applied, resulting in well-educated young researchers, ready for work in interdisciplinary teams.

Conclusion: Digital technologies are more than just tools; they are powerful catalysts for transforming education and research. To successfully adapt to these technologies, a strategic approach, a focus on adopting innovation, and continuous learning of both educators and researchers are necessary. The experience of IBIB PAN shows that Ph.D. students who are reluctant to acquire new skills and methodologies do not achieve significant scientific results within a given time, being unable to meet the interdisciplinary requirements in biomedical engineering. Therefore, the key factor is related to requirements and proper examination of candidates for Ph.D. study.

Acknowledgements: This work was supported IBBE PAS according to didactic duty for graduate and PhD students.

OP035

BME Education in Portugal: insights from the highest-ranked programs and the role of ANEEB

Margarida Maria LIMA, Martim Melo ROCHA

ANEEB - National Association of Biomedical Engineering Students, Portugal

* ***Corresponding author***. *E-mail address*: margaridaflima23@gmail.com ; martimrocha26@gmail.com

Keywords: Biomedical Engineering Education, ANEEB, Digital Health, Portugal, Curriculum Comparison

Motivation and Aim: Recent developments in digital health and the experience of the COVID-19 pandemic have brought both new opportunities and challenges to Biomedical Engineering (BME) education. As digital health technologies become mainstream in clinical settings, the alignment of academic curricula with these trends is essential. This paper introduces ANEEB, the National Association of Biomedical Engineering Students in Portugal, and presents a comparative overview of the country's top BME programs according to Shanghai Ranking[1] and EduRank[2]. The goal is to understand how well these programs are preparing students for the digital health era and to highlight ANEEB's role as a unifying and empowering platform that promotes the academic and professional development of Biomedical Engineering students across Portugal.

Novelty: Portugal offers a unique academic ecosystem where BME is taught at several high-ranking institutions (Aveiro, Porto, Coimbra, Lisbon, and Braga). Each program shares common foundations but presents distinct curricular approaches, particularly regarding the integration of digital health topics. This student-led analysis highlights those differences by identifying concrete innovations: the University of Coimbra, NOVA University of Lisbon and University of Lisbon (*Instituto Superior Técnico - IST*) offer structured units on Machine Learning in Medicine and Health Information Systems as optional and mandatory modules in the MSc in Biomedical Engineering; the University of Minho places a strong emphasis on medical device development, fostering technical and design skills relevant to digital health technologies; and the University of Porto promotes interdisciplinary projects involving informatics, signal processing, and wearable technologies. These varied strategies demonstrate how digital health is being progressively incorporated into BME curricula and serve as potential models for broader adoption. The analysis also explores how ANEEB acts as a collaborative platform between students, academics, and industry.

Methods: Curricular information will be gathered from official academic sources, including program websites and course plans. Interviews with students, professors, and professionals from Portuguese companies in the biomedical sector will be conducted to better understand the perception and incorporation of digital health topics in education.

Main results: The analysis revealed both overlapping and diverging trends among programs. Core subjects such as medical imaging, biomechanics, instrumentation, and signal processing are consistently present, while approaches to digital health and medical informatics differ across

institutions. A recurring challenge is the limited clinical exposure and hands-on experience provided to students. Some universities are addressing this by promoting internships or clinical placements. ANEEB also plays an active role by maintaining an internship platform that promotes opportunities from companies and research centers, while fostering connections between students, professionals, and industry stakeholders in the biomedical engineering field. Additionally, there is increasing discussion on solutions such as partnerships with healthcare institutions and the integration of simulation-based learning, aiming to strengthen practical training and bridge the gap between academic knowledge and professional practice. Findings from the national study "O Futuro da Engenharia Biomédica na nossa geração" [3], conducted by ANEEB, reinforce this need: students call for updated curricula, more practical components, greater access to internships, and increased exposure to market realities through alumni talks and career-oriented workshops. These insights highlight the urgency of aligning academic training with employers' expectations. Beyond organizing academic events and managing an internship platform, ANEEB also seeks to influence educational development by meeting with course coordinators at the beginning of each mandate to share feedback and results from national studies. Reports such as [3] consolidate student perspectives and aim to guide institutions in improving curricular relevance and professional preparedness.

Table 1: Overview of selected curricular components across top-ranked BME programs in Portugal (Aveiro, Coimbra, Lisbon - IST, Minho, and Porto).

University	Biomechanics	Bioinformatics	Biomaterials and Tissue Engineering	Medical Imaging	Biomedical instrumentation	Clinical Engineering
Aveiro	✗	✓	✓	✓	✓	✗
Coimbra	✗	✓	✗	✓	✓	✗
Lisbon (IST)	✓	✗	✓	✓	✓	✓
Minho	✓	✓	✓	✓	✓	✓
Porto	✓	✓	✓	✓	✓	✓

Conclusion: Portugal presents a diverse and evolving BME education landscape. Student-led coordination through ANEEB fosters collaboration, mobility, and knowledge-sharing across students from the various institutions.

Acknowledgements: We thank IFMBE for the invitation to contribute to the NBC 2025 SP10 session and for supporting student involvement in the global biomedical engineering community.

References:

[1] ShanghaiRanking's Global Ranking of Academic Subjects. Accessed April 13, 2025. https://www.shanghairanking.com/rankings/gras/2024/RS0208

[2] Portugal's best Biomedical Engineering universities [Rankings]. Accessed April 13, 2025. https://edurank.org/engineering/bioengineering/pt/

[3] "O Futuro da Engenharia Biomédica na nossa geração". Accessed April 26, 2025. https://drive.google.com/drive/folders/1Yk1UpFpNFzRULVugKrJDldBIRKIAbHZE

Oral Session OS05

Imaging Modalities and Medical Image Fusion

Chairs: Janis Spigulis (Latvia), Piotr Sawosz (Poland)

KL03, OP036–OP039

KL03

Development of Connectome MRI Techniques and Their Applications on Neurological Disorders

Li-Wei KUO[1*]

1 Institute of Biomedical Engineering and Nanomedicine, National Health Research Institutes, Miaoli County, Taiwan

* ***Corresponding author***. *E-mail address*: lwkuo@nhri.edu.tw

Keywords: Magnetic Resonance Imaging, Brain Connectome, Neurological Disorders

Motivation and Aim: During the past decade, mapping complex structural and functional networks in living human brain using non-invasive neuroimaging technologies has been widely developed and employed on a variety of cognitive and clinical neuroscience researches. Among all modern neuroimaging technologies, magnetic resonance imaging (MRI) has been considered as one of the most reliable and reproducible neuroimaging modalities for exploring the complex brain networks with superior spatial and temporal resolutions. The connectome MRI techniques may be capable of mapping the structural and functional alterations in the brains with neurological disorders. In these studies, we aimed to develop, optimize and utilize the connectome MRI techniques and demonstrate their potential use in applications on neurological disorders.

Novelty: The potential use of connectome MRI techniques in applications on neurological disorders was successfully demonstrated.

Methods: In our previous studies, we have developed a variety of connectome MRI techniques for mapping the brain structural and functional connectome in both *ex vivo* samples and *in vivo* applications. Additionally, we have also incorporated these connectome MRI techniques with multiple analysis approaches, including region-of-interest analysis, connectivity analysis and network analysis.

Main results: In this talk, I will introduce how we employ these connectome MRI techniques and analysis methods to map the brain connectivity and investigate the complex brain networks in healthy and diseased conditions. The pre-clinical and clinical applications on neurological disorders, such as stroke[1], dementia[2-4] and tremor[5], will be introduced and discussed.

Conclusion: We have developed connectome MRI techniques and the analysis approaches. The potential use of these techniques has been shown and demonstrated in the applications with neurological disorders.

Acknowledgements: We thank the National Health Research Institutes and the National Science and Technology Council in Taiwan for the funding supports.

References:

[1] Farrher, E.; Chiang, C. W.; Cho, K. H.; Grinberg, F.; Buschbeck, R. P.; Chen, M. J.; Wu, K. J.; Wang, Y.; Huang, S. M.; Abbas, Z.; et al. Spatiotemporal characterisation of ischaemic lesions in transient stroke animal models using diffusion free water elimination and mapping MRI with echo time dependence. Neuroimage 2021, 244, 118605. DOI: 10.1016/j.neuroimage.2021.118605.

[2] Tu, M. C.; Huang, S. M.; Hsu, Y. H.; Yang, J. J.; Lin, C. Y.; Kuo, L. W. Discriminating subcortical ischemic vascular disease and Alzheimer's disease by diffusion kurtosis imaging in segregated thalamic regions. Hum Brain Mapp 2021, 42 (7), 2018-2031. DOI: 10.1002/hbm.25342.

[3] Altunkaya, S.; Huang, S. M.; Hsu, Y. H.; Yang, J. J.; Lin, C. Y.; Kuo, L. W.; Tu, M. C. Dissociable Functional Brain Networks Associated With Apathy in Subcortical Ischemic Vascular Disease and Alzheimer's Disease. Front Aging Neurosci 2021, 13, 717037. DOI: 10.3389/fnagi.2021.717037.

[4] Hsu, Y. H.; Huang, S. M.; Lin, S. Y.; Yang, J. J.; Tu, M. C.; Kuo, L. W. Prospective Memory and Default Mode Network Functional Connectivity in Normal and Pathological Aging. J Alzheimers Dis 2022, 86 (2), 753-762. DOI: 10.3233/JAD-215293.

[5] Huang, S. M.; Ong, C. T.; Huang, Y. C.; Chen, N. H.; Leung, T. K.; Shen, C. Y.; Kuo, L. W. Resting-State Network Analysis Reveals Altered Functional Brain Connectivity in Essential Tremor. Brain Connect 2024, 14 (7), 382-390. DOI: 10.1089/brain.2024.0004.

OP036

Image subtraction versus data subtraction to create the dose calibration curve of radiochromic film for onsite dosimetry of CT dose

Toshizo KATSUDA[1*], Nobuyoshi TANKI[1], Rumi GOTANDA[2], Tatsuhiro GOTANDA[2], Tadao KUWANO[3], Kouichi YABUNAKA[4]

[1] Medical Radiation Technology, Shizuoka College of Medical Care Science, 2000, Hirakuchi, Hamana-ku, Hamamatsu-city, Shizuoka, 434-0041, Japan

[2] Faculty of Health Science and Technology, Kawasaki University of Medical Welfare, Okayama, 702-0193, Japan

[3] Department of Radiology, Osaka Center for Cancer and Cardiovascular Diseases Prevention, 1-6-107 Morinomiya, Jyoto-ku, Osaka, 536-8588, Japan

[4] Department of Ultrasound, Ono Memorial Hospital, 1-26-10 Minamihorie, Nishiku, Osaka, 550-0015, Japan

* ***Corresponding author. E-mail address: tkatsudajp@yahoo.co.jp***

Keywords: Calibration curve, onsite, fitting curve, radiochromic film, image subtraction, data subtraction.

Motivation and Aim:

Radiochromic films are used for dose measurement in diagnostic radiology. Especially, dose measurement for computed tomography (CT) [1)]. Also, quality control and quality assurance such as half-value layer measurement [2)].

To perform onsite creation of density-dose calibration curve for the radiochromic film dosimetry and quality assurance of low dose range to measure doses of CT. It is needed to improve convenience and immediacy. We evaluated the difference between the two subtraction processing methods for correction of nonuniformity to reduce the uncertainty of the radiochromic film.

The purpose of this study is to develop a method for creating a calibration curve, which is a preliminary step in measuring actual CT dose. The fitting curve is a method for easily visually comparing the non-uniformity corrections made by the two types of subtraction methods, and is a method for standardizing the relationship between film density and X-ray dose of CTs.

Novelty: The two differential methods for correcting for non-uniformity in the reaction layer of radiochromic film have not been compared.

Methods: Two RGB images were obtained, and the red channel was extracted from each image. One scanned image was irradiated with 385 nm UV-A rays to express the inhomogeneity of the active layer, and the other scanned image was X-rays were irradiated on the film. Two subtraction methods of a radiochromic film (Gafchromic XR-QA2) were compared, one was the image subtraction method that performed pixel by pixel subtraction between two images, and the other was the data subtraction method that performed subtraction of the mean pixel value in the regions of interest between two images. We evaluated and compared the shape of

the calibration curves and fitting curves created by the method for 16-bit images with a flatbed scanner and 8-bit images with a mobile scanner.

Main results: The calibration curve and fitting curve by the data subtraction method were more smoothly obtained than those by the image subtraction method using both 16-bit (Fig.1) and 8-bit images. Especially, uncertainty was reduced at very low dose ranges, such as less than 200 mGy.

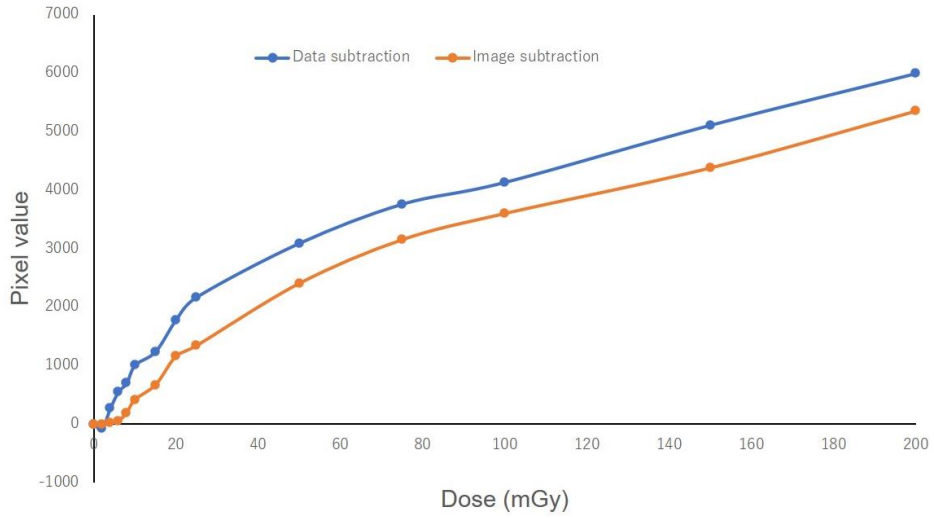

Fig. 1.

Conclusion: The data subtraction method was superior in reducing uncertainty at the extremely low dose range of the calibration curve. Moreover, convenience and immediacy can be improved by creating a calibration curve using 8-bit images with a mobile scanner.

References:

[1] Katsuda, T., Gotanda, R., Gotanda, T., Kuwano, T., Tanki, N., Yabunaka, K. Development of a three-dimensional dose evaluation method for computed tomography. J Appl Clin Med Phys. 24(2): e13897, 1-9 (2023). DOI: 10.1002/acm2.13897

[2] Gotanda, T., Katsuda, T., Gotanda, R., Kuwano, K., Akagawa, T., Tanki, N., Tabuchi, A., Shimono, T., Kawaji, Y., and Takeda, Y. Effective energy measurement using radiochromic film: application of a mobile scanner. Polish Journal of Medical Physics and Engineering; 22, 85-92 (2016). DOI: 10.1515/pjmpe-2016-0015

OP037

Speckle Contrast Optical Spectroscopy (SCOS) for monitoring of blood flow dynamics in process of diabetic wound healing supported with cold plasma therapy

Sara FATHOLLAH*, Stanislaw WOJTKIEWICZ, Wiktoria Kasprzak, Piotr SAWOSZ

Nalecz Institute of Biocybernetics and Biomedical Engineering, Polish Academy of Sciences, Trojdena 4, 02-109 Warsaw, Poland

* ***Corresponding author***. *E-mail address*: sfathollah@ibib.waw.pl

Keywords: SCOS, Blood Flow, Cold Plasma, Diabetic Wound

Motivation and Aim: The goal of this research is to develop the Speckle Contrast Optical Spectroscopy (SCOS) for non-invasive, contactless measurement of blood flow dynamics in diabetic wounds following plasma therapy. Diabetic foot ulcers (DFUs) are one of the most common complications of diabetes. Despite being largely preventable, they remain a major cause of mortality and reduced quality of life in diabetic patients [1, 2]. These patients often suffer from circulatory issues caused by atherosclerosis and microvascular dysfunction, leading to a lifetime risk of developing DFUs of approximately 15–25% [3-5]. Therefore, monitoring of blood flow dynamics in such wounds is crucial for understanding the healing process and optimizing treatments such as cold plasma therapy (CAP).

Novelty: We propose the use of SCOS [6,7] for assessing blood flow dynamics and microcirculation parameters in diabetic wounds undergoing cold plasma therapy (CAP). Unlike traditional histological methods, which are invasive and may disrupt wound healing, SCOS provides a non-invasive, contactless, real-time alternative, potentially with deeper tissue penetration than existing optical imaging techniques such as Hyperspectral Imaging (HSI) [8], Laser Doppler Imaging (LDI) [9], and similar to the Laser Speckle Imaging (LSI) [10]. This study aims to provide knowledge on oxygenation and perfusion changes during the plasma therapy on wound healing.

Methods: The SCOS system works by analyzing laser speckle patterns generated by the movement of red blood cells, providing real-time perfusion metrics. The system as presented in fig. 1 includes a high-speed, high resolution camera Chronos 2.1-HD (Kron Technologies, Canada) with a 1:1 macro lens, long coherence length diode laser (CrystaLaser, USA) with light attenuator, a medical-grade computer for data processing, all attached to an adjustable positioning arm and medical-grade cart with emergency power supply. The system allows to analyze speckle contrast in spatial (single pixel images size of a speckle) and temporal (few kHz camera frame rate) dimensions. The system is developed for a clinical measurement campaign involving 100 patients suffering from diabetic wounds, randomly assigned to two groups: Control Group (receiving standard diabetic wound care) and Plasma Group (receiving plasma therapy in addition to standard care). SCOS will analyze speckle contrast to quantify changes in blood perfusion over the healing process. Multiple regions of the wound will be imaged, including periphery and central zones, to evaluate regional perfusion variations.

Main results: The Speckle Contrast Optical Spectroscopy (SCOS) system has been successfully developed and optimized for contact-less monitoring of blood flow dynamics in diabetic wounds. Initial tests of the SCOS system demonstrated its ability to capture high-resolution speckle patterns, allowing for quantification of blood flow. Ongoing further refinements are in place to adjust the imaging system for the clinical phase.

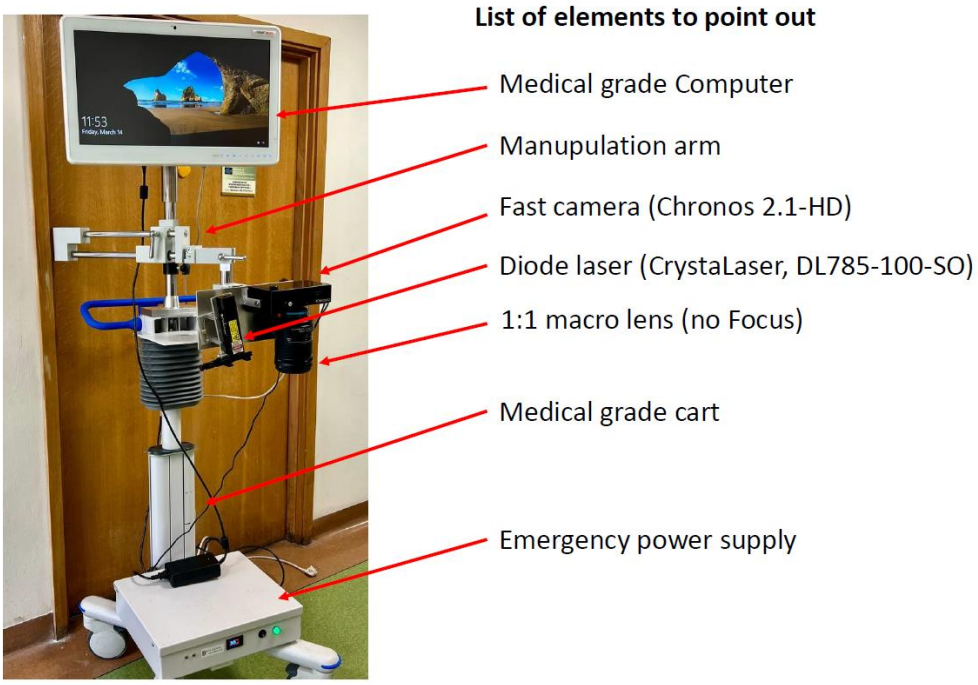

Figure 1. Optical system for SCOS

Conclusion: By advancing the capabilities of SCOS for contactless speckle observation in the special and temporal dimensions, this research will show the microvascular behavior in pathological conditions undergoing cold plasma supported wound healing process.

References:

[1] P. Valensi, I. Girod, F. Baron, T. Moreau-Defarges, and P. Guillon, "Quality of life and clinical correlates in patients with diabetic foot ulcers," Diabetes & metabolism, vol. 31, no. 3, pp. 263-271, 2005.
[2] N. C. Schaper et al., "Practical guidelines on the prevention and management of diabetes-related foot disease (IWGDF 2023 update)," Diabetes/Metabolism Research and Reviews, vol. 40, no. 3, p. e3657, 2024.
[3] W. Tang, Y. Zhao, Z. Cheng, J. Xu, Y. Zhang, and X. Liu, "Risk factors for diabetic foot ulcers: a systematic review and meta-analysis," Vascular, vol. 32, no. 3, pp. 661-669, 2024.
[4] S. A. Bus et al., "Guidelines on the prevention of foot ulcers in persons with diabetes (IWGDF 2023 update)," Diabetes/metabolism research and reviews, vol. 40, no. 3, p. e3651, 2024.
[5] C. f. D. Control and Prevention, "National diabetes fact sheet: national estimates and general information on diabetes and prediabetes in the United States, 2011," Atlanta, GA: US department of health and human services, centers for disease control and prevention, vol. 201, no. 1, pp. 2568-2569, 2011.
[6] K. Murali and H. M. Varma, "Multi-speckle diffuse correlation spectroscopy to measure cerebral blood flow," Biomedical optics express, vol. 11, no. 11, pp. 6699-6709, 2020.
[7] T. Dragojević et al., "Compact, multi-exposure speckle contrast optical spectroscopy (SCOS) device for measuring deep tissue blood flow," Biomedical optics express, vol. 9, no. 1, pp. 322-334, 2017.
[8] M. A. Calin, T. Coman, S. V. Parasca, N. Bercaru, R. Savastru, and D. Manea, "Hyperspectral imaging-based wound analysis using mixture-tuned matched filtering classification method," Journal of biomedical optics, vol. 20, no. 4, pp. 046004-046004, 2015.
[9] H. Hoeksema et al., "Accuracy of early burn depth assessment by laser Doppler imaging on different days post burn," Burns, vol. 35, no. 1, pp. 36-45, 2009.
[10] D. A. Boas and A. K. Dunn, "Laser speckle contrast imaging in biomedical optics," Journal of biomedical optics, vol. 15, no. 1, pp. 011109-011109-12, 2010.

OP038

Visible-NIR multispectral imaging of whole-body human skin

Janis SPIGULIS*, Edgars KVIESIS-KIPGE, Uldis RUBINS, Ilze IRBE, Marta SKRASTINA, Jekaterina TIHOMIROVA

Biophotonics Laboratory, Institute of Atomic Physics and Spectroscopy, Faculty of Science and Technology, University of Latvia, Riga, Latvia

* ***Corresponding author***. *E-mail address*: janis.spigulis@lu.lv

Keywords: Spectral line imaging, Whole-body dermoscopy, Multi-laser illumination

Motivation and Aim: To ensure efficient whole-body dermoscopy diagnostics and early screening of skin cancers, a laser multi-spectral-line imaging technique covering visible and near infrared (NIR) ranges has been developed.

Novelty: To our best knowledge, this is the first attempt to obtain and analyze a set of four spectral line images (three visible and one near-infrared), related to large areas or the whole body of human skin. Visible spectral images ensure sorting of malformations as pigmented or vascular, as well as mapping the distribution of three main skin chromophores over the malformations [1, 2]. In addition, the NIR images help to identify deeper (dermal) skin tumors, including malignant melanomas [3].

Methods: The snapshot multi-spectral-line imaging method [4] is applied in this study. Four laser spectral line (450 nm, 520 nm, 638 nm and 850 nm) illumination source is a side-emitting optical fiber spiral, Y-coupled to 3W RGB and 4W NIR lasers via SMA connectors – see Figure 1. High-resolution 61 Mpx Sony camera with removed infrared cut-off filter is placed within the illuminating fiber spiral. The camera-illuminator platform can be moved vertically up and down at typical heights 0.5 m and 1.5 m, while the patient changes his/her body position relatively to the camera, to enable imaging of any part of his/her skin with suspicious malformation(s). To avoid ambient illumination, the system and the patient are covered by a light-shielding tent. The system is operated from outside by means of Wi-Fi. Spectral line images are extracted from the camera digital image data set as described in [2].

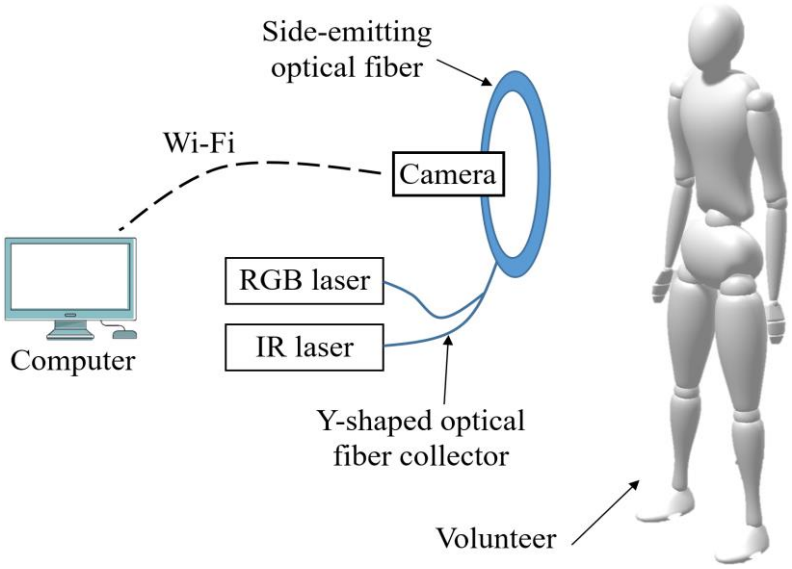

Figure 1. Schematic of the laser multispectral imaging setup.

Main results: Sets of four spectral line images (B - 450 nm, G - 520 nm, R – 638 nm, IR – 850 nm) of volunteer skin fragments comprising malformations in grayscale have been collected, the spectral image ratios were calculated, as well. In most cases, the number of malformations detected in the visible spectral images exceeded that detected in the 850 nm image, or all malformations disappeared at 850 nm; the image contrast always decreased with wavelength. A few malformations detected at all wavelengths most probably comprised higher chromophore concentration and/or were deeper penetrated in skin. At this stage of the project, only sets of distant skin spectral images of "relatively healthy" volunteers have been collected, without any clinical specifications of the imaged malformations. Clinical measurements with involvement of dermatologists are planned in March-August 2025, so by the time of conference enough oncology patient data would be available to discuss in more detail the potential advantages/disadvantages of this technology for skin cancer detection and early screening.

Conclusion: A new spectral imaging technology for distant assessment of skin tumors has been proposed, implemented and tested on volunteers. The set of combined 450/520/638/850 nm spectral images show a potential for advanced quantitative clinical diagnostics in dermatology.

Acknowledgements: This study is funded by the Recovery and Resilience Facility project "Internal and External Consolidation of the University of Latvia" (No.5.2.1.1.i.0/2/24/I/CFLA/007).

References:

1. J.Spigulis, U.Rubins, E.Kviesis-Kipge, I.Saknite, I.Oshina, E.Vasilisina, "Triple spectral line imaging of whole-body human skin: equipment, image processing, and clinical data", *Sensors* **24**, 7348 (2024). DOI:10.3390/s24227348.
2. J.Spigulis, I.Oshina, A.Berzina, A.Bykov, "Smartphone snapshot mapping of skin chromophores under triple-wavelength laser illumination", *J.Biomed.Opt.,* **22**(9), 091508 (2017). DOI: 10.1117/1.JBO.22.9.091508.
3. I.Kuzmina, I.Diebele, L.Valeine, D.Jakovels, A.Kempele, J.Kapostinsh, J.Spigulis, "Multi-spectral imaging analysis of pigmented and vascular skin lesions: results of a clinical trial", *Proc. SPIE,* **7883**, 788312 (2011). https://doi.org/10.1117/12.887207.
4. J.Spigulis. *Ultra-narrowband multispectral imaging. Techniques and applications*, 97 p. CRC Press / Taylor & Francis, Boca Raton, USA (2024). ISBN: 1032757299.

OP039

The Development of a Quadrature Surface Coil for Rat Brain MRI

Cheng-Che WU[1], Ming-Jye CHEN[2], Po-Hsun HE[2], Hsuan-Han CHIANG[2], Chang-Hoon CHOI[3], Li-Wei KUO[2], Kuan-Hung CHO[1*]

1 Department of Electronic Engineering, National United University, Miaoli, Taiwan

2 Institute of Biomedical Engineering and Nanomedicine, National Health Research Institutes, Miaoli, Taiwan

3 Institute of Neuroscience and Medicine - 4, Forschungszentrum Juelich, Juelich, Germany

* ***Corresponding author***. *E-mail address*: khcho@nuu.edu.tw

Keywords: MRI, quadrature, surface coil

Motivation and Aim: Phased array coils are widely used in modern clinical MRI systems due to their high signal-to-noise ratio (SNR), broad coverage, and adaptability to various geometries. However, conventional phased array coils require multiple RF receiver channels, limiting their accessibility. This study presents the development of an array-liked quadrature surface coil comprising two loop coils and a 90° hybrid coupler to enhance SNR in rat brain imaging. Experimental results demonstrate that the proposed coil increases SNR by over 50% in the cortex region compared to two conventional surface coils. This design facilitates multi-channel coil operation without additional RF receiver hardware, making it a cost-effective solution.

Novelty: This study develops a quadrature surface coil that enhances SNR in rat brain MRI without multiple RF receiver channels. This approach significantly boosts SNR, especially in the cortex and the middle brain regions, while maintaining comparable image coverage. By eliminating the need for additional receiver channels, this design offers a cost-effective and practical solution for laboratories with limited resources.

Methods: The quadrature coil coil consists of two overlapping surface coils (2 × 1.5 cm each), designed to minimize mutual interference and maintain signal integrity. A 90° hybrid coupler ensures equal power distribution and a phase shift, enabling in-phase signal summation to improve reception sensitivity. All MR measurements were performed using an high-strength gradient integrated 3 T whole-body MRI platform. To evaluate coil performance, T2-weighted images (T2WI) of rat brains were acquired with the following parameters: repetition time = 4000 ms, echo time = 68 ms, resolution = 0.117 × 0.117 mm², and slice thickness = 1 mm. For comparison, T2WI were also acquired using a single-loop surface coil (35 mm diameter, Doty Scientific, Columbia, SC, USA) and a homemade curved surface coil with an elliptical geometry (major axis: 28 mm, minor axis: 22 mm).

Main results: Figures 1a-c illustrate the proposed quadrature surface coil, single-loop surface coil, and curved surface coil, respectively. Figures 1d-f present SNR maps of the same slice position for each coil configuration. The proposed coil significantly improves SNR in the upper brain region while maintaining comparable imaging coverage. The SNR results from six different regions of interest (ROIs) are presented in Table 1 for quantitative comparison. In

regions close to the coil (ROIs 1–3), the quadrature surface coil demonstrated a significantly higher SNR, ranging from 89.4% to 120.5% greater than the single-loop surface coil and 45.8% to 58.8% higher than the curved surface coil. In the middle brain regions (ROIs 4 and 5), the quadrature surface coil outperformed the single-loop surface coil by 34.4% to 41.7% and exceeded the curved surface coil by 11.7% to 21.2%. In the deep brain region (ROI 6), the SNR achieved by the quadrature surface coil was similar to that of the curved surface coil, with both being lower than the single-loop surface coil.

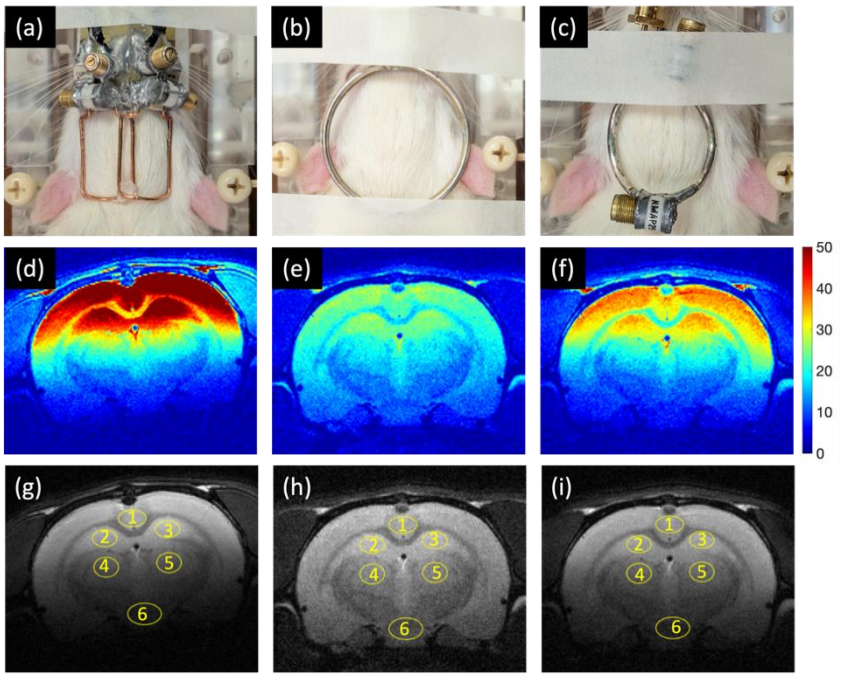

Figure 1: Comparison of T2-weighted images (T2WI) acquired using three different coil configurations. The top row displays (a) the quadrature surface coil, (b) the single-loop surface coil, and (c) the curved surface coil. The middle row presents SNR maps obtained with (d) the quadrature surface coil, (e) the single-loop surface coil, and (f) the curved surface coil. The bottom row shows the corresponding T2WI images acquired using (g) the quadrature surface coil, (h) the single-loop surface coil, and (i) the curved surface coil.

Table 1: The SNR results from 6 ROIs (Figrue 1g – i)

	ROI 1	ROI 2	ROI 3	ROI 4	ROI 5	ROI 6	S.D.
Proposed coil	50.5	48.1	54.0	24.6	24.8	8.1	373.2
Single-loop surface coil	22.9	25.4	24.9	18.3	17.5	10.2	284.2
Curved surface coil	31.8	33.0	34.9	20.3	22.2	7.5	328.9

Conclusion: This study successfully developed an array-liked quadrature surface coil optimized for rat brain imaging. The proposed coil significantly enhances SNR while maintaining comparable imaging coverage. Furthermore, the design eliminates the need for multi-channel scanning hardware, offering a practical and cost-effective alternative for resource-limited laboratories.

Acknowledgements: This work was supported by the National Science and Technology Council, Taiwan [NSTC 113-2221-E-239-004] and the National Health Research Institutes, Miaoli, Taiwan [NHRI-BN-114-PP-06].

Oral Session OS06
Biomaterials
Chair: Yuri Dekhtyar (Latvia), Katarzyna Arkusz (Poland)
OP040–OP045

OP040

Effect of Titanium-Doped Hydroxyapatite on Biofilm Formation of Pseudomona aeruginosa

Ángel Rodrigo ORTIZ JUÁREZ[1], Jimena Mariette ROBLEDO DORANTES[1], Araceli ZAPATERO-GUTIÉRREZ[2,3], Josué GARCÍA-ÁVILA[2,4], José Rafael ALANIS-GÓMEZ[2,5], Fabiola HERNÁNDEZ-ROSAS[2,3]

1 Programa de Ingeniería Biomédica, Universidad Anáhuac Querétaro, 76246 Zibatá, Querétaro, México

2 División de Ingeniería, Universidad Anáhuac Querétaro, 76246 Zibatá, Querétaro, México

3 Centro de Investigación, Universidad Anáhuac Querétaro, 76246 Zibatá, Querétaro, México

4 Stanford University, 94305 Stanford, California, USA

5 División de Investigación y Posgrado Facultad de Ingeniería, Universidad Autónoma de Querétaro, 76140,Querétaro, México

fabiola.hernandezro@anahuac.mx

Abstract. In this study, we synthesized titanium-doped hydroxyapatite (HAP- Ti) by microwave-assisted hydrothermal method and evaluated its antibacterial activity against Pseudomonas aeruginosa. The synthesis was optimized by con- trolling parameters such as temperature, reaction time, and molar ratio of precur- sors to favor the homogeneous incorporation of titanium into the crystalline struc- ture of hydroxyapatite. Structural and morphological characterization was per- formed by X-ray diffraction (XRD) to confirm the crystalline phase and scanning electron microscopy (SEM) to analyze the morphology and particle distribution. The antibacterial activity of HAP-Ti was evaluated by minimum inhibitory con- centration (MIC) assays, cell viability assays, and biofilm inhibition in P. aeru- ginosa cultures under controlled conditions. Different concentrations of the bio- material were exposed to bacterial cultures and cell viability was determined by spectrophotometry. Biofilm inhibition was analyzed by crystal violet staining and microscopy, observing the density and distribution of adhered structures. The re- sults showed a concentration-dependent inhibition, with a significant reduction in bacterial growth and biofilm formation in the presence of HAP-Ti. These find- ings highlight the potential of HAP-Ti for biomedical applications, particularly in the development of implants and prostheses with antimicrobial properties, which could contribute to the prevention of biofilm-associated infections and im- prove the biocompatibility of medical devices. Keywords: Hydroxyapatite, Titanium doping, Antibacterial activity, Biofilm inhibition, Biomedical applications

OP041

Electro-assisted nanodiamond integration into conducting polymer as a possible drug-delivery stent platform

Karolina CYSEWSKA[1*], Anita STOPPEL[2], Muhammad SAQIB[2], Birgit PAUL[3], Julia Kristin HUFENBACH[3], Joerg OPITZ[2], Natalia BESHCHASNA[2]

1 Faculty of Electronics, Telecommunications, and Informatics, and Advanced Materials Centre, Gdansk University of Technology, ul. Narutowicza 11/12, 80-233 Gdańsk, Poland

2 Fraunhofer Institute for Ceramic Technologies and Systems IKTS, Maria-Reiche Strasse 2, 01109 Dresden, Germany

3 Leibniz Institute for Solid State and Materials Research (IFW) Dresden, Helmholtzstrasse 20, 01069 Dresden, Germany

* ***Corresponding author***. *E-mail address*: karolina.cysewska@pg.edu.pl

Keywords: Conducting polymer, Degradable metal, Electrodeposition, Nanodiamond, Smart coating

Motivation and Aim: This study addresses the persistent challenges of in-stent restenosis and thrombosis in cardiovascular stents by exploring innovative coating strategies for biodegradable Fe-30Mn-1C (FeMnC) alloys [1]. While polymer-coated drug-eluting stents have reduced restenosis rates, they have also introduced complications such as delayed endothelial healing [2]. Conducting polymers like polypyrrole (PPy) offer a promising alternative due to their drug-eluting capabilities and potential to modulate iron-based stent degradation [3]. Additionally, nanodiamonds (NDs), known for their biocompatibility and functionalization potential, present an opportunity for targeted drug delivery.

This study aims to test the hypothesis that (1) one-step electrodeposition of a PPy coating on the surface of a cast biodegradable FeMnC alloy is feasible, and (2) nanodiamonds can be successfully incorporated into the polymer matrix during this process without altering the alloy's corrosion properties.

Novelty: The main novelty of this study lies in the one-step electrodeposition of PPy coatings on biodegradable FeMnC alloys, incorporating NDs directly into the polymer matrix during the deposition process. Unlike previous studies that relied on multi-step fabrication methods or pre-functionalization of NDs before polymer integration, this approach aims to achieve a uniform, drug-eluting coating in a single step, enhancing both the biodegradation control of the alloy and the targeted drug release capabilities of the stent. Additionally, the study explores how NDs influence the corrosion properties of FeMnC, ensuring that the integration does not compromise its mechanical integrity and degradation profile.

Methods: The FeMnC stent alloy was fabricated by melting pure elemental constituents in an Al_2O_3 crucible under an argon atmosphere in an induction furnace (Balzer). Subsequently, it was cast into a copper mould to receive the Fe69Mn30C1 (in wt%; FeMnC) ingot. Cast FeMnC samples were polished with SiC abrasive papers up to 2000 grid, rinsed with ethanol, and dried in the air. Pristine NDs were chemically functionalized during three steps of oxidation, hydroxylation, and arylation processes, yielding a highly stable water-based solution with a zeta

potential of -40 mV required for successful electrodeposition process. PPy coatings were electrosynthesized in an aqueous solution containing sodium salicylate and pyrrole, with or without NDs. The synthesis parameters were optimized regarding the physico-chemical and electrochemical properties of the resulting polymer coating on FeMnC. All the electrochemical studies were conducted in a three-electrode, water-jacketed cell controlled by a potentiostat Autolab PGSTAT204 (Metrohm, Herisau, Switzerland). The working electrode was either bare FeMnC or FeMnC coated with PPy or PPy-NDs, with an exposed area of 0.11 cm^2. The reference electrode was Ag/AgCl in saturated KCl, and the counter electrode was a platinum grid (BioLogic). The measurement temperature was maintained at 37° C +/- 1 °C using a thermostat TC120-ST26 (Grant Instruments, United Kingdom). Corrosion studies were performed in simulated body fluid (SBF) prepared according to Kokubo and Takadama's composition (Na^+ - 142 mmol L^{-1}, K^+ - 5 mmol L^{-1}, Mg^{2+} - 1.5 mmol L^{-1}, Ca^{2+} - 2.5 mmol L^{-1}, Cl^- - 148.6 mmol L^{-1}, HCO_3^- - 4.2 mmol L^{-1}, HPO_4^{2-} - 1.0 mmol L^{-1}, SO_4^{2-} - 0.5 mmol L^{-1}).

Main results: This study demonstrates the successful electrodeposition of the conducting polymer PPy on the surface of an active FeMnC alloy for potential temporary implant applications. It also establishes an effective chemical functionalization procedure for pristine NDs, yielding a highly stable water-based solution. Incorporating passivating salicylate and pyrrole monomer into the deposition process facilitated the formation of PPy coatings with embedded NDs on the FeMnC surface. The resulting PPy-ND matrix can serve as an efficient drug reservoir, paving the way for advanced drug-release systems, particularly degradable metallic implants. Indeed, to validate the system for these applications, studies regarding drug incorporation, long-term stability, and influence of PPy on FeMnC corrosion mechanism should be performed in the future.

Conclusion: This work presents a novel method for electrically integrating functionalized NDs into smart conducting polymer PPy coatings on highly active FeMnC alloy surfaces for stent applications. This innovative method facilitates the development of multifunctional coatings, providing a versatile platform for advanced bio-interfaces in medical implants. The study shows the feasibility of combining conducting polymers with nanomaterials to enhance surface functionality and tackle critical challenges in implantable device technologies.

Acknowledgements: The work was supported by Gdansk University of Technology IDUB Research University Excellence Initiative nr 16/1/2022/IDUB/IV.2a/Eu.

References:

[1] B. Paul, A. Hofmann, S. Weinert, F. Frank, U. Wolff, M. Krautz, J. Edelmann, M. W. Gee, C. Reeps, and J. Hufenbach, Effect of Blasting Treatments on the Surface Topography and Cell Adhesion on Biodegradable FeMn-Based Stents Processed by Laser Powder Bed Fusion, Adv Eng Mater **24**, 2200961 (2022).

[2] T. Donisan, L. Madanat, D. V. Balanescu, A. Mertens, and S. Dixon, Drug-Eluting Stent Restenosis: Modern Approach to a Classic Challenge, Curr Cardiol Rev **19**, E030123212355 (2023).

[3] K. Cysewska, L. F. Macía, P. Jasiński, and A. Hubin, Tailoring the electrochemical degradation of iron protected with polypyrrole films for biodegradable cardiovascular stents, Electrochim Acta **245**, 327 (2017).

OP042

Oxygen-Enhanced Hybrid Systems: A New Frontier in Biomedicine

Agata LIPKO[1*], Anna Grzeczkowicz[1], Monika DRABIK[1], Angelika KWIATKOWSKA[1], Tomasz MIŁEK[2,3], Ludomira GRANICKA[1]

1 Nalecz Institute of Biocybernetics and Biomedical Engineering, Polish Academy of Sciences, Warsaw, Poland

2 Cardinal Stefan Wyszyński University, Warsaw, Poland

3 Wolski Hospital, Warsaw, Poland

* ***Corresponding author***. *E-mail address*: alipko@ibib.waw.pl

Keywords: Wound healing, Chronic wounds, Perfluorocarbons

Motivation and Aim: Chronic wounds present a significant challenge in modern medicine due to their high treatment costs and severe impact on patients' quality of life. These wounds are particularly prevalent among ageing populations and individuals with comorbidities such as diabetes and cardiovascular diseases. Oxygen plays a crucial role in key physiological processes engaged in wound healing including cell proliferation, collagen deposition, and microbial burden reduction. However, chronic wounds are often characterized by inadequate oxygen supply, leading to hypoxic conditions that impair healing. Currently applied techniques aimed at increasing wound site oxygenation such as hyperbaric oxygen therapy and sub-atmospheric pressure dressings, though relatively effective, are costly and require specialized equipment. Consequently, there is an urgent need for novel, cost-effective, and accessible therapeutic solutions to enhance wound healing while minimizing hospitalization time and treatment expenses. To address these challenges, this study explores an innovative approach involving the incorporation of perfluorocarbons into wound dressing systems.

Novelty: Perfluorocarbons (PFCs) are synthetic compounds known for their exceptional capacity to dissolve and transport gases, particularly oxygen. This unique property has led to their exploration in medical applications, including their integration into wound dressings to enhance oxygen delivery to hypoxic tissues.

Several research initiatives have demonstrated the potential of PFC-infused dressings. For example, Patil et al. [1] investigated oxygenating wound dressings based on modified methacrylamide chitosan with pentadecafluorooctanoic chains, which were capable of maintaining elevated oxygen levels for up to 48 hours. These hydrogels promoted collagen production and accelerated wound healing in experimental models. Another study introduced gel-based wound dressings incorporating lyophilized nanometric additives capable of dissolving and delivering oxygen. This additive contained perfluorodecalin-encapsulated albumin nanoparticles, and its application significantly reduced hypoxia-inducible factors while expediting wound closure in a diabetic mouse model [2]. Despite these promising developments, the commercial availability of PFC-based wound dressings remains limited. By involving layered oxygenating modification into a bandage, this study aims to provide a safe and effective wound-healing environment.

Methods: The primary objective of the study was to evaluate *in vitro* the influence of an oxygenating layer on human dermal fibroblast function. An alginate-based layer containing oxygen-releasing elements was applied to a support, with perfluorocarbons serving as the oxygenating agent. The biological response of human dermal fibroblast cells exposed to these constructs was assessed, focusing on cell function and morphology. Flow cytometry, fluorescence microscopy, and scanning electron microscopy were employed to analyze cellular characteristics.

Additionally, the effectiveness and clinical applicability of a modified dressing incorporating an oxygenating layer has been under investigation. The research is focused on patients with chronic, non-healing wounds where conventional treatments had failed or yielded suboptimal results. The study examines whether oxygenating dressings could enhance healing rates, reduce inflammation, and improve overall patient outcomes. For this purpose, a specialized bandage with an oxygenating layer was has been developed and is being applied to patients with non-healing wounds. The dressing is changed at regular intervals, and healing progress is closely monitored. The study has been ongoing with full ethical approval, ensuring patient safety and informed consent.

Main results: The applied membrane coatings adsorbed onto the patch supported the viability of human fibroblasts cultured in the presence of modified supports for 10 days. Furthermore, fluorescence microscopy revealed that cells grown in the presence of the investigated material exhibited normal morphology. The treatment outcomes using the bandage with oxygenating elements, compared to the initial wound condition following treatment with unmodified dressings, demonstrated a beneficial effect of the dressing modification. To date, out of the 8 patients enrolled in the trial, 5 have completed the study. The inclusion criterion was the presence of a chronic, non-healing wound persisting for more than 3 months despite treatment with standard dressings at a local medical center. The applied dressing design, which maintains a moist wound environment and includes an oxygenation-enhancing layer, promoted healing of chronic wounds within 4 weeks in all 5 treated patients. Complete epithelialization was achieved in 2 patients, while the remaining wounds progressed to at least the granulation stage, with the majority demonstrating the formation of resistant epidermis.

Conclusion: The investigated platform, incorporating an oxygenating factor, supports the growth and morphology of human fibroblasts and can be recommended as a component of a dressing system. Furthermore, by evaluating the clinical efficacy of this novel therapeutic approach, the study aims to provide valuable insights into chronic wound management, potentially paving the way for more accessible and effective treatments that can be further implemented in medical practice.

References:

[1] Patil PS, Fountas-Davis N, Huang H, et al. Fluorinated methacrylamide chitosan hydrogels enhance collagen synthesis in wound healing through increased oxygen availability. *Acta Biomater*.2016;36:164-74. doi:10.1016/j.actbio.2016.03.022

[2] Yang Z, Chen H, Yang P, et al. Nano-oxygenated hydrogels for locally and permeably hypoxia relieving to heal chronic wounds. *Biomaterials.* 2022;282:121401. doi:10.1016/j.biomaterials.2022.121401

OP043

Using Backscattered Electrons to Determine Surface Charge on Laser-Treated Titanium Alloys

Arturs ABOLINS[1], Alberta AVERSA[2], Marks GOROHOVS[3], Yuri DEKHTYAR[3], Maris DORTIŅŠ[3], Lyubomir LAZOV[4], Arturs MAMAJEVS[3], Hermanis SOROKINS3, Edmunds SPRUDZS[4]

1 Rezekne Academy of Technologies (Food processing laboratory), Pils iela 23a, Rezekne, Lat-via, *arturs.abolins@rta.lv*

2 Politecnico di Torino, Italy, Department of Applied Science and Technology, Corso Duca de-gli Abruzzi, 24, Torino, Italy, *alberta.aversa@polito.it*

3 Riga Technical University, Mechanical and Biomedical Engineering Institute, Kipsalas 6B, Riga, Latvia, *marks.gorhovs@rtu.lv, jurijs.dehtjars@rtu.lv, hermanis.sorokins@rtu.lv*

4 Rezekne Academy of Technologies, Atbrīvošanas Aleja 115, Rezekne, Latvia, *lyubomir.la-zov@rta.lv*

Abstract. Oxidized titanium alloys, such as Ti 6Al 4V, are widely used in medical implants because their biocompatibility depends on surface properties like morphology, chemistry, and electrical charge. Laser processing in atmospheric, oxygenated conditions produces a thin oxide film with an embedded electrical charge, altering these surface characteristics. Although SEM is routinely employed to assess morphology and chemistry, its potential for evaluating surface charge is underexplored. In this study, we laser processed Ti 6Al 4V samples and used SEM in backscattered electron (BSE) mode to quantify surface charging. We correlated changes in BSE signal strength with work function measurements, finding that a work function increase from approximately 4.85 to 5.00 eV—indicative of greater surface charging—was accompanied by a measurable decrease in BSE image grey levels. Measurements at 10, 15, and 20 keV revealed a significant difference between 10 and 15 keV, while at 20 keV, the effect of surface charge on electron scattering was minimal. This approach demonstrates that BSE imaging can integrate charge analysis into routine SEM evaluations of laser-pro- cessed implant surfaces. Keywords: laser processing, titanium oxide, surface charge, scanning electron microscopy.

OP044

Thermal modification of hexagonal titanium dioxide nanotubes

Aleksandra JĘDRZEJEWSKA[1*], Ewa PARADOWSKA[1], Mieczysław JURCZYK[1], Katarzyna ARKUSZ[1]

1 Department of Biomedical Engineering, Faculty of Engineering and Technical Sciences, University of Zielona Gora, Zielona Gora, Poland

* ***Corresponding author***. *E-mail address*: jedrzejewska.ale@gmail.com

Keywords: titanium nanotubes, anodization, thermal modification, annealing, properties

Motivation and Aim: The aim of this study is to investigate the effect of annealing temperature (350 °C - 550 °C) on the structural, electrochemical and mechanical properties of hexagonal titanium dioxide nanotubes (hTNTs). It is expected that the results of this research will provide a complementary study of hTNTs to expand their applications in industry and medicine, especially for implants applications.

Novelty: While extensive research has been conducted on the effects of annealing on the properties of conventional circular titanium dioxide nanotubes, the emerging morphological variant—hexagonal titanium dioxide nanotubes - offers potential enhancements in mechanical, electrochemical, and corrosion properties. This study aims to provide novel insights into the thermal stability of hTNTs, thereby expanding their potential applications and contributing to a deeper understanding of how nanotube geometry influences their properties.

Methods: First, hexagonal titanium dioxide nanotubes were prepared by sonoelectrochemical anodization for 1 h at a potential of 20 V. Anodization was carried out in a two-electrode system in an electrolyte of composition: 94% ethylene glycol, 0.3 wt.% ammonium fluoride and 0.1 wt.% disodium edetate. The samples were then thermally modified in an argon atmosphere at temperatures: 350 °C, 450 °C, and 550 °C for 3 h. Scanning electron microscopy, Raman spectroscopy, nanoindentation, and electrochemical tests (open-circuit potential (OCP), electrochemical impedance spectroscopy (EIS), Tafel analysis) in Ringer's solution were used to characterize the samples.

Main results: Annealing does not affect the diameter value of hTNTs and slightly reduces their length. At 350 °C and 450 °C there is a transformation of the amorphous phase of hTNTs into the anatase crystalline phase, and at 550 °C into the anatase-rutile crystalline phase. Annealing removes fluorine ions remaining in hTNTs after anodizing. As the annealing temperature increased, an increase in OCP, hardness and Young's modulus of hTNTs was observed, and there were also a decrease in corrosion rate and corrosion current of hTNTs. Annealing at 550 °C improves the corrosion resistance, increase the open circuit potential and improves the adhesion strength of hTNTs to titanium while maintaining high Young's modulus and ductility.

Conclusion: The results confirm that annealing, especially at 550 °C, is an effective strategy for optimizing the properties of hTNTs. This modification improves the corrosion, mechanical, structural and electrochemical properties of hTNTs. The obtained parameters of thermally modified hTNTs make this material a promising technique for modifying titanium surfaces for medical applications. Further in vivo studies are required to evaluate the biocompatibility and long-term effects of applying hTNTs to implants.

OP045

The development of $(Ca/Zn)CO_3$ microparticles loaded with bacitracin as antibacterial and osteogenic materials for bone tissue engineering

Katarzyna RECZYŃSKA-KOLMAN[1*], Dorota OCHOŃSKA[2], Monika BRZYCHCZY-WŁOCH[2], Elżbieta PAMUŁA[1*]

[1] Department of Biomaterials and Composites, Faculty of Materials Science and Ceramics, AGH University of Krakow, al. Mickiewicza 30, 30-059 Kraków, Poland

[2] Department of Molecular Medical Microbiology, Faculty of Medicine, Jagiellonian University Medical College, ul. Czysta 18, 31-121 Kraków, Poland

* Corresponding authors: Katarzyna Reczyńska-Kolman, e-mail: kmr@agh.edu.pl and Elzbieta Pamuła, e-mail: epamula@agh.edu.pl

Keywords: $(Ca/Zn)CO_3$ microparticles, bacitracin, antibacterial, osteogenic

Motivation and Aim: Calcium carbonate ($CaCO_3$) microparticles are widely used in biomedical engineering, due to their excellent biocompatibility, biodegradability and porous microstructure suitable for drug loading [1,2]. Bacitracin (BCT), a promising antibacterial agent effective against a number of Gram positive bacteria species [3], has been recently shown to enhance osteogenic differentiation of mesenchymal stem cells [4,5], making it a perfect candidate for loading into $CaCO_3$ microparticles. Our previous studies aimed at immobilization of BCT on $CaCO_3$ microparticles had not been promising, therefore this study focused on the development of $(Ca/Zn)CO_3$ carriers for BCT.

Novelty: To the best of our knowledge this is the first study on the influence of Zn^{2+} addition to $CaCO_3$ microparticles to enhance the efficacy of BCT entrapment and biological performance of such microparticles including antibacterial efficacy and osteogenic potential.

Methods: $(Ca/Zn)CO_3$ microparticles were obtained by precipitation method from equimolar Na_2CO_3 and $(Ca/Zn)Cl_2$ solutions. For fabrication of Zn-enriched microparticles, 5%, 10% or 20% vol. of $CaCl_2$ solution used for precipitation was exchanged to equimolar $ZnCl_2$ solution. The morphology, size and surface area of the microparticles were evaluated. BCT was adsorbed on the microparticles form aqueous solution. The efficacy of BCT adsorption and subsequent BCT loading were determined using modified o-phthalaldehyde-based amine detection method. BCT release and degradation of the microparticles were assessed *in vitro* using phosphate-buffered saline (PBS), followed by the evaluation of microparticle cytotoxicity and osteogenic potential using human mesenchymal stem cells (hMSC). Antibacterial activity of the microparticles was determined using Kirby-Bauer agar diffusion assay on *Staphylococcus aureus* (ATTC 25923), *Staphylococcus epidermidis* (ATCC 700296) and *Streptococcus pyogenes* (ATCC 12384).

Main results: The morphology of the microparticles was strongly dependent on the addition of Zn^{2+} to the microparticles. The microparticles containing Zn^{2+} were larger, cubic in shape with predominant calcite structure. The adsorption efficacy of BCT increased significantly upon addition of Zn^{2+} (maximal drug loading of approximately 40%) due to strong affinity of BCT to Zn^{2+}. BCT was released from the microparticles within 24 h, the degradation of Zn^{2+} containing microparticles was three times slower than in the case of non-modified $CaCO_3$ microparticles. The microparticles were cytocompatible with hMSC, except the microparticles with the highest Zn^{2+} content. The microparticles with adsorbed BCT successfully inhibited the growth of *S. aureus*, *S. epidermidis*, and *S. pyogenes.* $(Ca/Zn)CO_3$ microparticles enhanced osteogenic differentiation of hMSC, however this effect might be also attributed to the release of Zn^{2+} rather than BCT.

Conclusions: The developed $(Ca/Zn)CO_3$ microparticles with adsorbed BCT could serve as antibacterial and osteogenic materials for the treatment of bacterial infections and regeneration of bone tissue.

Acknowledgments: The study was supported by Polish National Science Centre (project no. 2018/29/N/ST5/01543) and by the Program ”Excellence Initiative – Research University” for the AGH University of Krakow.

References:

1. Fadia P, Tyagi S, Bhagat S, et al. Calcium carbonate nano-and microparticles: synthesis methods and biological applications. *3 Biotech*. 2021;11:1-30.
2. Li L, Yang Y, Lv Y, Yin P, Lei T. Porous calcite $CaCO_3$ microspheres: Preparation, characterization and release behavior as doxorubicin carrier. *Colloids and Surfaces B: Biointerfaces*. 2020;186:110720.
3. Buijs N, Vlaming HC, van Haren MJ, Martin NI. Synthetic studies with bacitracin A and preparation of analogues containing alternative zinc binding groups. *ChemBioChem*. 2022;23(24):e202200547.
4. Ao H, Long T, Zhou J, Tang T, Yue B. Immobilizing bacitracin on titanium for prophylaxis of infections and for improving osteoinductivity: An *in vivo* study. *Colloids and Surfaces B: Biointerfaces*. 2017;150:183-191.
5. Li H, Du Z, Zhang S, Long T, Yue B. Bacitracin promotes osteogenic differentiation of human bone marrow mesenchymal stem cells by stimulating the bone morphogenetic protein-2/Smad axis. *Biomedicine & Pharmacotherapy*. 2018;103:588-597.

Special Symposium SE06b
IFMBE, Biomedical Engineering Education: Challenges, Digital Health Technology and Learning Methodology
Chairs:
Nicolas Pallikarakis (Greece), Martha Zequera (Colombia)
OP046–OP048, IP02

OP046

Current Landscape of Biomedical Engineering in Spain: Academic Opportunities, Professional Applications, and Technological Innovation

Jenny Pamela HARO BONILLA[1*], María Fernanda CABRERA UMPIERREZ[1]

1 Universidad Politécnica de Madrid, ETSI Telecomunicación, Life Supporting Technologies (LifeSTech), Madrid, España

* ***Corresponding author***. *E-mail address*: jenny.haro@alumnos.upm.es

Keywords: Biomedical Engineering, higher education, medical technology, Spanish universities, job placement, healthcare innovation

Motivation and Aim: Biomedical Engineering is consolidating its role as a key discipline in the face of pressing global health challenges, including the rise of chronic, neurodegenerative, and cardiovascular diseases. By integrating knowledge from engineering, medicine, and computer science, it enables the development of innovative technologies for diagnosis, therapy, and patient care. In recent years, Spain has witnessed a notable expansion in academic offerings related to this field, reflecting both educational demand and strategic national interest. This abstract aims to provide a comprehensive overview of Biomedical Engineering education in Spain, analyzing its academic breadth, pedagogical innovation, and alignment with current and emerging healthcare system needs.

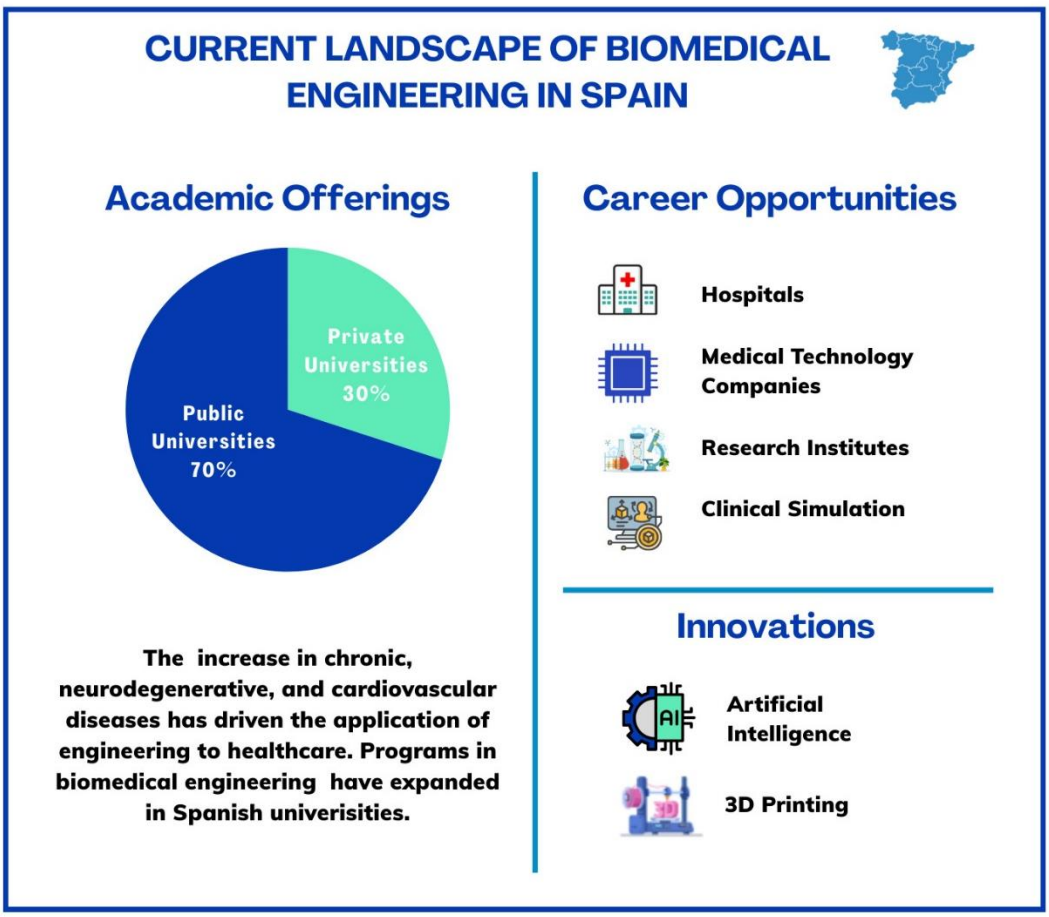

Novelty: This work offers a comparative and previously underexplored analysis of the Spanish academic landscape in Biomedical Engineering. It highlights how universities integrate emerging technologies—such as artificial intelligence, 3D printing, and telemedicine—within interdisciplinary curricula to respond to 21st-century health system needs. Additionally, it explores the connection between academic training and employability in medical technology sectors.

Methods: A qualitative descriptive analysis was conducted based on data collected from official university websites, national academic registries (e.g., RUCT), and postgraduate program repositories. Universities were included if they offered accredited undergraduate or master's degrees in Biomedical Engineering as of April 2025. Curricular mapping focused on teaching modalities (on-campus, hybrid, online), technological integration (AI, simulation, biosensors), and industry collaboration. Emphasis was placed on educational innovation and alignment with the biomedical labor market.

Main results: The analysis reveals a diverse and competitive academic ecosystem. Public universities such as Universidad Politécnica de Madrid, Universidad de Zaragoza, and Universitat Politècnica de València offer research-oriented programs with practical training in digital health, biosensors, and clinical engineering. Private institutions like Universidad de Navarra, Universidad San Pablo-CEU, and Universidad Internacional de Valencia emphasize flexible learning modalities and strong ties to the healthcare industry, supporting international mobility and job readiness.

All programs demonstrate a strategic focus on employability, preparing graduates for roles in hospitals, medical device companies, clinical services, and R&D centers. The synergy between education, technology, and innovation positions Biomedical Engineering as a driver of Spain's digital healthcare transformation. According to recent data, Biomedical Engineering graduates in Spain have an employment rate of approximately 96.9%, positioning the discipline among those with the highest employability nationally. This high employability is attributed to the strong alignment between academic curricula and labor market needs, particularly in sectors such as hospitals, medical device companies, clinical services, and R&D centers. The synergy between education, technology, and innovation positions Biomedical Engineering as a driver of Spain's digital healthcare transformation.

Table1. Spanish universities offering bachelor's and/or master's degrees in biomedical engineering

No	University	Bachelor's	Master's	Type	Key Features
1	Universidad de Navarra	x	x	Private	Hand-on training with a focus on applied research and collaboration with technology centers
9	Universidad Europea de Madrid	x		Private	Program taught in English, emphasizing advanced medical technologies and regenerative medicine
10	Universidad de Mondragón	x		Private	Training in the design of monitoring equipment and healthcare information systems
11	Universidad de Alicante	x		Public	Specialization in telemedicine, biomedical imaging and bioengineering devices
12	Universidad Rey Juan Carlos (URJC)	x		Public	Bilingual program with the opportunity to study at leading international universities
13	Universidad de Vigo	x		Public	Balanced training in technology, basic Sciences, and biomedicine, enabling interdisciplinary projects
14	Universitat Rovira I Virgili (URV)	x		Public	Multidisciplinary approach combining scientific, technical, and management knowledge
2	Universidad Carlos III de Madrid	x		Public	Strong foundation in biology and physiology, integrating engineering and science
3	Universidad Politècnica de Catalunya (UPC)	x	x	Public	Development and application of technological advances in medicine and healthcare
4	Universidad Politécnica de Madrid (UPM)	x	x	Public	Engineering problem-solving in the medical field, integrating knowledge in engineering and medicine

5	Universidad San Pablo – CEU	x	x	Private	Training to design and manage activities related to health and social care products and services
6	Universidad Pompeu Fabra (UPF)	x	x	Public	Focus on solving problems in medicine and biology through ICT (Information and Communication Technologies)
7	Universitat Politècnica de València (UPV)	x	x	Public	Notable academic offering with high demand for the Biomedical Engineering degree
8	Universidad de Barcelona	x	x	Public	Training in information and communication technologies applied to the biomedical field
15	Universidad de Girona	x		Public	Training to design and manage activities related to health and social care products and services
16	Universidad de Valladolid	x	x	Public	Training in telemedicni and biomedical sensor development
17	Universidad Pública de Navarra (UPNA)		x	Public	Emphasis on medical instrumentation and hands-on experiences in healthcare centers
18	Universidad de Zaragoza		x	Public	High technological component and innovation in biomedical devices
19	Universidad de Extremadura		x	Public	Close ties with local hospitals and clinical focus
20	Universidad Internacional de Valencia (VIU)		x	Private	Online format aimed at practicing professionals
21	Universidad del País Vasco (UPV/EHU)		x	Public	International cooperation and global health focus
22	Universidad Nacional de Asunción (Paraguay)		x	Public *	Program in collaboration with UPV/EHU
23	Universidad de Sevilla		x	Public	Focus on digital heath, big data, and emerging technologies
24	Universidad Autónoma de Madrid	x	x	Public	Update curriculum with focus on medical innovation and technology transfer
25	Universidad de Nebrija	x		Private	Interdisciplinary approach with a focus on digital health and entrepreneurship in biomedical technologies
* Program in collaboration with UPV/EHU					

Conclusion: Biomedical Engineering in Spain has positioned itself as a field of high academic relevance and social impact. The synergy between academic excellence, healthcare innovation, and technological integration has created a favorable environment for training professionals capable of leading digital transformation in health services. This discipline not only meets current educational and labor demands but also acts a driving force in the modernization of health care systems.

References:

[1] Universidades de Biomedicina. Uniscopio. Published May 6, 2024. https://uniscopio.com/universidad/universidades-biomedicina/

[2] Seib.org.es. Published 2025. Accessed April 22, 2025. https://seib.org.es/formacion/titulaciones-oficiales/

[3] Registro de Universidades, Centros y Titulos (RUCT) - Ministerio de Educaci?n, Cultura y Deporte. Educacion.gob.es. Published 2025. Accessed April 22, 2025. https://www.educacion.gob.es/ruct/consultaestudios?actual=estudios

[4] jcortazar. Mejores Universidades en España para Ingeniería Biomédica en 2024/2025. CampusHome. Published December 4, 2024. Accessed April 22, 2025. https://campushome.es/blog/mejores-universidades-en-espana-para-ingenieria-biomedica/

[5] Universidad Autónoma de Madrid. Grado en Ingeniería Biomédica | UAM. Universidad Autónoma De Madrid. https://www.uam.es/uam/biomedica.

[6] Unibertsitatea M. Grado en Ingeniería Biomédica. Mondragon Unibertsitatea. https://www.mondragon.edu/es/grado-ingenieria-biomedica.

[7] Grado en Ingeniería Biomédica Facultad Medicina - Valladolid. https://med.uva.es/grado-en-ingenieria-biomedica/.

[8] De Alicante U. Grado en Ingeniería Biomédica. Grado En Ingeniería Biomédica. https://web.ua.es/es/grados/grado-en-ingenieria-biomedica/. Published November 4, 2025.

[9] Grado en Ingeniería Biomédica : UPV. https://www.upv.es/titulaciones/GIB/menu_1014824c.html.

[10] Universidad CEU San Pablo. Grado en Ingeniería Biomédica en Madrid | CEU San Pablo. Universidad CEU San Pablo. https://www.uspceu.com/oferta/grado/ingenieria-biomedica.

[11] Ruiz J. Ingeniería Biomédica - Universidad Rey Juan Carlos. https://www.urjc.es/universidad/calidad/2001-ingenieria-biomedica. Published March 21, 2025.

[12] Grado en Ingeniería Biomédica. Universitat Pompeu Fabra Barcelona. https://www.upf.edu/es/web/graus/grau-enginyeria-biomedica.

[13] Universidad Politécnica de Madrid. https://www.upm.es/Estudiantes/Estudios_Titulaciones/EstudiosOficialesGrado/ArticulosRelacionados?fmt=detail&prefmt=articulo&id=551d88ff1da0f210VgnVCM10000009c7648a____.

[14] Ingeniería Biomédica - UPC Universitat Politècnica de Catalunya. UPC Universitat Politècnica De Catalunya. https://www.upc.edu/es/grados/ingenieria-biomedica-barcelona-eebe.

[15] Grado en Ingeniería Biomédica - Madrid. Universidad Europea. https://universidadeuropea.com/grado-ingenieria-biomedica-madrid/.

[16] Grados - landings. Landings. https://www.unav.edu/web/landings/grados?utm_medium=pmax&utm_source=google&utm_campaign=grados_2526&utm_content=nueva-estrategia&gad_source=1&gbraid=0AAAADrPcEYtMVmIWZGmnZt8rEZzvcwsX&gclid=CjwKC

Ajwn6LABhBSEiwAsNJrjtGO_BfMhsDbmos4_Bnv2VzgBWVeDvMvFX0q82U0dRg-zPD2Eri05RoC8X8QAvD_BwE.

[17] Ingeniería biomédica - G1074. Estudios. https://web.ub.edu/es/web/estudis/w/grado-g1074.

[18] Grado en Ingeniería Biomédica | UC3M. https://www.uc3m.es/grado/biomedica.

[19] Virgili URI. Grado en Ingeniería Biomédica URV | Universitat Rovira i Virgili. Universitat Rovira I Virgili. https://www.urv.cat/es/estudios/grados/oferta/enginyeria-biomedica/.

[20] Escola de Enxeñería Industrial. Grado en Ingeniería Biomédica - EEI. EEI. https://eei.uvigo.es/es/estudios/grados/grado-en-ingenieria-biomedica/. Published December 16, 2024.

[21] Estudia > Oferta formativa > Grados > Detalle. https://www.udg.edu/es/estudia/Oferta-formativa/Graus/Fitxes?IDE=1434&ID=3105G1517.

[22] Grado en Ingeniería Biomédica Universidad Nebrija. https://www.nebrija.com/lp/grado/ingenieria-biomedica/?Cod_TipoFRM=3028&utm_campaign=2024-25_Grado_Nacional-FCVN&utm_medium=Google&utm_source=GoogleSearch&utm_content=3028&gad_source=1&gbraid=0AAAACk16aVeFg1eiFc5OZmRZZwOwwRQR&gclid=CjwKCAjwn6LABhBSEiwAsNJrjp5Y0UmBdcKt3VXnARJ_yhnf_4wlO9STQUgzmwK9nmSCpjh9UFEYkhoC25sQAvD_BwE&gclsrc=aw.ds.

[23] UAM - Escuela Politécnica Superior - Máster Universitario en Ingeniería Biomédica (GTSTmuib). Www.uam.es. Published 2025. Accessed April 22, 2025. https://www.uam.es/ss/Satellite?c=Page&cid=1446837483518&language=es&nodepath=Grupos+de+Trabajo+de+Solicitud+de+Titulaciones+%28GTST%29&pagename=EscuelaPolitecnica%2FPage%2FUAM_sinContenido

OP047

Future vision: A strategic model for structured cooperation between Biomedical Engineers and Medical Physicists for mutual benefit

Carmel J CARUANA[1*], Eric PACE[1], Sam AGIUS[1]

[1]Medical Physics, Faculty of Health Sciences, University of Malta, Msida, Malta

* ***Corresponding author***. *E-mail address*: carmel.j.caruana@um.edu.mt

Keywords: Strategic planning, biomedical engineering, medical physics, inter-professional cooperation

Motivation and Aim: We live in unprecedented times: medical device technology is expanding at breakneck speed whilst disruptive developments such as artificial intelligence are impacting and sometimes redefining professional roles. Meanwhile, the Biomedical Engineering and Medical Physics professions both face difficult challenges resulting from external factors: chock-a-block curricula which can only accommodate additional content with very great difficulty, seemingly endless ongoing austerity economics leading to attempts at the over-commoditization of higher-level professional roles and competition from lesser qualified professions who seek to usurp part of their roles. In these circumstances strategic vision for both roles, strengthening of the respective Education and Training systems of both professions in line with that strategic vision and a symbiotic mutually-supportive alliance between the two professions are essential. However, a strategic, unified role-development and inter-professional cooperation model for providing strategic vision and to guide members of both professions does not exist.

Novelty: Although there have been many mostly informal discussions in the past regarding the relationship between the roles of Biomedical Engineers and Medical Physicists, these tended to be mostly on strategically inconsequential issues of role-overlap and regarding whether the two roles should be combined into a single profession. It has also been proposed that their education should be combined into a single academic programme[1]. However, these discussions do not acknowledge the obvious major differences in focus which are becoming increasingly wider given the external pressures arising from political, economic, social, technological and legislative issues. To our knowledge this is the first formal attempt at creating a model of the two roles and their inter-relationship for the benefit of both professions and which is both visionary and strategic in nature.

Methods: A search of the literature using the search strings: 'biomedical engineering AND role development', 'medical physics AND role development', 'biomedical engineering AND strateg*, 'medical physics AND strateg* and 'biomedical engineering AND medical physics' ([Title/Abstract]) was carried out using Pubmed and Web-of-Science and a model set up based on identified strategic role development issues.

Main results: A proposed model for both roles and for inter-professional cooperation between the two professions is shown in the diagram.

In order to fend off over-commoditization and competition the education and training of Biomedical Engineers should be geared towards the development of medical devices (*medical device development life cycle*). Biomedical Engineers relate to manufacturers and vendors and their education should focus on the major engineering disciplines, engineering design, *product development and medical device development related legislation*. *This will ensure that they remain at the forefront in the area of medical device development.*

On the other hand, Medical Physicists should focus totally on the effective, safe and optimized clinical use of such devices in hospitals (*intra-hospital medical device use cycle*) to ensure that they *too remain the top experts on the use of medical devices and on protection from physical agents within hospitals*. However, since medical physicists interact mostly with patients and healthcare professionals their education *should include also heavy doses of anatomy, physiology, pathology, medical ethics and communication and people skills. If possible, the learning of these subjects should be shared with healthcare professionals so that they may develop the essential inter-professional skills necessary to thrive in the hospital milieu*.

The two professions should *cooperate in an ongoing manner* particularly regarding medical device clinical trials, post-market device surveillance and intra-hospital device maintenance and upgrade. *Biomedical Engineers can help Medical Physicists resolve clinical problems which involve deep knowledge of the technological aspects of medical devices. In turn, Medical Physicists can help bridge the gap between Biomedical Engineers based in industry and the hospital inter-professional political environment.*

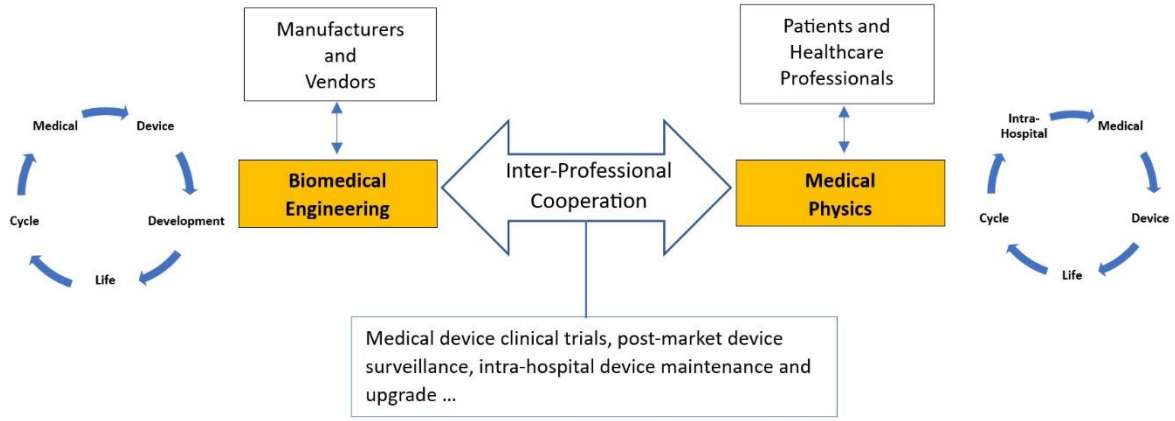

Conclusion: A strategic model for role development and structured cooperation between Biomedical Engineers and Medical Physicists has been presented. Both Biomedical Engineers and Medical Physicists are relatively small professions when compared to other healthcare professions. This weakness can only be overcome by adherence to strategic models which are designed to strengthen both professions and increase the cooperation between both professions for mutual support. The authors appreciate that such strategies may require changes to present cherished perspectives; however, history teaches that roles that do not adapt to environmental change and increase their competitive edge would slowly but surely be eventually replaced.

References:

[1] van der Putten WJM, Smith CE, Orton CG. Point/Counterpoint. The professions of Medical Physics and Clinical Engineering should be combined into a single profession 'Clinical Science and Technology'. *Med Phys* 2012;39(6):2953-5. doi: 10.1118/1.3694114.

OP048

Combining MRI and laser Doppler flowmetry for measurement of cerebral blood flow in neurointensive care

Stina MAURITZON[1*], Sofie TAPPER[1], Fredrik GINSTMAN[2], Anders TISELL[3], Peter ZSIGMOND[2], Karin WÅRDELL[1]

1 Department of Biomedical Engineering, Linköping University, Linköping, Sweden

2 Department of Neurosurgery and Department of Biomedical and Clinical Sciences, Linköping University, Linköping, Sweden

3 Department of Medical Radiation Physics and Department of Health, Medicine and Caring Sciences, Linköping University, Linköping, Sweden

* ***Corresponding author***. *E-mail address*: stina.mauritzon@liu.se

Keywords: laser Doppler flowmetry (LDF), microcirculation, magnetic resonance imaging (MRI), neurointensive care unit (NICU), subarachnoid haemorrhage (SAH)

Motivation and Aim: Subarachnoid haemorrhage (SAH) patients are carefully monitored in the neurointensive care unit (NICU) to prevent or minimise the impact of secondary brain injury. Although monitoring is extensive to ensure sufficient blood flow and oxygenation continuously, techniques related to cerebral blood flow (CBF) remain few and mainly focus on macrovascular CBF. Macrovascular blood flow, however, gives no guarantee that the microcirculation is functioning. Also, these different components of CBF may uncouple in times of critical illness and a common complication is loss of autoregulation. By combining different techniques, the advantages of each can be utilized to gain more information about the CBF. Therefore, we are investigating the feasibility of fibre-optical continuous microcirculation monitoring combined with blood flow MRI using a scanner located in the NICU.

Methods: Laser Doppler flowmetry (LDF) has been adapted for long-term monitoring of cerebral microcirculation [1], providing local microcirculatory data at high temporal resolution. A two-channel fibre optical probe evaluated for use during MRI scans of the brain was implanted and securely fixed during routine surgery. Long-term bedside monitoring took place 4-6 hours per day for up to 10 days in the NICU. Spatial coverage of global and regional CBF assessments was added through MRI. Arterial spin labelling (ASL) [2], generating absolute CBF maps of the whole brain, and 2D-flow MRI, estimating the total inflow to the brain, were performed with simultaneous LDF monitoring. The LDF system was placed in the MR control room during the MRI and connected to the patient using the 5m optical cable pulled through a wave trap. Risk analysis and training in case of emergency were carried out for the simultaneous measurements. Analysis studies are ongoing, comparing the different CBF methods to each other, and investigating and comparing long-term LDF data to clinical data, e.g. mean arterial pressure (MAP) and intracranial pressure (ICP), and clinical procedures such as drug boluses, ventilator adjustments, and head position changes.

Main results: The simultaneous MRI and LDF setup has been evaluated in three SAH patients and long-term bedside LDF monitoring has been achieved in nine patients to date, resulting in eight combined measurements and over 200 hours of bedside LDF data. The simultaneous MRI

and LDF measurements did not cause any complications for the patients or influence the data quality of either method, indicating that combined measurements are feasible in the NICU. Preliminary results from data analyses suggest that the combination of different CBF methods, covering both global and local CBF, and correlation analyses with clinical data like MAP and ICP, can provide several perspectives on blood flow and cerebral autoregulation at once, thus giving physicians more information for treatment decisions.

Conclusion:

In summary, this combined setup allows for simultaneous measurement of both macro- and microvascular components that can lead to increased understanding of CBF in critical illness, especially with LDF monitored bilaterally. The continuous mode of LDF can potentially give early warnings of deterioration, particularly in combination with the clinical monitoring data, which may indicate when another MRI is necessary to assess CBF comprehensively. With more data, it would be possible to investigate how these methods could complement each other during neurointensive care.

Acknowledgements: This research was funded by Swedish Foundation for Strategic Research, grant number RMX18-0056, and the Swedish Research Council Agency for Innovation Systems, grant number 2020-03131.

References:

1. Mauritzon, S., et al., *Analysis of laser Doppler flowmetry long-term recordings for investigation of cerebral microcirculation during neurointensive care.* Front Neurosci, 2022. **16**: p. 1030805.
2. Tapper, S., et al., *Method for detection of cerebral blood flow in neurointensive care using longitudinal arterial spin labeling MRI.* PLoS One, 2024. **19**(11): p. e0314056.

IP02

How to Promote Innovation and Entrepreneurship in the Classroom of Undergraduate Students

Martha Zequera

Oral Session OS07
Biomeasurements
Chairs: Halina Podbielska (Poland), Tilmann Sander-Thömmes (Germany)
OP049–OP054

OP049

A Blood Pressure Normalization Method for Aortic Pulse Wave Velocity

Kristina KÖÖTS, Kristjan PILT, Ivo FRIDOLIN,

Department of Health Technologies, Tallinn University of Technology, Ehitajate tee 5, 19086 Tallinn, Estonia

97ristina.koots@taltech.ee

Abstract. Arterial stiffness is an independent risk factor for cardiovascular dis- eases (CVD). Aortic pulse wave velocity (aoPWV) is a clinically used parameter for the arterial stiffness estimation, although it is influenced by blood pressure (BP). The aim of this study was to investigate whether and how aoPWV measurements obtained with a brachial single-cuff oscillometric device Arteriograph could be BP normalized. An exploratory study was conducted in 26 apparently healthy subjects (25-72 years). The aoPWV measurements were carried out in the supine position and during maneuvers designed to rise arterial BP. The aoPWV values were then normalized using mean arterial blood pressure (MAP). A moderate linear relation- ship ($r = 0.53$, $p < 0.001$) was observed between MAP and aoPWV with individ- ual-specific linear models describing the relationship for each subject. It was shown that the subjects with elevated arterial BP and aoPWV had a BP normalized aoPWV (aoPWVnorm) below 10 m/s. This indicates that the cause for an in- creased aoPWV (>10 m/s) was the increased BP rather than the increased intrin- sic stiffness of the arteries. Measurement of aoPWV at different BP levels is suggested to enable subject-specific BP normalization when estimating arterial stiff- ness.

Keywords: Arterial Stiffness, Blood Pressure, Aortic Pulse Wave Velocity, Pressure-normalized Aortic PWV

OP050

CT Assessment of the Hemidiaphragm Shape in Pleural Effusion and Its Association with Dyspnea

Anna M STECKA[1*], Katarzyna FABER[2], Elżbieta M. GRABCZAK[2], Marcin MICHNIKOWSKI[1], Rafał KRENKE[2], Tomasz GÓLCZEWSKI[1]

1 Nalecz Institute of Biocybernetics and Biomedical Engineering, Polish Academy of Sciences, Warsaw, Poland

2 Department of Internal Medicine, Pulmonary Diseases and Allergy, Medical University of Warsaw, Poland

* ***Corresponding author***. *E-mail address*: astecka@ibib.waw.pl

Keywords: Hemidiaphragm, Pleural Effusion, Dyspnea, Computer Tomography, Therapeutic Thoracentesis

Motivation and Aim: Pleural effusions, particularly large ones, have an impact on respiratory system mechanics and, therefore, patients' efficiency [1]. One of the initial and most frequent symptoms of pleural effusion is dyspnea (shortness of breath); nevertheless, the physiological mechanisms behind this have not been fully understood. This work aims to analyze thorax CT scans of patients with pleural effusion to assess the link between the hemidiaphragm shape and the levels of dyspnea reported by patients.

Novelty: This study is among the first to quantitatively assess the relationship between diaphragm shape and perceived dyspnea in patients with pleural effusion. By analyzing CT imaging alongside subjective symptoms, the research offers new insights into the physiological basis of dyspnea in pleural effusion cases.

Methods: All measurements and medical imaging took place at the Department of Internal Medicine, Pulmonary Diseases, and Allergy at the Medical University of Warsaw, all patients signed an informed consent to participate in the study. The study protocol was approved by the Medical University of Warsaw's Institutional Review Board (KB 105/2012) and registered at ClinicalTrials.gov (NCT02192138) on July 16, 2014. CT thorax scans from 21 patients (16 with right and 5 with left large pleural effusion) were analyzed, all images were obtained within 14 days prior to the therapeutic thoracentesis (TT). Measurements of the left and right hemidiaphragm positions were performed using Horos™ software, additionally, three-dimensional segmentations were created in the 3D Slicer image computing platform with the assistance of the Total Segmentator AI model. Measurements of hemidiaphragm shape were performed in three coronal sections of the thorax (Figure 1A – P1, P2, and P3) and two sagittal sections of the thorax (Figure 1A – P4 and P5). The contact point between the diaphragm and the chest wall on the contralateral side was marked and projected perpendicularly to the ipsilateral side. The diaphragm center was identified at the level where the inferior vena cava crosses it, defined as the midpoint between the vena cava and adjacent aorta. Straight lines were drawn from the contact points to this center. In the sagittal plane, measurements were taken between anterior and posterior contact points. The outlines of the left and right

hemidiaphragmatic domes were traced and measured, and lengths above the reference line were marked as positive (+), those below as negative (−); based on that the percentage of ipsilateral hemidiaphragm inversion was calculated. Dyspnea was evaluated in 17 patients immediately before the TT using the modified 10 point Borg scale.

Main results: The results of this work seem contradict the assumptions of other authors [2] and confirm our other analyses that the degree of dyspnea need not be related to improper hemidiaphragm work associated with its deformation (Figure 1B). Surprisingly, Spearman's correlations between the Borg dyspnea score and the percentage of ipsilateral hemidiaphragm inversion appeared to be negative (although statistically insignificant) and equal to -0.22 (p-0.404) and -0.37 (p=0.146) for the coronal and sagittal sections, respectively. The results confirm our previous analyses supported by computer simulations showing that anatomical inversion of the hemidiaphragm seen in USG imaging does not necessarily lead to functional inversion (pendulum breathing) [3].

Conclusion: Reasons for dyspnea in pleural effusion still seem to be uncertain and require further studies.

Acknowledgements: This study was supported by the National Science Center, Poland (grant N 2019/35/B/NZ5/02531) and The Nalecz Institute of Biocybernetics and Biomedical Engineering, Polish Academy of Sciences.

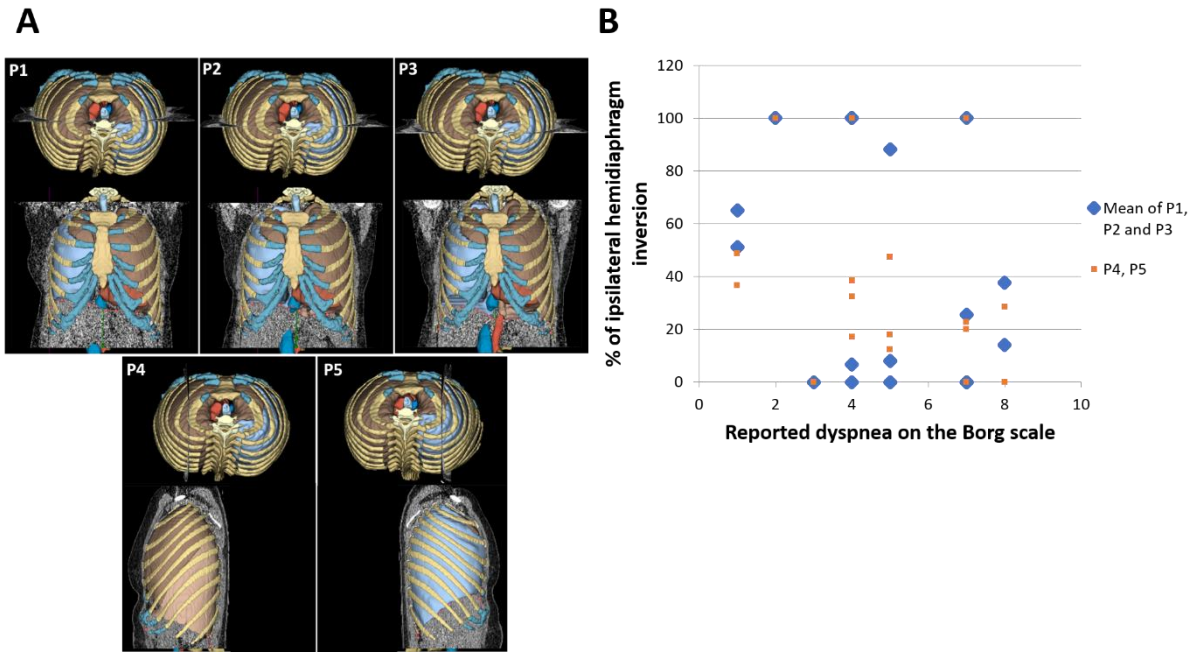

Figure 1. A) Measurement placement:P1, P2 and P3 are coronal sections of the thorax, P4 and P5 are sagital sections of the thorax. B) A chart illustrating the relationship between the percentage of ipsilateral hemidiaphragm inversion and the reported level of dyspnea on the Borg scale. The ipsilateral hemidiaphragm refers to the left or right side of the chest with the pleural effusion.

References:

[1] Shalaby HM, Ezzelregal HG. Assessment of diaphragmatic role in dyspneic patients with pleural effusion. Egypt J Bronchol. 2022;16(1):69. doi:10.1186/s43168-022-00170-6.

[2] Muruganandan S, Azzopardi M, Thomas R, et al. The Pleural Effusion And Symptom Evaluation (PLEASE) study of breathlessness in patients with a symptomatic pleural effusion. Eur Respir J. 2020;55(5):1900980. doi:10.1183/13993003.00980-2019.

[3] Gólczewski T, Stecka AM, Grabczak EM, Michnikowski M, Zielińska-Krawczyk M, Krenke R. Hemidiaphragm work in large pleural effusion and its insignificant impact on blood gases: a new insight based on in silico study. Front Physiol. 2025;16. doi:10.3389/fphys.2025.1539781

OP051

Magnetoencephalography in hearing threshold assessment

Anna JODKO-WŁADZIŃSKA[1*], Michał WŁADZIŃSKI[1], Tilmann SANDER[2], Tadeusz PAŁKO[1]

1 Warsaw University of Technology, Faculty of Mechatronics, Warsaw, Poland

2 Physikalisch-Technische Bundesanstalt, Berlin, Germany

* ***Corresponding author***. *E-mail address*: anna.wladzinska@pw.edu.pl

Keywords: magnetoencephalography, MEG, optically pumped magnetometers, OPM, SQUID, auditory evoked fields, hearing thresholds

Motivation and Aim: Measurement of Auditory Brainstem Responses (ABR) is the only method used in clinical practice which allows an objective assessment of hearing thresholds. Pure-tone audiogram can be reconstructed by determining the sound pressure level (SPL) for which wave V of the Auditory Evoked Potentials (AEP) is detectable.

Magnetoencephalography (MEG), as a technique complementary to electroencephalography (EEG), also has a potential to be used in the reconstruction of the pure-tone audiogram by determining the sound pressure level as an auditory response detection limit. MEG gives the possibility to perform non-contact measurements and avoid difficulties related to the use of scalp electrodes in EEG.

Traditional magnetometry is based on Superconducting Quantum Interference Devices (SQUIDs), which require liquid helium cooling to operate, generating high operating costs and limiting their widespread use. Novel sensors, Optically Pumped Magnetometers (OPMs), can be used at room temperature and placed closer to the signal sources, resulting in an increase in an amplitude of measured signal.

The aim of the presented research was to apply OPM technology to identify sound pressure level at which magnetic auditory evoked response M100 was detectable.

Novelty: There are very few studies in which the gold standard, SQUID MEG, was used in peri-threshold auditory evoked magnetic fields measurements [1][2][3]. The proposed method based on OPMs gives a new input to the field.

Methods: Hearing thresholds of each subject were assessed using the psychoacoustic (subjective) method, a classical tonal audiometry. The magnetic brain responses to sine stimuli at peri-threshold levels (5-10 dB SL, SL: sensational level) were recorded using a developed dedicated acoustic source, which did not interfere with measurements conducted inside a magnetically shielded room.

Signals were acquired using both systems, SQUID-MEG and OPM-MEG. Measurements using a 125-channel Yokogawa gradiometer based on SQUIDs were conducted at the Physikalisch-Technische Bundesanstalt (PTB) in Berlin, while OPMs (QZFM: QuSpin Zero Field Magnetometers) were used independently at PTB and Warsaw University of Technology. Individualized anatomy derived 3D-printed sensor holders for OPMs and EEG caps were used.

Obtained data were analyzed to assess the feasibility of magnetic measurements in objective hearing threshold assessment. The detectability of the M100 (100 ms latency) peak of auditory evoked fields, in relation to the sound pressure level of the stimulus was investigated.

Main results: The amplitude of the M100 auditory evoked response obtained using OPM-MEG was several times higher comparing to SQUID-MEG. Due to the dewar-related fixed geometry of SQUID system, magnetic dipoles of brain responses were only partially visible.

The M100 response was detected with both OPM- and SQUID-MEG for sound pressure level 10 dB above the subjectively determined thresholds (10 dB SL).

Conclusion: The OPM technology offers numerous advantages over traditional SQUID-based magnetometry, including the ability to position sensors directly on the subject's scalp, which improves signal reception and results in higher amplitudes of measured brain responses. Furthermore, their ease of use and lower maintenance cost is a clear advantage.

The conducted research showed that the registration of magnetic brain responses to tonal stimulation was possible for the sound pressure level 10 dB above individual hearing thresholds (10 dB SL). This is consistent with the research results available in the literature in which SQUID sensors were used. The feasibility of recording auditory evoked responses at peri-threshold levels was confirmed.

Hearing thresholds can be determined by identifying the sound pressure level at which the M100 magnetic auditory evoked response is detectable. This approach is a valuable complement to measurements of auditory evoked potentials, which currently provide the only objective method for determining hearing thresholds. Future work could be to compare the MEG AEF threshold with the AEP threshold within participants.

Acknowledgements: Research was partly funded within “Project PROM - International Scholarship Exchange for PhD Students and Academic Staff” financed from the European Social Fund under the Operational Program Knowledge Education Development, non-competitive project entitled International Scholarship Exchange for PhD Students and Academic Staff, contract number: POWR.03.03.00-00-PN13/18.

Research was funded by Warsaw University of Technology within the Excellence Initiative: Research University (IDUB) programme.

References:

[1] Lütkenhöner, B., Klein, J.-S., Auditory evoked field at threshold. Hearing Research. 2007;228(1-2):188–200. doi:10.1016/j.heares.2007.02.011

[2] Stufflebeam, S.M., Poeppel, D., Rowley, H.A., L. Roberts, T.P., Peri-threshold encoding of stimulus frequency and intensity in the M100 latency, NeuroReport. 1998;9(1):91-94. doi:10.1097/00001756-199801050-00018

[3] Kühler, R., Weichenberger, M., Bauer, M., Hensel, J., Brühl, R., Ihlenfeld, A., Ittermann, B., Sander, T., Kühn, S., Koch, C., Does airborne ultrasound lead to activation of the auditory cortex? Biomedical Engineering / Biomedizinische Technik, 2019, vol. 64, no. 4, pp. 481-493. doi:10.1515/bmt-2018-0048

OP052

Digital measurement modules for non-invasive monitoring of physiological parameters under extreme conditions

Ewelina SOBOTNICKA[1], Jan MOCHA[1,2], Grzegorz J. NOWAK[1,3] , Grzegorz BADURA[1], Aleksander SOBOTNICKI[1], Łukasz DZIUDA[4]

1 Lukasiewicz Research Network – Krakow Institute of Technology, Zakopianska St. 73,

30-418 Krakow, Poland

2 Silesian University of Technology, Department of Digital Systems, Akademicka St. 16,

44-100 Gliwice, Poland

3 Silesian University of Technology, Faculty of Biomedical Engineering, Roosevelta St. 40, 41-800 Zabrze, Poland

4 Military Institute of Aviation Medicine, 54/56 Z. Krasińskiego St., 01-755 Warsaw, Poland

ewelina.sobotnicka@kit.lukasiewicz.gov.pl

Abstract. The advancement of real time physiological monitoring technologies plays a vital role in ensuring the safety of individuals operating in extreme envi- ronments, including pilots, athletes, and professionals exposed to harsh environ- mental conditions. This article introduces a concept for digital measurement modules designed for non-invasive and continuous monitoring of critical physi- ological parameters. These include cardiovascular, respiratory, and musculoskel- etal system activity. The proposed solutions integrate advanced measurement technologies such as electrocardiography (ECG), impedance cardiography (ICG), electromyography (EMG), and Doppler ultrasonography to assess blood flow. The modules are optimized for mobile applications, offering high precision and resistance to external interferences. Their implementation enables the real- time collection and analysis of physiological data, facilitating early detection of potentially hazardous conditions. This is particularly relevant in scenarios where exposure to extreme gravitational forces, ischemic hypoxia, or other envi- ronmental stressors can significantly impact human performance and safety. A key advantage of these modules is the ability to provide continuous and reliable physiological assessment without restricting movement, making them suitable for use in dynamic environments. The collected data can also contribute to re- search on human adaptation to extreme conditions, helping to refine safety pro- tocols and enhance overall performance in aviation, professional sports, and other high risk industries. The developed technology represents a step forward in phys- iological monitoring, combining precision, mobility, and real time adaptability, thus offering a valuable tool for both safety and performance optimization.

Keywords: measurement modules, medical devices, physiological parameters, non-invasive monitoring, extreme conditions

OP053

Analytical equations for accurate sensitivity factors in near-infrared spectroscopy

Aleh SUDAKOU*, Stanislaw WOJTKIEWICZ, Roman MANIEWSKI, Adam LIEBERT

Nalecz Institute of Biocybernetics and Biomedical Engineering, Polish Academy of Sciences, Warsaw, Poland

* ***Corresponding author***. *E-mail address*: asudakou@ibib.waw.pl

Keywords: Near-infrared spectroscopy, sensitivity factors, recovery of optical properties.

Motivation and Aim: Near-infrared spectroscopy (NIRS) is widely used for non-invasive assessment of tissue optical properties. In scattering media such as biological tissues, especially when scattering (μ'_s) is much greater than absorption (μ_a), the mean photon pathlength (d) depends on optical properties μ_a and μ'_s. When μ_a increases, a smaller percentage of light penetrates deeper tissues compared to superficial tissues, causing d to decrease. Conversely, when μ'_s increases, light scatters more before reaching the detector, leading to an increase in d. Common data analysis approaches assume infinitesimally small changes in optical properties or, equivalently, that d remains constant, resulting in errors that grow as the magnitude of changes in optical properties increases.

Time-domain NIRS (TD-NIRS) measures distributions of times of flight of photons (DTOFs), providing information about light propagation. DTOFs allow for the analysis of attenuation (A), mean time of flight (m_1) and variance (V) [1]. Sensitivity factors [2] relate changes in these measurands to $\Delta\mu_a$, but they assume an infinitesimally small $\Delta\mu_a$. Data analysis based on sensitivity factors is an established method for recovering $\Delta\mu_a$.

Novelty: This study introduces analytical equations for non-linear sensitivity factors that extend the validity of existing data analysis approaches to large optical property changes. The equations allow recovering any magnitude of $\Delta\mu_a$ or $\Delta\mu'_s$, provided the diffusion approximation remains valid. Furthermore, we propose how the method can be accurately applied for multi-layered tissues, increasing their applicability.

Methods: We derived analytical equations for sensitivity factors in infinite (IM) and semi-infinite (SM) homogeneous media using the diffusion equation [3], which is an analytical solution of the radiative transfer equation (RTE) that relies on the diffusion approximation. Sensitivity factors were obtained by differentiating the definitions of A, m_1, and V with respect to μ_a, μ'_s, or r (source-detector distance). We extended the equations for large changes by introducing an averaging technique and making the sensitivity factor equations non-linear.

Main results: Results demonstrate that the derived sensitivity factors allow for accurate recovery of large $\Delta\mu_a$ or $\Delta\mu'_s$. The equations were verified for both IM and SM. The non-linear sensitivity factors eliminate errors introduced by assuming infinitesimally small perturbations in parameter recovery. We present an equation for A that may enable modelling tools to provide outputs in absolute units, provided reference value has been measured experimentally.

Conclusion: The non-linear sensitivity factors eliminate errors introduced by assuming infinitesimally small perturbations or a constant *d*, enabling more accurate parameter recovery in NIRS applications. Furthermore, even large changes can also be accurately recovered. These findings contribute to improving biomedical and clinical applications of NIRS by providing more reliable methods for analyzing tissue absorption and scattering properties.

References:

[1] Liebert, A., H. Wabnitz, D. Grosenick, M. Moller, R. Macdonald, and H. Rinneberg, Evaluation of optical properties of highly scattering media by moments of distributions of times of flight of photons. Appl Opt, 2003. 42(28): p. 5785-92.

[2] Liebert, A., H. Wabnitz, J. Steinbrink, H. Obrig, M. Moller, R. Macdonald, A. Villringer, and H. Rinneberg, Time-resolved multidistance near-infrared spectroscopy of the adult head: intracerebral and extracerebral absorption changes from moments of distribution of times of flight of photons. Appl Opt, 2004. 43(15): p. 3037-47.

[3] Patterson, M.S., B. Chance, and B.C. Wilson, Time resolved reflectance and transmittance for the non-invasive measurement of tissue optical properties. Appl Opt, 1989. 28(12): p. 2331-6.

OP054

The Advancing Brain Tumor Diagnosis: Vibrational Spectroscopy for Differentiation and Classification of Gliomas

Marlena GĄSIOR-GŁOGOWSKA[1*], Anastasija KRZEMIŃSKA[3], Bogdan CZAPIGA[2,3], Marta KOPACZYŃSKA[1]

1 Department of Biomedical Engineering, Faculty of Fundamental Problems of Technology, Wrocław University of Science and Technology, Wybrzeże Wyspianskiego 27, 50-370 Wrocław, Poland

2 Faculty of Medicine, Wrocław University of Science and Technology, Wybrzeże Wyspianskiego 27, 50-370 Wrocław, Poland

3 Department of Neurosurgery Unit, 4th Military Hospital in Wroclaw, ul. Rudolfa Weigla 5, 50-981 Wrocław

* ***Corresponding author***. *E-mail address*: marlena.gasior-glogowska@pwr.edu.pl

Keywords: Vibrational spectroscopy, Brain Tumor Differentiation, Glioma Classification

Motivation and Aim: Central Nervous System (CNS) tumors are among the most common cancers and leading causes of cancer-related deaths in adolescents, young adults, and children. With approx. 90,000 new cases annually, survival outcomes depend on age, tumor location, and grade, with WHO grade 4 tumors having the poorest prognosis(5-year survival: 6.8%) [1,2]. Brain tumors, particularly high grade gliomas [3], pose a significant challenge in neurosurgical oncology due to their infiltrative growth and blurred tumor margins. Neurosurgeons use various techniques for intraoperative visualization of tumor borders, such as intraoperative MRI [5], intraoperative ultrasound, neuronavigation, fluorescence-guided surgery [4], and intraoperative histopathology, each with limitations in availability, cost, and accuracy. Neuronavigation can be misleading post-resection due to brain tissue shift, while 5-5-Aminolevulinic acid (5-ALA) is limited to *glioblastoma multiforme* cases only. The lack of a rapid, effective, and affordable intraoperative technique for real-time tumor border identification highlights the urgent need for novel approaches.

In addition to the rapid identification of brain tumor borders, which affects the extent of tumor resection, there is a need to develop a method for the quick diagnosis of the tumor type (according to the WHO 2021 Classification of CNS Tumors) that would be as accurate as histopathological examination. Intraoperative diagnosis influences the neurosurgeon's decision regarding the extent of resection and could also shorten the patient's waiting time for adjuvant treatment after tumor resection. The aim is to develop and validate a database of Raman and infrared spectra of healthy and neoplastic brain tissues, including gliomas, meningiomas, and metastases. By applying vibrational spectroscopy, we seek to establish a robust, label-free, and real-time method for tumor identification and classification that can enhance surgical precision, minimize healthy tissue resection, and improve patient outcomes.

Novelty: This research aims to develop a novel classification algorithm for distinguishing healthy brain tissue from various neoplastic tissues, enabling neurosurgeons to make precise surgical decisions based on biochemical composition rather than relying solely on visual and

structural imaging techniques. The underlying hypothesis suggests that each type of brain tumor has a unique biochemical signature, which is reflected in its characteristic Raman spectral bands and infrared absorption patterns.

Methods: 69 brain tumor specimens were collected during planned tumor resection surgeries at the Operation Unit of the 4th Military Hospital. Under microscopic control, at least two adjacent 2×2 mm samples were obtained from an area with a high probability of tumor presence. One sample was washed in saline and immediately subjected to spectroscopic analysis, while the second sample was fixed in formalin and sent to the histopathology laboratory for validation. FT-Raman and ATR-FTIR spectrometers were used to analyze the biochemical composition of the tissue samples, providing insight into molecular alterations associated with tumor progression and differentiation from healthy brain tissue.

Main results: Spectroscopic analysis successfully differentiated healthy brain tissue from tumor-infiltrated regions, revealing distinct biochemical alterations between normal and neoplastic tissues. Initial findings suggest that nontumor brain tissue exhibits higher levels of structural lipids and well-preserved protein secondary structures, while tumor tissues show increased metabolic activity markers, a disrupted lipid-protein balance, and altered nucleic acid compositions. These observed differences lay the groundwork for the potential intraoperative differentiation of tumor margins using vibrational spectroscopy.

Conclusion: Our results highlight the clinical potential of vibrational spectroscopy as a non-invasive, label-free diagnostic tool for improving intraoperative tumor identification, optimizing resection strategies, and facilitating glioma classification. By correlating spectral data with histopathological and cytogenetic findings, we ensured the robust validation of spectral biomarkers. This approach supports the development of methodologies for differentiating healthy brain tissue from tumor-infiltrated regions and for subtyping gliomas, particularly distinguishing high-grade from low-grade gliomas.

Acknowledgements:

References:

[1] San Diego Brain Tumor foundation [online]. United States of America. 2020. [accessed on: 03.02.2024]. Available online: https://www.sdbtf.org/resources/brain-tumor-facts/

[2] Guo, X., Gu, L., Li, Y., Zheng, Z., Chen, W., & Wang, Y. (2023). Histological and molecular glioblastoma, IDH-wildtype: A real-world landscape using the 2021 WHO classification of central nervous system tumors. Frontiers in Oncology, 13, 1200815. https://doi.org/10.3389/fonc.2023.1200815

[3] Wang LM, Englander ZK, Miller ML, Bruce JN. Malignant Glioma. Adv Exp Med Biol. 2023;1405:1-30. doi: 10.1007/978-3-031-23705-8_1. PMID: 37452933

[4] Sun R, Cuthbert H, Watts C. Fluorescence-Guided Surgery in the Surgical Treatment of Gliomas: Past, Present and Future. Cancers (Basel). 2021 Jul 13;13(14):3508. doi: 10.3390/cancers13143508. PMID: 34298721; PMCID: PMC8304525.

[5] Krishna Kumar, G., Balasubramaniam, A., Pradeep, K., & Manohar, N. (2021). Intraoperative MRI in Brain Tumor Surgeries. IntechOpen. doi: 10.5772/intechopen.95588

Oral Session OS08
Biomedical Signal Processing: Brain and Physiological Function Analysis
Chairs: Gunta Krūmiņa (Latvia), Agnieszka Uryga (Poland)
OP055–OP058

OP055

Event-Related Potentials as Markers of Image Depth Perception

Mehrdad NADERI[1], Albina Abdullayeva[1], Gunta KRUMINA[1], Reinis ALKSNIS[2], Tatjana PLADERE[1]

1Department of Optometry and Vision Science, Faculty of Science and Technology, University of Latvia, Riga, LV-1004, Latvia

2Statistical Research and Data Analysis Laboratory, Faculty of Science and Technology, University of Latvia, Riga, LV-1004, Latvia

mehrdad.naderi@lu.lv

Abstract. Stereoacuity, the ability to perceive depth based on binocular disparity, is a crucial function of the human visual system. Traditional methods for assessing stereoacuity rely on subjective patient responses, making them potentially prone to bias. This study used electroencephalography (EEG) to investigate event-related potentials (ERPs) as potential markers for the objective assessment of depth perception based on binocular disparity. EEG data were collected for 32 participants, categorized into normal and abnormal stereoacuity groups, under controlled viewing conditions. Comparing participants' brain activity with normal and abnormal stereoacuity, data analysis revealed significant differences in ERP amplitudes within the 75-185 ms time window following the onset of visual stimulus (related to P1 and P2 components of ERP), particularly in the parietal regions. These findings suggest that specific ERP components could serve as neurophysiological indicators for objectively assessing depth perception.

Keywords: Electroencephalography (EEG), Event-Related Potential (ERP), Depth Perception, Stereoacuity

OP056

Analysis of the website accessibility influence on the cognitive workload of users with visual impairments

Piotr ZAJĄC, Aleksandra KRÓLAK

Institute of Electronics, Lodz University of Technology, Poland

piotr.zajac@dokt.p.lodz.pl, aleksandra.krolak@p.lodz.pl

Abstract. The aim of this study was to analyze the relationship be- tween the cognitive load when using selected online services and the level of accessibility of these services. The Zara website was selected for the study as a website with a low level of accessibility and the Zalando website as a website with a good level of accessibility. The accessibility of websites was determined on the basis of their compliance with the web content accessibility guidelines (WCAG) using automatic on- line tools supported by an expert evaluation. The cognitive workload was estimated based on the analysis of the time-domain HRV (heart rate variability) parameters and NASA-TLX inspired questionnaires. In the study participated 5 persons with visual impairments, 4 men and 1 woman, on average 40 years old. The results indicate a significant influence of the level of website accessibility on the mental workload of the users with visual impairments.

Keywords: cognitive workload, web accessibility, ECG, HRV, self-assessment questionnaire

OP057

Hemodynamic group activations from a multi-modal setup combining OPM-MEG and fNIRS

Pichaya TAPPAYUTHPIJARN[1*], Urban MARHL[2], Piotr SAWOSZ[3], Vojko JAZBINŠEK[2], Adam LIEBERT[3], Tilmann SANDER[1], Stanislaw WOJTKIEWICZ[3],

1 Physikalisch-Technische Bundesanstalt, Biosignals, Berlin, Germany

2 Institute of Mathematics, Physics and Mechanics, Ljubljana, Slovenia

3 Nalecz Institute of Biocybernetics and Biomedical Engineering, Warsaw, Poland

* ***Corresponding author***. *E-mail address*: Tilmann.sander-thoemmes@ptb.de

Keywords: functional near-infrared spectroscopy, magnetoencephalography, optically pumped magnetometers,

Motivation and Aim: Understanding neurovascular coupling (NVC) is important for neuroscience and has clinical value in studying various brain functions and neurological disorders such as stroke and Alzheimer's disease (AD). Two non-invasive modalities - functional near-infrared spectroscopy (fNIRS) and magnetoencephalography (MEG) - can be used to simultaneously measure cortical hemodynamics and neuronal activity[1].

Novelty: The combined measurement has become feasible due to the reduced size of optically pumped magnetometers (OPM) sensor in MEG and the development of an in-house fNIRS device[2], enabling concurrent measurements in a magnetically shielded room. A custom 3D-printed helmet, based on segmentation of each individual's anatomical MRI, ensures precise opodes placement. This experimental setup is flexible and can be used in combination with motor or visual activation for NVC studies.

Methods: Motor activation tasks included self-paced ball squeezing and finger opposition movements of the right hand for 20 seconds each. Four participants performed the tasks in sequence. Our in-house developed fNIRS system, consisting of 15 sources and 9 detectors, was used to measure the hemodynamic response. It records optical signals at 750 nm and 850 nm with a sampling rate of 15 Hz. The optode array was centered over C3. We focused on channels corresponding to the first and second nearest neighbors (source-detector pairs) with distances of 1.8 cm and 3.5 cm, respectively. Data analysis was performed using the MNE-NIRS software package (mne.tools/mne-nirs/). Channels with SCI values exceeding 0.5, which may indicate strong physiological signals, were excluded[3]. Subsequently, channels exceeding the threshold of coefficient of variation = 15% were considered to contain unphysiological noise and were excluded. To further clean the data, the negative correlation enhancement algorithm was applied[4]. Among the 81-channel grid, we selected only those channels that showed a statistically significant oxy-hemoglobin response for analysis. Subsequently, measurement epochs were averaged across three channels with the highest amplitude, followed by averaging across subjects.

Main results: As shown in Fig. 1, oxy-hemoglobin increases and reaches a plateau within the first 6 s and 8 s for the ball squeezing and finger opposition task, respectively. Then it remains almost stable until the end of stimulation at 20 s. Following stimulus cessation, a post-stimulus undershoot of oxy-hemoglobin peaks approximately 10 s later. This was observed in 3 out of 4 subjects in individual analysis. Finally, oxy-hemoglobin returns to baseline approximately 10 s later. On the contrary, deoxy-hemoglobin decreases during the ball squeezing task, and comes back to the baseline value at 10 s after stimulation ceases. However, during the finger tapping task, deoxy-hemoglobin does not decrease and remains near baseline throughout the task. The grand average value at the plateau (10 - 20 s) was extracted for one-sample t-test against the

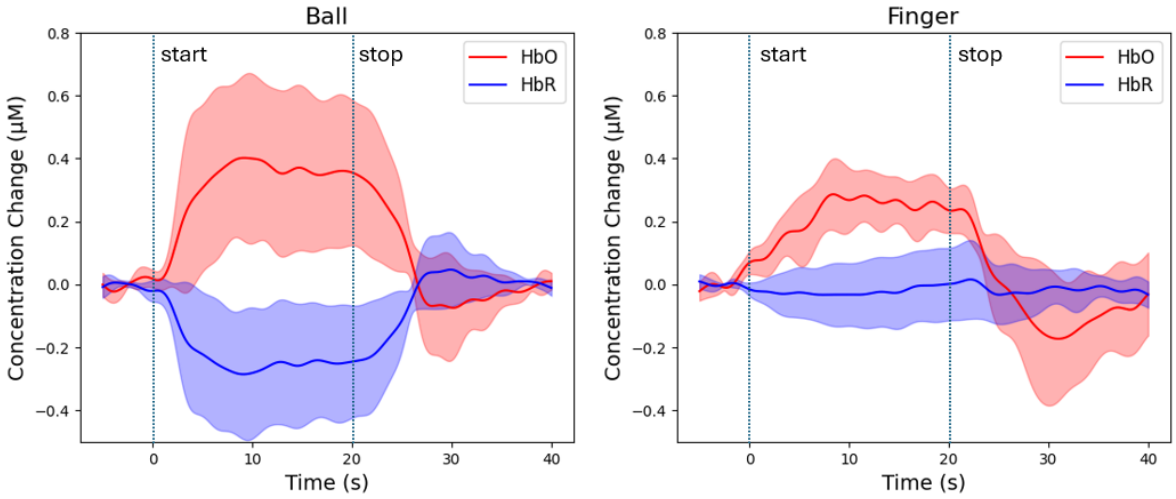

baseline (before the stimulation start). The average response is 0.36 ± 0.31 μM ($p = 0.0759$) for ball squeezing and 0.26 ± 0.07 μM ($p = 0.0083$) for finger tapping. There is greater variance in the ball-squeezing paradigm compared to the finger-tapping paradigm, likely due to differences in how subjects performed the task.

Fig. 1: The average epoch waveform response to ball squeezing (left) and finger tapping (right). Oxy-hemoglobin ("HbO") and deoxy-hemoglobin ("HbR") are shown in red and blue lines

Conclusion: We have demonstrated the feasibility of fNIRS group analysis in the developed simultaneous measurement setup. Future work will focus on incorporating visual or multi-sensory stimulation, mapping neuronal activity, and localizing activation sources, which will be valuable for further NVC studies

Acknowledgements: ARIS program P2-0348 and project N1-0283; by DFG project 505063244; and by NCN National Science Center Poland project 2021/43/I/ST7/02900.

References:

1. Marhl U, Wojtkiewicz S, Sawosz P, et al. Combined Measurement of Brain Activation During a Motor Task Using fNIRS and OPM-MEG. In: Jarm T, Šmerc R, Mahnič-Kalamiza S, eds. *9th European Medical and Biological Engineering Conference*. Vol 112. IFMBE Proceedings. Springer Nature Switzerland; 2024:170-177. doi:10.1007/978-3-031-61625-9_19

2. Wojtkiewicz S, Marhl U, Sawosz P, Jazbinsek V, Sander T, Liebert A. Multimodal fNIRS and oMEG for imaging of neurovascular coupling. In: *Proc. SPIE PC12828*. ; 2024:PC1282808. doi:https://doi.org/10.1117/12.3002625
3. Pollonini L, Bortfeld H, Oghalai JS. PHOEBE: a method for real time mapping of optodes-scalp coupling in functional near-infrared spectroscopy. *Biomed Opt Express*. 2016;7(12):5104. doi:10.1364/BOE.7.005104
4. Cui X, Bray S, Reiss AL. Functional near infrared spectroscopy (NIRS) signal improvement based on negative correlation between oxygenated and deoxygenated hemoglobin dynamics. *NeuroImage*. 2010;49(4):3039-3046. doi:10.1016/j.neuroimage.2009.11.050

OP058

Relationship between entropy of heart rate variability and cerebral autoregulation in healthy volunteers

Agnieszka URYGA[1*], Teodor BUCHNER[2], Magdalena KASPROWICZ[1]

1 Department of Biomedical Engineering, Wroclaw University of Science and Technology, Wroclaw, Poland

2 Faculty of Physics, Warsaw University of Technology, Warsaw, Poland

* ***Corresponding author***. *E-mail address*: agnieszka.uryga@pwr.edu.pl

Keywords: entropy, heart rate variability, cerebral autoregulation, cerebral blood flow velocity, arterial blood pressure

Motivation and Aim: Healthy heart is not a metronome, as the resting sinus rhythm of the heart is highly irregular and continuously adapts to respiratory activity, blood pressure fluctuations and neural impulses from autonomic centres [1]. Heart rate variability (HRV), by capturing the interplay between these regulatory systems, is considered a measure of heart–brain interactions [2]. An important aspect of heart–brain crosstalk is the maintenance of adequate cerebral perfusion. The integration and regulation of cerebral blood flow and systemic arterial blood pressure are governed by cerebral autoregulation. However, the contribution of the autonomic nervous system (ANS) to cerebral blood flow regulation remains understudied in the scenario of physiological challenges induced by respiration. This study aimed to analyze the relationship between entropy-based HRV measures and cerebral autoregulation during a controlled breathing maneuver.

Novelty: The impact of breathing at a fixed rate on the relationship between ANS activity and cerebral autoregulation remains unclear. The controlled breathing protocol applied in this study presents a non-invasive and easy implementable approach that induces substantial changes in respiratory rate (RR) and end-tidal CO_2 ($EtCO_2$), thereby stimulating both the baroreflex and chemoreceptors and altering cerebral autoregulation. Heartbeat irregularity and complexity were estimated using several entropy-based HRV metrics. These measures have been recently proposed as complementary to standard time and frequency-domain HRV metrics [3].

Methods: All signals were acquired non-invasively in young, healthy volunteers (Bioethical Committee agreements: KB-170/2014 and KB–179/2023/N). Arterial blood pressure (ABP) was measured using photoplethysmography. Cerebral blood flow velocity (CBv) was recorded using transcranial Doppler ultrasonography. RR and $EtCO_2$ were measured using capnography. A spontaneous breathing task was performed for 5 minutes, followed by three consecutive 5-minute controlled breathing sessions at fixed rates of 6, 10, and 15 bpm. The interbeat interval signal was derived from ABP. HRV entropy was estimated using multiscale entropy (MSEn), approximate entropy (ApEn), sample entropy (SampEn), and Fuzzy Entropy (FuzzEn) applying the Neurokit2 computational package in Python. Cerebral autoregulation was assessed using transfer function analysis (TFA) to evaluate phase shift (PS) and gain between ABP and CBv slow fluctuations in the very-low frequency (VLF; 0.02–0.07Hz) and breathing frequency (BF, [0.1,0.17,0.25]±0.02Hz) ranges. The analysis was performed in MATLAB following the CARNET guideline. A linear mixed-effects model (LMEM) was used to analyse the changes

in TFA metrics across the three combined RR, with subjects treated as random effects and RR, $EtCO_2$ and entropy metrics as fixed explanatory variables.

Main results: 70 healthy volunteers were included in the analysis (mean age 22±3 years). At higher fixed RR, $EtCO_2$ decreased ($p<0.001$), accompanied by a concomitant increase in ABP ($p<0.001$) and a decrease in CBv ($p=0.039$). PS at VLF gradually increased ($p=0.025$), while PS at BF decreased ($p<0.001$). ApEn, SampEn, MSEn and FuzzyEn significantly increased with higher RR ($p<0.001$). The LMEM model adjusted for $EtCO_2$ and RR demonstrated that PS at the VLF was significantly influenced by heartbeat irregularity (ApEn; $p=0.031$) and complexity (FuzzyEn; $p=0.044$). At BF, the LMEM model revealed that PS was affected by MSEn ($p=0.040$), while other entropy metrics were nonsignificant. Changes in gain at VLF and the BF were primarily explained by the RR and $EtCO_2$, with the impact of ANS metrics being negligible.

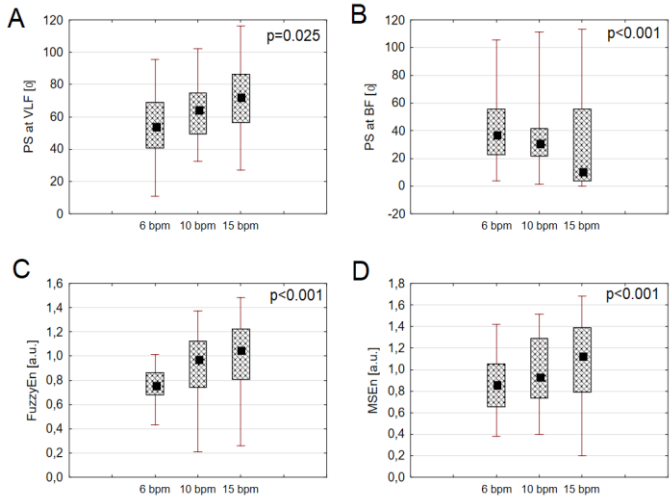

Fig.1 Changes in cerebral autoregulation metrics (phase shifts, PS) at (A) very-low frequency (VLF) and (B) breathing frequency (BF), as well as entropy metrics (C) fuzzy entropy (FuzzEn) and (D) multiscale entropy (MSEn) during controlled breathing. Data are presented as median (black square) with interquartile range (whiskers).

Conclusion: The controlled breathing protocol induces significant changes in HRV and cerebral autoregulation. The LMEM, adjusted for $EtCO_2$ and RR, showed that PS at both VLF and BF was significantly influenced by entropy metrics. Notably, the specific entropy metrics contributing to this influence varied depending on the analyzed frequency range: at VLF, ApEn and FuzzyEn were involved, whereas at BF, MSEn was a key determinant. This suggests that different entropy methods capture distinct aspects of heartbeat signal dynamics.

Acknowledgements: We would like to thank Piotr Urbański, MD and Tomasz Szczepański, MD PhD for assisting in laboratory measurements. This work was supported by the National Science Centre, Poland (grant no UMO-2022/47/D/ST7/00229).

References:

[1] Shaffer F, McCraty R, Zerr CL. A healthy heart is not a metronome: an integrative review of the heart's anatomy and heart rate variability. *Front Psychol*. 2014; 30(5):1040.

[2] McCraty R., Atkinson M., Tomasino D., Bradley R. T. The coherent heart: heart-brain interactions, psychophysiological coherence, and the emergence of system-wide order. *Integral Rev.* 2009; 5: 100–115.

[3] Byun S, Kim AY, Jang EH, Kim S, Choi KW, Yu HY, Jeon HJ. Entropy analysis of heart rate variability and its application to recognize major depressive disorder: A pilot study. *Technol Health Care*. 2019; 27(S1):407-424.

Special Symposium SE07a
IFMBE, Students and Recent Graduates Working Group: How Can We Bring Innovation to Socially Impactful Research Through the Effective Use of Emerging Technologies?
Chairs: Martha Zequera (Colombia), Piotr Ladyzynski (Poland), Anna Stecka (Poland)
OP059–OP062

OP059

Intelligent System for Monitoring Sedentary Behaviour to Support Elderly Care

Santiago LYNETT[1], Santiago MESA[1], Wilder CASTELLANOS[1], Martha ZEQUERA[1],

Pilar CASTELLANOS[2]

1 Department of Electronic Engineering, Pontificia Universidad Javeriana, Colombia

{santiagolynett, santiagoa.mesan, wecastellanos, mzequera}@javeriana.edu.co

2School of Medicine, Universidad Pedag´ogica y Tecnol´ogica de Colombia

jessica.castellanos@uptc.edu.co

Abstract. The ageing population poses significant challenges to health- care systems, particularly regarding the monitoring and prevention of sedentary behaviour among the elderly. Prolonged inactivity is associated with increased risks of chronic diseases and reduced quality of life. This study aims to evaluate an innovative IoT-based intelligent monitoring system designed to track sedentary behaviour and automate attendance registration in elderly care centers. The system integrates a miniaturized and ergonomically designed wearable device with a fixed station to monitor physical activity levels and attendance in real-time. Data is transmitted to an IoT platform, providing caregivers with action- able insights and timely alerts regarding prolonged sedentary periods. A pilot study involving three elderly volunteers was conducted primarily to assess technological feasibility and the accuracy of the system in distinguishing between sedentary and non-sedentary behaviour using the Metabolic Equivalent of Task (MET) as a reference. Results indicate that the system accurately differentiates activity states; however, further studies with larger sample sizes are recommended to validate these findings comprehensively and achieve statistically significant outcomes.

Keywords: IoT, elderly care, sedentary behaviour monitoring, wearable devices, healthcare technology, MET index, real-time monitoring, RFID attendance tracking

OP060

Hybrid Respiratory System Model as a Foundation for Modular Physiological Simulation Framework

Zofia KNAPIŃSKA[1*], Krzysztof ZIELIŃSKI[1]

1 Nalecz Institute of Biocybernetics and Biomedical Engineering PAS, Warsaw, Poland

* ***Corresponding author***. *E-mail address*: zknapinska@ibib.waw.pl

Keywords: hybrid modeling, respiratory simulation, modular architecture, spirometry, mechanical ventilator testing, physiological modeling, lung mechanics

Motivation and Aim: Accurate, data-driven simulations of human physiological functions are increasingly important for advancing medical research while minimizing risks and costs associated with human trials. This study explores the feasibility of developing a modular simulation framework capable of realistically modeling human body systems and physiological processes occurring within them. As a proof of concept, this presentation focuses on developing a hybrid respiratory system model. The aim is to investigate how such a model, which combines hardware and software, can enhance the precision, safety, and efficiency of medical examinations regarding the respiratory system and lead to the development of adaptable, patient-tailored protocols operating on devices such as mechanical ventilators.

Novelty: The presentation focuses on the initial implementation of a modular hybrid modeling approach, demonstrating how the respiratory system can be simulated using integrated software and hardware components. While the long-term objective is to build a comprehensive, scalable environment incorporating multiple body systems, this contribution focuses primarily on the respiratory module. It highlights its potential to adapt its functioning to diverse patient profiles, integrate seamlessly with clinical decision support systems and existing medical devices such as mechanical ventilators, and advance precision medicine by fostering a patient-centered approach.

Methods: A hybrid respiratory model was developed as the first module within a modular physiological simulation framework. The system integrates a software component, simulating diverse, patient-specific breathing cycles with hardware that mimics respiratory mechanics via two mechanically driven cylinders. It interfaces with medical devices and supports standardized testing protocols like spirometry to enable precise lung function analysis. In this case, a hybrid approach allows for flexibility in research applications and medical device optimization.

Main results: The hybrid respiratory model accurately replicated lung mechanics across a wide range of simulated patient conditions and profiles. It allowed for controlled interaction with ventilators and generated reliable spirometry data. These results demonstrate the model's adaptability and potential for improving the design and validation of respiratory medical devices.

Conclusion: The hybrid respiratory system model establishes a strong foundation for a hybrid, modular physiological simulation framework. By enabling realistic, hardware-integrated simulations, it advances medical device development, supports personalized clinical decision-making, and opens the path for future integration of additional physiological modules representing other body systems.

Acknowledgements: This work was supported by the National Science Centre, Poland (Grant No 2021/43/D/ST7/01912).

OP061

Bridging Innovation and Society: ANEEB Perspective on Emerging Technologies

Andreia MARTINS[1,2]; Diogo Henrique Vieira ANDRADE[1,3]

1 ANEEB - National Association of Biomedical Engineering Students, Portugal

2 University of Minho – School of Engineering

3 University of Porto – Faculty of Engineering

* ***Corresponding author***. *E-mail address: martinsandreia15@gmail.com; diogohva02@gmail.com*

Keywords: Biomedical Engineering Education, ANEEB, Technology, Innovation

Motivation and Aim: The lack of access to real-world data and practical tools in academic settings, combined with the considerable gap between technology creators and end users, has led to challenges in generating projects with a strong social impact. In this context, the National Association of Biomedical Engineering Students (ANEEB) promotes initiatives that bridge the intersection between education, technology, and society from the early stages of students' academic careers in Portugal. The goal of this study is to demonstrate that student-led initiatives can meaningfully engage with emerging technologies in a practical, ethical and socially relevant manner, efficiently preparing students to become innovation-driven, addressing real challenges even before entering the job market.

Novelty: This study highlights the strategic role of student associations, such as ANEEB, in promoting the adoption of emerging technologies within education and research to address both societal and industrial needs. It explores how ANEEB facilitates closer connections between academic theory and real-world challenges by leveraging international collaboration and prioritizing social impact. Through initiatives including online job fairs, competitions, pedagogical sessions, summer internship platforms, and scholarship programs, the association fosters the development of digital technology skills.

Methods: ANEEB actively integrates the use and exploration of emerging technologies, examples include Hackatons where participants develop innovative prototypes and solutions using artificial intelligence and digital platforms, promoting practical problem-solving and technological creativity [3]; Pedagogical sessions and project competitions emphasize artificial intelligence and optimization techniques, helping students gain familiarity with cutting-edge tools and methodologies; Career platforms such as online job fairs and summer internship programs connect students with real-world opportunities [4]; Summarized articles and active social media engagement keep students updated on the latest scientific and technological advances [2].

All these projects are designed with a strong emphasis on ethics, interdisciplinarity, accessibility, and active student engagement, ensuring that future biomedical engineers are equipped to apply emerging technologies in ways that are both responsible and socially impactful.

Main results: Participation in ANEEB-led initiatives has resulted in the development of innovative prototypes and policy proposals, enhanced digital literacy and a greater understanding of biomedical engineering and has increased national visibility and tangible contributions to curricular reforms and early-stage research.

Notably, ANEEB played a crucial role in establishing a new Biomedical Engineering college under the Portuguese Order of Engineers (OE), giving students a stronger voice in curriculum planning and accreditation processes. Feedback indicates that students not only broaden their academic and professional horizons through these initiatives but also contribute to shaping the future of biomedical engineering in Portugal.

Conclusion: Student associations are not merely support structures, they are powerful engines of innovation with tangible social impact. The ANEEB experience shows that when these organizations are driven by competent, motivated, and socially conscious students, emerging technologies can be harnessed as essential tools for purposeful research. By fostering collaboration from the early stages of higher education, we are building a scientific culture focused on inclusion and social responsibility, effectively bridging the gap between tomorrow's professionals and the evolving needs of society.

Acknowledgements: We would like to thank the International Federation for Medical and Biological Engineering (IFMBE) for inviting us and promoting our participation in the NCB 2025 SP11 session, and for being a beacon of support for student involvement in the global biomedical engineering community.

References:

[1] ANEEB – National Association of Biomedical Engineering Students. Accessed April 13, 2025. https://aneeb.pt/

[2] Criação de Colégio da Especialidade de Engenharia Biomédica é "momento marcante para todos" e destaque na Conferência Nacional da ANEEB. HealthNews. Accessed April 14, 2025. https://healthnews.pt/2024/09/10/criacao-de-colegio-da-especialidade-de-engenharia-biomedica-e-momento-marcante-para-todos-e-destaque-na-conferencia-nacional-da-aneeb/

[3] Health Hackathon: 24 horas de inovação em saúde no Hospital da Luz. HealthNews. Accessed April 14, 2025. https://healthnews.pt/2024/11/15/health-hackathon-24-horas-de-inovacao-em-saude-no-hospital-da-luz/

[4] ANEEB oferece estágios para preparar estudantes de Engenharia Biomédica e amenizar transição para o mercado de trabalho. HealthNews. Accessed April 14, 2025. https://healthnews.pt/2024/08/07/aneeb-oferece-estagios-para-preparar-estudantes-de-engenharia-biomedica-e-amenizar-transicao-para-o-mercado-de-trabalho/

OP062

Time-domain near-infrared spectroscopy: advancing brain oxygenation monitoring

Aleh SUDAKOU*, Adam LIEBERT

Nalecz Institute of Biocybernetics and Biomedical Engineering, Polish Academy of Sciences, Warsaw, Poland

* ***Corresponding author***. *E-mail address*: asudakou@ibib.waw.pl

Keywords: Time-correlated single-photon detection, depth-resolved StO_2, TD-NIRS

Motivation and Aim: Monitoring brain oxygenation and metabolism using near-infrared light is valuable for diagnosing and managing neurological conditions such as stroke, traumatic brain injury, and neurodegenerative diseases. Near-infrared spectroscopy (NIRS) offers advantages in portability, real-time monitoring, and cost. Advancements in emerging technologies and instrumentation, including pulsed broadband lasers and single-photon detectors for time-domain NIRS (TD-NIRS) at multiple wavelengths [1], are enabling various new applications and research [2].

Novelty: This study explores how the effective use of advancements in TD-NIRS instrumentation led to new research and applications.

Methods: TD-NIRS measures time-of-flight (and possibly wavelength) of single photons that have travelled from a laser source to a detector. This enables depth-resolved assessment of optical properties at multiple wavelengths. We used a state-of-the-art TD-NIRS system developed at IBIB PAN. We improved data analysis method and developed a two-layered blood-lipid phantom, which enabled accurate recovery of tissue oxygen saturation (StO_2) in both deep and superficial layers and its validation. Two layers mimic cerebral and extracerebral tissues for measurements on a head.

Main results: Advancements in instrumentation and data analysis have significantly reduced the influence of superficial StO_2 on measurements of deep StO_2, such as in brain monitoring.

Conclusion: These advancements bring TD-NIRS closer to routine clinical applications, such as real-time, non-invasive monitoring of cerebral StO_2, which is highly valuable in both clinical and research settings.

References:

[1] Lange, F., L. Giannoni, and I. Tachtsidis, The Use of Supercontinuum Laser Sources in Biomedical Diffuse Optics: Unlocking the Power of Multispectral Imaging. Applied Sciences, 2021. 11(10): p. 4616.

[2] Sudakou, A. (doctoral thesis, 2024). Depth-resolved assessment of tissue oxygen saturation using time-domain near infrared spectroscopy. Nalecz Institute of Biocybernetics and Biomedical Engineering PAS.

Special Symposium SE08
Meet the Editor
Chairs: Zahra Moussavi (UK), Adam Liebert (Poland)
KL04, KL05

KL04 Keynote Lecture: Meet the Editor of the Medical & Biological Engineering & Computing

Zahra Moussavi

KL05

Meet the Editor-in-Chief of the Biocybernetics and Biomedical Engineering: why I reject the manuscripts?

Adam LIEBERT

In this presentation, I will offer practical guidance on best practices for publishing scientific papers in the field of biomedical engineering, based on my experience as Editor-in-Chief of *Biocybernetics and Biomedical Engineering*, a journal published by Elsevier. The journal focuses on publishing high-quality research that integrates mathematical, physical, chemical, and engineering approaches with biomedical applications. The Editorial Board is particularly interested in studies that enhance our understanding of physiological processes and contribute to the development of diagnostic, monitoring, or therapeutic systems used in biology and medicine.

Drawing on my editorial experience, I will discuss the most common reasons manuscripts are rejected. These include a poor fit with the journal's scope, insufficient analysis or discussion of the authors' own data, methodological flaws, weak organization and presentation, and ethical concerns. The goal of this talk is to help researchers— especially early-career scientists — understand the expectations of the editorial board and how to avoid frequent mistakes. By aligning submissions with the journal's mission and maintaining high scientific and ethical standards, authors can significantly improve their chances of successful publication.

Oral Session OS09
Modeling Physiological Systems in Health and Disease
Chairs: Joanna Stachowska-Piętka (Poland), Leszek Pstraś (Poland)
OP063–OP066

OP063

Linear vs. nonlinear diffusion according to Linear Nonequilibrium Thermodynamics

Jacek WANIEWSKI

Nalecz Institute of Biocybernetics and Biomedical Engineering PAS, Warsaw, Poland
Corresponding author. *E-mail address*: jwaniewski@ibib.waw.pl

Keywords: membrane transport, diffusion, convective transport, osmosis

Motivation and Aim: In spite of widely used linear Fickian description of diffusion, the derivation of transport equations from Linear Nonequilibrium Thermodynamics by Kedem and Katchalsky (KK) in 1958 yielded the diffusion parameter proportional to solute concentration [1]. We attempted an alternative derivation that, depending on assumptions, provides the KK formula or, for non-osmotic case, constant diffusion parameter as proposed by Fick [2].

Novelty: The new derivation yields linear diffusion of solute in solvent, but in osmotically active media (permselective membranes, porous structures an additional term proportional to osmotic pressure decreases the effectiveness of diffusive transport.

Methods: The general scheme of mass transport processes of Linear Nonequilibrium Thermodynamics is applied with specific assumptions for the Onsager parameters. The case of ideal diluted solution is considered and the transport equations are transformed for the description of volumetric flux and separate description of diffusion and convective transport. The hydrostatic pressure gradient is eliminated from the solute transport equation.

Main results: The obtained formula for solute diffusivity parameter, D, according to the KK model is: $D_{KK} = RT\left(L_{S,KK} - \sigma^2 L_V\right)c$, c.f. [1], whereas according to the new model is: $D_N = RT\left(L_{S,N} - \sigma^2 L_V c\right)$, where $L_{S,KK}$, $L_{S,N}$ and L_V are derived from the Onsager solute and volume transport parameters, σ is the Staverman reflection coefficient, and c is the molar concentration of solute. Note that free diffusion parameter, i.e., without induced osmosis, $\sigma = 0$, in the KK model is still dependent on concentration, while according to the new formula it is a constant as in [2].The general equation for solute transport contains also the convective component, and the description of volumetric flux is the same in both models [1]. The exemplary numerical simulations for of the transport in diffusion chamber show the possible difference between the investigated transport models and the Fick formula.

Conclusion: The linear Fickian diffusive law can be derived from Linear Nonequilibrium Thermodynamics for free diffusion, however in the osmotically active media the diffusive parameter is modified due to osmotic effect and contains a component proportional to solute concentration.

References:

[1] Kedem O, Katchalsky A. Thermodynamic Analysis of the Permeability of Biological Membranes to Non-Electrolytes. Biochim Biophys Acta. 1958;27(2):229-46.

[2] Fick A. On Liquid Diffusion (Reprinted from the London, Edinburgh, and Dublin Philosophical Magazine and Journal of Science, Vol 10, Pg 30, 1855). J Membrane Sci. 1995;100(1):33-8.

OP064

Indirect application of machine learning to estimate parameters of cancer growth and response to treatment in individual patients

Jarosław ŚMIEJA*, Krzysztof ŁAKOMIEC, Artur WYCIŚLOK, Andrzej ŚWIERNIAK, Krzysztof FUJAREWICZ

Silesian University of Technology, Gliwice, Poland

* ***Corresponding author***. *E-mail address*: Jaroslaw.Smieja@polsl.pl

Keywords: Mathematical modeling, Cancer treatment, Personalized medicine, Machine learning

Motivation and Aim: Black-box models using machine learning techniques for predicting individual treatment outcomes in personalized medicines are very useful but have two important disadvantages. First, they are useless if a new type of treatment or significantly changed treatment protocol is introduced as they require new learning cycle based on available clinical data to provide reliable prognosis. Second, they do not answer the questions why a specific outcome is predicted and how it could be improved. On the other hand, models based on describing treatment with ordinary differential equations (ODEs) provide means to test alternative treatment protocols but require model parameters estimation which is difficult, if possible at all, for individual patients, due to scarcity of available data that would relate directly to processes taken into account in the model. Construction of a hybrid model that would combine ODE modeling with machine learning used to estimate parameters of the model, instead of the treatment outcome should help in using the best of these two approaches.

Novelty: This paper presents an universal method combining ODE and machine learning techniques to describe disease dynamics, predict treatment outcome and provide information about patient data crucial for estimating model parameters. Using adjoint sensitivity analysis makes it possible to apply backpropagation technique to train the artificial neural network whose desired output (actual parameter values) is not known. Instead, training is based on the output of a dynamical model that is compared to clinical data. Such hybrid model allows to test alternative treatments for an individual patient in silico, taking into account current patient state. Applicability of such approach has been tested with analysis of cancer growth, metastasis and anticancer treatment with Kaplan-Meier survival curves showing Metastasis Free Time and average prediction error for metastasis time as quality indices.

Methods: Cancer growth, metastasis and response to adjuvant radio- and chemotherapy was modeled by a simple ODE model [1] and related to clinical data on non-small cell lung cancer patients. A multilayer artificial neural network was used to determine parameters of this model. Training was performed using clinical data on metastasis free time and overall survival. Blood morphology results were entered as input data for the artificial neural network. For backpropagation in training, the adjoint sensitivity analysis [2] was applied.

Main results: Kaplan-Meier survival curves obtained from simulation corresponded to the clinical curves, proving applicability of the proposed method. Predictions of metastasis free

time for individual patients varied with respect to their accuracy, depending on the cancer stage at the moment of diagnosis. However, it must be stressed that only basic blood morphology results were used and they might not be of sufficient predictive value. Nevertheless, using the machine learning subsystem that provides means for linking clinical data to model parameters of a dynamical system not only facilitates reliable testing of alternative treatment protocols but through that linking opens way for a new explainable AI in biomedical applications.

Conclusion: Though only a single instance of the proposed method was developed for specific group of patients and specific treatment, the method that combines machine learning and ODE-based modeling opens new application areas. It allows to overcome one of the major obstacles in effectively using mathematical modeling as a tool for planning individual patient treatment and predicting its outcome

Acknowledgements: This work was partially supported by the SUT internal grant 02/040/BK_25/1070 and project FESL.10.25-IZ.01-07E7/23

References:

[1] Wyciślok A, Śmieja J, Metastasis modelling approaches - comparison of ideas. In: The latest developments and challenges in biomedical engineering. Proceedings of the 23rd Polish Conference on Biocybernetics and Biomedical Engineering, Lodz, Poland, September 27-29, 2023 / Strumiłło Piotr [et al.] (eds.), Lecture Notes in Networks and Systems, 2024, vol. 746, Cham, Springer, s.199-214, doi:10.1007/978-3-031-38430-1_16

[2] Fujarewicz K, Lakomiec K. Adjoint sensitivity analysis of a tumor growth model and its application to spatiotemporal radiotherapy optimization. *Math Biosci Eng.* 2016;13(6):1131-1142. doi:10.3934/mbe.2016034

OP065

Prognostic Value of Early Interictal Epileptiform EEG Patterns in Ischemic Stroke: A Predictive Model for Functional Outcomes

Katerina ISCRA[1], Edoardo RICCI[2], Andrea BONINI[1], Giovanni FURLANIS[2], Michele MALESANI[2], Paola CARUSO[2], Marcello NACCARATO[2], Paolo MANGANOTTI[2], Agostino ACCARDO[1], Miloš AJČEVIĆ[1]

1 Department of Engineering and Architecture, University of Trieste, Italy

2 Clinical Unit of Neurology, Department of Medical Sciences, University Hospital and Health Services of Trieste, University of Trieste, Italy

katerina.iscra@phd.units.it

Abstract. An accurate prediction of clinical outcomes in acute ischemic stroke is essential for improving patient management. There is growing research interest in EEG- based neurophysiological biomarkers. In this context, although the prevalence of epileptiform patterns is emerging, their role as potential predictors of outcome is still poorly investigated. In this study, we investigate whether interictal epileptiform discharges (IEDs) detected in the acute phase can contribute to predicting long-term functional outcomes in treated ischemic stroke patients and to the development of a predictive model. We retrospectively analyzed clinical, neurophysiological, and neuroimaging data from 228 acute ischemic stroke patients (mean age: 74±14 years; 122 females). Patients were classified into two groups based on their 3-month modified Rankin Scale (mRS) scores: good outcomes (mRS 0–2, 127 patients) and poor outcomes (mRS 3–6, 101 patients). Standard 19-channel EEG recordings were conducted to assess epileptiform abnormalities and IEDs. Feature selection was performed based on the Gain Ratio method, and predictive models were developed using five different machine learning (ML) techniques: classification tree, logistic regression, naïve Bayes, artificial neural network, and support vector machine. Our results identified the National Institutes of Health Stroke Scale (NIHSS) at admission, mRS anamnestic, chronic heart failure, acute infectious disease, sum of lobes with a infarct area, atrial fibrillation, and IEDs as significant predictors of ischemic stroke functional outcomes. Logistic regression achieved the best performance, with an accuracy of 81% and an AUC of 0.83. These findings confirm the importance of clinical and radiological features while also highlighting the predictive value of interictal EEG epileptiform patterns for stroke outcome prediction.

Keywords: EEG, Interictal epileptiform discharges, Ischemic stroke, Machine learning

Special Symposium SE07b
IFMBE, Students and Recent Graduates Working Group: How Can We Bring Innovation to Socially Impactful Research Through the Effective Use of Emerging Technologies?
Chairs: Martha Zequera (Colombia), Piotr Ladyzynski (Poland), Anna Stecka (Poland)
OP067–OP070

OP067

Development of an Innovative Methodological Model for the Integration of Emerging Technologies in the Development of Medical Devices with Social Impact

Leslie Y. CIEZA HUANE

Universidad Peruana Cayetano Heredia, Faculty of Engineering, Lima, Peru

* ***Corresponding author***. *E-mail address*: leslie.cieza@upch.pe

Keywords: Medical Devices, Emerging Technologies, GAITS, VDI

Motivation and Aim: The integration of emerging technologies such as artificial intelligence (AI), the Internet of Things (IoT), big data, and blockchain into medical device development has significant potential to transform healthcare delivery. Despite these advantages, major challenges persist in interoperability, data privacy, regulatory complexities, and high implementation costs. This research aims to propose an innovative and structured methodological model that effectively addresses these challenges, facilitating the successful integration of emerging technologies into medical devices while ensuring significant social impact.

Novelty: Recent literature underscores the significance and complexity of integrating emerging technologies in medical device development. Ching et al. (2024) identified critical challenges such as data interoperability, ethical concerns, and cybersecurity but did not propose a structured methodological framework. Ferri et al. (2022) focused on clinical and economic evaluation frameworks without detailing a clear methodology for technological integration. Sharma et al. (2024) emphasized interdisciplinary stakeholder involvement but lacked a structured methodological model. The existing gap, therefore, is the absence of a systematic and replicable methodological framework that explicitly integrates technological feasibility, regulatory compliance, ethical considerations, and stakeholder engagement in medical device development. This research addresses this gap by uniquely combining the GAITS (Guidance and Impact Tracking System) and VDI (Verein Deutscher Ingenieure) methodologies, providing a structured and comprehensive approach specifically designed to overcome these complexities.

Methods: The proposed methodological model integrates GAITS and VDI frameworks to create a structured process encompassing technological feasibility, regulatory compliance, ethical considerations, and stakeholder involvement. This approach has been empirically validated through its application in the Biomedical Instrumentation course at Universidad Peruana Cayetano Heredia, where engineering students developed innovative medical device prototypes addressing real-world healthcare challenges.

Main results: Several case studies demonstrate the feasibility and impact of the proposed methodology. Students successfully developed prototypes integrating IoT, AI, and data analytics, improving elderly patient monitoring and safety. A comparative analysis of prototypes highlights key advantages, including increased autonomy, real-time health tracking, and early warning systems. Until now we have obtained data for 225 students.

Conclusion: The integration of GAITS and VDI methodologies offers a robust solution for overcoming the technical, ethical, and regulatory challenges inherent in developing innovative medical devices. The proposed model ensures effective technology integration with substantial social impact, making it a valuable tool for academia and industry stakeholders aiming to foster sustainable and impactful healthcare innovation.

Acknowledgements: The author acknowledge Universidad Peruana Cayetano Heredia for supporting the implementation of this study

References:

1. Ching KW, Tan SY, Lee PH. Developing medical devices with emerging technologies: trends, challenges, and future direction. F1000Research. 2024;13:1007.
2. Sharma A, Kumar V, Singh R, Gupta D. Developing medical devices with emerging technologies: trends, challenges, and future direction. ResearchGate. 2024. Available from: https://www.researchgate.net/publication/383768835
3. Ferri S, Drummond M, Tarricone R. Emerging Technologies for Medical Devices: A Health Technology Assessment Perspective. Value in Health Regional Issues. 2022;32:100-107.

OP068

A Robotic System Integrating the Semmes-Weinstein Monofilament (SWM10g) for Automated Plantar Sensory Evaluation: Novel Approach for Early DPN Detection

César Augusto MORENO BARACALDO[1], Martha ZEQUERA DÍAZ, PhD[2]

1 Pontificia Universidad Javeriana, Department of Electronics Bioengineering Lab Baspi-Footlab

caugustomorenob@javeriana.edu.co, mzequera@javeriana.edu.co

Bogotá D.C. Colombia

Abstract. The present study introduces an automated device for the controlled application of the Semmes-Weinstein 10g monofilament (SWM-10g), designed for quantitative assessment of plantar sensitivity and early detection of diabetic peripheral neuropathy (DPN). As a common complication of diabetes mellitus, DPN increases the risk of lower extremity ulceration and amputation. Our research introduces an innovative automated application technique for SWM10g, characterized by its unique design, efficient methodology, and significant advantages in reduced size and enhanced portability compared to previous approaches documented in scientific literature [19], [20], [21]. Ten healthy Colombian volunteers (4 men, 6 women; aged 20-50 years) participated with University Ethics Committee approval. Assessments covered six regions on each foot's plantar surface, with three repetitions per region, totaling 360 measurements. Results were consistent between both methods, reporting normal tactile plantar sensitivity thresholds below 5.0 grams-force with a mean of approximately 1.0 grams-force. Participants reported positive sensitivity with the traditional manual SWM-10g monofilament test, which demonstrated 100% specificity. Sensitivity comparisons across all contact points revealed that the 1st metatarsal and calcaneal branch points exhibited significantly lower sensitivity compared to other evaluated points ($p < 0.01$). Gender-based comparative analysis yielded no statistically significant differences. This research is preliminary and focuses on the innovation of a device for the evaluation and measurement of plantar sensitivity, with clinical evaluation not being its main objective. The clinical assessment and results presented in this study constitute complementary work carried out to test the equipment's functionality, which also explains the limited number of subjects included in the study. Further refinement of the development is recommended before subsequent evaluation in patients with DPN, complemented by comparisons with nerve conduction studies (NCS) and autonomic function testing (AFT) for early detection of sensitivity loss. The methodology establishes groundwork for the quantitative assessment of plantar sensitivity thresholds and demonstrates potential for enhanced accuracy.

Keywords: Diabetes mellitus, Foot ulcer prevention, Medical robotics, SWM-10g monofilament, Electronic measurement system, Embedded electronic device, Nerve conduction studies (NCS), Autonomic function testing (AFT)

OP069

AI-based tool to support clinical decisions using predictive factors derived from tumor-infiltrating lymphocyte quantification in breast cancer

Shrief ABDELAZEEZ[1*], Alessio FIORIN[2,3,4], Carlos LOPEZ[2,3,4], Laia ADALID[2,3], Marylene LEJEUNE[2,3,4], Anna KORZYNSKA[1]

1 Laboratory of Analysis and Processing of Microscopic Image, Nałęcz Institute of Biocybernetics and Biomedical Engineering Polish Academy of Sciences, Ks. Trojdena 4, 02-109 Warsaw, Poland

2 Oncological Pathology and Bioinformatics Research Group, Institut d'Investigació Sanitària Pere Virgili, Tortosa, Spain

3 Department of Pathology, Hospital de Tortosa Verge de la Cinta, Institut Català de la Salut, Tortosa, Spain

4 Department of Computer Engineering and Mathematics, Universitat Rovira i Virgili, Tarragona, Spain

* ***Corresponding author***. *E-mail address*: sabdelazeez@ibib.waw.pl

Keywords: Artificial Intelligence, Tumor-Infiltrating Lymphocytes (TILs), Breast Cancer, Histopathological Imaging, Stromal TILs Quantification, Clinical Decision Support, Active Learning, Deep Learning

Motivation and Aim: Breast cancer is one of the most common cancers globally, and measuring stromal Tumor-Infiltrating Lymphocytes (sTILs) is crucial for predicting patient outcomes and guiding treatment. However, the manual quantification of sTILs by pathologists is time-consuming, subjective, and prone to human error. This study aims to develop an AI-based tool to automate the quantification of sTILs in histopathological images, helping pathologists make accurate and consistent clinical decisions.

Novelty: This work introduces a novel dual-pathway AI framework designed to analyze breast cancer histopathological images. Unlike existing methods, the proposed tool integrates two parallel deep learning pathways: one for the detection and segmentation of TILs and another for the identification of stromal regions. The outputs are combined using a quantification algorithm to estimate the sTILs score. Additionally, the framework incorporates an active learning approach, where pathologists provide offline feedback to refine the TILs segmentation model, reducing false positives, false negatives and enhancing reliability. This combination of dual-pathway analysis and active learning represents a significant advancement in the field of computational pathology.

Methods:

The AI tool leverages a dual-pathway deep learning framework to analyze regions of interest (ROIs) in H&E-stained whole slide images (WSIs) of breast cancer. The first pathway employs an AttentionUNet model for TILs detection and segmentation, chosen for its ability to focus on relevant features and improve segmentation accuracy in histopathological images. The second pathway utilizes a DeepLabV3+ model with a ResNet101 backbone for stromal region

segmentation, chosen for its superior feature extraction capabilities and efficiency in processing large-scale image data. The outputs from both pathways are integrated using a quantification algorithm that calculates the sTILs score by estimating the area of TILs within the stroma divided by the total stromal area, multiplied by 100 to yield a percentage score.

To enhance model performance, an active learning approach was implemented, where pathologists provided feedback on false-positive TILs predictions, enabling iterative refinement of the segmentation model. The study utilized two datasets: a private dataset comprising 10 WSIs for TILs segmentation annotated by three different pathologists and 60 WSIs for sTILs scoring evaluation (with ROIs annotated and scored by a single pathologist), and the publicly available BCSS dataset for stroma region segmentation. *Figure 1* provides a comprehensive overview of the AI tool's framework, highlighting the dual-pathway architecture, the quantification process, and the active learning feedback loop.

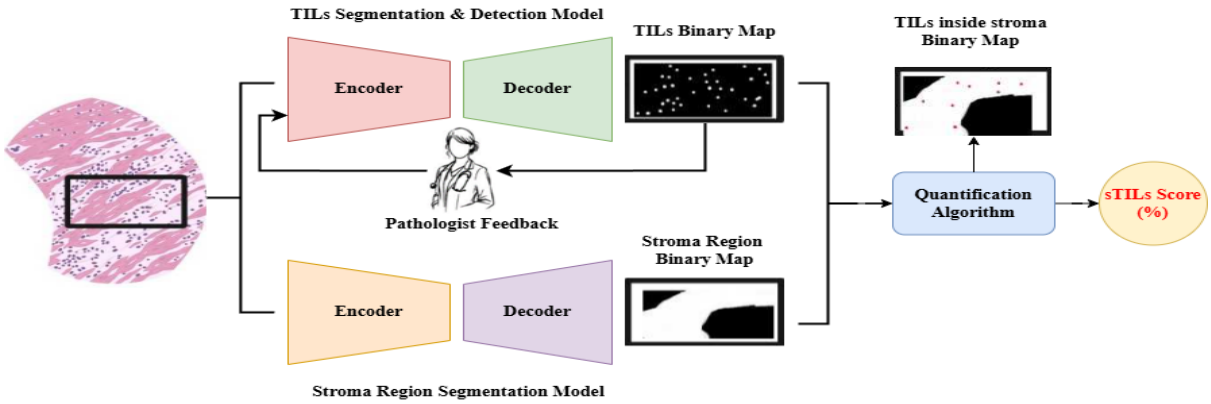

Figure 1: AI Tool Framework for sTILs Scoring.

Main results: The proposed AI tool demonstrated strong performance in sTILs quantification, achieving a high correlation with pathologist evaluations. Regression and correlation analyses were conducted on the 60 ROIs, and the results are presented in a detailed *Table 1*. The tool's ability to accurately quantify sTILs across varying levels of immune infiltration highlights its potential as a reliable decision-support tool in clinical settings.

Table 1: Statistical Analysis to assess AI tool performance

Correlation Analysis	Regression Analysis	Agreement
Spearman	R2 Square	Kappa Index
0.6928	0.7554	0.6608

Conclusion: This study introduces a robust AI tool for sTILs quantification in breast cancer histopathology, overcoming manual assessment limitations. By combining a dual-pathway deep learning framework with active learning, it delivers accurate, reproducible sTILs scores, aiding pathologists in clinical decision-making which improve processes in healthcare, enables personalized patient treatment and care.

Acknowledgements: This study is part of the BOSOMSHIELD European Project, funded under the Horizon Europe Research and Innovation Program (Grant Agreement No. 101073222).

OP070

Deep Learning-Based Classification of Thermograms from Plantar Region

Santiago MARTINEZ[1*], Marta ZEQUERA[2]

1 Pontificia Universidad Javeriana, Electronics department, Bogotá, Colombia

2 Pontificia Universidad Javeriana, Electronics department, Bogotá, Colombia

* ***Corresponding author***. *E-mail address*: *ramirez_santiago@javeriana.edu.co*

Keywords: Plantar Thermograms, Deep Learning, Convolutional Neural Networks

Motivation and Aim: Diabetic foot complications are a major health concern, often leading to severe conditions such as ulcers and amputations if not detected early. Thermographic imaging has emerged as a promising, non-invasive tool for identifying abnormal temperature patterns associated with diabetic foot pathology. However, accurately classifying plantar thermograms remains a challenge due to variations in temperature distribution and the need for robust automated analysis methods.

This study aims to develop a deep learning-based classification model for plantar thermograms using Convolutional Neural Networks (CNNs) to improve detection accuracy. By incorporating advanced architectures such as ResNet and U-Net, along with data augmentation techniques, and a new dataset taken in the Footlab-BASPI laboratory, we seek to enhance model generalization and optimize classification performance under 5 classes based on the thermal change index (TCI).

Novelty: This study introduces a comparison between deep learning-based approaches for classifying plantar thermograms, specifically designed for diabetic foot screening. We employ Convolutional Neural Networks (CNNs), including ResNet and U-Net architectures, to enhance feature extraction and classification accuracy. Additionally, we apply data augmentation techniques to a dataset of 374 thermograms, from 132 diabetic patients and 55 healthy controls to improve model generalization.

Methods: This study compares deep learning methods to classify plantar thermograms, aiming to detect abnormal temperature patterns linked to diabetic foot complications. The normal temperature pattern is the butterfly pattern, found in the control group, the TCI measures how far is the distribution of temperatures from the control group in 5 classes, as shown in table 1. A dataset of 374 thermograms was expanded and diversified through data augmentation techniques such as rotation, flipping, scaling, and intensity adjustments. These enhancements aimed to improve the model's robustness and generalization across varied thermogram samples.

Table 2. TCI ranges for each class.

Class	TCI range (℃)	Quantity of thermograms	Quantity of thermograms after data augmentation
Class 1	$TCI \leq 2$	110	330
Class 2	$2 < TCI \leq 3$	50	150
Class 3	$3 < TCI \leq 4$	55	165
Class 4	$4 < TCI \leq 5$	68	204

Class 5	TCI > 5	91	273

Comparisons between Convolutional Neural Networks (CNNs) were made, specifically between ResNet for its feature extraction capabilities and U-Net to enhance the segmentation of key temperature regions. A hybrid model combining both architectures was also tested and compared. The models were trained on thermograms categorized into five classes based on the Thermal Change Index (TCI), with performance evaluated through metrics coming from the confusion matrix (accuracy, precision, recall, F1-Score). Hyperparameter tuning further refined the models, the dataset was split into 80% train and 20% validation and test.

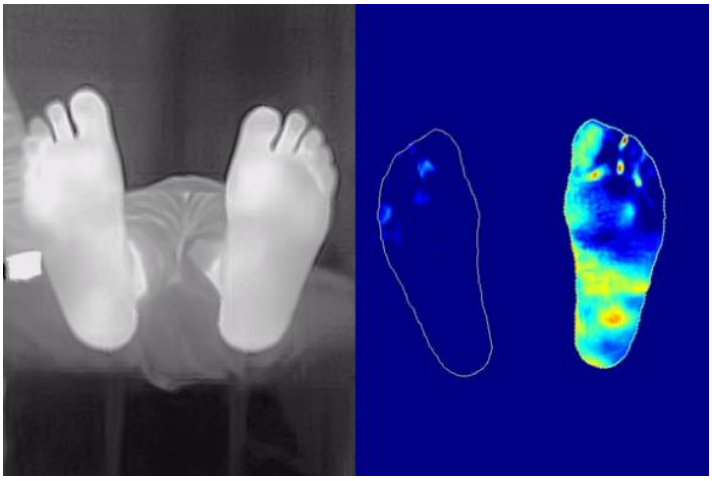

Figure 2. Example from the database taken in the Footlab BASPI laboratory (STANDUP project).

Main results: The hybrid deep learning-based classification approach demonstrated strong performance in distinguishing plantar thermograms based on the Thermal Change Index (TCI). The combination of ResNet and U-Net architectures proved to be particularly effective, enhancing both feature extraction and spatial analysis of thermographic patterns, with an accuracy of 87%. The application of data augmentation techniques contributed to improved model generalization, enabling robust classification across an expanded dataset. Additionally, evaluation on thermograms from the Footlab - BASPI laboratory confirmed the model's applicability in real-world conditions.

Overall, the hybrid architecture achieved promising classification results, highlighting the potential of deep learning techniques for advancing diabetic foot screening through automated thermogram analysis.

Conclusion: This study demonstrates the potential of deep learning-based approaches for the classification of plantar thermograms, offering a promising solution for early detection of diabetic foot complications. By leveraging a combination of the architectures ResNet and U-Net, along with data augmentation techniques, we have developed a robust and efficient model capable of accurately classifying thermograms based on the Thermal Change Index (TCI).

The results indicate that deep learning, particularly CNNs, can significantly improve the accuracy and reliability of thermogram analysis, supporting clinical decision-making and enhancing the screening process for diabetic foot conditions. With the successful application of this approach to the Footlab - BASPI dataset, we highlight the feasibility of integrating deep learning models into clinical practice for non-invasive, automated diabetic foot screening.

Oral Session OS10
Assistive Technologies and Rehabilitation Engineering
Chairs: Lenka Lhotska (Czech Republic), Paweł Strumiłło (Poland)
OP071–OP074

OP071

Vision and Vibration-Based Feedback System to Support Situational Awareness of Uniformed Services Officers

Mateusz URBAN[1*], Ignacy STENCEL[2], Mateusz SUDEJKO[3], Szymon CYGAN[1]

1 Warsaw University of Technology, Faculty of Mechatronics, Institute of Metrology and Biomedical Engineering, Poland
2 Warsaw University of Technology, Faculty of Mechatronics, Institute of Micromechanics and Photonics, Poland
3 Warsaw University of Technology, Faculty of Mathematics and Information Science, Poland
**Corresponding author. E-mail address: mateusz.urban2.stud@pw.edu.pl*

Keywords: Vibration-Based Feedback, Hazard Detection, Wearable Technology

Motivation and Aim: Law enforcement officers often face threats from outside their field of vision, limiting their situational awareness and increasing the risk of injury [1]. This study aims to develop a vibration-based feedback system that enhances users' ability to detect and locate potential hazards outside their visual field using real-time computer vision and vibration-based stimulation.

Novelty: The proposed system integrates object detection cameras with vibration-based actuators to create an intuitive, wearable hazard detection system. The system maps detected objects to vibration-based feedback zones, offering real-time guidance for the user. Unlike previous solutions, this approach provides spatial awareness without visual or auditory distractions [2].

Methods: The system employs two cameras for object detection and depth estimation using YOLOv8 and stereo vision techniques [3, 4]. The detected object's angular and distance coordinates are transmitted via Bluetooth to a microcontroller, which activates vibration-based actuators. Six actuators correspond to six 20° angular ranges, while detection distances of up to 18 meters are divided into six subranges, each with distinct vibration patterns. The prototype was tested on 33 volunteers, who identified simulated threats based solely on vibration-based feedback. Accuracy and error patterns were analyzed.

Main results: The system achieved a 68.4% accuracy rate in hazard localization across 297 test points. Analysis of error patterns revealed that angular misinterpretations were more frequent than distance errors. Common user feedback highlighted issues with device comfort,

actuator density, and signal interpretation. Notably, hazards within 1.5 meters were identified with 94% accuracy, suggesting strong potential for close-range threat detection.

Conclusion: This study demonstrates the feasibility of a vibration-based feedback system for enhancing situational awareness in law enforcement. Improvements in actuator placement, signal differentiation, and device ergonomics are necessary for practical implementation. Future research will focus on optimizing signal processing, expanding testing cohorts, and refining the system for real-world deployment.

Acknowledgements: This research was supported by the Institute of Metrology and Biomedical Engineering, Warsaw University of Technology as a part of the Assistant Intern position.

References:

[1] FBI. 'LEOKA' Law Enforcement Officers Killed and Assaulted. Retrieved from https://ucr.fbi.gov/leoka
[2] Dagnelie, G. Visual Prosthetics: Physiology, Bioengineering, Rehabilitation. Springer, 2011.
[3] Leigh, R. J., & Zee, D. S. The Neurology of Eye Movements. Oxford University Press, 1999.
[4] Howard, I. P., & Rogers, B. J. Binocular Vision and Stereopsis. Oxford University Press, 1995.

OP072

Enhancing Cognitive and Motor Skills through Personalized Digital Games

Petr NOVAK[1],Lenka LHOTSKA[1,2]

1 Czech Institute of Informatics, Robotics and Cybernetics, Czech Technical University in Prague, Jugoslavskych partyzanu 1580/3, 160 00 Prague 6, Czech Republic

2 Faculty of Biomedical Engineering, Czech Technical University in Prague, nam. Sitna 3105,

272 01 Kladno, Czech Republic

lhotska@cvut.cz

Abstract. Maintaining cognitive function and fine motor skills is crucial for healthy aging, enabling older adults to remain independent, engaged, and enjoy a high quality of life. However, both cognitive abilities and motor skills can de- cline with age, impacting daily activities and overall well-being. Cognitive games, particularly those incorporating a motor component, offer a promising approach to address this challenge. In the paper we describe our ongoing research that is focused on design and development of a suite of digital games and tasks designed to train fine hand motor skills, eye-hand coordination, perception, visual field, and other cognitive abilities. These games are specifically tailored for individuals who cannot use standard mouse and keyboard interfaces, primarily targeting the elderly, post-stroke patients, and individuals recovering from upper limb fractures. We present already developed games and results of analysis based on user acceptance testing. In the conclusion we propose future enhancements.

Keywords: cognitive game, motor skills, cognitive impairment, personalization, user acceptance

OP073

Detection of Limb Movement Related Events from EEG Signals Using ARMA Models

Bartłomiej SZTYLER*, Paweł STRUMIŁŁO

Institute of Electronics, Lodz University of Technology, Poland

* ***Corresponding author***. *E-mail address*: bartlomiej.sztyler@dokt.p.lodz.pl

Keywords: EEG, Motor Imagery, Signal modelling, AR, ARMA

Motivation and Aim: Motor imagery (MI) and motor execution (ME) classification play a crucial role in the development of brain-computer interfaces (BCIs), offering potential applications in neurorehabilitation, assistive technologies, and human-computer interaction[1]. While ME detection is relatively well-established due to its stronger neural activation, MI classification remains challenging due to its inter-subject variability[2]. Traditional spectral analysis methods, such as power spectral density (PSD), may not always be optimal for capturing the temporal dynamics of EEG signals, while modern machine learning and deep neural network approaches[3], despite their potential, are often computationally expensive, and may not be well-suited for real-time applications.

The aim of this study is to evaluate the effectiveness of parametric autoregressive (AR) modelling techniques[4] in extracting discriminative features for MI and ME classification.

Novelty: Unlike previous applications of AR modelling in EEG analysis, our work focuses on its optimization for the classification of motor imagery (MI) and executed movements (ME). The idea lies in determining coefficients that capture differences between MI and ME states, leading to improved ME and MI detection accuracy.

Methods: The data used in this study were obtained from the "EEG Motor Movement/Imagery Dataset"[5], a publicly available dataset provided by PhysioNet. This dataset contains EEG recordings of subjects performing motor execution and motor imagery tasks. The methodology consists of the following steps:

1. EEG Preprocessing: raw EEG signals are filtered using a bandpass filter (8–30 Hz) to isolate sensorimotor rhythms, particularly the μ (8–13 Hz) and β (13–30 Hz) bands, which are associated with motor activity. A common average reference (CAR) is applied to minimize noise and inter-electrode variability. EEG trials are segmented into fixed-length windows based on event markers, ensuring sufficient temporal resolution for classification.
2. Stationarity Analysis: the Augmented Dickey-Fuller (ADF) test is applied to assess whether EEG signals are suitable for AR modelling.
3. Feature Extraction via AR Modelling: an AR model of order p is fitted to each EEG segment, where p is optimized using Akaike Information Criterion (AIC) to prevent under and overfitting. The AR coefficients serve as feature vectors representing the temporal dynamics of EEG signals for classification.
4. Classification using LDA: Extracted AR features are used as input for a Linear Discriminant Analysis (LDA) classifier. LDA is chosen due to its computational efficiency and ability to maximize class separability, making it well-suited for real-time EEG classification.

Main results: The proposed parametric modelling approach demonstrates promising results in detecting MI and ME states. Key findings include:

- Classification Accuracy: The mean classification accuracy across all patients is 76.37%, with a standard deviation (SD) of 4.26%. highlighting the robustness of parametric features for executed movement detection. The mean classification accuracy for MI is 67.66%, with SD of 7.14%., reflecting the inherent challenges of distinguishing imagined movements based on EEG signals.
- Feature Discriminability: AR coefficients extracted from ME trials exhibited higher discriminability compared to MI trials, suggesting that executed movements produce more distinct neural signatures.
- Inter-Subject Variability: While AR modelling provides stable features for ME classification, MI feature patterns showed significant variability across subjects, indicating the need for subject-specific model adaptation.

.

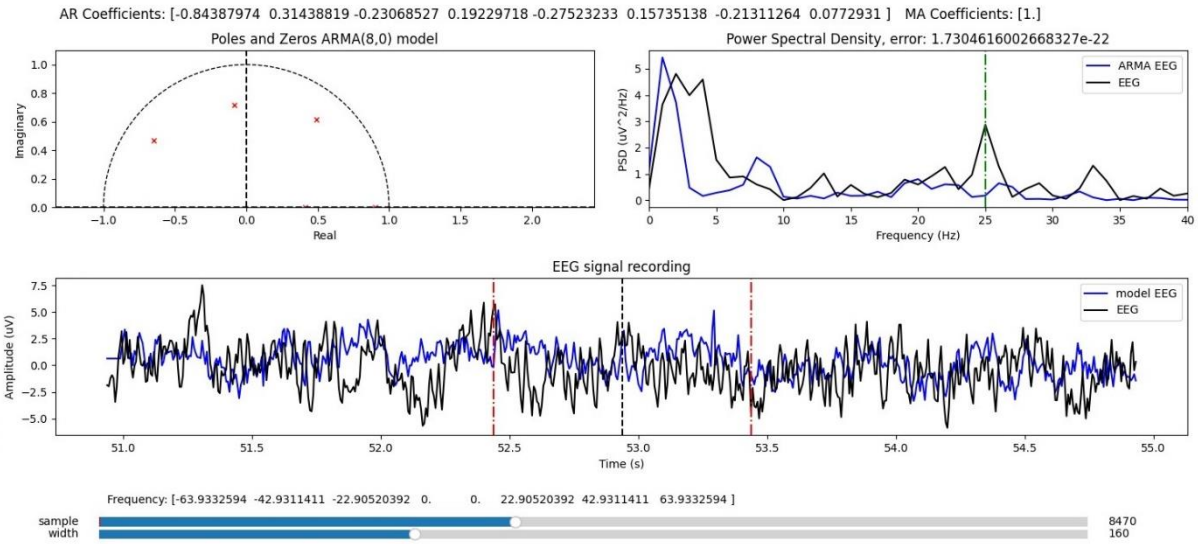

Figure 3 Screenshot of the developed application illustrating the EEG signal analysis from channel C3 for patient S014. The figure presents real and modeled signals, Z-plane plot, spectral representation, and time-domain graph with vertical markers indicating the analysis window width. Two sliders at the bottom allow for the selection of the measurement moment and the adjustment of the analysis window width.

Conclusion: This study demonstrates the potential of parametric modelling, specifically AR-based feature extraction, for EEG classification in MI and ME tasks. The findings suggest that AR coefficients can serve as meaningful features for BCI applications, particularly in executed movement detection. However, the lower classification accuracy for MI underscores the need for additional feature detection techniques, e.g. based on deep learning or hybrid approaches, to improve performance.

Acknowledgements: This work has been completed while the first author was the Doctoral Candidate in the Interdisciplinary Doctoral School at the Lodz University of Technology, Poland.

References:

[1] Mulder T. Motor imagery and action observation: cognitive tools for rehabilitation. J Neural Transm (Vienna). 2007;114(10):1265-78. doi: 10.1007/s00702-007-0763-z. Epub 2007 Jun 20. PMID: 17579805; PMCID: PMC2797860.
[2] Padfield, N., Zabalza, J., Zhao, H., Masero, V., Ren, J.: Eeg-based brain-computer interfaces using motor-imagery: Techniques and challenges. Sensors 19(6), 1423(2019)
[3] Al-Saegh, A., Dawwd, S.A., Abdul-Jabbar, J.M.: Deep learning for motor imagery eeg-based classification: A review. Biomedical Signal Processing and Control 63, 102172 (2021)

[4] Haderlein, J.F., Peterson, A.D., Burkitt, A.N., Mareels, I.M., Grayden, D.B.: Autoregressive models for biomedical signal processing. In: 2023 45th Annual International Conference of the IEEE Engineering in Medicine & Biology Society (EMBC).pp. 1–6. IEEE (2023)
[5] Schalk G, McFarland DJ, Hinterberger T, Birbaumer N, Wolpaw JR. BCI2000: a general-purpose brain-computer interface (BCI) system. IEEE Trans Biomed Eng. 2004;51(6):1034-1043. doi:10.1109/TBME.2004.827072

PLENARY LECTURE 4

PL4

High-Resolution Magnetoencephalography: A New Window to Human Brain Function?

Prof. Lauri Parkkonen, PhD (Finland)

The main research area of Parkkonen is non-invasive neuroimaging, mainly instrumentation and data analysis methods related to MEG as well as human neuroscience of sensory modalities and cognition. He has contributed to MEG instrumentation and signal processing methods that are currently in active use in over 100 laboratories world-wide. Currently he pursues the use of optically-pumped magnetometers for MEG, exploits real-time feedback of measurements of brain activity to study cognition and plasticity, both for basic neuroscientific research and for clinical applications. He is also coordinating a national consortium to develop a biobank for functional brain-imaging data.

Parkkonen has also contributed to ultra-low-field MRI research and to invasive monitoring of local cortical activity. In cognitive neuroscience, Parkkonen has shed light on the neural mechanisms of sensory processing, particularly conscious visual perception. Recently he has pioneered the emerging field of social neuroscience to uncover brain mechanisms supporting social interaction by using hyperscanning i.e. simultaneous recording of the brain activity of the interacting participants.

Aalto Brain Centre

Department of Neuroscience and Biomedical Engineering,

Aalto University School of Science

Finland

Oral Session OS11
Artificial Intelligence in Healthcare: Diverse Applications
Chairs: Paulo de Carvalho (Portugal), Fabiola Martinez-Licona (Mexico)
OP075–OP080

OP075

Neurosymbolic AI approach for dry and wet AMD classification using OCT images

Aleksandar MILADINOVIĆ[1], Alessandro BISCONTIN[1], Miloš AJČEVIĆ[2], Agostino ACCARDO[2], Dario MARANGONI[3], Daniele TOGNETTO[3], Leandro INFERRERA[3]

1 Institute for Maternal and Child Health IRCCS "Burlo Garofolo", Trieste, Italy

2 Department of Engineering and Architecture, University of Trieste, Trieste, Italy

3 Department of Medicine, Surgery and Health Sciences, Ophthalmology Clinic, University of Trieste, Trieste, Italy

Abstract. Accurate classification between dry and wet age-related macular degeneration (AMD) is crucial for determining appropriate treatment strategies and improving patient outcomes. However, deep learning convolutional neural networks (CNNs) often face challenges when working with small datasets, particularly in the context of rare pathologies, which can hinder their robustness and generalizability. To address these issues, we employed a neurosymbolic approach that integrates medical knowledge in the form of symbolic AI, enhancing the model's interpretability and reasoning capabilities. The aim of this study was to improve the classification of retinal conditions, specifically dry AMD, wet AMD, and healthy retinas. Our results demonstrated an overall accuracy of 93%, indicating the effectiveness of this methodology in accurately classifying retinal diseases. These findings suggest that the neurosymbolic approach holds promise for advancing diagnostic support in ophthalmology while providing a transparent decision-making framework.

Keywords: Neurosymbolic AI, Optical Coherence Tomography, OCT, Retinal imaging

OP076

Estimation of body ratios from Low-Resolution, Dual-Energy X-ray Images Using Convolutional Neural Networks

Kamil JANCZYK[1,2], Jacek RUMIŃSKI[1], Tomasz NEUMANN[1], Aleksandra SZYMCZYK[3], Piotr WIŚNIEWSKI[4]

1 Gdansk University of Technology, FETI, Department of Biomedical Engineering,

Gdansk, 80-233, Poland

kamil.janczyk@pg.edu.pl,

2 Ship Hydromechanics Division, Maritime Advanced Research Centre, Poland,

3 Department of Emergency Medicine, Medical University of Gdansk, Poland,

4 Department of Endocrinology and Internal Diseases, Medical University of Gdansk,

Poland

Abstract. Estimating body ratios from X-rays is an interesting re- search topic important for clinical applications such as assessing chil- dren's development or deviations from expected growth patterns. Re- search on these issues typically involves time-consuming and resource-intensive methods, such as manual body length measurements or high- resolution image annotations. We have proposed a preprocessing frame- work and adapted pre-trained convolutional neural network models to estimate the lengths of the body parts of children and young adults from low-resolution, dual-energy, whole-body, X-ray absorptiometry images. Furthermore, we proposed a solution for the automatic estimation of body ratios and the determination of samples significantly deviating from the average. The dataset of X-ray absorptiometry images was expanded with annotations of the length of individual body parts performed un- der the supervision of a specialist. The experimental results show that the proposed preprocessing techniques and the adapted convolutional neural network model achieved a mean relative error of up to 4.24 be- tween the estimated and annotated lengths of body parts percent and the Lin correlation coefficient of convergence of 0.92. It was shown that, by employing low-resolution images and deep learning methods, one can accurately estimate the lengths of specific body parts, facilitating the precise detection of samples that deviate from the average.

Keywords: Dual-energy absorption, convolutional neural network, body ratios

OP077

Genetic Algorithm for Predicting Primary Imatinib Resistance in Locally Advanced or Metastatic Gastrointestinal Stromal Tumors

Martina SASSI[1,2], Jacopo VITALE[1], Maria Elisabetta PAGNANO[1], Laura RISI AMBROGIONI[2], Margherita A.G. MATARRESE[1], Bruno Vincenzi[2], Leandro PECCHIA[1]

1 Research Unit of Intelligent Technology for Health and Wellbeing, Department of Engineering, Universit`a Campus Bio-Medico di Roma, Via Alvaro del Portillo, 21, 00128 Rome, Italy

2 Fondazione Policlinico Universitario Campus Bio-Medico di Roma, Via Alvaro del Portillo, 200, 00128 Rome, Italy

martina.sassi@unicampus.it

Abstract. Gastrointestinal stromal tumors (GISTs) are the most com- mon mesenchymal neoplasms, primarily driven by KIT or PDGFRA mutations. While tyrosine kinase inhibitors (TKIs), such as imatinib, have transformed treatment, resistance remains a significant challenge. Alter- native TKIs offer options but with increased toxicity and inconsistent efficacy. This study investigates artificial intelligence-driven radiomics for predicting primary TKI resistance in GIST patients. Sixteen patients were classified as imatinib-sensitive or -resistant based on CT scans taken at baseline and one year post-treatment. Expert radiologists manually segmented CT scans and extracted the volume of interest, composed of the principal mass and metastasis. A total of 93 radiomic features were extracted from each axial slice from the axial view. A genetic algorithm was implemented for feature selection and model hyperparameter optimization. The Support Vector Classifier demonstrated the highest accuracy (95%), underscoring the potential of AI-driven radiomics to guide personalized GIST treatment.

Keywords: artificial intelligence, genetic algorithm, gastrointestinal stromal tumors, machine learning, radiomics

OP078

Can machine learning models help identify infected wounds requiring antibiotic treatment?

Piotr FOLTYNSKI[1*], Piotr LADYZYNSKI[1], Karolina KRUSZEWSKA[2], Arkadiusz KRAKOWIECKI[3], Bozena CZARKOWSKA-PACZEK[2]

[1] Nalecz Institute of Biocybernetics and Biomedical Engineering, Polish Academy of Sciences, Warsaw, Poland

[2] Department of Clinical Nursing, Medical University of Warsaw, Warsaw, Poland

[3] PODOS Wound Care Clinic, Warsaw, Poland

* ***Corresponding author***. *E-mail address*: pfoltynski@ibib.waw.pl

Keywords: Wound infection, Image classification, Machine learning

Motivation and Aim: One of the reasons that slows down the healing of a wound is its infection. Therefore, it is important to recognize this condition, perform a microbiological test and introduce antibiotics for treatment. On the other hand, excessive use of antibiotics in wound treatment leads to the emergence of antibiotic-resistant strains, which is an undesirable phenomenon. Therefore, it is very important to correctly identify wounds that require antibiotic treatment. The aim of the study was to develop a machine learning (ML) model for wound image classification that would enable automatic determination of whether the wound is uninfected or it is infected and the patient requires antibiotic treatment.

Novelty: The accuracy of the model will be compared with the results of expert clinicians and nursing students.

Methods: We selected 445 photos showing wounds without infection. These wounds were not microbiologically tested. The remaining 454 photos showed infected wounds that had a positive microbiological test and the patient received antibiotic treatment. The photos were taken with Xiaomi Redmi Note 7 smartphone or Sony DSC-W810 compact camera. First, we created a test set by randomly selecting 82 images showing 42 uninfected and 40 infected wounds. Then from the remaining images, we randomly selected 154 for the validation set. The remaining 663 were the training set. We used five pretrained models from YOLO generation 8. These models were trained on the train data set and then their accuracy was verified on the test set. Accuracy was calculated as the ratio of well-classified wounds to the number of wounds that were assessed.

Main results: The models achieved a mean accuracy (±SD) of 0.929±0.013. The images from the test set were also evaluated for infection by six experts and six nursing students. They achieved an accuracy of 0.732±0.084 and 0.689±0.056, respectively. Statistical analysis revealed that the ML models were significantly better than the experts and the students, while the results of experts and students did not differ significantly.

Conclusion: The results of ML models in classifying wound images could significantly help physicians and clinicians in making decisions about prescribing antibiotics to patients with wounds.

OP079

Deep Multiple Instance Learning for Automated Tumor Positivity Score Prediction in Non-Small Cell Lung Cancer

Krzysztof PYSZ[1], Witold DYRKA[1*], Artur BARTCZAK[2], Jarosław KWIECIEŃ[3], Piotr KRAJEWSKI[3]

1 Politechnika Wrocławska, Wrocław, Poland

2 Specjalistyczny Szpital Chorób Płuc w Zakopanem, Zakład Patomorfologii, Zakopane, Poland

3 Cancer Center, Wrocław, Poland

* ***Corresponding author***. *E-mail address*: witold.dyrka@pwr.edu.pl

Keywords: Non-Small Cell Lung Cancer (NSCLC), Tumor Positivity Score (TPS), Deep Learning, Multiple Instance Learning (MIL), Histopathological Image Analysis

Motivation and Aim: Accurate assessment of TPS in NSCLC is critical for treatment planning and prognosis. However, current methods involve extensive manual labor and expertise due to the need for annotating individual slides. The aim of this study is to develop an automated deep learning approach using MIL to predict TPS at the slide level. This would reduce reliance on time-intensive manual annotations and expert resources while providing assistance by highlighting regions of high diagnostic value and offering preliminary TPS for experts' reference.

Novelty: The proposed method introduces an end-to-end pipeline that leverages MIL for predicting TPS without requiring detailed region-of-interest (ROI) labeling. By combining embedding extraction with a multilabel classification network and an aggregation model, this approach efficiently automates the assessment of TPS in NSCLC while drastically reducing the need for additional annotations, requiring only the overall score value.

Methods: The framework consists of two key components:

1) A multilabel classification deep neural network based on the MobileNetV3Large [1] architecture and trained on a publicly available dataset [2]. The architecture was chosen due to the combination of high accuracy in classifying tumor and background regions (92% and 99% respectively) and low parameter count, ensuring computational efficiency. While predicting the tissue type in each patch of an entire whole-slide image (WSI), the network effectively captures relevant histopathological features. As a result, it also functions as a low-resource embedding extractor by average-pooling activations from the final layer before the classifier. These embeddings are then passed to the next stage of the pipeline

2) A lightweight MIL model with gated attention trained on 136 WSIs, which leverages embeddings from tumor-classified patches to predict the overall TPS (0-100) for the entire slide. In addition, the model generates an attention map highlighting regions of interest,enabling further analysis of the most relevant patches.

OP080

Artificial Intelligence Models for Age and Sex Estimation from Electrocardiograms

Daniel ALBORNOZ[1], Cristian SPOSATO[1], Gustavo MESCHINO[1], Santiago MANZOLILLO[2], Virginia BALLARIN[1]

1 FASTA University, Mar del Plata, Argentina

2 Cardiology Institute of Corrientes, Argentina

vballari@ufasta.edu.ar

Abstract. The electrocardiogram (ECG) is a fundamental tool in cardiovascular evaluation, widely used in clinical settings due to its accessibility, low cost, and ease of application. Recent advances in artificial intelligence (AI) have expanded the potential applications, enabling the estimation of demographic characteristics such as age and sex from ECG signals. This study aims to develop and validate an AI model capable of estimating age and sex from ECG records in a local population, evaluating its performance compared to previous studies and analyzing its potential impact on clinical applications. A convolutional neural network (CNN) was trained using a dataset of 275,000 anonymized ECGs. The model achieved an 87% accuracy in sex classification and an average absolute error of 9 years for age estimation. These results suggest that the predicted age may serve as a biomarker for biological aging and cardiovascular risk. The integration of this AI tool into clinical practice could lead to more efficient patient stratification and optimize healthcare resource allocation

Keywords: Electrocardiogram, Artificial Intelligence, Age Estimation, Sex Classification, Machine Learning

Special Symposium SE09
IFMBE, Industry Committee – From Lab to Market: Bridging the Gap in Biomedical Innovation
Chairs: Piotr Ładyżyński (Poland), Jari Hyttinen (Finland), Martha Zequera Diaz (Colombia)
KL6, OP081–OP084

KL6

A journey of +25 years in the ecosystem of spin-off creation: a perspective of the academic innovators of ETRO.RDI

Johan STIENS

Vrije Universiteit Brussel, ETRO.RDI, Brussels, Belgium

* ***Corresponding author***. *E-mail address*: johan.stiens@vub.be

Keywords: Spin-off companies, Readiness levels, Entrepreneurial personality, Medical and Clinical affairs

Motivation and Aim: Spin-off creation is an important fuel for academic valorization and a catalyst for an innovative economy. However, the journey towards the creation of the academic spinoff is very bumpy. In an era of global grand challenges, the societal impact dimension is utmost crucial. This presentation aims at sharing the experience of successes and failures in crossing the chasm and discusses the role and importance of the interaction between all stakeholders in the ecosystem of today.

Novelty: In this presentation the journey of more than 25 years involvement in spinoff creation in the large research group "ETRO.RDI" recognized since 2005 as a group of expertise in applied research at VUB, will be critically assessed within the context of the evolution of the academic and societal framework. We highlight the importance of each single element in the value chain: alignment of the technical expertise with business acumen and navigating regulatory frameworks..

Methods: A multidimensional analysis of the spinoff venture from the academic entrepreneurial point of view will be discussed. All the readiness levels, far beyond the well-known technology readiness level (TRL) will be discussed. For ventures in the domain of biomedical engineering and healthcare, the extra dimension of the critical assessment of clinical, quality and regulatory affairs adds to the multi-dimensionality.

Main results: The complex interactions between all the stakeholders of the ecosystem are discussed to deliver the utmost important outcome to translate the innovative idea in business: the value proposition. Timing, regulatory affairs, agility, serendipity, resilience, and a multi-sectoral network are crucial elements of the matrix on the road to success..

Conclusion: This talk aims to equip attendees with practical insights to transform engineering breakthroughs into thriving enterprises. Whether you are considering launching a spin-off or

looking to refine your approach, this session offers a roadmap for turning engineering expertise into impactful, scalable businesses..

Acknowledgements: Author thanks the VUB for the financial support over the last 20 years for the IOF-GEAR program financing, more in particular the funding of the Tech4Health consortium for the period 2020-2025.

References:

[1] Spin-offs: reinforcing a vector of value creation for EU-27, The Deep Tech Opportunity, EU report 25-02-2025, https://digital-strategy.ec.europa.eu/en/library/spin-offs-driving-innovation-across-eu-27

OP081

Bioimpedance Method for Monitoring Chronic Wounds

Jari VIIK[1*], Atte KEKONEN[1,2], Magdalena ANTOSZEWSKA[3]

1 Faculty of Medicine and Health Technology, Tampere University, Finland

2 CutoSense, Littoinen, Finland

3 Department of Dermatology, Venereology and Allergology, Medical University of Gdansk, Poland

* ***Corresponding author***. *E-mail address*: jari.viik@tuni.fi

Keywords: Wound, Bioimpedance, Quantitative, Long-Term, Monitoring

Motivation and Aim: Chronic wounds pose a significant global health burden, often leading to prolonged suffering, increased healthcare costs, and elevated risk of complications. Current wound assessment methodologies are predominantly subjective, relying on visual inspection and manual measurement, and typically require the removal of dressings. This process not only disrupts the wound environment but also increases the risk of infection. There is a critical need for the development of quantitative assessment method that enables continuous monitoring of chronic wound status and healing progression without unnecessary dressing removal.

Novelty: The developed measurement system, WoundWatch®, enables non-invasive, long-term monitoring of chronic wounds without the need to remove the dressing. It incorporates an electrode-dressing array allowing for the simultaneous assessment of a larger wound area. The developed quantitative parameter, the Wound Status Index (WSI), provides an objective measure of wound healing progression.

Methods: The WoundWatch® system incorporates a purpose-built bioimpedance device, mobile measurement software, and a screen-printed electrode array. The method employs a two-electrode measurement technique to capture bioelectrical signals. The superficial layers of the skin exhibit high impedance, while the presence of a wound markedly reduces impedance. As the wound heals, the impedance increases. The impedances of the wound and healthy skin are measured separately. By relating the impedances of the wound and the impedance representing surrounding healthy skin, we have defined the quantitative parameter WSI representing the wound status[1]. The measuring device is connected to a connection cable from the electrode array located outside the dressing, eliminating the need to remove the dressing. The method and equipment[2] were tested on several acute wounds before the clinical proof-of-concept study[3]. The reference method in the clinical proof-of-concept study was the measurement of wound surface area using planimetry. The WoundWatch® system was further developed based on insights gained from the proof-of-concept study, leading to a clinical study measuring hard-to-heal wounds of various etiology[4] having digital planimetry as a reference. Currently, a clinical trial[5] concerning the monitoring of venous ulcers is ongoing at University Clinical Centre in Gdansk (Poland) and in Wound Center, Tampere University Hospital (Finland).

Main results: Initial evidence of the bioimpedance-based method's capability for assessing wound status was provided through testing with four acute wounds[1]. Long-term measurement was demonstrated by 142 hours of continuous monitoring of wound healing from beneath the

primary dressings[2]. The clinical proof-of-concept of the measurement system and method were assessed in an open, non-randomized follow-up study of seven venous ulcers[3]. A strong correlation was found between the WSI and the wound surface area, with a Pearson correlation coefficient of $r(93) = -0.84$, $p < 0.001$. Following enhancements to the WoundWatch® system, the feasibility of bioimpedance measurement and method for the monitoring of chronic wounds in the clinical setting was demonstrated with 14 hard-to-heal chronic ulcers[4]. Again, a strong correlation was found between the WSI and the wound surface area, $r(91) = -0.86$, $p<0.001$. Most recent, ongoing study with venous ulcers is also yielding promising results.

Conclusion: The WoundWatch® system represents a scientifically advanced, non-invasive, quantitative, and long-term wound monitoring solution. By leveraging bioimpedance measurements and the novel Wound Status Index (WSI), it provides healthcare professionals with an objective tool to track wound healing progression accurately. The system is designed for application in both home care settings and healthcare facilities. Ongoing clinical trials in Gdańsk and Tampere are focused on securing the medical device designation and CE marking

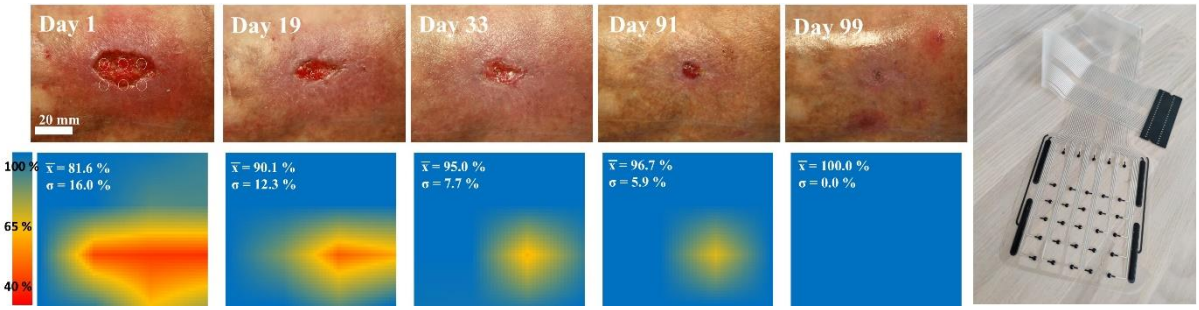

to facilitate the system's integration into clinical practice.

References:

[1] Kekonen A, Bergelin M, Eriksson J-E, Vaalasti A, Ylänen H, Viik J. Bioimpedance measurement based evaluation of wound healing. Physiol Meas. 2017;38(7):1373-1383. doi:10.1088/1361-6579/aa63d6.

[2] Kekonen A, Bergelin M, Johansson M, Kumar Joon N, Bobacka J, Viik J. Bioimpedance Sensor Array for Long-Term Monitoring of Wound Healing from Beneath the Primary Dressings and Controlled Formation of H2O2 Using Low-Intensity Direct Current. Sensors (Basel). 2019;19(11):2505. doi:10.3390/s19112505.

[3] Kekonen A, Bergelin M, Eriksson J-E, Vaalasti A, Ylänen H, Kielosto S, Viik J. Bioimpedance method for monitoring venous ulcers: Clinical proof-of-concept study. Biosens Bioelectron. 2021;178:112974. doi:10.1016/j.bios.2021.112974.

[4] Antoszewska M, Spychalski P, Kekonen A, Viik J, Barańska-Rybak W. Bioimpedance sensor array for monitoring chronic wounds: Validation of method feasibility. Int Wound J. 2024; 21(8):e14899. doi:10.1111/iwj.14899.

[5] ClinicalTrials.gov. Monitoring of Venous Ulcers Using a Bioimpedance Measurement Based Method and System (WoundWatch®). ClinicalTrials.gov ID: NCT05805137. https://clinicaltrial.be/en/details/264117.

OP082

From an idea to the product – Brain Optics quantitative near infrared spectroscopy device

Stanislaw WOJTKIEWICZ*, Mateusz ŻBIK, Adam LINKOWSKI, Michał WAŚKIEWICZ, Dominik DOMAŃSKI, Hamid DEHGHANI, Piotr SAWOSZ

Brain Optics sp. z o.o., Kredytowa 28,15-336 Białystok, Poland

* ***Corresponding author***. *E-mail address*: swojtkiewicz@brainoptics.eu

Keywords: NIRS, quantitative near infrared spectroscopy, tissue oxygen consumption

Motivation and Aim: There is no medical grade instrumentation to measure cortex oxygenation in absolute units and without calibration. Device, to be used in monitoring of brain in surgery theatres (e.g. cardiac surgeries, mechanical thrombectomies), in acute respiratory failure, traumatic brain injuries, strokes, intensive care units, etc..

This abstract and presentation will tell the story of shifting from an idea to a product from the perspective of an active researcher.

Novelty: BRAINmed – calibrationless, quantitative near infrared spectroscopy (qNIRS) to measure tissues haemodynamic properties in absolute units.

Methods:

The process of shifting from an idea to a product:

1. The idea for a product: From the very beginning, be sure who has the rights. If your affiliated institution works on the same topic, consider a spin-off with the institution. Otherwise, as in our case, make sure (document) there is no crossing points in the research. Additionally, build your own lab, equipped by you. Otherwise, consider the spin-off.
2. Check the market: define users of your product and a client (the person who makes decision on buying). Find them, approach and ask what do they know about the technology, will they use it and is it actually needed. Maybe they do not know yet that they want it. Pay for the consultancy as needed. Talk to the final users and client as soon as possible to verify the idea. If possible, talk with potential strategic investor as soon as possible.
3. Find the team: technical knowledge on electronics, programming, scientists recognizable in the field (be one yourself or convince others to join the team). A business developer person would be an ideal addition as well. The cheapest option is to make the team members shareholders. They might do some work for the future revenue. Keep the key competences and technologies within the company. Limit number of main shareholders to the core team members and sign contracts with complementary team members, where shares will be transferred after meeting certain milestones.
4. Apply for soft or investing money: a R&D project is most recommended. However, remember that this might be hard to get and you need to pay at least 20% of your own contribution. A venture capital money is challenging and may not be recommended for everyone as the seeding money is an order of magnitude less than the R&D project and investors expect the revenue of minimum 10 times the investment in 3 to 4 years. They will

pump-up the value of the company and sell you to the highest bidder in the next investment round. Look for the smart money, where the investor takes the responsibility in running the company, provides resources, business knowledge, contacts, etc.. Calculate and plan financial liquidity and react in advance if financial problems arise in your calculation.

5. Execute the project: make sure you have a solid R&D manager who knows the technology and has an experience in running projects (this is most probably you), apply professional tools to manage tasks, the team will not work just by itself as often happens in the academia. Plan the development work until entering the market, not only when you have money from an R&D project. If a clinical trial is needed, this will take 1-2 years and will be heavily expensive. Apply for a patent.
6. Launch the product: Start selling, lending, giving samples of your product to the research. Try to be as open as possible with your data. Scientists do not like closed systems.
7. Sell: the company or the product. Preferably, sell the company with the developed product to a strategic investor. The more your product is developed the better selling conditions. Stay with the new owner as the R&D team if desired. If selling the product on your own, build sell forces. However, the financial success look much better if selling the company.
8. Pivot: if the original project fails, pivot to other market if applicable or to a new product. Do not hold to the original idea for too long.

Main results:

The method of elevating the idea to the product is based on the example of the BRAINmed device as shown in fig. 1.

Figure 1. BRAINmed – quantitative Near Infrared Spectroscopy

Key features of the system as in fig. 1: frequency domain NIRS, multi-frequency technique (up to 63), 0.5 ms measurement time per frequency, frequency band 80 MHz – 450 MHz, absorption and reduced scattering measurements in absolute unit of 1 /mm^{-1}, haemoglobin concentrations in absolute units of μM, no calibration on physical phantoms nor measurements of the baseline needed. Turn on and measure.

Conclusion:

Some of the key points to successfully develop a product: know your market, invest in an external market research, apply for R&D projects and a patent, look for smart money – not just money, keep the key competences and technologies within the company, be ready to sell it all, do not attach yourself too much to the technology you have been developing for past few years.

The developed qNIRS device might not only measure the tissue saturations, but the venous oxygen saturation as well. Where the ratio of venous and tissue oxygen saturations shows the actual tissue oxygen consumption, critical in monitoring brain state (actual oxygen consumption within the brain), e.g. at intensive care units or operation theatres.

OP083

From identification of unmet clinical need to commercialization - story of tissue sensing injection needle

Jari HYTTINEN*,

1 Faculty of Medicine and Health Technology, Tampere University, Tampere, Finland

* ***Corresponding author***. *E-mail address*: jari.hyttinen@tuni.fi

Keywords: Commercialization of MedTech, bioimpedance, needle, local anesthesia, lumbar puncture

Motivation and Aim: The commercialization of biomedical engineering and med tech innovations is normally initiated by identification of unmet clinical need or sometimes by novel technology producing new opportunities for nee products and applications. After this phase a real work starts to push the innovation towards products and finally successful sales. This is a story of the path of new MedTech technology, finding the go-to market need, and the challenges to reach the sales and acquiring the funding in present world situation,

Novelty: New method to integrate bioimpedance sensor and fast impedance spectra measurement into an ordinary anesthesia or puncture needle was developed, Further, tissue identification methods were developed so that the tissue where the needle tip is can be identified. A company Injeq was established 2011 to commercialize the technology.

Methods: The technology to sensor integration, measurement and tissue identification was tested using finite element modelling[1], fantom in-vitro experiments, animal tissue and live animal testing as well as four major clinical trials in three different application areas namely finger joint injections[2], liver biopsy guidance and cancer identification[3], and lumbar puncture [4]. Further several user interview and reports were completed to identify the go-to market area.

Main results: The developed technology clearly helped finding the needle target tissue in all application areas. The pediatric lumbar puncture was selected as market entry area. With several million funding received from various investors including three successful crowdfunding rounds, a CE mark based on the MDR for this target application was secured by Injeq company in late 2021. With secured dealership contracts throughout the Europe and beyond, the company was intended to go public early the 2022 with target 8M€ new investments. However, the European political environment changed dramatically 24th February 2022 diminishing the investment opportunities, thus the company decided to delay the public offering and IPO. This forced the company to try to attract other funding with greatly reduced strategic maneuverability. With still not fully polished product in challenging MedTech market, the sales were not picking up as expected and the company run out of financing in 2024 filing bankruptcy.

Conclusion: The story of the Injeq intelligent needle commercialization highlights the challenges in MedTech area, finding the actual target need, pushing a novel product to an established and low margin market, and the challenges of finding long term funding that would enable companies to dully prove the technology market potential.

Acknowledgements: All personnel, leadership and the team behind the Injeq and several iinvestors including 1500+ private people investing the company through crowdfunding schemes.

References:

[1] Halonen, S., Kari, J., Ahonen, P., Kronström, K., & Hyttinen, J. (2019). Real-time bioimpedance-based biopsy needle can identify tissue type with high spatial accuracy. *Annals of biomedical engineering*, *47*(3), 836-851.

[2] Halonen, S., Kankaanpää, E., Kari, J., Parmanne, P., Relas, H., Kronström, K., ... & Peltomaa, R. (2017). Synovial fluid detection in intra-articular injections using a bioimpedance probe (BIP) needle—a clinical study. *Clinical Rheumatology*, *36*, 1349-1355.

[3] Halonen, S., Ovissi, A., Boyd, S., Kari, J., Kronström, K., Kosunen, J., ... & Hyttinen, J. (2022). Human in vivo liver and tumor bioimpedance measured with biopsy needle. *Physiological Measurement*, *43*(1), 015006.

[4] Sievänen, H., Kari, J., Halonen, S., Elomaa, T., Tammela, O., Soukka, H., & Eskola, V. (2021). Real-time detection of cerebrospinal fluid with bioimpedance needle in paediatric lumbar puncture. *Clinical Physiology and Functional Imaging*, *41*(4), 303-309.

OP084

Towards commercialization of an optical guidance system for neurosurgery

Karin WÅRDELL[1*], Johan RICHTER[1,2]

1 Department of Biomedical Engineering, Linköping University, Linköping, Sweden

2 Department of Neurosurgery, Linköping University Hospital, Linköping, Sweden

* ***Corresponding author***. *E-mail address*: karin.wardell@liu.se

Keywords: fluorescence spectroscopy, laser Doppler flowmetry (LDF), brain tumor, biopsy, deep brain stimulation (DBS)

Motivation and Aim: The aim is to give an overview of the technology transfer of an optical guidance system for neurosurgery.

Methods: Laser Doppler flowmetry (LDF) is well recognized for microcirculation studies [1], and five aminolaevulinic acid (5-ALA) fluorescence microscopy is FDA approved for brain tumor surgery [2]. FluoRa, is a probe-based optical system combining LDF and 5-ALA fluorescence for guidance during neurosurgery [3]. Malignant tissue is detected in situ during brain tumor biopsies and resection. Simultaneously microcirculation and grey-white matter changes are identified with LDF. For stereotactic neurosurgery as DBS implantations, the probe acts as a guide and a "vessel alarm". FluoRa is developed for invasive use in the nervous system and is thus a Class III device. The parts are designed and constructed in line with the General Safety and Performance Requirements.

Main results: Over 15 years the technique has been systematically improved, and evaluated in different studies including more than 130 DBS implantations [4, 5], 45 needle biopsies [6, 7] and 75 tumor resections [8]. The latter includes children with brain tumors undergoing resection (Phase II, Eudrat 2013-005565-40) [9]. A summary of all studies is found in [10]. In parallel to the research, technology transfer towards commercialization was initiated more than 5 years ago when the spin-off company, FluoLink AB, was founded. Covid-19 and thereafter the Medical Device Regulations (MDR) has slowed down the process. A multicenter investigation according to Good Clinical Practice, of an updated version of FluoRa, was submitted in 2023 to the Swedish Medical Product Agency. Despite major efforts it has not been approved. This has prohibited evaluation of the device in additional neurosurgical clinics. The presentation will give an overview of the steps and hurdles so far of technology transfer towards commercialization of the optical device for neurosurgical use.

Conclusion: A system for optical guidance in neurosurgery has been developed and proof of concept shown. Due to the complexity of MDR, the technology transfer process towards commercialization of new investigational devices is slowed down. Additionally, MDR has a major negative impact on research in biomedical engineering, including clinical evaluations of novel medical devices.

Acknowledgements: This research was funded by Swedish Foundation for Strategic Research (RMX18-0056). Swedish Agency for Innovation Systems (2023-03943).

References:

1. Nilsson, G.E., G.E. Salerud, N.O.T. Strömberg, and K. Wårdell, *Laser Doppler perfusion monitoring and imaging.* In Biomedical Photonics Handbook, 2003: p. Chapter 15, 1-24.
2. Hadjipanayis, C.G. and W. Stummer, *5-ALA and FDA approval for glioma surgery.* J Neurooncol, 2019. **141**(3): p. 479-486.
3. Klint, E., S. Mauritzon, B. Ragnemalm, J. Richter, and K. Wårdell, *FluoRa - a System for Combined Fluorescence and Microcirculation Measurements in Brain Tumor Surgery.* Annu Int Conf IEEE Eng Med Biol Soc, 2021. **2021**: p. 1512-1515.
4. Wårdell, K., P. Zsigmond, J. Richter, and S. Hemm, *Relationship between laser Doppler signals and anatomy during deep brain stimulation electrode implantation toward the ventral intermediate nucleus and subthalamic nucleus.* Neurosurgery, 2013. **72**(2 Suppl Operative): p. ons127-40.
5. Zsigmond, P., S. Hemm-Ode, and K. Wårdell, *Optical Measurements during Deep Brain Stimulation Lead Implantation: Safety Aspects* Stereotact Funct Neurosurg, 2017. **Jan 5;95(6):392-399**.
6. Richter, J., N. Haj-Hosseini, P. Milos, M. Hallbeck, and K. Wårdell, *Optical Brain Biopsy with a Fluorescence and Vessel Tracing Probe.* Oper Neurosurg (Hagerstown), 2021. **21**(4): p. 217-224.
7. Klint, E., J. Richter, P. Milos, M. Hallbeck, and K. Wårdell, *In situ optical feedback in brain tumor biopsy: A multiparametric analysis.* Neurooncol Adv, 2024. **6**(1): p. vdae175.
8. Richter, J.C.O., N. Haj-Hosseini, M. Hallbeck, and K. Wårdell, *Combination of hand-held probe and microscopy for fluorescence guided surgery in the brain tumor marginal zone.* Photodiagnosis Photodyn Ther, 2017. **18**: p. 185-192.
9. Milos, P., N. Haj-Hosseini, J. Hillman, and K. Wårdell, *5-ALA fluorescence in randomly selected pediatric brain tumors assessed by spectroscopy and surgical microscope.* Acta Neurochir (Wien), 2023. **165**(1): p. 71-81.
10. Wårdell, K., E. Klint, and J. Richter, *Probe-Based Fluorescence Spectroscopy for In Situ Brain Tumor Measurements During Resection and Needle Biopsies.* Biomedicines, 2025. **13(3)**(537): p. 1-15.

Special Symposium SE10
Young Polish Society for Biomedical Engineering Meeting
Chairs: Marek Darowski and The Main Board of the Polish Society for Biomedical Engineering (Poland)
OP085–OP091

OP085

Development of a neural network-based method for analyzing muscle interactions in biomechanics and medical fields

Julia WILK[1*], Cezary RZYMKOWSKI[1]

1 Division of Theory of Machines and Robots, Warsaw University of Technology, Warsaw, Poland

* ***Corresponding author***. *E-mail address*: julia.wilk2.dokt@pw.edu.pl

Keywords: neural networks, electromyography, muscle cooperation, biomechanical simulations, machine learning

Motivation and Aim: This publication introduces a new approach for analyzing muscle cooperation using neural networks in biomechanics and medical applications. Various neural network models, including Echo State Networks (ESN), Long Short-Term Memory (LSTM), and recurrent neural networks, were utilized with electromyographic (EMG), kinematic, and dynamic data. The objective was to assess individual muscle contributions to overall muscle force production. The methodology involved training and testing neural networks on datasets representing lower limb muscle activity, predicting force generation, and validating results against biomechanical simulations in OpenSim. The findings highlight the potential of neural networks for accurate muscle function modeling, with applications in rehabilitation and sports injury prevention. This interdisciplinary approach connects machine learning with biomechanics, creating new avenues for research and practical use.

Novelty: Human movement is complex due to the intricate interactions between muscles, joints, and neural inputs. Understanding muscle cooperation is crucial in fields such as biomechanics, rehabilitation, and sports science. Conventional methods for modeling muscle behavior often depend on simplified mathematical models, like Hill-based muscle models, which struggle to accurately represent nonlinear interactions [1]. This publication combines neural network technology with biomechanical data to introduce a new approach for modeling muscle cooperation. By utilizing electromyography (EMG), kinematic, and dynamic data, this method aims to predict the individual contributions of muscles to overall muscle force generation.

Methods: The dataset used in this study was sourced from an open-access biomechanical repository [2], containing EMG signals, kinematic, and dynamic data from eight lower limb muscles. Preprocessing involved filtering the EMG signals, normalizing the kinematic data, and splitting the dataset into training and testing sets. Five different neural network architectures were evaluated: Echo State Networks (ESN), Long Short-Term Memory (LSTM), support

vector machines (SVM), random forests, and regression models [3]. Training and testing were performed in MATLAB, with validation through biomechanical simulations in OpenSim. Error analysis focused on the absolute and relative differences between the predicted and simulated forces. To assess generalizability, models were also tested on movements not part of the training set, such as knee lifts and stair descents [4].

Main results: The neural networks demonstrated varying degrees of accuracy in predicting muscle forces. Recurrent and LSTM models performed the best, especially in capturing the nonlinear relationships between EMG signals and muscle forces. While SVM and random forest models delivered satisfactory results, they faced challenges in generalizing to untrained movements. Error analysis showed that recurrent models were particularly effective in predicting complex movements, while LSTM models provided computational efficiency for real-time applications. The findings underscore the potential of neural networks to improve biomechanical modeling by providing accurate, non-invasive estimates of muscle activity. However, limitations include the need for high-quality input data and difficulties in generalizing the results to different populations.

Conclusion: This study illustrates the potential of using neural networks to model muscle cooperation in biomechanics. By integrating EMG, kinematic, and dynamic data with machine learning, a strong framework is established for analyzing muscle contributions to movement. The proposed method has practical applications in rehabilitation, allowing for personalized therapy plans, and in sports, enhancing training programs and injury prevention strategies. Future research should aim to expand the dataset to include a wider range of subjects and movements, improve model robustness, and explore real-time implementation possibilities.

References:

[1] Delp, S. L., Anderson, F. C., Arnold, A. S., et al. OpenSim: Open-source software to create and analyze dynamic simulations of movement. IEEE Transactions on Biomedical Engineering, 54(11), 1940-1950, 2007.

[2] Luan, Y et al. HAR-sEMG: A Dataset for Human Activity Recognition on Lower-Limb sEMG. Knowledge and Information Systems, 63, 2791–2814, 2021. DOI: 10.1007/s10115-021-01598-w.

[3] Hochreiter, S., & Schmidhuber, J. Long short-term memory. Neural Computation, 9(8), 1735-1780, 1997.

[4] Rymkiewicz, C. et al. Advanced approaches to EMG-based muscle modeling in biomechanical research. Journal of Biomechanics, 54, 105-118, 2022.

OP086

Analysis of the influence of the basal geometry of the auxetic layer in the intervertebral disc endoprosthesis on the distribution of stress and strain in the lumbar spine structures

Martyna MYSZOGRAJ[1*], Piotr POSADZY[1]

1 Poznan University of Technology, Poznan, Poland

* ***Corresponding author***. *E-mail address*: martyna.myszograj@doctorate.put.poznan.pl

Keywords: spine, intervertebral disc endoprosthesis, FEA, auxetics

Motivation and Aim: Diseases and injuries of the spine are increasingly common, with many cases requiring surgical intervention involving implants. Dynamic intervertebral disc endoprostheses offer the potential to preserve mobility in the implanted segment, thereby reducing the risk of postoperative complications such as adjacent segment disease. This study aims to design and evaluate an intervertebral disc endoprosthesis incorporating auxetic structures to improve its mechanical performance and reduce stress on spinal structures.

Novelty: The research explores the use of auxetic structures with different geometries in intervertebral disc endoprostheses. Unlike the designs with conventional structures, the study investigates how auxetic properties can influence stress and strain distribution, potentially leading to improved implant longevity.

Methods: The study included a literature review of the mechanical properties and biomechanics of the lumbar spine, the current state-of-the-art in auxetic structures, and experimental and numerical studies of auxetic structures used in biomedical engineering. In the design and research part, the design of an intervertebral disc endoprosthesis using auxetic structures with different basic geometries was proposed and numerical studies were carried out on the effect of the used geometry on the distribution of stresses and strains in the endoprosthesis structure and lumbar spine structures.

Main results: The analysis revealed that the honeycomb-type auxetic structure placed in the insert, due to the accumulation of stresses, is destroyed and thus fails to fulfill its role in the intervertebral disc endoprosthesis. In contrast, the use of a star-type auxetic structure presents a potential solution to the problem of overloading the anatomical structures of the spine after the implantation of an intervertebral disc endoprosthesis. The maximum stress value was found to be located on the insert, specifically on the auxetic layer. This contrasts with the conventional endoprostheses, where the maximum stress occurs on the spherical part of the insert. The maximum stress value on the endoprosthesis (442.12 MPa) is higher than the values reported by other researchers. Nevertheless, the stress values do not exceed the yield strength of the material (908 MPa). The maximum stresses on the anatomical structures of the spine were found to be smaller than those reported in studies.

Conclusion: In conclusion, the honeycomb-type auxetic structure in the insert is unsuccessful due to stress accumulation, while the star-type auxetic structure offers a potential solution to reduce overloading of the spine after implantation. The maximum stress is concentrated on the auxetic layer, in contrast to conventional implants where it occurs on the spherical component. The findings suggest that incorporating star-type auxetic structures in intervertebral disc endoprostheses may positively influence the stress and strain distribution, potentially improving the longevity and functionality of the implant. The maximum stress (442.12 MPa) remains below the material's yield strength (908 MPa), thereby ensuring structural integrity. Additionally, the stress on the spine's anatomical structures is lower, indicating an improvement in implant performance.

OP087

Multifunctional chitosan-based hydrogels enriched with biologically active substances

Weronika GURA[1*], Szymon SALAGIERSKI[1], Michał DZIADEK[1,2], Katarzyna CHOLEWA-KOWALSKA[1]

[1]AGH University of Krakow, Department of Glass Technology and Amorphous Coatings, Faculty of Materials Science and Ceramics, 30 Mickiewicza Av., 30-059 Krakow, Poland

[2] Department of Materials Engineering, University of British Columbia, Vancouver, British Columbia, Canada

* ***Corresponding author***. *E-mail address*: gura@agh.edu.pl

Keywords: hydrogel, chitosan, bioactive glass, Schiff's base crosslinking, retinol, resveratrol

Motivation and Aim: Modern biomedical engineering continuously strives to develop innovative materials that can be applied in regenerative medicine and tissue engineering. Hydrogels based on biopolymers such as chitosan exhibit promising potential as biomaterials supporting tissue regeneration. The combination of chitosan with bioactive glass and the addition of biologically active substances such as retinol and resveratrol may further enhance their therapeutic properties. The aim of this study was to design and manufacture hydrogel materials based on chitosan and whey protein isolate, crosslinked with functionalized dextran and enriched with high-calcium bioactive glass, retinol, and resveratrol. The research focuses on assessing the impact of these components on mechanical properties, bioactivity, and the ability to release active substances, contributing to the development of advanced regenerative therapies.

Novelty: This study presents novel hydrogel materials based on chitosan and whey protein isolate, crosslinked with oxidized dextran and enriched with bioactive glass, retinol, and resveratrol. For the first time, a detailed investigation into the impact of these components on bioactivity, mechanical properties, and the controlled release of biologically active substances has been conducted. The results indicate the possibility of precisely modifying biomaterial properties, which could contribute to the advancement of modern tissue engineering therapies.

Methods: The hydrogels were obtained by crosslinking chitosan and whey protein isolate with functionalized dextran. These materials were produced in two forms: injectable hydrogels and lyophilized, highly porous three-dimensional scaffolds. Structural analysis was performed using FTIR spectroscopy and SEM-EDS microscopy. Mechanical properties were evaluated through compression and rheological tests. The bioactivity of the materials was assessed by incubation in simulated body fluid (SBF), while the controlled release of biologically active substances was analyzed using UV-VIS spectroscopy. Antioxidant properties were determined using the ABTS• assay, and cytotoxicity and metabolic activity effects on RAW 264.7 and N2a cell lines were examined.

Main results: The obtained hydrogels exhibited high bioactivity and the ability to support mineralization in SBF solution. Bioactive glass improved the mechanical properties and structural stability of the materials, while resveratrol enhanced their antioxidant properties. The

release profile of active substances depended on their concentration in the material, with higher concentrations of resveratrol leading to intensified release, whereas the effect for retinol was the opposite. High concentrations of resveratrol demonstrated cytotoxicity toward the tested cell lines, while bioactive glass improved cell viability and metabolic activity.

Conclusion: The results showed that the introduction of bioactive glass and biologically active substances significantly improved the therapeutic properties of the hydrogels. The materials demonstrated the ability to promote tissue regeneration, which was confirmed through tests on cell lines. Physicochemical analyses indicated adequate stability and structure of the hydrogels, and mechanical tests confirmed their suitability for medical applications.

The conducted studies confirmed that the developed hydrogels have significant potential as biomaterials for tissue engineering, particularly in bone and cartilage regeneration. Bioactive glass improved the mechanical parameters and bioactivity of the materials, while resveratrol exhibited strong antioxidant effects. Optimizing the concentration of active substances may enable controlled drug release and the customization of biomaterials for specific medical applications.z

Acknowledgements: This work was supported by the National Science Centre, Poland (Grant no. 2023/49/N/ST11/02999) and the “Excellence Initiative – Research University” program at AGH University.

OP088

The influence of simulated microgravity on cells cultured on polymeric scaffolds and microspheres

Barbara SZAFLARSKA[1,2*], Kamila WALCZAK[2], Agata KOŁODZIEJCZYK[1,3], Elżbieta PAMUŁA[2]

1 AGH University of Kraków, AGH Space Technology Centre, Kraków, Poland

2 AGH University of Kraków, Faculty of Materials Science and Ceramics, Kraków, Poland

3 Analog Astronaut Training Center, Kraków, Poland

* ***Corresponding author***. *E-mail address*: bszaflarska@agh.edu.pl

Keywords: Microgravity, tissue engineering, polymeric scaffolds, microspheres, PLGA, bone tissue

Motivation and Aim: Spaceflight poses a variety of dangers to the human body, among them radiation and microgravity. Adaptation to this harsh environment can cause serious health problems. One of the most threatening issues that astronauts experience during space missions is bone tissue deterioration. It is thought to be caused by the dysregulation between bone formation and resorption, resulting in tissue density loss, however, the exact mechanisms are still not fully understood. To study those effects, microgravity-simulating devices have been developed, although each of them introduces certain artifacts to the experiment. The aim of this study was to establish a protocol for studying MG-63 osteoblast-like cells cultured on polymeric scaffolds and microspheres in simulated microgravity conditions and to characterize their behavior.

Novelty: Research on skeletal changes in space is complicated by inconsistencies between studies and the limitations of *in vitro* models of the isolated cells. Since extracellular matrix (ECM) influences cellular responses to microgravity, incorporating scaffolds mimicking bone tissue can provide more accurate insights into bone adaptation in space.

Methods: The study includes preparation of the scaffolds and microspheres made from poly(L-lactide-coglycolide)(PLGA), characterization of their properties, and experiments on osteoblast-like MG-63 cells in simulated microgravity conditions on a random positioning machine (RPM) in terms of their morphology, viability, and proliferation. Cell morphology was examined using scanning electron microscopy (SEM), while cell viability was evaluated using the Alamar Blue assay and live/dead fluorescence staining. Moreover, the cytotoxicity of the system was assessed by measuring lactate dehydrogenase (LDH) release. Additionally, pH of the culture medium was measured as a function of culture time.

Main results: Three experiments were performed and, as a result, a protocol for culturing MG-63 osteoblast-like cells on PLGA biomaterials on the RPM was successfully established. The study showed that cells remained viable up to 7 days of culture in simulated microgravity conditions, both on scaffolds and microspheres. Cells cultured on the microspheres exhibited

weak adhesion to their surfaces but preferentially formed spheroids. Moreover, cells in the samples exposed to the RPM demonstrated increased metabolic activity; although, these conditions also resulted in higher cytotoxicity. This finding suggests greater cell activity and proliferation under RPM conditions.

Conclusion: The study demonstrated that the development of material-cell constructs based on PLGA scaffolds and osteoblast-like cells can serve as a research model for assessing the impact of microgravity on bone tissue.

Acknowledgements: This study was supported from the subsidy for the Faculty of Materials Science and Ceramics, AGH University of Krakow (No. 16.16.160.557).

OP089

Unsupervised segmentation of defective skulls in volumetric data by using deep networks dedicated to modality transfer

Kamil KWARCIAK

AGH University of Krakow, Kraków, Poland

* ***Corresponding author***. *E-mail address*: kamil.kwarciak@gmail.com

Keywords: Generative artificial intelligence, Deep learning, Modality translation, Synthetic data

Motivation and Aim: Skull segmentation from MR images is a crucial yet challenging task in modern computational medicine. MRI primarily focuses on soft tissues rather than bone structures, making direct skull segmentation difficult. While CT imaging provides well-established skull segmentation techniques, its radiation exposure poses health risks, highlighting the need for an MRI-based approach. This study aims to develop an unsupervised skull segmentation methodology by leveraging modality translation techniques. By converting MR images into synthetic CT representations, this approach enables effective skull segmentation without requiring labeled MR data, addressing both clinical and computational challenges.

Novelty: This study introduces a novel approach to MRI-based skull segmentation by transforming the problem into a modality translation task, followed by CT-based segmentation. Unlike traditional supervised methods that rely on annotated MRI datasets, presented method leverages deep generative models such as generative adversarial networks, denoising diffusion models, and contrastive learning techniques to achieve unsupervised segmentation. Additionally, integration of the super-resolution strategy addresses the lower resolution of MRI compared to CT, ensuring high-quality segmentation results. This methodology not only surpasses existing supervised methods but also outperforms a cutting-edge foundation medical segmentation model and other modality translation techniques.

Methods: This study employs an unsupervised skull segmentation pipeline that leverages modality translation techniques to convert MR images into synthetic representations. A diverse set of deep generative models is explored, including generative adversarial networks (GANs), denoising diffusion models, and contrastive learning methods. Once MR images are transformed into their CT counterparts, well-established CT-based segmentation techniques are applied. Additionally, a super-resolution approach is integrated to compensate for the lower resolution of MRI data, ensuring high-quality segmentation suitable for clinical applications.

Main results: The proposed methodology outperforms traditional supervised segmentation methods, demonstrating superior accuracy and robustness in MRI-based skull segmentation. It also surpasses a state-of-the-art foundation medical segmentation model and outperforms existing modality translation techniques. The integration of super-resolution further enhances the quality of segmentation, addressing the limitations of MRI's lower resolution. Additionally, ablation studies highlight the effectiveness of MR-to-CT translation for unsupervised skull

segmentation, showcasing its potential in applications such as infant skull imaging and defective skull reconstruction. These results establish the proposed approach as a significant advancement over conventional segmentation techniques.

Conclusion: This study presents a novel unsupervised approach to MRI-based skull segmentation by leveraging modality translation techniques, transforming the problem into a more manageable CT-based segmentation task. The proposed methodology outperforms traditional supervised methods and state-of-the-art segmentation models while maintaining fast inference for volumetric data. Additionally, the integration of super-resolution ensures high-quality segmentation, addressing the resolution gap between MRI and CT. The results demonstrate the potential of MR-to-CT translation for broader applications, such as infant skull imaging and defective skull reconstruction, opening new research area in computational medical imaging.

Acknowledgements: The work on this project was done under Lider Grant no: LIDER13/0038/2022 (DeepImplant) by The National Centre for Research and Development, Poland. Additional appreciations are directed to HPC infrastructure PLGrid support for the opportunity to perform GPGPU high performance computations that were conducted with the AGH Cyfronet Athena and Helios Supercomputers on NVIDIA graphics cards within computational grants no. PLG/2023/016239 and PLG/2024/017079.

OP090

Multifunctional alginate-based capsules for theranostic applications

Malwina FURGAŁA[1,2*], Patrycja DOMALIK-PYZIK[2*]

1 AGH University of Krakow, Faculty of Electrical Engineering, Automatics, Computer Science and Biomedical Engineering, Krakow, Poland

2 AGH University of Krakow, Faculty of Materials Science and Ceramics, Department of Biomaterials and Composites, Krakow, Poland

* ***Corresponding author***. *E-mail address*: malwinafurgala@gmail.com

Keywords: theranostics, hollow hydrogel capsules, silver nanoparticles, magnetic-core particles, cancer treatment

Motivation and Aim: Cancer remains one of the leading causes of death worldwide, and the therapy of this disease has been a significant challenge [1]. Conventional treatment methods, such as chemotherapy and radiotherapy, often lack specificity, leading to side effects and damage to non-cancerous tissues. Therefore, there is a pressing need for more specific and efficient therapeutic approaches. Theranostics represents a new paradigm that integrates therapeutic and diagnostic modalities within a single system, providing an appealing alternative [2]. The aim of the research was to develop, synthesize, and assess innovative multifunctional particles with potential theranostic applications. Two types of materials were researched in this study: hollow hydrogel capsules and magnetic-core nanoparticles, both functionalized with metal nanoparticles to enhance therapeutic efficacy.

Novelty: This work presents the fabrication of silver or copper alginate multifunctional hydrogel capsules through a template-assisted synthesis pathway utilizing calcium carbonate particles. Furthermore, iron oxide nanoparticles were synthesized and subsequently coated with silver or copper alginate, achieving a novel integration of diagnostic and therapeutic capabilities. In comparison to traditional drug delivery systems, these materials facilitated controlled release, improved targeting, and potential imaging in the future, positioning themselves as promising candidates for next-generation cancer treatments.

Methods: Multifunctional alginate-based capsules were synthesized using calcium carbonate templates and further modified with silver or copper (*Fig.1*). Moreover, iron oxide nanoparticles were developed and coated with either silver or copper alginate. The obtained materials were characterized through scanning electron microscopy (SEM), transmission electron microscopy (TEM), and Fourier-transform infrared spectroscopy (FTIR). *In vitro* cytotoxicity studies were performed to assess their biocompatibility and anticancer properties.

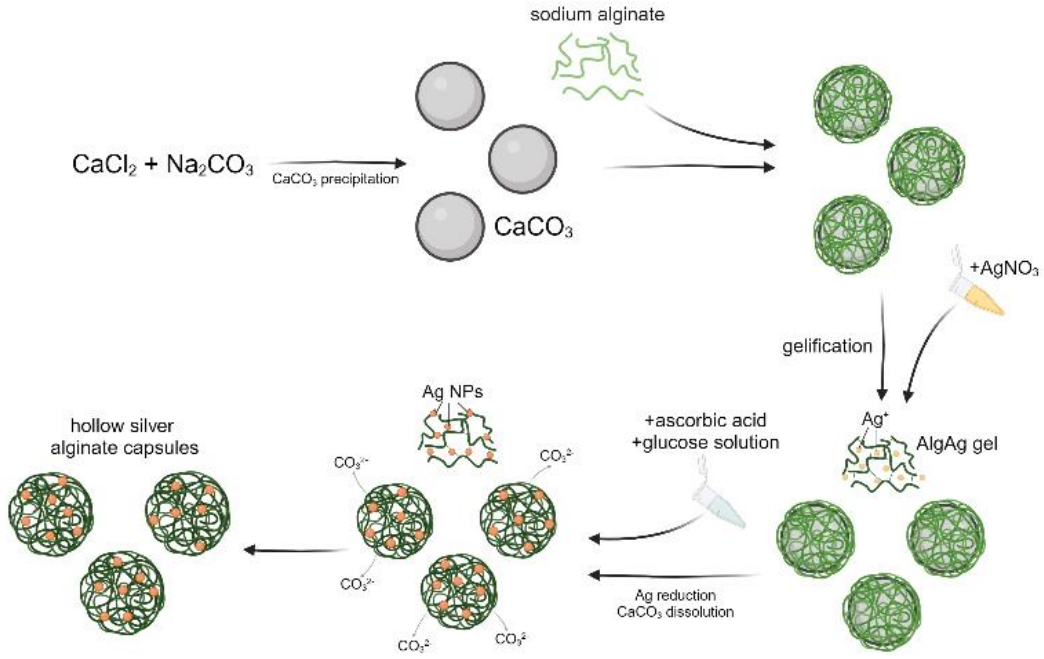

Fig.1 Fabrication process of silver alginate hydrogel capsules

Main results: The structural and physicochemical characterization confirmed the successful fabrication of hydrogel capsules and hydrogel-coated iron oxide nanoparticles. The capsule size was controlled by adjusting the size of the calcium carbonate sacrificial templates, which were produced either by regular mixing or ultrasonication. Metal-alginate hybrid structures were formed through reduction of silver nitrate/copper sulfate with the use of ascorbic acid. Silver alginate hydrogel capsules demonstrated the highest anticancer efficacy. Magnetic-core nanoparticles coated with copper alginate also exhibited promising results, suggesting their potential for further investigation in theranostic applications.

Conclusion: The present study demonstrated the potential of multifunctional hydrogel capsules and magnetic-core nanoparticles as effective theranostic agents for cancer treatment. Among the tested materials, silver alginate hydrogel capsules emerged as the most promising candidate. Nevertheless, copper alginate-coated magnetic-core nanoparticles also revealed considerable potential, and therefore additional studies aimed at optimization and *in vitro* validation are justified.

Acknowledgements: This study was funded by the National Science Centre in Poland under the project „Theranostic nanoplatforms for therapy and diagnostics of ovarian cancer - preliminary studies”, no 2024/08/X/ST11/01187.

References:

[1] L. Zhang, S. Sanagapalli, and A. Stoita, "Challenges in diagnosis of pancreatic cancer," *World J Gastroenterol*, vol. 24, no. 19, pp. 2047–2060, May 2018, doi:10.3748/wjg.v24.i19.2047

[2] B. K. Kashyap, V. V. Singh, M. K. Solanki, A. Kumar, J. Ruokolainen, and K. K. Kesari, "Smart Nanomaterials in Cancer Theranostics: Challenges and Opportunities," *ACS Omega*, vol. 8, no. 16, pp. 14290–14320, April 2023, doi:10.1021/acsomega.2c07840

OP091

Computer Methods to Support Diagnosis and Therapy of Scoliosis Using Spinal Radiograms and Clinical Data

Anna Maria BERENT*

Warsaw University of Technology, Faculty of Electronics and Information Technology, Poland

* ***Corresponding author***. *E-mail address*: ankaberent@gmail.com

Keywords: adolescent idiopathic scoliosis (AIS), diagnosis support, treatment support, Cobb angle, mobile app, radiogram, deep neural networks

Motivation and Aim: This work focuses on supporting the diagnosis and treatment of scoliosis. The motivation for choosing this topic stems from the author's personal experience with adolescent idiopathic scoliosis (AIS) and interest in technological solutions that support medicine. AIS affects 2-3% of the population and accounts for 80% of all scoliosis cases. It is a three-dimensional deformity of the spine, characterized by a lateral curvature greater than 10 degrees, often accompanied by vertebral rotation. The progression of the disease is typically assessed through Cobb angle measurements on radiographs. Since these measurements form the basis for diagnosis and treatment decisions, including invasive scoliosis correction surgery, they should be as reliable and efficient as possible.

This study challenges the assumption that Cobb angle measurement is the most critical factor in scoliosis diagnosis and treatment. The goal was to develop an effective support system for scoliosis patients by addressing broader needs beyond Cobb angle measurement, focusing on improving communication and access to reliable information.

Novelty: A literature review highlighted the need for increased accuracy and repeatability of Cobb angle measurements. However, it also revealed a lack of access to databases that could facilitate the verification and improvement of measurement methods. While many studies emphasize the importance of Cobb angle measurement, this work identifies a gap in understanding its practical significance in clinical settings.

Interviews with doctors who regularly perform Cobb angle measurements revealed that, in practice, the accuracy of this measurement is not the primary concern. Instead, it is just one of several important factors considered when assessing scoliosis, alongside body balance and the overall clinical evaluation. A physiotherapist specializing in scoliosis treatment confirmed these findings, emphasizing that X-ray examinations should be viewed as part of a broader treatment process.

To incorporate the perspectives of patients and their families, a pilot survey was conducted among 23 individuals affected by scoliosis (18 patients and 5 parents). The results indicated that the most significant area requiring support is communication – both between patients and specialists and among patients themselves. Additionally, access to reliable information about scoliosis emerged as a key concern.

This study ultimately concludes that the most critical aspect of scoliosis diagnosis and treatment is not just improving Cobb angle measurement accuracy but rather enhancing communication and access to trustworthy information for patients.

Methods: To address these identified needs, a comprehensive approach was taken. The study involved: **a literature review** to examine existing methods and their limitations, particularly regarding Cobb angle measurement; **interviews with specialists**, including doctors and physiotherapists, to understand the real-world importance of Cobb angle measurement and the broader diagnostic and therapeutic proces; **a pilot survey** conducted with scoliosis patients and their families to determine their primary concerns and needs.

Based on these findings, a **mobile application concept** was developed to comprehensively support scoliosis patients by improving access to information and communication with specialists.

Main results: As a response to the identified needs, a mobile application named **"SKOLIOŻApka"** was designed. The app serves as a comprehensive support tool for scoliosis patients by offering: reliable information about scoliosis, a database of specialists recommended by patients, personal stories from other patients to provide emotional suport, tools to help patients accept their appearance, a platform for improved communication between patients and specialists, as well as among patients themselves.

Additionally, the app is planned to include **automatic Cobb angle measurement** with accuracy comparable to manual methods and will allow a smartphone to function as a scoliometer.

Conclusion: The paper confirms that while improving Cobb angle measurement accuracy is important, a more pressing need exists in supporting patient-specialist communication and access to reliable scoliosis-related information. The findings justify the development and implementation of the proposed mobile application, which aligns with the needs identified through literature analysis, specialist interviews, and patient surveys.

If the application is to be further developed, enhancements will be necessary, including refining its graphical interface and adding additional functionalities. Collaboration between the app administrator, patients, and specialists will be crucial to ensure its effectiveness.

Future research should also explore **new solutions** that directly support medical professionals, such as: automating the analysis of X-ray images, including Cobb angle measurement and body balance parameters, developing more precise methods for assessing spinal curvature and establishing new clinical guidelines for scoliosis treatment.

Special Symposium SCC
IFMBE Scientific Challenge Competition – Segmentation Challenge: Wounds and Markers in Focus
Chairs: Paulo de Carvalho (Portugal), Piotr Foltynski (Poland), Jorge Henriques (Portugal), Piotr Ladyzynski (Poland)
OP092–OP097

OP092

Advanced Multi-Class Wound Segmentation Using EfficientNet UNet

A Comprehensive Approach to Automated Wound Assessment

Athanasios KALLIPOLITIS[1], Melina TZIOMAKA[1], Argyrios ZAFEIRIOU[1], Ilias MAGLOGIANNIS[1]

1 Department of Digital Systems, University of Piraeus, Piraeus, Greece

nasskall@unipi.gr, tziomakamel@unipi.gr, zafeiriou@unipi.gr, imaglo@unipi.gr

Abstract. Accurate wound image analysis is important for effective treatment planning and monitoring healing progression. This paper introduces a deep learn- ing methodology for automated wound segmentation by developing an innova- tive framework that uses EfficientNet and UNet architectures. Our research tack- les essential issues in wound assessment, which involve multi-class segmentation along with boundary precision and test-time augmentation. To enhance segmen- tation quality, the proposed methodology employs a composite loss function combining focal, boundary-aware, and dice loss modules. The experimental re- sults show equivalent or better performance than current methodologies with our three-class model achieving an average F1 score of 0.8876. This work represents a significant advancement toward comprehensive wound assessment systems that can support decision-making across diverse healthcare settings.

Keywords: Wound Segmentation, Deep Learning, Medical Image Analysis, Computer Vision, Boundary-Aware Loss, Multi-class Segmentation

OP093

Automated Segmentation of Wound and Scale Markers Areas Using a U-Net-Based Neural Network

Zuzanna BŁASZKOWSKA, Karolina DZWONKOWSKA, Piotr STEFAŃSKI, Piotr M. SZCZYPIŃSKI

Lodz University of Technology, Lodz, Poland

This paper presents a method for automated segmentation of wound areas and scale markers in medical images using a U-Net-based neural network. The model was trained on a dataset of 371 original images, augmented through rotations to increase its generalization ability. Training was conducted over 100 epochs, with dynamic learning rate adjustments to stabilize the process. The model's performance was evaluated using accuracy, loss metrics, and confusion matrices, with segmentation quality assessed through Dice-Sørensen and Jaccard indices. Results show good performance in segmenting wound areas and scale markers, with the model achieving a median Dice-Sørensen coefficient of 0.7068 for wounds and 0.9397 for scale markers. Future work may include expanding the training dataset and exploring the use of classification-oriented neural networks as encoders to further improve segmentation accuracy.

Keywords: Medical image segmentation, U-Net, Deep learning, Wound detection, Scale markers localization, Convolutional neural networks (CNNs), Dice- Sørensen coefficient, Jaccard index, Data augmentation

OP094

Towards efficient wound management: An automatic Deep Learning model for accurate wound image segmentation

Aleksandar MILADINOVIĆ[1], Alessandro BISCONTIN[1], Andrea BONINI[2], Francesco BASSI[2], Simone KRESEVIC[2], Alessandra RAFFINI[2], Katerina ISCRA[2], Agostino ACCARDO[2], Miloš AJČEVIĆ[2]

1 Institute for Maternal and Child Health IRCCS "Burlo Garofolo", Trieste, Italy

2 Department of Engineering and Architecture, University of Trieste, Trieste, Italy

aleksandar.miladinovic@burlo.trieste.it

Abstract. Untreated wounds may lead to serious complications, underscoring the need for consistent monitoring. In clinical practice, wound imaging offers a potential tool for objective assessment. However, obtaining quantitative analysis requires accurate semantic image segmentation, a task that is often time-consuming. Despite deep learning has shown effectiveness in image segmentation, several challenges remain, especially in occluded or low-light images. This study aims to provide a novel semantic segmentation approach for wound images, designed to overcome some of these limitations. A semantic segmentation framework that combines a Convolutional Neural Network-based encoder with a lightweight multilayer perceptron decoder was proposed. A dataset consisting of 451 images was employed for the training, validation, and testing of a semantic segmentation architecture. During the training phase, the model achieved a pixel accuracy of 99.02%, with 98.82% on the validation set and 98.27% on the test set. The corresponding F1 scores were 0.97 for both training and validation, and 0.95 for the test set. The deigned framework and the produced model provided a valuable solution for automatic wound assessment through precise image segmentation approach. The proposed method offers a remarkable contribution to telemedicine, providing a significant advancement for automatic wound management.

Keywords: Wound healing monitoring, Semantic segmentation, Deep Learning.

OP095

Dual-Attention U-Net++ with Class-Specific Ensembles and Bayesian Hyperparameter Optimization for Precise Wound and Scale Marker Segmentation

Daniel CIEŚLAK[1,2]*, Miriam RECA[1], Olena ONYSHCHENKO[1], Jacek RUMIŃSKI[1]

1* Faculty of Electronics, Telecommunications and Informatics, Gdańsk University of Technology, Gdańsk, Poland.

2 IDEAS NCBR, Warsaw, Poland.

*Corresponding author(s). E-mail(s): cieslak.a.daniel@gmail.com;

Abstract

Accurate segmentation of wounds and scale markers in clinical images remains a significant challenge, crucial for effective wound management and automated assessment. In this study, we propose a novel dual-attention U-Net++ architecture, integrating channel-wise (SCSE) and spatial attention mechanisms to address severe class imbalance and variability in medical images effectively. Initially, extensive benchmarking across diverse architectures and encoders via 5- fold cross-validation identified EfficientNet-B7 as the optimal encoder backbone. Subsequently, we independently trained two class-specific models with tailored preprocessing, extensive data augmentation, and Bayesian hyperparameter tuning (WandB sweeps). The final model ensemble utilized Test Time Augmentation to further enhance prediction reliability. Our approach was evaluated on a bench- mark dataset from the NBC 2025 & PCBBE 2025 competition. Segmentation performance was quantified using a weighted F1-score (75% wounds, 25% scale markers), calculated externally by competition organizers on undisclosed hard- ware. The proposed approach achieved an F1-score of 0.8640, underscoring its effectiveness for complex medical segmentation tasks.

Keywords: Image segmentation, Wound assessment, Deep learning, Medical imaging, U-Net++, Attention Mechanism, Bayesian Optimization

OP096

Wound area detection with nnU-Net v2 architecture

Franciszek KUBALA, Piotr MATUSIEWICZ, Dominik MIKA, Dominik ZAWLOCKI, Zbisław TABOR

AGH University of Krakow, Karkow 30-059, Poland

Abstract. Diabetic foot ulcers are a dangerous complication of diabetes and, if uncared for, can lead to significant health risks. In treatment, wound annotation and measurements are crucial. The development of AI models has the potential to significantly transform medical diagnostic techniques and greatly benefit the daily work of medical staff. With the support of deep learning, we aim to expand on new ways to implement convolutional neural networks (CNNs) in the daily work of medical staff. In this study we used the well renowned nnU-Net 2.0 architecture. The models are trained using custom loss function which improves segmentation accuracy compared to the state of the art approaches. Segmentation was performed using an ensemble of models. For the dataset, we obtained 451 wound pictures with ground truth segmentations of wounds and scale markers and split the dataset into a holdout test part of 15% images and 85% of training/validation images. Various models achieved accuracy of 90,91%, 90.88% and 91.65%. Model ended up with big accuracy and could be used in a medical setting.

Keywords: Wound area segmentation; Convolutional neural networks; Deep learning; nnU-Net

OP097

Segmentation challenge: wounds and markers in focus

Piotr POTRZEBOWSKI, Arkadiusz KARBOWSKI, Kamil STERNIUK, Aleksandra KRAJNA, Zuzanna CEMKA, Krystian OPALA, Jacek RUMIŃSKI

Gdańsk University of Technology, Faculty of Electronics, Telecommunications and Informatics, G. Narutowicza 11/12, 80-233 Gdańsk, Poland

Abstract. Accurate segmentation of wound images is critical for effective diagnosis, treatment planning, and monitoring of wound healing. In this study, we introduce an advanced deep learning framework for the simultaneous segmentation of wounds and scale markers. Our approach leverages state-of-the-art architectures—including U-Net++, DeepLabV3+, and Segformer—combined with pre-trained encoders and diverse transfer learning strategies (full fine-tuning, decoder-only tuning, and partial tuning) to address the challenges posed by limited and heterogeneous clinical datasets. Evaluations conducted on the NBC2025 Challenge dataset demonstrate the effectiveness of our method, with models achieving high F1-scores, including 0.8934 on the test dataset, and competitive mean Intersection over Union (mIoU) values on the validation set. Extensive data augmentation further enhances model generalization, ensuring robust segmentation performance. The promising results under- score the potential of deep learning-based segmentation as a reliable tool for objective wound assessment, thereby supporting improved clinical decision-making and patient care.

Keywords: wound segmentation, deep learning, medical image analy- sis, convolutional neural networks, transfer learning, semantic segmentation

Special Symposium SE11
Biosensing Devices
Chairs: Chia Ming Yang (ROC Taiwan), Dorota G. Pijanowska (Poland)
IP03, OP098–OP102

IP03

Introduction to biosensing devices

Dorota G. PIJANOWSKA

Nalecz Institute of Biocybernetics and Biomedical Engineering, PAS, Trojdena 4, Warsaw, Poland

Biosensing devices are analytical tools that combine a biological recognition element, such as enzymes, antibodies, or nucleic acids, with a physical transducer to detect specific biological or chemical targets. While this definition is widely recognized, a closer examination reveals its multi-faceted nature, providing a foundation for deeper exploration of biosensing technologies (bioSTs) and their applications. Technological advances in areas such as nanomaterials, microfluidics, and semiconductor-based sensors have greatly improved biosensor sensitivity, miniaturization, and real-time detection capabilities. These innovations have expanded their use across diverse fields, including medical diagnostics, environmental monitoring, and point-of-care testing. In this session, we will explore how emerging interdisciplinary approaches that shaping the next generation of intelligent biosensing platforms. This session will highlight selected aspects of biosensing technology, including: (1) silicon-based sensor interfacing circuits, (2) novel bioreceptors and capture systems, and (3) a semiconductor chip designed for cell separation and other cellular assays.

OP098

Silicon Technology Based Sensor Interfacing Circuit Development for Urolithiasis Prevention

CHUNG[1*], Wen-Yaw Danny; RAMEZAN[1,2], Roozbeh; F. CAYA[1,3], Meo Vincent; SILVERIO[1], Angelito A.; LIU[1], Yen-Wei.; YANG[4], Chia-Ming; TSAI[5], Vincent F.

1 Department of Electronics Engineering, Chung Yuan Christian University, Zhongli, Taiwan, R.O.C.

2 Graduate Institute, Prospective Technology of EECS, National Chin-Yi University of Technology, Taichung, Taiwan, R.O.C.

3 School of Electrical, Electronics, and Computer Engineering, Mapua University, Manila, Philippine

4 Department of Electronics Engineering, Chang-Guan University, Lin-Kuo, Taiwan, R.O.C

5 Department of Urology, Taipei Tzu Chi Hospital, Taipei, Taiwan, R.O.C.

* ***Corresponding author***. *E-mail address*: eldanny@cycu.edu.tw

Keywords: Sensor interfacing circuit, Urolithiasis, Kidney stone, Silicon technology

Motivation and Aim: With the advanced silicon based processes have been continuously developed in past two decades, the conventional "Moore's Law" predicts the transistor number in a chip will be doubled every eighteen months, so it gets more challenged due to the limit of the device sizes' shrinking. However, the concept of "More than Moore's Law" is playing a more important role as device scaling is becoming more difficult and expensive, different approaches have been explored to solve the limitation of Moore's law, such as the development of 3D devices and package, the integration of diversified sensor and signal processing unit/system on a chip become a good way to extend the scope of "More than Moore's Law". In addition, the development of microfabrication technology brings the new medical applications based on Biological CMOS with Biological Micro-Electro-Mechanical System, MEMS process becomes more popular offered by famous foundry services such as TSMC, UMC, Infineon Technology etc.

Furthermore, Point-of-Care-Test, POCT devices in daily health-care system provide significant help for aging society and modern life, most popular examples developed are blood pressure meter and glucose meter, they reduce the risk of stroke and complex syndrome happened based on daily monitoring parameters and profile analysis. Same concepts can be applied in the risk evaluation of urolithiasis (kidney stone) formation in early stages. According to the statistics of Dept. of Family Medicine, Taoyuan General Hospital in Taiwan, MOHW (Ministry of Health and Welfare), one of the 10 adults experience urolithiasis. The treatment cost of kidney stone spends huge health-care insurance budget every year in Taiwan.

Therefore, to solve the health-care problem such as urinary stone forming prediction by using sensors integrated system on a silicon chip become more important and possible in advanced silicon process for new POCT device applications.

Novelty: This paper presents diversified silicon based sensor technology and their readout circuit design for measuring four major parameters including pH, calcium ions concentration (Ca2+), uric acid level and conductivity (indicator for total dissolved solids) from the sample of the first void urine in the morning. Three kinds of sensors, i.e., potentiometric, amperometric and conductivity sensors are used in this system development. Multi-parameter sensing system integrated with signal processing chips as well as A.I. skill will be explored and discussed in this paper.

Methods: This research presents the electronics system of multi-sensor platform in modular-based approach that successfully developed for measuring and data-collection of four key parameters in urine sample to evaluate the risk of kidney stone formation in early stages. In addition, the on-chip sensor development and CMOS sensor interfacing circuits were designed and implemented in 0.35um and 0.18um technology.

Main results: The system was designed for sensing range of pH between 2.0 and 10.0 with resolution of 0.1 and overall accuracy better than 10%, for calcium ion concentration the range is between pCa 1.0 and pCa 4.0 with pCa 0.1 resolution and accuracy better than 10%. Uric acid sensor was formed by an electrochemical cell. A wide-range amperometric readout circuit with ability to work with both two-electrode and three-electrode sensors was utilized. Measurement range for uric acid was between 20 ppm and 500 ppm with resolution of 1 ppm and accuracy better than 10%. Electro-conductivity was an index that used for measurement of total dissolved electrolytes in urine. A gold-coated four-electrode conductivity sensor was used for measurement of conductivity.

Conclusion: This paper presented the design and implementation of a silicon technology based multi-sensor platform for the measurement and data collection of four key parameters in urine samples to evaluate the risk of urolithiasis in its early stages. Verification with standard solutions has shown that our system correlates well with measurements from standard instruments. To provide a potential point-of-care test device usage for kidney stone prediction, more clinical urine test data will be collected and analyzed for more accurate, reliable rick factor estimation.

Acknowledgements: The authors would like to thank MOST's two-year research project funding, Bioptik Technology Inc. and acknowledge the Ten Chen Medical Group, the National Center for High-Performance Computing in Taiwan, as well as the Taiwan Semiconductor Research Institute (TSRI), Taiwan, ROC for the technical support.

References:

[1] Robertson, W.G. Methods for diagnosing the risk factors of stone formation. *Arab. J. Urol.* **2012**, *10*, 250–257.

[2] Chou, Y.-H.; Li, C.-C.; Wu, W.-J.; Juan, Y.-S.; Huang, S.-P.; Lee, Y.-C.; Liu, C.-C.; Li, W.-M.; Huang, C.-H.;Chang, A.-W. Urinary Stone Analysis of 1,000 Patients in Southern Taiwan. *Kaohsiung J. Med. Sci.* **2007**,*23*, 63–66.

[3] Silverio, A.A.; Chung, W.-Y.; Cheng, C.; Hai-Lung, W.; Chien-Min, K.; Chen, J.; Tsai, V.F.S. The potential of at-home prediction of the formation of urolithiasis by simple multi-frequency electrical conductivity of the urin e and the comparison of its performance with urine ion-related indices, color and specific gravity. *Urolithiasis* **2015**, *44*, 127–134.

[4] Marickar, Y.M.F. Electrical conductivity and total dissolved solids in urine. *Urol. Res.* **2010**, *38*, 233–235.

[5] Chung, W.-Y.; Ramezani, R.F.; Cheng, C.-Y.; Wu, C.-H.; Ger, T.R.; Hsiung, N.S.K.; Wang, S.-H.; Tsai, V.F.S. Dual Key-Parameter Sensing System Development for Urolithiasis Recurrence Prevention. In Proceedings of the 2020 10th International Conference on Biomedical Engineering and Technology, Tokyo, Japan, 15–18 September 2020; Association for Computing Machinery: New York, NY, USA, 2020; pp. 11–16.

OP099

Novel DNA-based bioreceptor for label-free lactoferrin detection

Agnieszka PAZIEWSKA-NOWAK[1*], Marcin URBANOWICZ[1], Dorota Genowefa PIJANOWSKA[1]

1 Nalecz Institute of Biocybernetics and Biomedical Engineering PAS, Warsaw, Poland

* ***Corresponding author***. *E-mail address*: apaziewska@ibib.waw.pl

Keywords: surface plasmon resonance, DNA-type lactoferrin bioreceptor, affinity label-free biosensing, impedimetric biosensor

Motivation and Aim: A key challenge in determining clinically significant proteins is the lack of sensitive and selective analytical tools, which limits their use in routine diagnosis. For example, lactoferrin (Lf), an iron-regulatory glycoprotein, influences inflammation and modulates the immune response through various mechanisms. It is a putative marker for autoimmune inflammatory diseases like Leśniowski-Crohn's and neurodegenerative diseases such as Alzheimer's. This study presents a comprehensive method for developing DNA-based bioreceptors and demonstrates their implementation in selective Lf biosensors.

Novelty: Developing new bioreceptors is a challenge. In the case of DNA-type bioreceptors, like aptamers, it is time-consuming and resource-intensive, requiring Systematic Evolution of Ligands by Exponential Enrichment (SELEX) and sequencing methods. Producing antibodies is even more costly, as it involves animal or plant models and encounters stability issues due to environmental changes like pH or temperature. Lactoferrin's ability to bind with DNA makes it a promising candidate for a bioreceptor. Hence, predefined DNA sequences were utilized, and their affinity was rapidly screened using an optical method to select the optimal Lf-binding sequence, which lowered the production costs and ensured high stability and selectivity – essential factors for pre-clinical diagnostics of inflammatory and neurodegenerative diseases. Furthermore, transferring this technology to an impedimetric platform facilitated easy adaptation to biological samples, signifying a substantial advance in developing cost-effective and efficient biosensing methods.

Methods: Two label-free methods, surface plasmon resonance (SPR) and electrochemical impedance spectroscopy (EIS), were used for lactoferrin detection. SPR is a key technique for studying intermolecular binding affinity and dynamics. This label-free method quantifies receptor-analyte interactions in real time. It enabled the affinity screening of DNA oligonucleotides to identify the one with the highest affinity for Lf, providing kinetic data essential for evaluating DNA sequences as Lf bioreceptors. The selectivity study determined

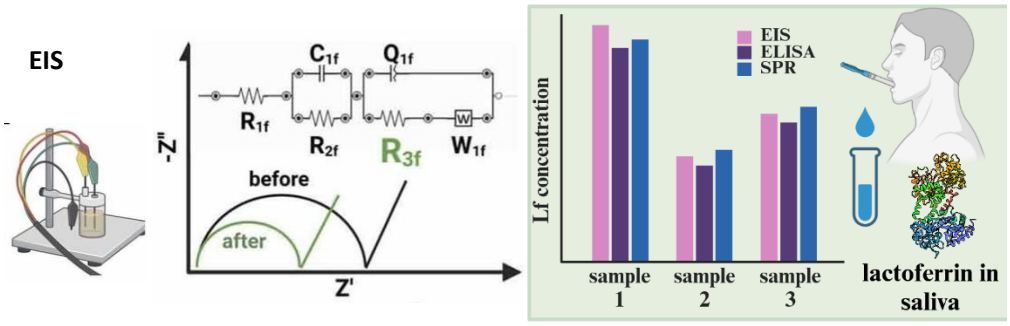

Fig. 1. Scheme of EIS and reference (SPR, ELISA) measurements in saliva samples.

the DNA strand's suitability for an Lf biosensor, while thermodynamics offered insights into interaction driving forces. We also employed electrochemical impedance spectroscopy (EIS) to construct the Lf biosensor, analyzing the system's electrical properties through equivalent circuit model parameters and analyte concentration changes. Further efforts adapted the biofunctionalization protocol for an impedimetric Lf biosensor. Lf quantification was achieved by comparing signals pre- and post-interaction with the DNA bioreceptor layer. Finally, the performance of the developed Lf biosensors was evaluated using human saliva samples.

Main results: The affinity screening results allowed for the rapid distinction of 72-mer *ds*DNA 5'[TAGAGGATCAAAAAA]$_4$TAGAGGATCAAA3' having the highest affinity to Lf. The kinetic analysis indicated a fast association and a considerably slower dissociation. An equilibrium dissociation constant $<10^{-6}$ showed a high specificity of Lf binding to the proposed DNA oligonucleotide, thereby providing a foundation for biosensing application. Thermodynamic parameters showed endothermic DNA-Lf complex formation, where positive enthalpy and entropy changes suggested an entropically driven process primarily influenced by hydrophobic forces supported by electrostatic binding. The selectivity study found minimal protein interference (<3%), confirming the bioreceptor's satisfactory selectivity for biosensing applications [1]. The biofunctionalization of electrochemical sensors was performed under the optimized molar ratio 1:10 of the linear linker/blocker. The changes in Lf concentration were correlated with resistance R_{3f} of the equivalent circuit model, where the calibration was established as ratio of charge transfer resistance before and after interaction ($R_{3f\_before}/R_{3f\_after}$) vs. Lf concentration ($C_{Lf}$) and characterized within a physiologically relevant Lf concentration range. Notably, the detection (1.25 nM) and quantification limits (2.5 nM) were the lowest of all the label-free methods and at least one order of magnitude lower than for immunosensors. Furthermore, the biosensors exhibited good shelf-life stability for 21 days of storage. Lastly, they were applied to measure Lf levels in human saliva (n=3), yielding consistent results with reference ELISA tests and confirming the utility of the proposed biosensor in saliva [2].

Conclusion: This work presents a label-free approach to developing DNA-based biorecognition layers and sensing proteins like lactoferrin. Effectively tackling bioreceptor design challenges, the DNA sequence with the highest affinity for Lf and its kinetics and thermodynamics of interaction with the target protein were identified. The bioreceptor showed remarkable selectivity for Lf over interferents and, when applied to the label-free impedimetric method, revealed high stability, sensitivity, and repeatability. The ability to quantify salivary Lf highlights the biosensor's potential for preclinical inflammation screening.

Acknowledgements: The research was funded by Nalecz Institute of Biocybernetics and Biomedical Engineering PAS, grant no. FBW/1.2/22.

References:

[1] Paziewska-Nowak A, Urbanowicz M, Sadowska K, Pijanowska DG. DNA-based molecular recognition system for lactoferrin biosensing. *Int J Biol Macromol*. 2023; 253(P3):126747. doi:10.1016/j.ijbiomac.2023.126747

[2] Paziewska-Nowak A, Urbanowicz M, Pijanowska DG. Label-free impedimetric biosensor based on a novel DNA-type receptor for selective determination of lactoferrin in human saliva. *Sensors Actuators B Chem*. 2024; 405:135377. doi:10.1016/j.snb.2024.135377

OP100

Selective Capture of Extracellular Vesicles by Peptide-Functionalized Hollow Fiber Membranes

Loredana DE BARTOLO[1,*], Simona SALERNO[1], Antonella PISCIONERI[1], Sabrina MORELLI[1], Alessandro GORI[2], Elena PROVASI[3], Paola GAGNI[2], Lucio BARILE[4,5], Marina CRETICH[2] and Marcella CHIARI[2]

National Research Council of Italy, [1]Institute on Membrane Technology CNR- ITM Rende,

[2]Institute of Chemical Sciences and Technologies "G. Natta", CNR- SCITEC, Milan, Italy

[3]Lugano Cell Factory, Istituto Cardiocentro Ticino, Lugano, Switzerland

[4]Cardiovascular Theranostics, Istituto Cardiocentro Ticino, Bellinzona, Switzerland

[5]Faculty of Biomedical Sciences, Università della Svizzera Italiana (USI), Lugano, Switzerland

* ***Corresponding author***. *E-mail address*: l.debartolo@itm.cnr.it

Keywords: Hollow fiber membranes, Peptide functionalization, Extracellular vesicles

Motivation and Aim: Membranes find utility in different biomedical applications, including drug delivery, artificial organs, tissue regeneration, diagnostic devices, and bioseparations [1-2]. Recently, membrane processes have been employed for the separation and concentration of subcellular components such as extracellular vesicles (EVs), which play a pivotal diagnostic and therapeutic role in numerous pathological conditions. However, the separation and isolation of specific EV populations from other components found in biological fluids is still challenging. We developed a peptide-functionalized hollow fiber (HF) membrane module to achieve the separation and enrichment of highly pure EVs derived from human cardiac progenitor cells.

Novelty: The strategy is based on the functionalization of Polysulfone HF membranes with a BPt peptide sequence able to bind extracellular vesicles characterized by highly curved membranes.

Methods: HF membranes were modified by a nanometric coating with a copoly azide polymer Copoly (DMA-NAS-N_3-MAPS) to limit non-specific interactions and to enable the conjugation with BPt peptide ligand (sequence: RPPGFSPFR-(O2Oc)-RPPGFSPFR-K-G-(O2Oc)2-Prg), by click chemistry reaction [3-4]. The BPt-functionalized module was integrated into a TFF process to facilitate the design, rationalization, and optimization of EV isolation. The isolation efficiency of the BPt functionalized HF membranes under TFF process was demonstrated by using a heterogeneous EV population derived from the culture media of human cardiac progenitor cells.

Main results: The TFF integrated BPt-functionalized membrane module demonstrated the ability to selectively capture EVs with diameter <200 nm into the lumen of fibers while effectively removing contaminants such as albumin. EVs successfully captured within the lumen of BPt-functionalized HFs were gently released by divalent metal cations solution. The captured and released EVs contain the common markers including CD63, CD81, CD9 and syntenin-1. Moreover, they retained round shape morphology and structural integrity as visualized by TEM images, highlighting the ability of this approach to concentrate and purify

EVs minimizing shear stress. Additionally, it achieved the removal of contaminants such as albumin with high reliability and reproducibility, reaching a removal of 93%.

Conclusion: The integration of BPt functionalized membrane within the TFF system allows to overcome one of the drawbacks of the current size-based isolation which is the presence of a large number of particles and/or aggregates with the same size of EVs and of other contaminants. Furthermore, the use of TFF BPt-functionalized membrane module reduces membrane fouling and the formation of the undesirable adsorption phenomena of non EVs components responsible of the filtration impairment.

Acknowledgements: The Authors acknowledge the financial support from the European Union's Horizon 2020 research and innovation program under grant agreements No. 951768 (project MARVEL).

References:

[1] S. Morelli, A. Piscioneri, E. Curcio, S. Salerno, C.-C. Chen, L. De Bartolo, Membrane bioreactor for investigation of neurodegeneration, Mater. Sci. Eng. C 2019; 103: 109793

[2] S Morelli, U D'Amora, A Piscioneri, M Oliviero, S Scialla, A Coppola, D De Pascale, F Crocetta, MP De Santo, M Davoli, D Coppola, L.De Bartolo. Methacrylated chitosan/jellyfish collagen membranes as cell instructive platforms for liver tissue engineering. Int J Biol Macromol. 2024; 281:136313.

[3] S. Salerno, S. Morelli, A. Piscioneri, M. Frangipane, A. Mussida, L. Sola, R. Frigerio, A. Strada, G. Bergamaschi, A. Gori, M. Cretich, M. Chiari, L. De Bartolo. Multifunctional membranes for lipidic nanovesicle capture. Separation and Purification Technology 2022; 298: 121561

[4] S. Salerno, A. Piscioneri, S. Morelli, A. Gori, E. Provasi, P. Gagni, L. Barile, M. Cretich, M. Chiari, L. De Bartolo. Extracellular vesicles selective capture by peptide-functionalized hollow fiber membranes. Journal of Colloid And Interface Science 2024; 667: 338–349

OP101

A controllable and multifunctional semiconductor chip for neuronal cells for separation, culture and potential sensing

Chia-Ming YANG[1,2,3,4*], Leung Sze TSUI[2], Ping-Han HSIEH[3], Yu-Fan XUE[1]

1 Institute of Electro-Optical Engineering, Chang Gung University, Taoyuan, Taiwan

2 Department of Electronic Engineering in Chang Gung University, Taiwan

3 Department of Biomedical Engineering in Chang Gung University, Taiwan

3 Department of Neurosurgery, Chang Gung Memorial Hospital at Linkou, Taoyuan City, Taiwan

* ***Corresponding author***. *E-mail address*: cmyang@mail.cgu.edu.tw

Keywords: LAPS, neuron, ODEP, potential

Motivation and Aim: Evaluating neuronal cells typically involved cell culture and quantitative analysis using immunology [1], electrophysiology [2], molecular biology [3], and optical imaging techniques [4] in the past. However, limitations of these methods could be poor spatial resolution, destructiveness, complexity and high costs. The most commercial tool in electrophysiology could be microelectrode arrays (MEAs) with high unit price and non-controllable for the distribution of neuronal cell growth and differentiation [5]. The low efficiency could be further improved by using new technology. In this work, we propose a controllable and multifunctional semiconductor chip for neuronal cells for separation, culture and potential sensing by means of the integration of 2 platforms including optically-induced dielectrophoresis (ODEP) and light-addressable potentiometric sensor (LAPS).

Novelty: A semiconductor layer, hydrogenated amorphous silicon on indium tin oxide (ITO) on a glass, is applied for common substrate for the operation of ODEP and LAPS. Also the custom-designed system with 2 different operation schemes can be easily performed. In ODEP scheme, DC illumination with virtual electrode design and AC bias was applied to chip. After ODEP operation, the quick switch can be easily achieved by changing to AC illumination with defined patterns and DC bias applied to chip in this system. With this 2-in-1 functional chip, the neuronal cell separation, culture and measurement could be easily performed with an affordable cost.

Methods: A microfluidic chip was fabricated with 4 different layers from substrate of a-Si:H/ITO/glass, adhesive tape with channel, top ITO/glass and polydimethylsiloxane connector. A peak-to-peak voltage (VPP) of 10V with frequency of 1 MHz was applied between top ITO and bottom ITO layer. Then B35 cells were introduced into channel, which can be manipulated by positive ODEP force with defined projected light pattern of rectangular shape. Due to the operation mechanism of LAPS measurement, an insulator should be added on a-Si:H layer. Therefore, different high dielectric constant layers including Al_2O_3, HfO_2 and NbOx were fabricated on a-Si:H/ITO/glass substrate to study the feasibility of the culture for neuronal neuroblast cell line (B35) from the central nervous system of a 4-to-10-month-old rat with neuroblastoma.

Main results: Al_2O_3 is the most suitable surface to culture B35 cells based on optical microscope check. With and without Al_2O_3 layer, B35 cells could be both collected by positive ODEP force but different manipulation velocity. Certain B35 cells can be easily located in the defined location by virtual electrodes operation. Differentiation of B35 cells was optimized by using retinoic acid (RA) to have a synapse length of 150 μm. The effective potential shift could be found with approximately +250 mV with cultured B35 cells of 1×10^4 cells on Al_2O_3 LAPS surface after 2 days. With 4-aminopyridine (4-AP) of 1 mM treatment, the potential shift is 10 mV.

Conclusion: A controllable and multifunctional semiconductor chip and the custom-designed system are both developed for neuronal cell relative electrophysiology researches. Neuronal cells can be selected and separated by ODEP and culture in microfluidics. Surface potential generated by cells and drug could be both quantitatively measured by LAPS. In the future, stimulus signal within ms level could be realized by a high-speeding scanning given LAPS system optimization, which could be more friendly promoted to neuron electrophysiology studies.

Acknowledgments: The authors would like to thank the National Science and Technology Council of R.O.C. for financially supporting this research under contract of 111–2923-E-182–001-MY3, 111–2221-E-182–023-MY3 and the Chang Gung University for UERPD2N0071.

References:

[1] Scanziani M, Häusser M. Electrophysiology in the age of optical imaging. *Nature*. 2009;461(7266):930-939. doi:10.1038/nature08493.

[2] Deng XH, Qiu Y, Li XX, et al. The role of the mitochondrial membrane potential in neuronal differentiation. *Neuroscience*. 2006;141(2):645-661. doi:10.1016/j.neuroscience.2006.04.017.

[3] Geloso MC, de Guglielmo G, Bernardi G, et al. Experimental models of neuroinflammation: from the mouse to human disease. *Neurochem Int*. 2011;58(6):729-738. doi:10.1016/j.neuint.2011.04.015.

[4] Drobac E, Desrosiers P, Cacace A, et al. The role of nitric oxide in the regulation of synaptic transmission in the hippocampus. *J Neurosci Res*. 2010;88(3):695-711. doi:10.1002/jnr.22379.

[5] Sakmann B, Neher E, Sigworth FJ, et al. The physiology of membrane channels in excitable cells. *Annu Rev Physiol*. 1984;46:455-472. doi:10.1146/annurev.ph.46.030184.002323

OP102

Development of a Biosensing Flow Cytometry-Based Assay for Predicting Drug Resistance in Leukemia Cells

Aleksandra KACZOROWSKA[1*], Wojciech KAŁAS[2], Przemysław SAREŁO[1,3], Marlena GĄSIOR-GŁOGOWSKA[1], Ewa ZIOŁO[2], Marta SOBAS[4], Halina PODBIELSKA[1], Marta KOPACZYŃSKA[1]

1 Department of Biomedical Engineering, Faculty of Fundamental Problems of Technology, Wrocław University of Science and Technology, Wybrzeże Wyspianskiego 27, 50-370 Wrocław, Poland.
2 Department of Experimental Oncology, Ludwik Hirszfeld Institute of Immunology and Experimental Therapy, Polish Academy of Sciences, Rudolfa Weigla 12, 53-114 Wrocław, Poland.
3 Pre-clinical Research Center, Wrocław Medical University, Karola Marcinkowskiego 1, 50-368 Wrocław, Poland.
4 Department and Clinic of Hematology, Cellular Therapies and Internal Medicine, Faculty of Medicine, Wrocław Medical University, Wybrzeże Pasteura 4, 50-367 Wrocław, Poland.

****Corresponding author***. *E-mail address: aleksandra.kaczorowska@pwr.edu.pl*

Keywords: Chemoresistance, Acute Myeloid Leukemia, Flow Cytometry, Anthracycline Antibiotics, Functional Assay

Motivation and Aim: Chemoresistance remains a major challenge in the treatment of acute myeloid leukemia (AML), which is the deadliest blood cancer. AML is a highly heterogeneous disease with surprisingly few mutations, suggesting that non-genetic factors are also relevant to AML outcomes. While molecular markers are valuable for prognosis, they do not fully account for drug resistance. Many studies show that lab tests can predict chemoresistance. However, such tests use a complex and time-consuming methodology and require long-term cell culture and specialized instrumentation. Nevertheless, such tests rarely are used outside clinical studies. There is an urgent need to examine another approach to chemoresistance testing. Functional assays offer promising alternatives for real-time drug response profiling. This study aims to develop a novel flow cytometry-based biosensing assay that can rapidly predict topoisomerase II inhibitors (e.g. daunorubicin (DNR)) resistance in leukemia cells, focusing on real-time drug accumulation and efflux kinetics. Our results will be correlated with the cell's sensitivity in in vitro testing and, retrospectively, with the therapy outcome.

Novelty: We introduce novel fluorescence-based parameters, that quantitatively describe DNR accumulation and efflux kinetics in leukemia cells. These parameters strongly correlate with IC50 values and provide a functional assessment of resistance, offering a clinically relevant alternative to traditional long-term cytotoxicity assays.

Methods: Leukemia cell lines with varying sensitivities to DNR (AML-007 – primary leukemia cell line, derived from the blood marrow of 66-years-old patient diagnosed with AML at the Clinic of Hematology, Blood Neoplasms, and Bone Marrow Transplantation, Wrocław Medical University; K562, and others) were evaluated. Using flow cytometry, intracellular DNR accumulation was measured over time, taking advantage of the drug's intrinsic fluorescence. Three parameters were introduced to assess drug susceptibility: Fluorescence Density (FD),

which measures drug accumulation relative to cell size; Susceptibility Index (S-index), derived from FD, indicating cell susceptibility to the drug; and Deviation from Linearity (DfL), which quantifies how much the fluorescence accumulation pattern deviates from a linear model. These parameters collectively reflect drug uptake and sensitivity. Confocal microscopy was used to visualize DNR intracellular localization and co-localization with nuclei and mitochondria. Spectroscopic analysis further examined biochemical differences in membrane composition and rigidity, providing insight into the physical properties contributing to drug resistance.

Main Results: AML-007 cells exhibited higher intracellular DNR accumulation and lower DfL values compared to the resistant K562 cells, which showed reduced drug uptake and deviations from linear accumulation patterns. Short-term exposure (30–120 min) enabled rapid differentiation between sensitive and resistant cells, demonstrating the power of flow cytometry-based biosensing for functional drug testing. Confocal microscopy revealed that sensitive cells exhibited DNR fluorescence in the area of cell nuclei, while resistant cells exhibited cytoplasmic localization of drug. Spectroscopic analysis confirmed altered membrane properties in drug-resistant cells, which may impact drug uptake. The S-index demonstrated a strong correlation with IC50 values across multiple cell lines, validating its utility as a predictive biosensing marker.

Conclusion: This study introduces a novel flow cytometry-based biosensing assay for the rapid prediction of daunorubicin resistance in leukemia cells. The identified fluorescence-based parameters offer a fast, functional measure of drug susceptibility with significant potential for clinical applications. Validation in patient-derived samples may enable real-time resistance profiling, paving the way for personalized treatment strategies and improved outcomes in AML. We are convinced that developing a reliable and practical method of predicting chemoresistance would not only allow avoiding overtreatment but also challenge the existing standard of care for AML patients. First, it would help identify high-risk patients that will be directed to the transplantation without inefficient induction therapy. Second, early identification of high-risk patients with chemoresistant illnesses will ethically allow them to participate in clinical studies.

Acknowledgements: This work was supported by NCN grant no. 2017/25/B/NZ5/02608, statutory programme of Hirszfeld Institute of Immunology and Experimental Therapy, Polish Academy of Sciences, and statutory funds of the Department of Biomedical Engineering, Faculty of Fundamental Problem of Technology, Wrocław University of Science and Technology.

Special Symposium SE12
Information Content Analysis in Cardiovascular and Respiratory Systems
Chair: Gerard Cybulski (Poland)
OP103–OP108

OP103

Magnetocardiography adds information to electrocardiographic recordings

Kazimierz PĘCZALSKI[1*], Judyta SOBIECH[2], Mateusz BROCZKOWSKI[1], Natalia JUREK[2], Tadeusz PAŁKO[1], Teodor BUCHNER[2*]

[1] Faculty of Mechatronics, Warsaw University of Technology, Warsaw, Poland

[2] Faculty of Physics, Warsaw University of Technology, Warsaw, Poland

* ***Corresponding author***. *E-mail address*: teodor.buchner@pw.edu.pl

Keywords: Magnetocardiography, electrocardiography, cardiological diagnosis

Motivation and Aim: Magnetocardiography (MCG) has been recently demonstrated as a method that allows for the diagnosis of cardiac patients better than a sole ECG, due to its ability to embrace electrically silent phenomena, such as intracellular ionic currents and vortex currents [1,2,3]. Modern MCG equipment can be used at the bedside, which significantly increases its availability. To achieve this aim, it is important to build the new guidelines for the measurement and interpretation of the MCG curve: its morphology depends on the measurement site.

Novelty: We demonstrate the results of measurement of cardiogenic magnetic field in clinical conditions, using a novel atomic sensor, based on optical measurement of alkali atoms, in a spin enhanced relaxation free (SERF) regime. Such results were hard to obtain so far, as the superconducting quantum interference device (SQUID) required liquid helium, which made it expensive and immobile, and the previous generations of SERF sensors required magnetically shielded rooms (MSRs).

Methods: We have used the SERF sensor to obtain the MCG signal in healthy volunteers, outside the MSR, and have simultaneously measured the synchronized electrocardiogram (ECG).

Main results: The figure presents an exemplary signal. The magnetic QRS complexes are well visible. The T wave morphology has been obtained by signal window averaging with overlapping windows aligned by QRS complexes.

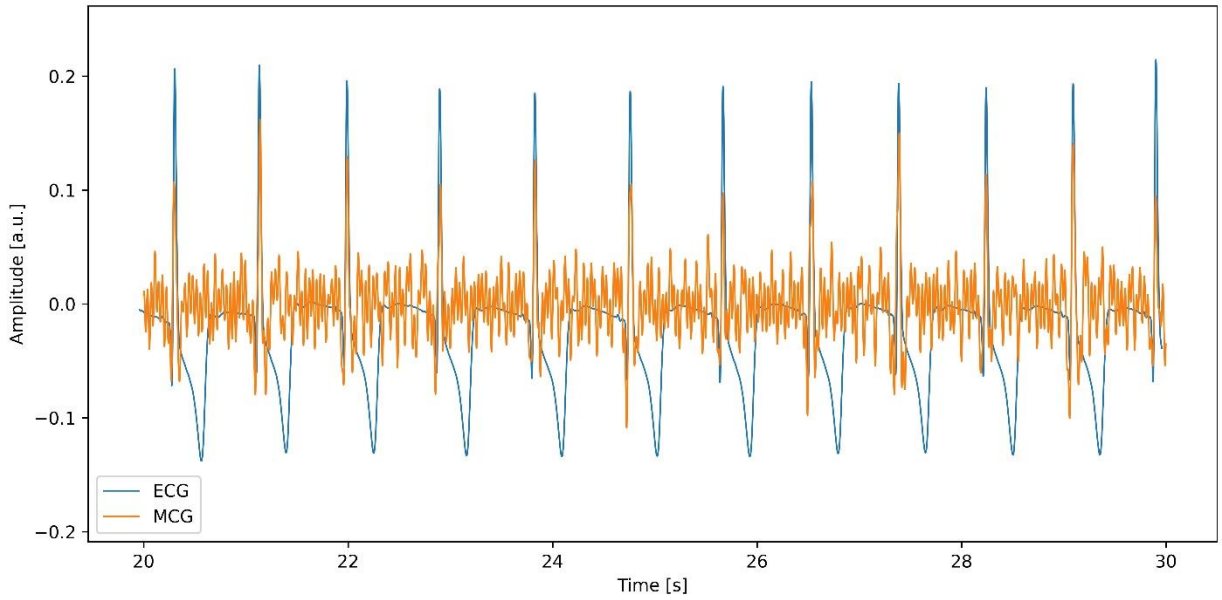

The MCG is potentially suitable for the assessment of: 1) low volume pathologies, such as microvasculature related cardiac insufficiency, which are undetected in the ECG due to low sensitivity, 2) broad pathologies, which are symmetric, and hence undetectable in the bipolar measurement. Unlike the ECG, the MCG is a true unipolar recording whose amplitude is strictly dependent on the location of the source [3]. The interpretation of the magnetic phenomena is still developing; specifically, the multi-ionic nature of the MCG [3] has to be further confirmed.

Conclusion: The MCG is a valuable method, which allows for complementing the ECG, due to its truly unipolar nature. Further research is required to interpret the physiological and physical mechanisms responsible for various features of the MCG, in order to assure proper physiological interpretation of the MCG information content.

References:

[1] Pęczalski K, Sobiech J, Buchner T, et al. Synchronous recording of magnetocardiographic and electrocardiographic signals. Sci Rep. 2024; 14(1):4098.

[2] Fenici R, Picerni M, et al. An advanced vision of magnetocardiography as an unrivalled method for a more comprehensive non-invasive clinical electrophysiological assessment. American Heart Journal Plus: Cardiology Research and Practice. 2025; 52:100514.

[3] Wessel N, Kim JS, Joung BY, et al. Magnetocardiography at rest predicts cardiac death in patients with acute chest pain. Front. Cardiovasc Med. 2023; 10. doi:10.3389/fcvm.2023.1258890

OP104

Information content of the electrocardiogram

Sebastian WILDOWICZ[1], Tomasz GRADOWSKI[1], Igor OLCZAK[1], Izabela GHAFOUR[1] Aleksandra BEDEŁEK[1], Maciej STANDERSKI[1], Teodor BUCHNER [1*]

[1] Faculty of Physics, Warsaw University of Technology, Warsaw, Poland

* ***Corresponding author***. *E-mail address*: teodor.buchner@pw.edu.pl

Keywords: electrocardiogram, machine learning, information content

Motivation and Aim: The widespread use of machine learning (ML) techniques opens the old question on information content in the 12-lead electrocardiogram (ECG). The context for the question is also new: an optimal choice of feature vector is essential to reduce the models, so that they can be integrated into wearable sensors. Optimal choice of electrodes allows to reduce the redundancies, aiming at maximization of diagnostic yield at minimal equipment cost.

Novelty: The utilization of ML models, namely PhysECG – the physically motivated projection of the ECG enables us to resolve the cardiac electric activity per each electrode separately, despite the fact that the 12-lead ECG measurements are essentially bipolar. The potential of Wilson Central Terminal (WCT) was shown to exhibit large departures from zero, so the question of whether the surface ECG can be truly unipolar is still open. The PhysECG projection is based on an assumption that unipolar electrode potentials may be treated as convolutions of a typical membrane potential with an electrode-specific function, which we refer to as the activity function. It may be interpreted as the mass of the activated ventricle within the sensitivity field of each electrode.

Methods: With help of PhysECG we have extracted the activity function (AF) resolved per electrode. The AF were then validated by inverse procedure: reconstruction of the QRS which demonstrated the low error level. This allows us to identify and correlate the information content per electrode and not per lead. It allows us to observe the activity of each ventricle separately. The model was built on the 21799 recordings of the PTB-XL database, and the presented data was analyzed in the group of 80 recordings of a control group from PTB database. First, we analyzed the stability of the representation. Next, we calculated the cosine similarity (CS) between each pair of electrodes: $CS = \cos \quad \varphi = \langle AB \rangle / (|A||B|)$. The similarity of AF is positive definite, as the numerator is a dot product of two positive definite AF. In consequence, the CS is 1 for a maximum correlation and 0 for a minimum correlation.

Main results: The representation was shown to be stable. The morphology of the activity functions was qualitatively similar across the whole patient group. The cosine similarity revealed many interesting relations.

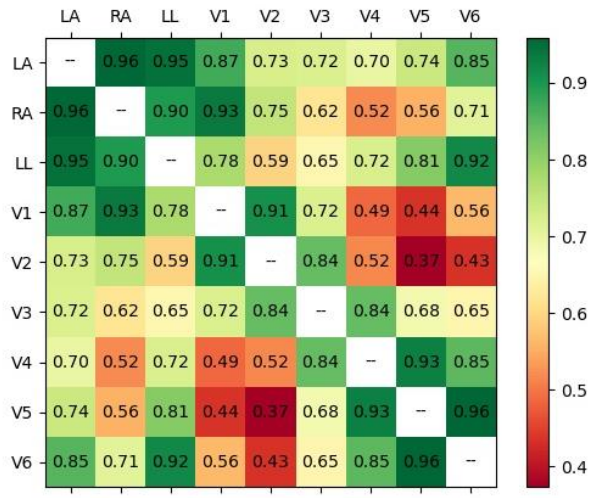

1. The correlation between the limb leads (LL) is one of the highest. This is understandable, as since the introduction of unipolar leads by Wilson, it is known that the information delivered by the LL is insufficient to precisely represent the electrical state of the myocardium. 2. There is a high correlation RA-V1, as both of them are related to the right ventricular activity (RVA). 3. Similarly, there is a high correlation LL-V6. The LA-V6 correlation is high as well. Both correspond to the left ventricular activity (LVA). 4. The lowest correlation observed is between V1, V2 and V4-V6, which validates our initial assumption, that the information delivered by this measure shows the LVA and the RVA separately [1]. 5. The precordial lead (PL) which has nearly equal (and low) correlations to all the LL is V3, which well corresponds with the results obtained with help of other ML models [2]. 6. The correlation between the LL, LA, and the LVA seen by V4-V6 seems to increase with the number of PL. This could be the manifestation of increased conductance between the postural wall and the LL, which was conjectured in [3]. Interestingly, the correlation between the RA and these leads increases as well. This subject requires further analysis.

Conclusion: In general, it may be concluded, that: 1) the high correlation between the LL confirms the decision to introduce the PL by Wilson, 2) utilization of a single LL should be a sufficient proxy for the WCT at reduced number of leads, 3) the V3 electrode seems to be the most promising candidate for a single PL, as its statistical independence from all the LL seems to be the highest, which means that it adds the most value, as compared to all other PL.

Moreover, it was demonstrated that the PhysECG technique reveals many interesting facts about the electrical activity of the heart. We have a strong feeling that we are starting to unleash the potential of this physically motivated projection.

References:

[1] Wildowicz S, Gradowski T, Figura P et al. Physically motivated projection of the electrocardiogram, Biocybernetics and Biomedical Engineering, in review. https://arxiv.org/abs/2410.11504

[2] Gradowski T, Buchner T, Deep learning model for ECG reconstruction reveals the information content of ECG leads, https://arxiv.org/abs/2502.00559.

[3] Buchner T, Molecular theory of biopotentials (in Polish), Oficyna Wydawnicza Politechniki Warszawskiej (2022).

OP105

Application of Impedance Cardiography for Differentiating Control Group from subjects with Presyncopal Symptoms During the LBNP test

Katarzyna TESSMER[1*], Grzegorz GRAFF[1], Gerard CYBULSKI[2]

[1] Gdańsk University of Technology, Faculty of Applied Physics and Mathematics & BioTechMed Center, Narutowicza 11/12, 80-233 Gdańsk, Poland

[2] Faculty of Mechatronics, Institute of Metrology and Biomedical Engineering, Warsaw University of Technology, Św. A. Boboli 8, 02-525 Warsaw, Poland

* Corresponding author: kattessm@pg.edu.pl

Impedance cardiography (ICG) is a valuable tool in cardiovascular research and clinical practice due to its non-invasiveness, cost-effectiveness, and ability to provide real-time hemodynamic monitoring. The Lower Body Negative Pressure (LBNP) test is used to simulate orthostatic stress by shifting blood volume away from the upper body to the lower extremities, mimicking the effects of standing up. ICG can be effectively applied in this test to monitor hemodynamic responses in real time and differentiate between individuals with normal and abnormal autonomic control.

In this study, 24 healthy men underwent graded LBNP exposure at -15, -30, and -50 mmHg. Each exposure has lasted for 10 minutes or until presyncope symptoms or signs occurred. Participants were divided into two groups: 13 individuals who successfully completed the test and 11 subjects who exhibited presyncopal symptoms or signs. For each participant, mean values of the intervals RR, CC, RC, CR, as well as the ratios RC/RR and CR/RR were calculated from 1-minute signal segments recorded at 0 mmHg and -30 mmHg. For the definition of the respective intervals, see [1]. Additionally, means and standard deviations were computed for both groups. At 0 mmHg, signals were analyzed starting from the 3rd minute of the beginning of the recording. At -30 mmHg, data were assessed from the 23rd minute for the control group, whereas for the presyncopal group, analysis focused on the period preceding symptom onset. To identify statistical differences between groups, Student's t-test and the Mann-Whitney U test were applied, depending on the data distribution. Moreover, differences were examined separately for both groups before the test started (0 mmHg) and during the test (-30 mmHg). We found statistically significant differences between the groups at -30 mmHg (in particular, $p = 0.004$ for CC intervals) and within each group separately at 0 mmHg and -30 mmHg. In particular, for CC intervals and the control group, $p = 0.01$, and for the presyncopal group, $p = 0.0001$. Moreover, most measures were higher in the control group. However, no statistically significant difference was observed between the groups at 0 mmHg before the start of the LBNP test.

In conclusion, our findings suggest that impedance cardiography parameters can effectively distinguish individuals with presyncopal symptoms from those who tolerate LBNP well, particularly at -30 mmHg. To further enhance the diagnostic and predictive value of this approach, future investigations could benefit from more refined, nonlinear measures of cardiovascular regulation.

References:

[1] Cybulski G. *Ambulatory Impedance Cardiography. The systems and their Applications*. Springer Science & Business Media; 2011.

[2] Gąsiorowska A., Nazar K., Mikulski T., Cybulski G., Niewiadomski W., Smorawiński J., et al., Hemodynamic and neuroendocrine predictors of lower body negative pressure (LBNP) intolerance in healthy young men. *J. Physiol. Pharmacol. 56 (2005) 179–193.*

OP106

The Effect of Data Filtering Methods on Heart Rate Asymmetry Measures

Rafal PAWLOWSKI[1*], Katarzyna BUSZKO[1]

1 Ludwik Rydygier Collegium Medicum in Bydgoszcz Nicolaus Copernicus University in Toruń, Bydgoszcz, Poland

* ***Corresponding author***. *E-mail address*: rpawlowski@cm.umk.pl

Keywords: Heart Rate Asymmetry, Heart Rate Variability, Poincare Plot, Artefacts Filtering

Motivation and Aim: Heart Rate Asymmetry (HRA) refers to an imbalance between accelerations and decelerations in human Heart Rate (HR). This phenomenon is commonly observed in young, healthy individuals, although its extent varies depending on the applied assessment method. Standard approaches to HRA analysis rely on Poincaré plots, which interpret the distribution of points corresponding to HR accelerations and decelerations. During our research, we observed that different data filtering methods significantly impact HRA outcomes. Therefore, we decided to investigate this phenomenon in greater depth. To eliminate the potential influence of outliers resulting from a specific data acquisition method, we analyzed the impact of various filtering techniques on HRA results using synthetically generated RR interval sequences.

Novelty: To the best of our knowledge, this is the first study to conduct a comparative analysis of the impact of different filtering methods on HRA measures. Using synthetic dataset allows for an unbiased assessment of preprocessing effects, and provides new insights into the methodological variability in HRA analysis.

Methods: We analyzed 1000 synthetically generated heartbeat interval series (300 RRs each), designed to closely resemble natural tachograms, including ectopic beats [1]. Our study evaluated the most commonly used HRA measures: Porta Index (PI), Guzik Index (GI), and Ehlers Index (EI), as well as less frequently applied metrics such as the Area Index (AI), Slope Index (SI), and Deceleration Input (DI). To identify potentially incorrect heartbeat intervals, we employed two automated detection methods: a square-based approach (excluding intervals outside the 300 – 2000 ms range) and a quotient-based approach (marking intervals as incorrect if the change between consecutive intervals exceeded 20%). The results obtained using these filtering methods were compared to each other and to those derived from unfiltered data. Additionally, we assessed the impact of filtering by comparing the outcomes with values obtained from shuffled interval series.

Main results: In four out of six HRA measures (GI, EI, AI, and SI), the differences caused by various filtering methods exceeded those observed between shuffled heartbeat series and their filtered counterparts. E.g. the median of differences in GI obtained by square and quotient filtering is -0.037 whereas the median of differences between shuffled data and quotient filtering is -0.011. Other differences between GI results obtained with different filtering methods are presented on boxplots in figure below. This finding suggests that the choice of filtering method has a greater impact on HRA results than the underlying data itself.

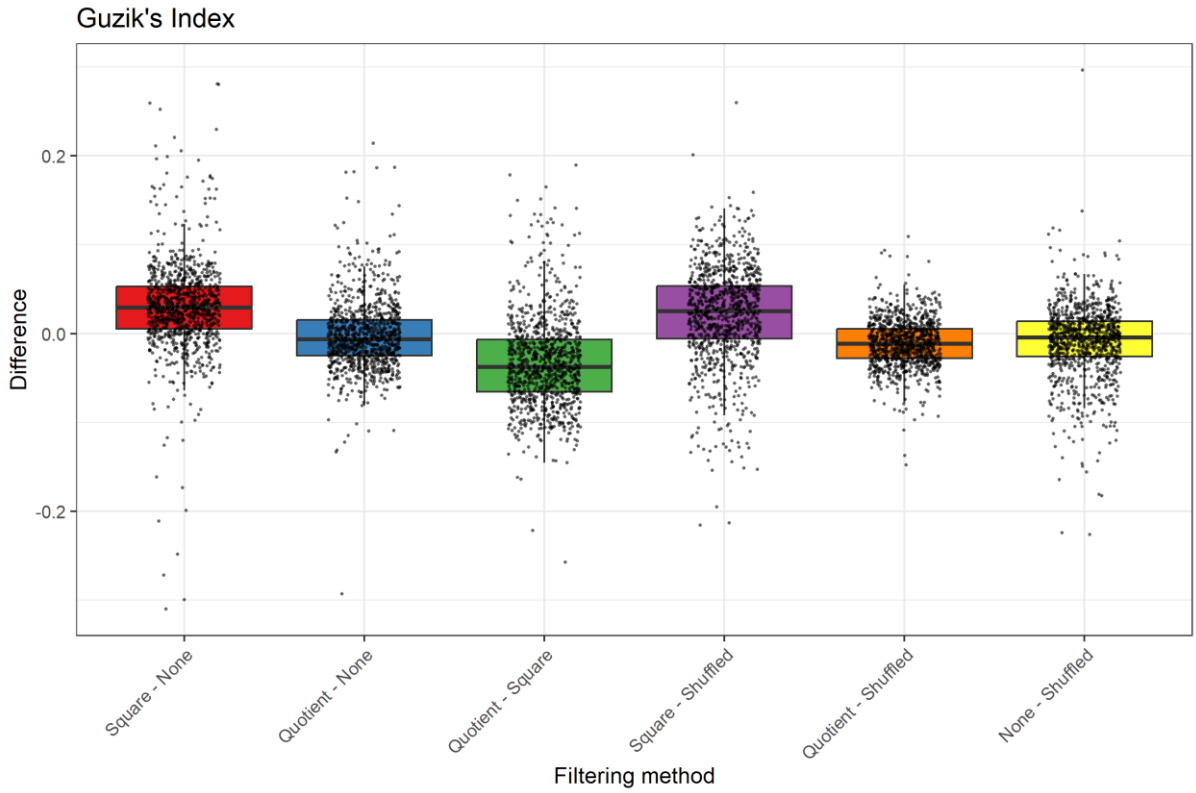

Conclusion: When manual identification of incorrect HR intervals is not feasible, it is crucial to provide detailed information about the automated detection method used. Without this transparency, meaningful comparisons between different studies become challenging, potentially leading to inconsistencies in findings. Addressing these discrepancies could enhance the reproducibility and reliability of HRA analyses in future research.

Acknowledgements: None

References:

[1] McSharry PE, Clifford G, Tarassenko L, Smith LA. Method for generating an artificial RR tachogram of a typical healthy human over 24-hours. In: Computers in Cardiology. ; 2002:225-228. doi:10.1109/CIC.2002.1166748

OP107

Comparison of three methods of identification the characteristic points in impedance cardiography signal

Milena CHOŁUJ[1], Bartosz ŚMIGIELSKI[1], Edward KOŹLUK[2], Ewa MICHALAK[3], Gerard CYBULSKI[1*]

1 Warsaw University of Technology, Department of Mechatronics, Institute of Metrology and Biomedical Engineering, Warsaw, Poland

2 Międzylesie Specialist Hospital Warsaw, Poland

3 Department of Noninvasive Cardiology, Institute of Cardiology, Warsaw, Poland

* ***Corresponding author***. *E-mail address*: Gerard.Cybulski@pw.edu.pl

Keywords: impedance cardiography, systolic time intervals, biomedical measurement uncertainty

Motivation and Aim: Impedance cardiography is an non-invasive technique allowing long-term monitoring of signal reflecting the mechanical activity of the heart: systolic time intervals and beat-to-beat changes in stroke volume. One of the essential problems with transforming ICG method from research type to clinical applications is uncertainty in proper calculations of hemodynamic parameters, caused by ambiguous identification of characteristic points on the ICG curve. Among them, as reported from literature and our researches [1-5], the detection of the B-ICG point, which denotes the end of pre-ejection period (PEP) and the beginning of left ventricular ejection time (ET), seems to be the most difficult part of automatic analysis of ICG signals. Since the ICG signal is slowly fluctuating around the electrical zero it is necessary to estimate baseline level for each cardiac cycle to calculate properly the maximal amplitude of first derivative of ICG signal (dZ/dt) and identify the point B.

Novelty: In this study we compared three methods of identifying B-ICG and the dedicated for each cycle level of fluctuating baseline. We used two methods known from literature [2, 5] and introduced a new one, based on calculating the integral of the signal during each heart cycle.

Methods: For baseline level estimation and B-ICG identification we applied Miyamoto et al. method [2] modified later by Cybulski [3] (denoted by MC), the method described by Naidu et al. (denoted as SN) [5] and our algorithm (IC) where the baseline is identified for each cycle as the line for which area under and below line is equal within the cycle from Q-ECG (i) to Q-ECG (i+1). We presumed that the sum of inflow and outflow of blood from the chest segment limited by receiving electrodes should be 0 within the cycle. Since dz/dt reflects volume flow rate changes, the areas below and above the dz/dt curve (for positive or negative values, respectively, should be equal. The same unfiltered, raw signals were used in all three cases, and the same algorithms were used for identifying Q, B, X points.

We compared the results of systolic time intervals (PEP and ET) evaluated using each method with the results acquired by means of pulsed Doppler echocardiography in the ascending aorta from a suprasternal projection in supine position performed in young, healthy subjects. For recalculations we used echocardiographic data obtained in supine position (ES) from the study published earlier [6]. The comparisons were performed between mean values of 100

beat cycles calculated for each subject using each of three methods MC, SN, IC and the ES by means of t-test for unpaired samples. **Main results:** For PEP the differences (d_{XX}) between ICG and Echo values using three methods of automatic calculations IC, SN and MC, were respectively: d_{IC} = 1,6±16.7 ms, d_{SN} = -14.6 ±24.7 ms, d_{MC} = -30.7±22.7 ms. For ET the differences (d_{XX}) between ICG and Echo values using three methods of automatic calculations IC, SN and MC, were respectively: d_{IC} = 17.6±22.4 ms, d_{SN} = 24.6±35.5 ms, d_{MC} = 40.8±26.9 ms.

Conclusion: We found that the discrepancies between the systolic time interval values estimated using ICG signal and those provided using pulsed Doppler visualizations were the smallest for newly introduced method (IC) based on calculating the integral of dZ/dt signal. However, we have to underline, that these comparisons were performed between mean values of automatic calculations for each subject and the mean values in each subject using echocardiographic method; thuse there were no beat-to-beat comparisons.

Acknowledgements: The research programs of institutions the authors are affiliated with supported this study. There was no external source of funds.

References:

[1] Lozano D.L, Norman G, Knox D et al. (2007) Where to B in dZ/dt. Psychophysiology, 44(1), 113–119

[2] Miyamoto Y, Tamura T, Takahashi T, Mikami T. Transient changes in ventilation and cardiac output at the start and end of exercise. Jpn J Physiol. 1981;31(2):153-68. doi: 10.2170/jjphysiol.31.153. PMID: 7289222.

[3] Cybulski G (1988) Computer method for automatic determination of stroke volume using impedance cardiography signals. Acta Physiologica Polonica, 39(5-6):494-503

[4] Cybulski G (2011) Ambulatory Impedance Cardiography. The Systems and their Applications. Series: Lecture Notes in Electrical Engineering, Vol. 76, 1st Edition, Springer-Verlag Berlin and Heidelberg GmbH & Co. KG

[5] S. M. M. Naidu, U. R. Bagal, P. C. Pandey, S. Hardas and N. D. Khambete, "Detection of characteristic points of impedance cardiogram and validation using Doppler echocardiography," 2014 Annual IEEE India Conference (INDICON), Pune, India, 2014, pp. 1-6, doi: 10.1109/INDICON.2014.7030596.

[6] Cybulski G, Michalak E, Koźluk E et al. (2004) Stroke volume and systolic time intervals: beat-to-beat comparison between echocardiography and ambulatory impedance cardiography in supine and tilted positions", Medical and Biological Engineering and Computing, 42, pp 707-711

OP108

Simulations study of pulmonary secretion removal using a closed suction system in two artificial lungs ventilated by a single ventilator and the Ventil divider

Krzysztof ZIELIŃSKI[1*], Zofia KNAPIŃSKA[1]

1 Nalecz Institute of Biocybernetics and Biomedical Engineering PAS, Warsaw, Poland

* ***Corresponding author***. *E-mail address*: kzielinski@ibib.waw.pl

Keywords: modelling and simulations, respiratory system, split ventilation, closed suction system, removal of pulmonary secretions, Ventil, COVID-19

Motivation and Aim: A closed suction system (CSS) is a device for pulmonary secretion removal in mechanically ventilated patients. Although the application of CSS and its effect on the entire respiratory circuit have been previously investigated [1, 2], the effect of CSS in the case of two patients ventilated by a single ventilator remains unknown. During the COVID-19 pandemic, multi-patient ventilation using a single machine was analyzed. The aim of this study is to assess the effect of CSS by investigating pressure and flow transmission across the entire respiratory circuit consisting of two ventilated subjects, connected to one ventilator by Ventil – a pneumatic divider for independent ventilation.

Novelty: To the best of the authors' knowledge, no studies have investigated the application of CSS in two subjects mechanically ventilated by a single ventilator.

Methods: Two artificial lungs (TestLung 2000, IMT Analytics), representing mechanical properties of the respiratory system of two ventilated subjects, were connected to the Ventil device (its output channels). The Ventil was then connected to a pneumatic, piston-based system that mimicked a ventilator operating in mandatory, pressure-controlled ventilatory mode. CSS was mimicked by another smaller piston-based system generating negative pressure with different time and amplitude. The simulation of secretion removal was performed during both the inspiratory and expiratory phases for diverse resistances (5-50 $mbar \cdot s \cdot L^{-1}$) and compliances (25-75 $mL \cdot mbar^{-1}$) of both artificial lungs. CSS simulation was performed only for the left artificial lung. Pressure and flow signals, recorder during the CSS procedure in the right artificial lung and in the connection between the 'ventilator' and the Ventil, were analyzed.

Main results: Due to the one-way valves in the Ventil's outputs, the negative pressure in the respiratory tract of the left artificial lung, affected by the CSS procedure, was not transferred to the respiratory tract of the right artificial lung. When negative pressure occurs in the left respiratory tract it helps maintain a secure seal, by enhancing the closing action of the one-way valve in the right Ventil's output. However, negative pressure can still transfer from CSS to the connection tube placed between the Ventil and the ventilator, potentially causing an emergency stop the ventilation from the latter. Moreover, an unexpected Ventil's behavior can occur due to its control system instability. Thus, CSS in the one ventilated subject may indirectly and adversely affect the ventilation of the second ventilated subject. A relief valve preventing the negative pressure is recommended between the ventilator and the Ventil.

Conclusion: The COVID-19 pandemic and the associated ventilator shortage now seem to be under control. However, these results could provide relevant clinical insights for future similar crises, such as terrorist threats or sudden respiratory pandemics.

Acknowledgements: This work was supported by the National Science Centre, Poland (Grant No 2021/43/D/ST7/01912).

References:

[1] Nakstad ER, Opdahl H, Heyerdahl F, Borchsenius F, Skjønsberg OH. Manual ventilation and open suction procedures contribute to negative pressures in a mechanical lung model. BMJ Open Respir Res. 2017;4(1):e000176.

[2] Jung F, Chou S-SP, Yang S-H, Lin J-C, Jow G-M. Closed Endotracheal Suctioning Impact on Ventilator-Related Parameters in Obstructive and Restrictive Respiratory Systems: A Bench Study. Applied Sciences. 2021;11(11):5266.

Oral Session OS12
Biomedical Signal Processing: Cardiovascular, Muscular and Cognitive Signals
Chairs: Stanislaw Wojtkiewicz (Poland)
OP109–OP112

OP109

Cross evaluation of diffuse correlation spectroscopy and intravoxel incoherent motion MRI in measuring tissue blood flow

Neda MOGHARARI*, Kamil LIPIŃSKI, Stanislaw WOJTKIEWICZ, Adam LIEBERT, Michal KACPRZAK

Nalecz Institute of Biocybernetics and Biomedical Engineering, Polish Academy of Sciences, Poland

* ***Corresponding author***. *E-mail address*: nmogharari@ibib.waw.pl

Keywords: Diffuse correlation spectroscopy, tissue blood flow, tissue blood perfusion

Motivation and Aim: Diffuse correlation spectroscopy (DCS) is a noninvasive optical technique to monitor tissue blood flow. The blood flow index (BFI) measured by the DCS (BFI_{DCS}) has been validated against several techniques which typically expressed the blood flow/perfusion with the units of $mL.100g^{-1}.min^{-1}$ or $cm.s^{-1}$ [1-3], leading to the lack of direct comparison with BFI_{DCS} expressed by the unit of mm^2/s. In this study, we compared the BFI_{DCS} with the diffusion, perfusion and flow parameters measured by the intravoxel incoherent motion magnetic resonance imaging (IVIM-MRI). IVIM-MRI technique provides information on the motion of water molecules in two components expressed in mm^2/s: the slow one refers to the water molecular diffusion in tissues and the fast one reflecting blood perfusion in vessels [4, 5].

Novelty: In this study, for the first time, we cross-evaluated the DCS ability to detect the Brownian like motion of scatterers and RBCs versus IVIM-MRI technique sensitive to Brownian motion and perfusion related incoherent motion of water molecules, all with the same unit of mm^2/s.

Methods: To compare the DCS and IVIM-MRI techniques in monitoring the tissue blood flow, we have carried out series of experiments on a tissue-mimicking phantom and muscle occlusion test on healthy adult volunteers. We utilized a container, with parallel holes to pass the transparent silicon tubes with the inner diameter of 1 mm representing a simplified model of muscle tissue with vessels. To mimic various blood velocities in muscles capillaries [Ivanov, 1985 #402], silicon tubes were connected to the programmable syringe pump and four flow rates of 1, 2, 4 and 6 mm/s within the tube were applied. The container was filled with an agar-gel mixture doped with $NiCl_3$. The lipid-based liquid (SMOFlipid 20, Fresenius Kabi) was added to the mixture to obtain a turbid material with reduced scattering coefficient of μ'_s = 1 mm^{-1} and absorption coefficient of μ_a = 0.003 mm^{-1}. SMOFlipid, is a highly scattering fatty emulsion that consists of spherical oil droplets within a lipid membrane with $\sim 0.5\ \mu m$ diameter [6]. The liquid mixture to pump through the tubes was prepared using a SMOFlipid as the scatterers (i.e., mimicking the RBCs) and distilled water.

The occlusion test was performed on the gastrocnemius muscles of the healthy adult volunteers in partial venous occlusion (60 mmHg) and arterial occlusion (180 mm Hg).

We have considered Pearson's correlation (R^2) approaches for statistical data analysis and evaluate the correlation between the flow index measured by the DCS and IVIM derived diffusion, perfusion and flow parameters.

Main results: Based on tissue-mimicking phantom results, a strong positive correlation was found between the flow index measured by DCS and the IVIM-derived perfusion ($R^2 = 87,\ p < 0.05$) and flow ($R^2 = 80,\ p < 0.05$) parameters. In-vivo experiments on healthy adult volunteers during leg muscle occlusion showed moderate positive correlation ($R^2 = 64,\ p < 0.05$) between the BFI_{DCS} and the IVIM-derived perfusion parameter representing the blood perfusion. However, the BFI_{DCS} is weakly correlated ($R^2 = 26,\ p > 0.05$) with the diffusion parameter referring to the water molecular diffusion in tissues. Finally, the weak correlation ($R^2 = 26,\ p > 0.05$) between the BFI_{DCS} and blood flow parameter is reported as the IVIM-derived flow parameter is influenced by tissue blood volume fraction, which was not changing linearly during the leg muscle occlusion.

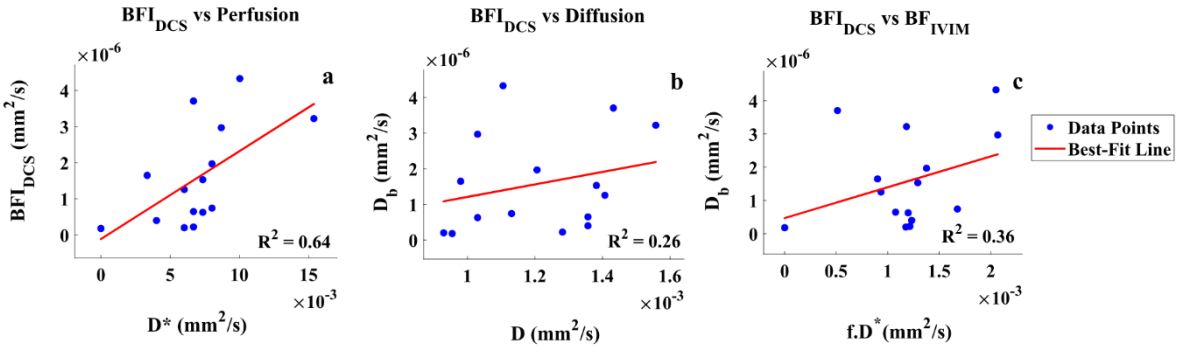

Correlations of BFI_{DCS} (blood flow index measured by DCS) versus (a) IVIM-derived perfusion, (b) IVIM-derived diffusion, (c) IVIM-derived blood flow during baseline, venous, and arterial leg occlusion measured on 5 healthy adult volunteers.

Conclusion: The moderate positive correlation between the BFI_{DCS} and the blood perfusion parameter measured by IVIM-MRI indicates that BFI_{DCS} primarily arises from scattered photons due to RBCs motion in the capillaries and intravascular blood perfusion. The weak correlation between the BFI_{DCS} and D confirms the fact that BFI_{DCS} is mostly influenced by blood perfusion in intravascular comparing to water molecular diffusion in extravascular.

Acknowledgements: The study was financed by the National Science Centre of Poland (NCN) in the framework of projects 2019/33/B/ST7/01387, 2020/39/D/ST7/03425, and by the Nalecz Institute of Biocybernetics and Biomedical Engineering PAS, grant no. FBW/2.3/22 and ST253

References:

1. Durduran, T., et al., *Optical measurement of cerebral hemodynamics and oxygen metabolism in neonates with congenital heart defects.* Journal of Biomedical Optics, 2010. **15**(3): p. 037004.
2. Buckley, E.M., et al., *Validation of diffuse correlation spectroscopic measurement of cerebral blood flow using phase-encoded velocity mapping magnetic resonance imaging.* J Biomed Opt, 2012. **17**(3): p. 037007.
3. Carp, S.A., et al., *Validation of diffuse correlation spectroscopy measurements of rodent cerebral blood flow with simultaneous arterial spin labeling MRI; towards MRI-optical continuous cerebral metabolic monitoring.* Biomed Opt Express, 2010. **1**(2): p. 553-565.
4. Bihan, D.L., et al., *Separation of diffusion and perfusion in intravoxel incoherent motion MR imaging.* Radiology, 1988. **168**(2): p. 497-505.
5. Shiraishi, T., et al., *Evaluation of diffusion parameters and T2 values of the masseter muscle during jaw opening, clenching, and rest.* Acta Radiologica, 2012. **53**(1): p. 81-86.

6. Skouroliakou, M., et al., *Physicochemical stability assessment of all-in-one parenteral emulsion for neonates containing SMOFlipid.* European Journal of Hospital Pharmacy: Science and Practice, 2012. **19**(6): p. 514-518.
7. Irwin, D., et al., *Influences of tissue absorption and scattering on diffuse correlation spectroscopy blood flow measurements.* Biomed Opt Express, 2011. **2**(7): p. 1969-85.
8. Shthialingam, E., *Hematocrit significantly confounds diffuse correlation spectroscopy measurements of blood flow.* Biomedical Optics Express, 2020. **11**: p. 4786-4799.

OP110

QRS detection based on the Matching Pursuit algorithm

Mohammed OWAHIDUR RAHMAN[1], Piotr AUGUSTYNIAK[1], Elzbieta OLEJARCZYK[1,2]

1 Department of Biocybernetics and Biomedical Engineering, AGH University of Krakow, Krakow 30-059, Poland

2 Nalecz Institute of Biocybernetics and Biomedical Engineering, Polish Academy of Sciences, Warsaw 02-109, Poland

eolejarczyk@agh.edu.pl

Abstract. The purpose of this study was the detection of QRSs in ECG signals using the Matching Pursuit (MP) method. Five groups of patients were consid- ered: healthy controls (NORM), patients with ST-T change (STTC), myocardial infarction (MI), conduction disturbance (CD), and hypertrophy (HYP). The ECG signals were decomposed using MP algorithm in set of functions, so called atoms, characterized by specific energy, amplitude, frequency and scale, corresponding to different ECG patterns, QRS complexes and T waves. A threshold for fre- quency ranging from 6 Hz to 45 Hz and scale value from 0.02 to 0.069 was ap- plied to identify the QRS patterns. The proposed algorithm allowed for the iden- tification of QRSs with a high performance independently on the patient group. The average values of sensitivity, specificity, and positive and negative predic- tive values were 98.94 %, 100%, 100%, and 99.30 %, respectively. The QRSs detection using an algorithm based on MP decomposition and on the application of two thresholds for frequency and scale is very efficient, and it can be applied in ECG wearable devices for monitoring patients in real time.

Keywords: ECG, QRS detection, Matching Pursuit method

OP111

Estimation of Cognitive Flow Level During Gait with Metrorhythmic Stimulation Using Physiological Data and Machine Learning

Patrycja ROMANISZYN-KANIA[1], Anita POLLAK[2], Aleksandra TUSZY[1*], Damian KANIA[3], Andrzej W. MITAS[1]

1 Faculty of Biomedical Engineering, Silesian University of Technology, Gliwice, Poland

2 Institute of Psychology

3 Institute of Physiotherapy and Health Sciences, The Jerzy Kukuczka Academy of Physical Education in Katowice, Katowice, Poland

* ***Corresponding author***. *E-mail address*: aleksandra.tuszy@polsl.pl

Keywords: physiological signals, psychological factors in physiotherapy, objective assessment methods, machine learning

Motivation and Aim: Cognitive flow (also called "flow") is a phenomenon derived from the theory of positive psychology and was a particular focus of Mihály Csíkszentmihályi, who first described this concept. Flow largely explains why people remain highly engaged in tasks despite the absence of external rewards [1]. Experiencing a high level of flow can lead to increased efficiency and productivity. Maintaining such engagement is a key aspect of developing non-pharmacological interventions like rhythmic auditory stimulation for gait re-education process. It may fluctuate due to various factors, including changes in the parameters of the applied auditory stimuli. Therefore, continuous monitoring of flow seems reasonable. However, it would be beneficial to establish objective measures of flow and better understand the body's physiological response to the experience. The aim of this study was to estimate low and high flow levels based on physiological data recorded during gait with metronomic stimulation, using machine learning methods.

Novelty: This study explores the concept of objectifying low and high flow level assessment based on physiological signals recorded in real-time during exercises, which could, in a broader perspective, contribute to the optimization of therapeutic interventions and the improvement of their effectiveness.

Methods: The study had a pilot character and continued the authors' previous work [2]. The research group comprised 36 healthy individuals (15F/21M, 20-38 years old). The physiological signals were measured using the Empatica E4 device placed on the wrist, which enables recording electrodermal activity (EDA), local body temperature, accelerometric signals from three axes, and blood volume pulse (BVP). All participants performed six transitions around the lab (about 2 min per transition), synchronizing their steps with the rhythm heard through the headphones (with 100%, 105%, and 95% of the preferred tempo with two different sound meters). The Flow Frequency Scale (11-item, 1-6 scale) questionnaire was filled in by participants after each given task. Recorded signals from every transition separately were processed as described in detail in [2,3,4]. The basic components of the EDA signal - tonicity, phase, and additive error - were determined. The calculated features of this signal included 18

statistical values and eight related to galvanic skin responses. Additionally, five features of the BVP signal were calculated, and based on this same signal, 14 parameters related to HRV were determined. The total number of computed characteristics was 46. The research group was divided into low and high flow level subgroups by the median flow value of 61, based on scores from all 216 data points.

Three independent classifiers, Support Vector Machine (SVM), k-Nearest Neighbor (kNN), and Naive Bayes, were used to build the flow level estimation model. The most differentiating features were selected using the Neighborhood Component Analysis algorithm, and the level of perceived flow (low/high) was determined based on the median score in the study group. The performance of the models was evaluated using k-fold cross-validation.

Main results: Among the characteristics that most differentiate the groups in terms of flow level were EDA, BVP, and HRV metrics. Electrodermal activity-related features included the minimum value of skin conductance level, rapid phasic movements, the number of galvanic skin responses, and the number of significant galvanic skin response events. BVP signal features included low and high bandpass filtering and the fundamental signal frequency. HRV parameters covered the standard deviation of successive differences, the standard deviation of normal-to-normal intervals, the root mean square of successive differences, the percentage of successive RR intervals differing by more than 50ms, the triangular index, the baseline width of the RR interval histogram, very low frequency, low frequency, high frequency, and heart rate. kNN model achieved the highest accuracy (71.25%), followed by Naïve Bayes (70.00%) and SVM (68.75%). It also had the highest True Positive Rate (77.27%), indicating strong sensitivity in detecting high-flow states. Naïve Bayes excelled in Positive Predictive Value (80.85%), suggesting it produced the most reliable positive predictions.

Conclusion: In our study, the kNN model achieved the highest accuracy and True Positive Rate. The observed results indicate satisfactory performance of the models. Similar machine learning applications have been described in some literature reports, such as using Naïve Bayes in [5]. The use of additional modalities with high measurement reliability, e.g. electroencephalography, can probably contribute to even higher accuracy of the proposed methods. The results suggest that objectification of flow level measurement may be possible. However, to fully confirm these observations, further work would need to be done, and similar studies should be conducted on an increased group of subjects.

References:

[1] Csikszentmihalyi M, Csikszentmihalyi IS. Optimal Experience: Psychological Studies of Flow in Consciousness. Cambridge University Press; 1988.

[2] Kania D, Romaniszyn-Kania PM, Bugdol M, et al. Flow and Physiological Response Assessment during Exercise Using Metrorhythmic Stimuli. Journal of Human Kinetics. 2024;94:243-254. doi:10.5114/jhk/187804.

[3] Romaniszyn-Kania P, Pollak A, Danch-Wierzchowska M, et al. Hybrid system of emotion evaluation in physiotherapeutic procedures. Sensors. 2020;20(21):6343. doi:10.3390/s20216343.

[4] Romaniszyn-Kania P, Pollak A, Bugdol MD, et al. Affective state during physiotherapy and its analysis using machine learning methods. *Sensors*. 2021;21(14):4853. doi:10.3390/s21144853.

[5] Graft J, Romine W, Watts B, et al. A Preliminary Study of the Efficacy of Using a Wrist-Worn Multiparameter Sensor for the Prediction of Cognitive Flow States in University-Level Students. Sensors. 2023; 23(8):3957. https://doi.org/10.3390/s23083957.

OP112

Evaluation of Factors-of-Interest in Muscle Phantoms Based on Ultrasonic Data

Vladislavs AGARKOVS[1], Aleksandrs SISOJEVS[1;2], Alexey TATARINOV[1], Tamara LAIMIŅA[1]

1 Institute of Electronics and Computer Science, 14 Dzerbenes St., LV-1006, Riga, Latvia

2 Riga Technical University, 6A Kipsalas Street, Riga LV-1048, Latvia

alexiv@inbox.lv

Abstract. Subcutaneous adipose tissue (SAT) and intermuscular adipose tissue (IMAT) are two forms of body fat. The differential assessment of SAT and IMAT contents in sarcopenia and obesity by ultrasonic measurements is difficult due to their complex influence. In the present study, the possibility of using pattern recognition methods applied to ultrasound propagation signals to discriminate SAT and IMAT values was investigated using muscle tissue mimicking phan- toms. The muscle mimicking phantoms were made of gelatin (muscle) with oil (fat) outer layers (SAT) and oil inner inclusions (IMAT) with gradually varying SAT and IMAT contents from zero to 50 % with a step 12.5%. The set included a net of 25 phantoms with five grades of SAT and IMAT, each varied inde- pendently. Each phantom (object under study) passed multiple repeatable ultra- sonic tests. For each object, a set of parameters was extracted from the set of ultrasonic signals, including speed of sound, ultrasound attenuation at two frequencies and signal amplitude integrals. Decision rules were constructed for all objects based on the set of the extracted parameters. The efficiency of the con- structed rules was checked using the signals of the examination object. The re- sults of the experiments demonstrated the potential effectiveness of the proposed approach for determining SAT and IMAT values separately. **Keywords**: Quantitative Ultrasound, Pattern Recognition, Tissue Mode

Oral Session OS13
ICT in Medicine and Health Technology Assessment
Chairs: Tomasz Neumann (Poland)
OP113–OP116

OP113

Detection of electronic protected health information in DICOM objects: rule-based methods vs. LLMs

Dmytro TKACHENKO, Milena SOBOTKA, Antoni GÓRECKI, Jakub KŁOPOTEK-GŁÓWCZEWSKI, Tomasz NEUMANN, Jacek RUMIŃSKI

Gdansk University of Technology, FETI, Department of Biomedical Engineering, Gdansk,

80-233, Poland

dmytro.tkachenko@pg.edu.pl,

Abstract. This study evaluates and compares the effectiveness of rule- based methods and Large Language Models (LLMs) in detecting elec- tronic protected health information (ePHI) within DICOM files, with a particular focus on Polish names and identifiers. The research utilized multiple test datasets containing DICOM and JSON data with identifiers and popular, rare Polish names, as well as false names, which do not ex- ist. We compared several approaches: rule-based methods (STRICT and ANY mode), state-of-the-art (SOTA) models (GPT-4o, DeepSeek v.3, Bielik v.2, and Llama v3.3), and the RoBERTa De-ID Named Entity Recognition (NER) model. Results demonstrated that rule-based meth- ods achieved high precision and recall for structured data, with near- perfect performance for popular and rare names. However, LLMs, while flexible, require high false positive rates and significant processing time. Rule-based algorithms are currently more effective for ePHI detection in DICOM attributes, but they struggle with free-text attribute values. Fine-tuning LLMs is suggested as a potential improvement for ePHI de- tection in medical imaging data.

Keywords: healthcare informatics, ICT in medicine, DICOM, large lan- guage models

OP114

User expectations on wearable medical devices in Latvia

Nadezhda SEMJONOVA[1], Roberts MALNIEKS[1], Alexei KATASHEV[2]

1 Economics and Business Institute, Riga Technical University, Kipsalas street 6b, Riga, LV1048, Latvia

2 Mechanical and Biomedical Engineering Institute, Riga Technical University, Kalnciema street 6, Riga, LV1048, Latvia

Nadezda.Semjonova@rtu.lv

Abstract. This study explores expectations of potential users of wearable medi- cal devices in Latvia. The opinions of healthy individuals were collected using on-line free survey portal, this limited the study to the population of active in- ternet and IT users. Out of 89 respondents, 44 already use wearable devices, like smart watches of fitness activity meters. Latvian respondents consider price as the most important factor, determining intention to purchase the device. This is different from other developed countries, where easiness to use is perceived as the most important factor. Alongside, Latvian respondents perceive wearable devices as mostly suitable for fitness activity monitoring and seldom see any health benefits except of fitness tracking. The medical doctors could change this opinion, as the Latvian users consider medical doctors as the most creditable in- formation sources about wearable medical devices.

Keywords: Wearable devices, Fitness tracking, Health monitoring, User expec- tations, Latvia

OP115

Relationship between accelerometer-based walking activity and subjective health

Robert RÓŻAŃSKI[1], Piotr WIŚNIEWSKI[12*], Jacek RUMIŃSKI[3]

1 Lab4Life Sp. z o.o., Gdynia, Poland

2 Chair and Department of Endocrinology and Internal Diseases, Medical University of Gdańsk, Gdańsk, Poland

3 Gdansk University of Technology, Department of Biomedical Engineering, Gdańsk, Poland

* ***Corresponding author***. *E-mail address*: *piotr.wisniewski@gumed.edu.pl*

Keywords: accelerometer, feature engineering, subjective health, walking activity

Motivation and Aim: State of the art studies report that walking is important in preventing diseases and increasing life expectancy. The study aims to analyze the relationship between objective, accelerometer-based walking activity features and reported subjective health.

Novelty: This is the first cross-dataset study with a set of features derived for objectively measured walking activity signals compared to subjective health analyzed using absolute and relative probability distributions. The study shows that the sum of steps, variance of walking activity, and non-physical activity (NPA) periods are more related to poor health rating than the intuitively assumed relation with age.

Methods: We used data from two studies: NHANES (2005-2006, random sample) [1] and UK Biobank [2] (non-random s.). The UKB dataset has almost 100000 examples with raw accelerometer data, measured for 7 days. The NHANES datasets contain derived step values per minute (7*24*60=1440 samples per subject, *step_signal={steps_per_ith_minute}, i*=1..1440). We preprocessed the UKB raw data to step signals based on the approach described in [3]. We derived subjective health ratings (NHANES: range 1-5, 5=worst; UKB: range 1-4, 4=worst), selected the same age range (45-77 y.). Seven physical activity features (f_{PA}) were calculated for each step signal: sum for steps per day, NPA events (<10 steps/min), Hjorth activity (signal variance), signal energy, cadence (an average of max values in all 30-minute windows), Gini inequality index and the PA aggregation measure. Data were categorized into good health rating (NHANES 1-3, UKB 1-2) and poor health rating (NHANES 4-5, UKB 3-4) to further evaluate the probability of poor health rating with age. Next, we introduce the distribution of probabilities of poor health rating P_i as a function of given feature:

$$P_i = P(poor\ health | f_{PA} \geq i) = \frac{Npg_i}{Npg_i + Nng_i} \qquad RPR_i = \frac{P(f_{PA} \geq i | poor\ health)}{P(f_{PA} \geq i | good\ health)} = \frac{Npg_i / Np_i}{Nng_i / Nn_i}$$

where *Npg* is the ***N***o. of ***p***ositive events (i.e., poor health rating) for the f_{PA} ***g***reater that *i* (≥ threshold); *Nng* the same for negative events (i.e., good health rating).

The value of P_i is calculated for each possible feature value *i*, e.g., for the sum of steps $P_{i=1000}$ is the probability of finding an observation with a poor health rating when sum of steps per day is ≥ 1000. Additionally, we introduce the Relative Probability Ratio, comparing the probabilities for poor and good health ratings under given conditions. By changing *i* value we can obtain the distribution of *P* and *RPR*.

Main results: For the NHANES dataset, there is no statistical difference between subjective health rating categories 2 vs. 3 (p=0.831) and 4 vs. 5 (0.696) concerning age (Fig. 1). Additionally, for both datasets and all categories, the effect size (rank biserial correlation), is very small, with maximum of 0.071. However, there is an observable relationship between objectively measured PA features and subjective health ratings. Comparing all categories, the p-value is less than 0.05 for "sum of steps," activity, cadence, and npa. For example, for the activity feature, the rank biserial correlation for the above examples is -0.145 for 2 vs. 3 and -0.21 for 4 vs. 5. In Fig. 1, examples of P_i and RPR_i distributions are presented for "sum of steps", activity (variance of step signals), and NPA.

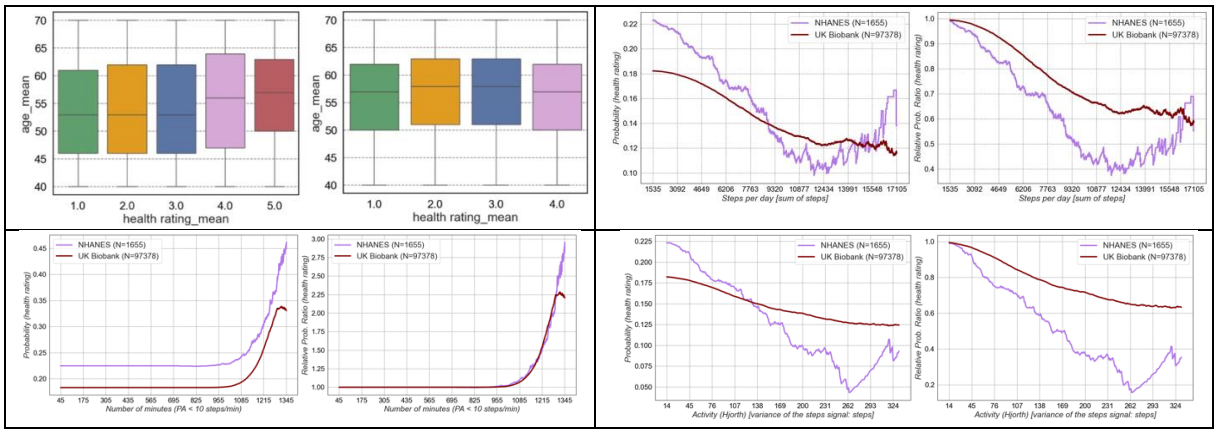

Fig. 1. From the top, left: age statistics for original subjective health ratings groups (NHANES, UKB), P_i and RPR_i as a function of the sum of steps, NPA, and activity (N-No. of preprocessed examples).

The interesting finding is that walking activity features are more related to poor health rating (P_i) than the intuitively assumed relation with age. P_i decreases until about 11000 steps are taken daily. Then, the distribution is flattened (UKB), and even $P_{i>11000}$ increases for NHANEs (smaller sample size). For example, for men: $f_{PA} \geq 11000$ -> $Npg_{11000} = 20$ (poor health), $Nng_{11000} = 191$ (good h.), while $f_{PA} < 11000$ -> $Npl_{11000} = 141$ (poor h.), $Nnl_{11000} = 471$ (good h.). For both datasets similar trend is observed. The variance of walking signal is also related to subjective health rating, reaching a decrease of P_i of ~80% for NHANES. Finally, the RPR for NPA shows almost perfectly overlapping results for both datasets, showing an exponential increase in poor health ratings when the average NPA is high.

Conclusion: The sum of steps, variance of walking activity, and NPA periods are more related to poor health rating than the intuitively assumed relation with age. The results were obtained for two different sets (random sample, small size vs. non-random sample, big size), indicating the same trends.

Acknowledgements: This study was supported by the National Centre for Research and Development (NCBiR) under grant no. POIR.01.01.01-00-1221/18. This research has been conducted using data from the UK Biobank, a major biomedical database (application 56598), and the NHANES study.

References:

[1] Centers for Disease Control and Prevention (CDC). National Center for Health Statistics (NCHS). National Health and Nutrition Examination Survey Data. Hyattsville, MD: U.S. Department of Health and Human Services, Centers for Disease Control and Prevention, 2024, https://wwwn.cdc.gov/nchs/nhanes/.

[2] Sudlow C, Gallacher J, Allen N, Beral V, Burton P, Danesh J, et al. UK biobank: An open access resource for identifying the causes of a wide range of complex diseases of middle and old age. PLoS medicine. 2015;12(3):e1001779.

[3] Dinesh J, et. al, What Is a Step? Differences in How a Step Is Detected among Three Popular Activity Monitors That Have Impacted Physical Activity Research. Sensors (Basel). 2018 Apr;18(4): 1206

OP116

Subjective Evaluation of Phantoms in X-ray Breast Imaging Research: Insights from Bulgaria

Tsvetelina TENEVA[1], Antonio SARNO[2], Nikolay DUKOV[1], Vasileios ELEFTERIADIS[3], Zhivko BLIZNAKOV[1], Panagiotis PAPADIMITROULAS[3], Kristina BLIZNAKOVA[1]

1 Medical University of Varna, Varna, BULGARIA

2 University of Milan, Milan, ITALY

3 BIOEMTECH, Athens, GREECE

kristina.bliznakova@mu-varna.bg

Abstract. This work aims at defining a validation approach to subjectively assess the realism of breast phantom images acquired with x-ray systems. Various breast phantoms were used to address specific questions. First, the realism of a breast neoplasm model was evaluated. Second, different materials for phantom produc- tion were evaluated for x-ray contrast, sharpness, inhomogeneity, and artifacts. Third, 3D printing techniques for manufacturing breast tissues were explored. Lastly, computational models were assessed by comparing manual and automatic segmentations of the breast tissues. Two distinct grading scales were introduced to aid radiologists in evaluating the phantoms. The first scale assesses computa- tional phantoms based on the realism of glandular tissue distribution, morphol- ogy, and the preservation of fine parenchymal structures. The second scale is designed to support the validation of physical phantoms, focusing on the realism of the generated x-ray image. The scales have been applied to the selected cases and will be further used in studies involving the production of anthropomorphic phantoms.

Keywords: radiologist evaluation, anthropomorphic phantoms, breast imaging, breast neoplasm, segmentation

Oral Session OS14
Neural Engineering and Neuroinformatics
Chairs: Chih-Wei Peng (ROC Taiwan), Leon Bobrowski (Poland)
OP117–OP120

OP117

Therapeutic Effects of Temporal Interference Stimulation on Post-Stroke Motor Function Recovery: An Animal Study

Chih-Wei PENG[1,*], Chun-Wei WU[1], Yu-Ting Li[2]

1 School of Biomedical Engineering, College of Biomedical Engineering, Taipei Medical University, Taipei, Taiwan

2 The Instrument Technology Research Center, National Applied Research, Hsinchu, Taiwan

* ***Corresponding author***. *E-mail address*: *cwpeng@tmu.edu.tw*

Keywords: Transcranial temporal interference stimulation, stroke, motor function, rehabilitation

Motivation and Aim: Traditional non-invasive brain stimulation techniques, such as direct current stimulation (tDCS) and alternating current stimulation (tACS), have shown potential in promoting post-stroke functional recovery. However, their therapeutic efficacy is significantly limited by the shielding effects of the scalp and skull, which reduce the effectiveness of electrical stimulation as tissue depth increases. Transcranial temporal interference stimulation (TIS) is an emerging non-invasive deep brain stimulation technique that has the potential to overcome these limitations.

Novelty: The therapeutic effects and neuroregulatory mechanisms of TIS in stroke treatment remain largely unexplored. This study aims to investigate the efficacy of TIS in improving motor function following ischemic stroke.

Methods: A middle cerebral artery occlusion (MCAO) rat model was employed to simulate stroke and evaluate post-treatment behavioral outcomes. One week before inducing stroke, stainless steel screw electrodes (1.4 x 8 mm) for minimal-invasive transcranial stimulation were implanted into the left cranial bone of the rats and secured with bone cement. On the day of the stroke induction, the rats underwent a 1.5-hour MCAO procedure, followed by the removal of the suture, wound closure, and recovery. The TIS treatment was initiated immediately after, involving intermittent theta burst stimulation (iTBS) at 1 mA for 15 minutes. In the sham-treatment control group, carrier currents of the same frequency were applied without generating low-frequency interfering waves in the brain tissue. In the non-stroke control group, the same surgical procedures were performed without occluding the middle cerebral artery, and no stimulation was administered post-surgery. Behavioral assessments, mNSS and grid-walking tests, were conducted on days 4, 7, 14, and 21 post-stroke to evaluate motor function.

Main results: The results showed that post-stroke, the neurological deficit scores and grid-walking errors significantly increased in the MCAO and MCAO+TIS groups compared to the non-stroke control group, indicating marked impairment in motor function. Following 5 consecutive days of TIS treatment, rats in the treatment group (MCAO+TIS) exhibited a more pronounced recovery trend compared to the untreated group (MCAO).

Conclusion: These findings suggest that 5 consecutive days of TIS stimulation hold potential for improving motor impairments caused by ischemic stroke in the middle cerebral artery, providing a promising avenue for stroke rehabilitation.

OP118

Digital Cognitive Assessments and Smart Environments

Ankica BABIC[1,2] *, Gina FARSIROTOS[2]

1 University of Linkoping, IMT, Linkoping, Sweden

2 University of Bergen, INFOVIT, Bergen, Norway

** Corresponding author. E-mail address: ankica.babic@uib.no, ankica.babic@liu.se*

Keywords: Cognitive decline, digital health, remote monitoring, aging, health technologies

Motivation and Aim

Cognitive decline associated with aging, including conditions such as mild cognitive impairment (MCI) and early dementia, is a growing public health concern. As global populations age, innovative solutions are needed to support early detection, personalized interventions, and continuous monitoring outside traditional clinical settings. Information technologies (IT) offer promising tools to detect subtle cognitive changes, engage users in cognitive training, and provide remote support for both patients and caregivers. This abstract presents an overview of emerging IT solutions, focusing on their potential to enhance cognitive health management in aging populations.

Novelty

Recent advances in sensor technologies, mobile health applications, and artificial intelligence (AI) have enabled a new generation of cognitive monitoring tools. Unlike traditional cognitive assessments, which are often conducted episodically in clinical environments, modern IT-based systems offer continuous, real-time data collection in naturalistic settings. This shift towards longitudinal and passive data capture opens new possibilities for detecting subtle cognitive changes that may indicate early decline.

Methods

This work reviews and synthesizes recent research on IT-based solutions for cognitive decline, including:

- Wearable and ambient sensors for monitoring daily activities and behavioral patterns.
- Smartphone-based cognitive screening tools and interactive applications for cognitive training.
- AI-driven analysis of speech, typing patterns, and activity data for detecting cognitive changes. The focus is on solutions validated in research or clinical settings, with special attention to usability and acceptability among older adults.

Main results

Table 1 summarizes key categories of IT tools, their primary functions, and selected examples from recent literature.

Technology Type	Primary Function	Examples
Wearable sensors	Activity, sleep monitoring	Smartwatches, fitness trackers
Smartphone apps	Cognitive screening, training	BrainHQ, Lumosity
Ambient sensors	Daily activity tracking	Smart home systems
Speech analysis AI	Cognitive change detection	Voice biomarkers from calls

These tools demonstrate high potential for early risk detection and engagement in cognitive health promotion. However, challenges related to data privacy, digital literacy, and clinical integration remain.

Conclusion

IT-based technologies hold great promise for supporting healthy cognitive aging through early detection, continuous monitoring, and digital cognitive interventions. Future work should focus on improving interoperability between systems, ensuring clinical validation, and enhancing user-centered design to maximize adoption among older adults. Multidisciplinary collaborations between clinicians, engineers, and social scientists will be essential to translating these technologies into effective, scalable solutions for cognitive health management.

References

1. Dodge HH, Zhu J, Mattek NC, et al. Use of High-Frequency In-Home Monitoring Data May Reduce Sample Sizes Needed in Clinical Trials. PLoS One. 2015;10(9):e0138095.
2. Kourtis LC, Regele OB, Wright JM, et al. Digital biomarkers for Alzheimer’s disease: the mobile/wearable devices opportunity. NPJ Digit Med. 2019;2:9.
3. Deeg DJH, Bath PA. Self-Rated Health, Gender, and Mortality in Older Persons: Introduction to a Special Section. Gerontologist. 2003;43(3):369–371.

OP119

Creating structures from formal neurons

Leon BOBROWSKI

[1] Faculty of Computer Science. Bialystok University of Technology

[2] Nalecz Institute of Biocybernetics and Biomedical Engineering, Polish Academy of Sciences (IBBE PAS) , Poland

Corresponding author. *E-mail address* l.bobrowski@pb.edu.pl

Keywords: formal neurons, structuring neural networks. high learning

Data mining procedures are aimed at extracting useful patterns from multidimensional data sets [1]. Patterns extracted from data sets are used, among others, in computer systems of artificial intelligence. A large group of data mining methods is based on models of neural networks

Neural networks are built using various types of neuron models [2]. Of great importance are networks built from formal neurons, often called multilayer perceptrons. In the middle of the last century, the perceptron was the first model of the learning process in the human nervous system. This model initiated the rapid development of neural networks and their versatile applications

Designing neural networks for a specific task involves choosing their structure, e.g. the number of layers and the number of neurons in each layer, and setting the parameters (weights) of individual neurons in the network. According to the currently widely used back-propagation method, the choice of structure is made at the beginning of the design process, often heuristically or experimentally based on a series of trials and errors. The back-propagation method is the basis of deep learning, the currently dominant methodology in computer artificial intelligence (*AI*) systems [3].

In the presented work, a strategy of bottom-up formation of structures from formal neurons is presented. According to this strategy, the structure of the layered network is formed gradually starting from the lowest layers. The structure of subsequent layers is formed based on training feature vectors, created on the basis of data sets in accordance with the current task. According to the pattern recognition methodology, we take into account only such categories (classes) that can be represented by example feature vectors created on the basis of the data set.

The concept of bottom-up formation of hierarchical structures from formal neurons has been presented as the leading idea of the high learning method [5]. According to the high learning method, the lower layers of the neural structure are formed using a dipolar strategy [4]. Dipolar layers are designed in the network to aggregate the learning vectors in a separable manner. Learning vectors are aggregate in a separable manner if the number of the vectors or their dimension is reduced, provided that the learning sets remain separable. The highest layer of the hierarchical network is created at the end of the formation process according to the ranked strategy [4]. The ranked layer is a decision layer of the network that implements the mapping of all feature vectors representing one class into one output vector of the network with components equal to zero or one.

The creatio of hierarchical structures of formal neurons based on large, multidimensional training sets can be efficiently performed using the basis exchange algorithms [4]. These algorithms are similar to linear programming and are aimed at minimizing convex and piecewise linear criterion functions, Computations according to the basis exchange algorithms are spatially limited to a finite number of dual vertices in the multidimensional parameter space, which allows for increasing the efficiency of computations [6] The quality of the final solutions based on dual vertices can be further improved by maximizing the margins based on the L_1 norm [7].

References:

[1] Duda, O. R., Hart, P. E., Stork, D. G.: *Pattern Classification*, J. Wiley, New York, 2001
[2] Aggarwal C. C.: *Neural Networks and Deep Learning*, Springer Verlag, 2023
[3] Bishop C. M, Bishop H.: *Deep Learning: Foundations and Concepts*. Springer Verlag, 2023
[4] Bobrowski L.: *Data Exploration and Linear Separability*, pp. 1 - 172, Lambert Academic Publishing, 2019
[5] Bobrowski L.: High Learning Hierarchical Neural Networks., pp. 295–304 in: *Computational Collective Intelligence* (*ICCCI* 2024), Nguyen Ngoc Thanh *et al.* (*eds.*), Springer Verlag, 2024
[6] Bobrowski L.: Computing on vertices in data mining, pp. 1 - 19, *Data mining*, Intech Open 2021
[7] Bobrowski, L.: Feature Selection with L_1 Regularization in Formal Neurons, pp.343-353 in: E*ngineering Applications of Neural Networks* (*EANN* 2024), Iliadis L. *et al.* (*eds.*), Springer Verlag, 2024

Joint 20th Nordic-Baltic Conference on Biomedical Engineering and the 24th Polish Conference on Biocybernetics and Biomedical Engineering (NBC 2025 & PCBBE 2025)

June 16 - 18, Warsaw, Poland

BOOK OF ABSTRACTS

POSTER SESSION

Rapid Fire Poster Presentations RF1
Artificial Intelligence in Healthcare, Biomaterials, Biomedical Sensors and Instrumentation
Chairs: Anna Stecka (Poland)
PP01–PP25

PP01

Control of scanner quality and consistency for deep learning models in collaborative digital pathology

Shrief ABDELAZEEZ[1*], Lukasz ROSZKOWIAK[1], Krzysztof SIEMION[1,2,3], Antonina PATER[1], Alessio FIORIN[4,5,6], Carlos LOPEZ[4,5,6], Laia ADALID[4,5], Marylene LEJEUNE[4,5,6], Anna KORZYNSKA[1]

1 Laboratory of Analysis and Processing of Microscopic Image, Nałęcz Institute of Biocybernetics and Biomedical Engineering Polish Academy of Sciences, Ks. Trojdena 4, 02-109 Warsaw, Poland

2 Medical Pathomorphology Department, Medical University of Bialystok, Bialystok, Poland

3 Faculty of Medical and Health Sciences, University of Radom, Radom, Poland

4 Oncological Pathology and Bioinformatics Research Group, Institut d'Investigació Sanitària Pere Virgili, Tortosa, Spain

5 Depart. of Pathology, Hospital de Tortosa, Institut Català de la Salut, Tortosa, Spain

6 Depart. of Computer Engineering and Mathematics, Universitat Rovira i Virgili, Tarragona, Spain

* ***Corresponding author***. *E-mail address*: sabdelazeez@ibib.waw.pl

Keywords: Digital pathology, Quality control, Deep learning, Transfer learning, AI based method

Motivation and Aim: Quality control in digital pathology is essential for ensuring diagnostic accuracy, especially in cross-site collaborations where variability in scanners, staining protocols, and lab practices can lead to inconsistencies. This study aims to compare quality of digital images scanned by six different scanners using the same glasses. The goal is to identify scanner-specific artifacts that can influence results of tissue evaluation by AI based model performance, enabling their mitigation before diagnosis, thereby improving the reliability of digital pathology workflows in multi-institutional settings.

Novelty: This work introduces a comprehensive framework for evaluating scanner quality in whole slide images produced by various scanners. It utilizes a VGG16 model trained on inflammatory spindle cell lesions and fine-tuned using transfer learning on breast cancer data. The study uniquely compares scanner quality across various institutions available in BosomShield project. This tool is prepared to provide insights into the variability introduced

by different devices and in future investigation their impact on deep learning-based diagnostic tools.

Methods:

The study analyzed two H&E-stained cancer biopsy datasets. The training set comprised annotated inflammatory spindle cell lesions from the Medical Pathomorphology Department in Bialystok, Poland, digitized at 40X magnification to train a VGG16 model. For fine-tuning, we

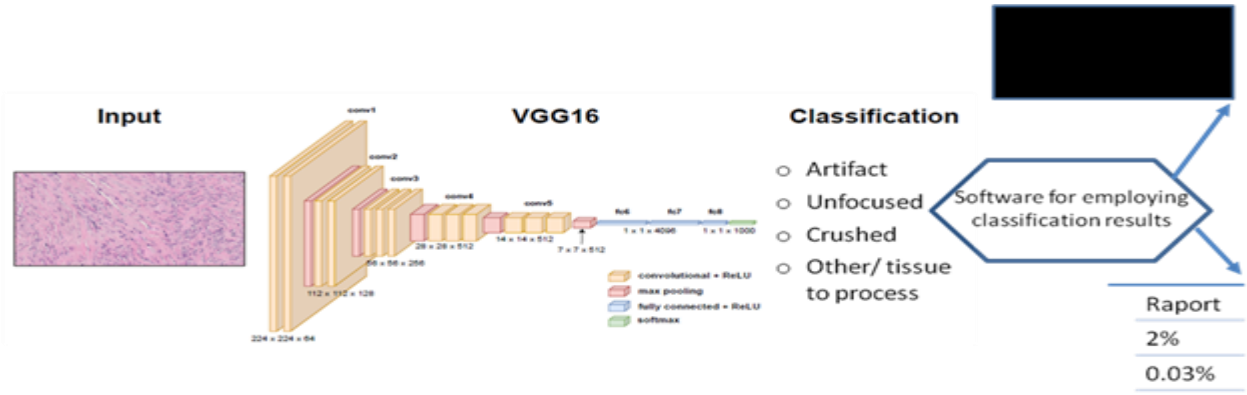

used breast cancer tissue samples from the BosomShield project (Hospital de Tortosa Verge de la Cinta, Spain). The developed model detected artifacts, crushed tissue, and unfocused regions. Evaluation involved 50 slides scanned by multiple devices (VS200 Olympus, Aperio AT2, Ventana DP200, Pannoramic 3DHISTECH, and two NanoZoomer 2.0HT systems) at 20X and 40X magnifications from partner institutions across Spain, Italy, and France. Scanner quality assessment quantified artifacts in five TILs-relevant breast cancer fragments per device, as illustrated in Figure *4*.

Figure 4: Framework for scanner quality assessment

Main results: Our VGG16 model effectively identified image quality issues (AUCs: 0.942 artifacts, 0.935 focus). Lower values indicate better scanner performance. Aperio AT2 had perfect focus (0±0); VS200 Olympus worst (0.57±0.1 unfocused). DP200 Roche detected largest crushing area (0.16±0.07) overestimated it, while VS200 Olympus led in artifacts area detection (0.3±0.03) also overestimated it. Zero values confirm true artifact absence. Pannoramic 3DHISTECH performed best (<0.001 artifacts) as relevant area for TILs evaluation was chosen by pathologies to be without artifact.

Table 3: Fraction of areas classified across different scanners.

Type of Scanner	Unfocused	Crushed	Artifact
Pannoramic 3DHISTECH	0.002 ± 0.00006	0.0006 ± 0.03	0.0003 ± 0.02
DP200 Roche	0.028 ± 0.002	**0.16 ± 0.07**	0.0088 ± 0.0003
NanoZoomer-2.0 HT C9600 (Spain)	0.004 ± 0.0002	0.006 ± 0.0003	0.008 ± 0.099
Aperio AT2 Leica	**0 ± 0**	0.006 ± 0.0003	0.013 ± 0.001
NanoZoomer-2.0 HT C9600 (France)	0.2 ± 0.1	0.004 ± 0.07	0.03 ± 0.187
VS200 Olympus	**0.57 ± 0.1**	0.0003 ± 6.67E-07	**0.3 ± 0.03**

Conclusion: The proposed framework integrates transfer learning and fine-tuning methods for quality evaluation in digital images scanned from E&H stained biopsy samples. The prepared model shows that the Aperio AT2 Leica, Pannoramic 3DHISTECH Scanner and NanoZoomer-2.0 HT C9600 Hamamatsu scanners do not introduce unfocused area because of their good deep estimation measurement and do not detect false crushed and artifact area.

Acknowledgements: This work was supported by the Academic Center of Pathomorphological and Genetic-Molecular Diagnostics, Bialystok, Poland, and the Bosom Shield project (Horizon Europe, Grant No. 101073222).

PP02

Impact of Input Color Models on Breast Cancer Binary Classification Using CNNs

Jakub JAWORSKI[1*], Lukasz ROSZKOWIAK[2]

1 WIT Academy, Warsaw, Poland

2 Nalecz Institute of Biocybernetics and Biomedical Engineering Polish Academy of Sciences, Warsaw, Poland

* ***Corresponding author***. *E-mail address*: Jakub.Jaworski@wit.edu.pl

Keywords: machine learning, AI, CNN, color models

Motivation and Aim: The effectiveness of convolutional neural networks (CNNs) in medical image classification is influenced by various factors, including the choice of input color model. While RGB is commonly used, alternative representations may provide distinct advantages in feature extraction and classification performance. Understanding the impact of different color models on CNN-based breast cancer classification is essential for optimizing diagnostic accuracy and computational efficiency.

Novelty: Despite the widespread use of CNNs in medical imaging, few studies have systematically investigated the impact of color space manipulation on classification performance. Most research relies on standard RGB input, overlooking the potential benefits of alternative color representations. While some models explore specific color models, comprehensive evaluations comparing multiple color spaces remain scarce. By providing insights into the role of color representation in CNN-based diagnostics, this study contributes to the refinement of automated breast cancer detection methods and the broader application of deep learning in medical imaging. The findings offer valuable guidance for optimizing preprocessing strategies and improving classification performance in medical image analysis.

Methods: This study systematically examines the influence of input color models on binary classification performance in breast cancer detection. To achieve this, the research framework Iro was developed to train CNNs using images processed in the red-green-blue (**RGB**), grayscale (**GSC**), hue-saturation-value (**HSV**), and CIE LAB (**LAB**) color spaces. The MobileNet architecture was selected for its efficiency and suitability for medical image analysis. For consistency, all models were trained for 20 epochs using the RMSprop optimizer with a learning rate of 0.00001 and a batch size of 4, using 3-fold cross-validation method. The BreakHis dataset [1] was used, which contains histopathological images of breast tumors at different magnifications (40×, 100×, 200×, and 400×). The analysis was conducted separately for each magnification level to assess the impact of color representation across varying image resolutions. Performance evaluation was carried out using visualization techniques and statistical testing to identify patterns, assess model accuracy, and explore potential improvements in classification outcomes.

Main results: The evaluation revealed that the HSV color model achieved the best classification performance (apart from 40× magnification), while the grayscale representation performed the worst. Interestingly, these findings contrast with the results obtained for general

image classification using the CIFAR10 dataset, where all colorspaces demonstrated similar effectiveness [2]. The detailed results are presented in Figure 1.

Conclusion: The study demonstrated that the choice of input color model significantly influences the performance of convolutional neural networks in breast cancer classification. The HSV color space yielded the highest accuracy, while grayscale performed the worst, contradicting findings from general image classification on the CIFAR10 dataset. The lower performance of grayscale images may be attributed to the simplification of the input data by reducing it to a single channel instead of the three channels provided by other color models. This discrepancy suggests the domain-specific impact of color representation in CNNs, emphasizing the need for tailored preprocessing strategies in medical imaging applications and further studies.

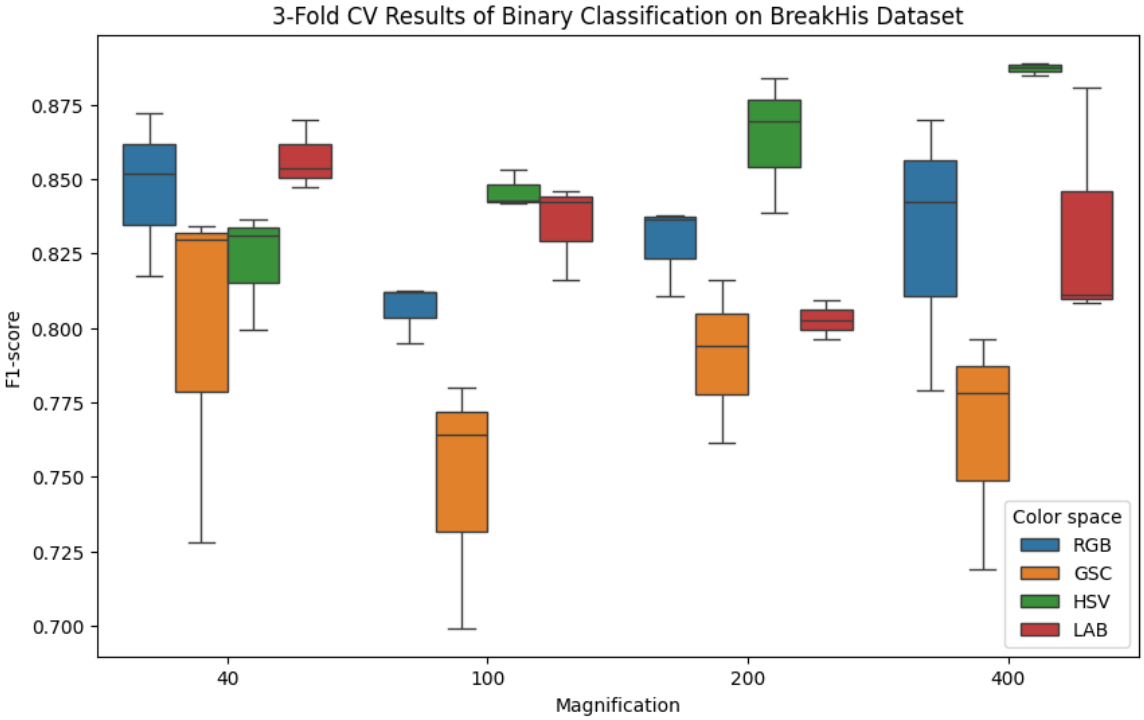

Figure 1 3-Fold CV Results of Binary Classification on BreakHis Dataset. The central line inside each box represents the median F1-score, while the box edges indicate the interquartile range (IQR) – spanning the 25th to 75th percentiles. The whiskers extend to the most extreme data points within 1.5×IQR from the lower and upper quartiles.

References:

[1] Spanhol FA, Oliveira LS, Petitjean C, Heutte L. A dataset for breast cancer histopathological image classification. IEEE Trans Biomed Eng. 2016;63(7):1455-1462. doi:10.1109/TBME.2015.2496264.

[2] Jaworski J. Analysis of the Impact of the Applied Color Model on Classification Using Convolutional Neural Networks. [Dissertation]. Warsaw, Poland: WIT Academy; 2025.

PP03

Artificial artifacts detection in raw EEG signal using Neural Networks

Kacper FILIPEK[1*], Patryk ZYCH[1], Adam PATALAS[1]

1 Institute of Mechanical Technology, Poznan University of Technology, Poznan, Poland

* ***Corresponding author***. *E-mail address*: kacper.filipek@student.put.poznan.pl

Keywords: Hybrid Neural Network, EEG, Artifact detection, CNN, MLP

Motivation and Aim: Artifacts in biomedical signals, such as electrical disruptions in electrodes readings, can sometimes be overlooked, which creates a risk of extracting patterns or features from corrupted data without realizing the presence of measurement device errors that can compromise the reliability of the analysis[1]. In this study, we explored the accuracy and usability of simple neural network models in detecting an artificially introduced artifact in raw electroencephalography (EEG) signals representing resting-state brain activity. The signal consisted of 34048 samples, recorded at sampling frequency of 512 Hz. The primary objective of the study was to compare the efficiency of these models in terms of training time, as signal characteristics can vary significantly between patients and across individual resting-state recordings.

Novelty: An artificial artifact, simulating a brief, spike-like disruption, was injected into dataset at a random location on one of the 64 EEG channels. This enabled systematic analysis of classification accuracy in a controlled environment. The performance of MLP, CNN, and deep CNN models was compared, with achieved accuracies of approximately 80%.

Methods: Raw EEG data were used for the analysis, with impulse-like artifacts artificially added to clean recordings. Each signal trace contained an artificially added artifact at random location with the addition of a mask used to inform the models during training about channel on which the artifact occurs. The neural network models were trained to perform binary classification: presence or absence of an artifact. Feature extraction was intentionally omitted in order to assess the potential of neural networks in processing raw time-dependent data. Additionally, the use of hybrid neural network architectures, such as CNNs with integrated LSTM layers [2], was explored to enhance sensitivity to time-dependent variations in the signal.

Main results: All tested models performed well under controlled conditions. However, the CNN model, despite improvements in accuracy and F1 score, required significantly more computational resources and longer training time.

Table 4 Performance of models in artifact detection

Model	Accuracy	F1 score
MLP	67%	62%
CNN	73%	58%
Deep CNN	79%	60%

Conclusion: The results suggest that even simple neural networks can successfully identify basic artifacts prior to any signal processing. Expanding model architectures with hybrid elements may lead to improved performance in detecting more complex artifacts commonly observed in EEG acquisition, as well as in capturing time-dependent patterns within the signal. Furthermore, the use of generative adversarial networks (GANs) presents a promising direction for generating more complex training scenarios and enhancing model robustness [3].

References:

1. Ingolfsson TM, Benatti S, Wang X, et al. Minimizing artifact-induced false-alarms for seizure detection in wearable EEG devices with gradient-boosted tree classifiers. *Sci Rep*. 2024;14(1). doi:10.1038/s41598-024-52551-0

2. Li H, Ding M, Zhang R, Xiu C. Motor imagery EEG classification algorithm based on CNN-LSTM feature fusion network. *Biomed Signal Process Control*. 2022;72:103342. doi:10.1016/j.bspc.2021.103342

3. Habashi AG, Azab AM, Eldawlatly S, Aly GM. Generative adversarial networks in EEG analysis: an overview. *J NeuroEngineering Rehabil*. 2023;20(1):40. doi:10.1186/s12984-023-01169-w

PP04

Color normalization in conventional Pap smear images

Antonina PATER[1*], Łukasz ROSZKOWIAK[1,] Anna KORZYŃSKA[1]

1 Nałęcz Institute of Biocybernetics and Biomedical Engineering Polish Academy of Sciences, Warsaw, Poland

* ***Corresponding author***. *E-mail address*: apater@ibib.waw.pl

Keywords: Color normalization, Cervical cytology, Computational pathology, GAN

Motivation and Aim: Color normalization methods allow to reduce color variability between observed images. In histology and cytology, the colors of tissue samples are determined by the stains applied during the preparation process. Numerous color normalization methods have been proposed for digitized histopathological samples, improving the consistency of analysis[1,2]. Cytological images differ from histopathological images in structure; however, they contain similar objects (cells) at a similar scale and are prepared with dyes used also for histopathological slide preparation. Therefore, methods proposed for histopathological slide normalization may have a similarly beneficial impact on cytological images.

Novelty: Although color normalization methods have been previously evaluated on cervical liquid-based cytology (LBC) images, their performance on conventional cervical smears remains unexplored. In this study, we evaluated the effectiveness of color normalization on digitized fragments of conventional cervical smear slides stained with Papanicolaou stain. This is particularly significant, as conventional cervical cytology differs from LBC in terms of structure and cell distribution.

Methods: Classical normalization methods of Reinhard, Macenko, Vahadane and Khan, as well as deep learning-based methods, adaptive color deconvolution (ADC) [1], including two GAN methods, contrastive unpaired translation (CUT) and CycleGAN[2], were applied to two Papanicolau-stained cervical cytology datasets: Bialystok[3] and CRIC[4]. The GAN-based methods were trained on 80% of each dataset and tested on the remaining part. The ACD was fitted on 5 images of each dataset due to memory limits. The classical methods used one target image of each dataset because of the methods' constraints. The results of the normalization methods performed on test images (185 Bialystok images and 78 CRIC images) were evaluated using structure-describing metrics – RMSE, PSNR, and SSIM (from the scikit-image package) – which assess noise, texture, color, and object shape, and the difference in luminance from the source or target dataset, given by the following formula:

$$\Delta L_B = \left| \langle median(L_{ij}) \rangle_A - \langle median(L_{ij}) \rangle_B \right|$$

where:
L_{ij} – luminance of the pixel in the i^{th} column and j^{th} row of the analyzed image,
$\langle ... \rangle_A$ – mean calculated for the set of normalized images.
$\langle ... \rangle_B$– mean calculated for the set of reference images (target or source dataset).

Main results: The ACD method reached the lowest RMSE and highest PSNR and SSIM when Bialystok was normalized to the CRIC dataset, and vice versa. The CUT method reached the lowest luminance difference (ΔL) from the target dataset for normalization in both ways. The

detailed results of the methods assessment are provided in Table 1. A visual example of normalization methods performance is shown in Figure 1.

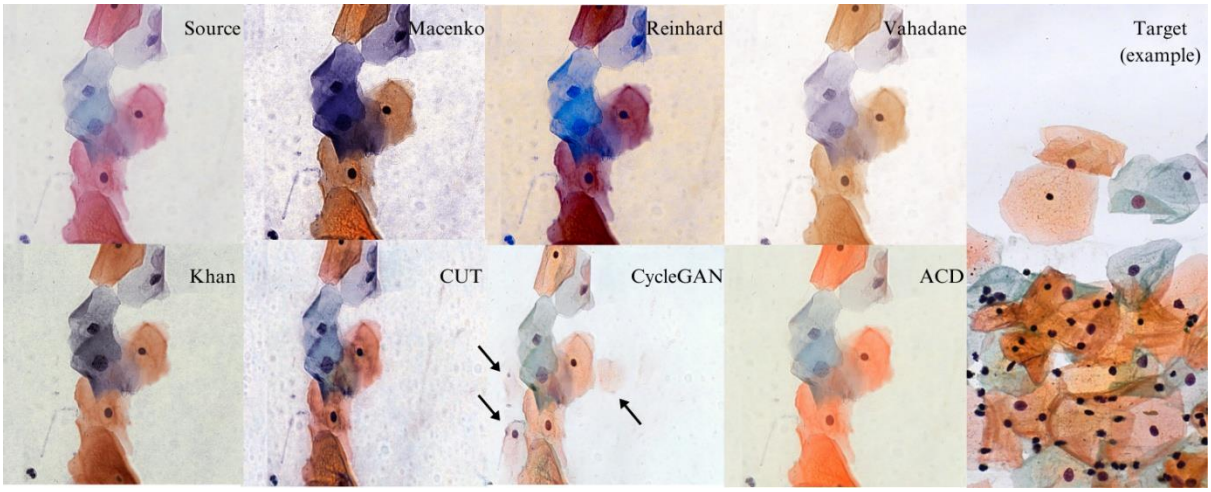

Figure 1: Image normalized with the assessed normalization methods

Table 1: Quantitative assessment of color normalization methods using RMSE, PSNR, SSIM, and luminance difference. Measures shown with one standard deviation.

Normalization	Method	RMSE	PSNR	SSIM	$\Delta L_{Bialystok}$	ΔL_{CRIC}
Bialystok to CRIC	ACD	14.5 ± 6.3	24.3 ± 3.0	0.94 ± 0.02	3.7 ± 1.1	1.0 ± 1.1
	CUT	26.8 ± 7.0	19.7 ± 2.0	0.70 ± 0.08	5.3 ± 1.1	0.6 ± 1.1
	CycleGAN	36 ± 10	17.0 ± 2.1	0.70 ± 0.10	5.9 ± 0.9	1.1 ± 0.9
	Khan	27.5 ± 8.1	19.3 ± 2.9	0.63 ± 0.14	3.6 ± 1.2	1.1 ± 1.2
	Macenko	34.1 ± 9.4	17.7 ± 2.0	0.69 ± 0.20	3.8 ± 0.9	1.0 ± 0.9
	Reinhard	30 ± 15	18.6 ± 3.9	0.79 ± 0.16	0.1 ± 1.1	4.8 ± 1.1
	Vahadane	33.1 ± 6.1	16.6 ± 1.4	0.91 ± 0.03	6.3 ± 1.1	1.6 ± 1.1
CRIC to Bialystok	ACD	11.1 ± 4.2	27.8 ± 3.3	0.94 ± 0.03	3.1 ± 2.1	1.6 ± 1.8
	CUT	41 ± 11	14.1 ± 2.2	0.67 ± 0.10	1.3 ± 1.2	6.0 ± 1.2
	CycleGAN	36.6 ± 6.2	15.1 ± 1.7	0.68 ± 0.08	2.6 ± 1.8	7.5 ± 1.8
	Khan	28.0 ± 9.4	19.1 ± 3.1	0.81 ± 0.09	3.6 ± 1.2	1.6 ± 1.2
	Macenko	25 ± 18	21.7 ± 6.2	0.87 ± 0.08	9.2 ± 1.2	4.4 ± 1.6
	Reinhard	30 ± 24	20.0 ± 8.0	0.88 ± 0.12	9.2 ± 0.9	4.5 ± 0.9
	Vahadane	13.9 ± 6.9	26.1 ± 4.2	0.91 ± 0.05	4.4 ± 1.7	0.3 ± 1.7

Conclusion: Color normalization methods proposed for histopathological slides can be applied to cytological images but have several drawbacks. GAN-based methods offer a low ΔL from the target dataset but tend to produce background artifacts, such as nonexistent cells and shapes (Figure 1, arrows), and can be more burdensome in cytological smear images than densely packed cells in histological images. Classical normalization methods, using a single target image, are limited by its content. The range of colors present in the target image can particularly increase ΔL from the target dataset if it does not reflect the target dataset's diversity. The effect can be more pronounced in Pap smear images because of the use of 5 stains instead of one or two, which is typical for histopathology samples.

References:

1. Roy S et al. A study about color normalization methods for histopathology images. Micron. 2018;114:42-61.
2. Salvi M et al. Generative models for color normalization in digital pathology and dermatology: Advancing the learning paradigm. Expert Systems with Applications. 2024;245:123105.

3. Pater A et al. Conventional cervical cytology image dataset with cell outline annotations. In: 2023 International Symposium on Image and Signal Processing and Analysis (ISPA). IEEE; 2023:1-6.
4. Rezende MT et al. Cric searchable image database as a public platform for conventional pap smear cytology data. Sci Data. 2021;8(1):151.

PP05

Development of PES-PUR Scaffolds for Cartilage Tissue Engineering

Monika WASYŁECZKO[1*], Cezary WOJCIECHOWSKI[1], Judyta DULNIK[2], Wioleta SIKORSKA[1], Andrzej CHWOJNOWSKI[1]

1 – Institute of Biocybernetics and Biomedical Engineering, Department of Biomaterials and Biotechnological Systems, Warsaw, Poland
2 – Institute of Fundamental Technological Research Polish Academy of Sciences, Laboratory of Polymers and Biomaterials, Warsaw, Poland

* - *Corresponding author*. *E-mail address [mwasyleczko@ibib.waw.pl]*

Keywords: articular cartilage, tissue engineering, biodegradable scaffolds, polymer scaffolds, regenerative medicine.

Motivation and Aim:

Cartilage injuries often lead to long-term joint dysfunction due to the limited regenerative capacity of hyaline cartilage. Tissue engineering aims to develop scaffolds that support the growth of chondrocytes and stem cells while recreating the native tissue environment. In this study, polyethersulfone (PES) and polyurethane (PUR) scaffolds were designed and evaluated. These scaffolds featured an interconnected macroporous structure with pore diameters exceeding 100 μm. This architecture supports cell growth, enables nutrient transport, and facilitates the production of proteins essential for cartilage repair. The scaffolds exhibited favorable mechanical properties, suitable hydrophilicity, and partial biodegradability in simulated physiological conditions, confirming their potential for use in regenerative medicine focused on articular cartilage repair.

Novelty:

The proposed scaffolds combine PES and PUR using wet-phase inversion and salt-leaching methods, integrating gelatin nonwovens to create an interconnected macroporous network. This approach ensures suitable porosity, hydrophilicity, and mechanical properties for cartilage tissue engineering. Moreover, this study provides the first evidence that PES undergoes partial degradation under simulated physiological conditions. Until now, its biodegradation has only been reported in in vivo studies. This finding expands the current understanding of PES behavior in biomedical applications and highlights its potential as a component of degradable scaffolds.

Methods:

Scaffold fabrication involved wet-phase inversion and salt-leaching, utilizing gelatin nonwovens as macropore precursors. Structural analysis included scanning electron microscopy (SEM) and MeMoExplorer software for porosity evaluation. Wettability was assessed via contact angle and swelling ratio, while mechanical properties were tested under stress conditions exceeding 10 MPa. Degradation in simulated body fluid (SBF) was monitored, with Fourier-transform infrared spectroscopy (FT-IR) confirming hydrolysis through ester bond disappearance (~1730 cm^{-1}).

Main results:

Mechanical tests confirmed the possible suitability of the S1-S3 scaffolds for knee joint applications, with all scaffolds showing Young's modulus above 10 MPa, comparable to native cartilage. Contact angles were less than 62°, confirming a hydrophilic surface that promotes cell adhesion and nutrient transport.

The scaffolds also showed excellent fluid absorption, with swelling ratios exceeding up to 500% after 24 hours in PBS, indicating high water absorption capacity supporting cell viability and scaffold degradation.

After four weeks in simulated body fluid (SBF), S1-S3 scaffolds showed controlled degradation. Weight loss reached 11% for S1 (PES:PUR 2:1), 29.1% for S2 (1:1) and 32.7% for S3 (1:2). A control membrane made of pure PES showed a loss of 12%. Porosity increased by up to 13.1%, and the area of large pores (>300 μm^2) more than doubled in S3 (from 16.5% to 36.5%). Notably, partial degradation of PES in SBF was demonstrated for the first time.

Conclusion:

The PES–PUR scaffolds demonstrated favorable mechanical, structural, and degradation properties, meeting key requirements for cartilage tissue engineering. Notably, the study revealed, for the first time, partial in vitro degradation of PES in simulated physiological conditions. These findings highlight the potential to tailor scaffold performance by adjusting polymer composition. Further studies are planned to assess their effectiveness in hyaline cartilage regeneration.

Acknowledgements:

This research was supported by statutory funds of Laboratory of Electrostatic Methods of Bioencapsulation in Nalecz Institute of Biocybernetics and Biomedical Engineering, Polish Academy of Sciences (IBBE PAS).

References

Chen, M. *et al.* (2024) 'Advancements in tissue engineering for articular cartilage regeneration', *Heliyon*. Elsevier Ltd, 10(3), p. e25400. doi: 10.1016/j.heliyon.2024.e25400.

Cui, M. *et al.* (2023) 'Developments of polyurethane in biomedical applications: A review', *Resources Chemicals and Materials*. Elsevier B.V., 2(4), pp. 262–276. doi: 10.1016/j.recm.2023.07.004.

Jakutowicz, T. *et al.* (2024) 'Comparative Study of Autogenic and Allogenic Chondrocyte Transplants on Polyethersulfone Scaffolds for Cartilage Regeneration', *International Journal of Molecular Sciences*, 25(16). doi: 10.3390/ijms25169075.

Płończak, M. *et al.* (2023) 'Intraarticular Implantation of Autologous Chondrocytes Placed on Collagen or Polyethersulfone Scaffolds : An Experimental Study in Rabbits', pp. 4–7.

Wang, M. *et al.* (2024) 'Articular cartilage repair biomaterials: strategies and applications', *Materials Today Bio*. Elsevier Ltd, 24(December 2023), p. 100948. doi: 10.1016/j.mtbio.2024.100948.

Wasyłeczko, M. *et al.* (2023) 'Scaffolds for Cartilage Tissue Engineering from a Blend of Polyethersulfone and Polyurethane Polymers', *Molecules (Basel, Switzerland)*, 28(7), pp. 1–6. doi: 10.3390/molecules28073195.

Wasyłeczko, M., Sikorska, W. and Chwojnowski, A. (2020) 'Review of synthetic and hybrid scaffolds in cartilage tissue engineering', *Membranes*, 10(11), pp. 1–28. doi: 10.3390/membranes10110348.

Wasyłeczko, M., Wojciechowski, C. and Chwojnowski, A. (2024) 'Polyethersulfone Polymer for Biomedical Applications and Biotechnology', pp. 37–42.

Zhang, H. *et al.* (2023) 'From materials to clinical use: advances in 3D-printed scaffolds for cartilage tissue engineering', *Physical Chemistry Chemical Physics*. Royal Society of Chemistry, 25(36), pp. 24244–24263. doi: 10.1039/d3cp00921a.

PP06

Polymer-Modified PEO Coating: Corrosion Behavior and Cytotoxicity Assessment

Barbara RYNKUS[1*], Maciej SOWA[2], Ada ORŁOWSKA[1], Joanna JAWORSKA[3], Katarzyna JELONEK[3], Aneta SAMOTUS[4], Janusz SZEWCZENKO[1]

1 Department of Biomaterials and Medical Device Engineering, Faculty of Biomedical Engineering, Silesian University of Technology, Zabrze, Poland

2 Department of Inorganic Chemistry, Analytical Chemistry and Electrochemistry, Faculty of Chemistry, Silesian University of Technology, Gliwice, Poland

3 Centre of Polymer and Carbon Materials of the Polish Academy of Sciences, Zabrze, Poland

4 Foundation for the Development of Cardiac Surgery, Zabrze, Poland

* ***Corresponding author***. *E-mail address*: barbara.rynkus@polsl.pl

Keywords: magnesium alloys, plasma electrolytic oxidation (PEO), biodegradable polymer coatings, electrochemical impedance spectroscopy, cytotoxicity

Motivation and Aim: Magnesium alloys have good mechanical properties and are widely considered to be biocompatible with the human body, strengthening their potential for biomedical applications[1]. In addition, Mg alloys have the unique property of being biodegradable in body fluids, which translates into the possibility of using them as temporary implants. The use of biodegradable magnesium implants in orthopedics has a number of advantages, the most important of which is that there is no re-surgery associated with the need to remove the implant from the patient's body. However, Mg alloys also have several drawbacks that require further work on their widespread use, relating to poor corrosion resistance and too rapid degradation, which occurs before bone fusion and affects implant functionality[2]. In order to overcome this, surface modifications are used to ensure adequate properties of the biomaterial. Coatings obtained by plasma electrolytic oxidation (PEO) are widely used in biomaterial engineering due to their effectiveness in providing good corrosion resistance. However, due to their porous structure, they may be insufficient protection in terms of long-term degradation of Mg alloys in a biological environment. The use of an additional polymer layer can improve the protective and biological properties of the material, making such a solution promising for biomedical applications[3,4]. The aim of this study is to develop and characterize a duplex coating consisting of a calcium-phosphate coating obtained by the PEO method and an additional polymer layer.

Novelty: The novelty of this work was the development of a new combination of coatings to provide control of magnesium alloy degradation. To achieve this, the bath required to produce the Ca-P coating by PEO was designed using sodium hexametaphosphate and calcium acetate. The use of these reagents has not previously been reported in the literature. In addition, a newly designed polymer was used, which was specifically developed to provide an adequate degradation rate for the magnesium alloy.

Methods: Coatings were produced on WE43 (Mg-Y-RE-Zr) alloy with an AC+DC high-voltage power supply in two-steps procedure. First, the PEO process was carried out in a phosphate bath, which consisted of 12 g/L $(NaPO_3)_6$ and 0.05 M KOH. The coating-forming

process was carried out until a voltage of 350V was reached. The second bath was based on the first electrolyte with the addition of 1.038 g/L $Ca(CH_3COO)_2 \times H_2O$. The samples were oxidized under these conditions for 10 min. The following oxidation parameters were used: a duty ratio (DR) of 50% and current ratio (R) of 1.6. L-lactide-glycolide- trimethylene carbonate terpolymer (LP 454) (L-La 70% Gl 10% TMC 20%) - P(L/G/TMC) was used to produce the polymer coating. P(L/G/TMC) was applied to the samples after PEO by ultrasonic spraying. The coating was applied in 20 layers using a frequency of 60 kHz. In order to characterize the produced coatings, the surface morphology was assessed by scanning electron microscopy and then subjected to corrosion tests. Electrochemical impedance spectroscopy and potentiodynamic polarization tests were carried out. In addition, the effect of the formed coatings on biological properties was investigated with the human osteosarcoma cell line MG-63.

Main results: The results of the observations using the SEM showed a clear change in the surface structure of the PEO samples after application of the polymer coating. The applied polymer filled a major part of the micropores formed during the plasma electrolytic oxidation process, at the same time sealing the previously visible micro-cracks in the structure. Analysis of the corrosion test results confirmed the beneficial effect of the polymer coating on the corrosion resistance of the PEO-oxidized Mg alloy substrate; a significant increase in polarization resistance was observed. In addition, biological evaluation showed reduced cytotoxic effects observed in direct contact with the material, while maintaining cell proliferation-promoting effects.

Conclusion: The corrosion results obtained indicate that the design of duplex systems is a promising approach to ensure appropriate degradation rates for magnesium alloys used in orthopedics. The use of the polymer coating had a positive effect on the biological properties of the modified magnesium alloy, which is important in terms of biocompatibility and potential for application.

Acknowledgements: The research was funded by the European Funds for Silesia 2021-2027 Program co-financed by the Just Transition Fund - project entitled “Development of the Silesian biomedical engineering potential in the face of the challenges of the digital and green economy (BioMeDiG)”. Project number: FESL.10.25-IZ.01-07G5/23.

References:

1. Peron M, Berto F, Torgersen J. *Magnesium and Its Alloys as Implant Materials: Corrosion, Mechanical and Biological Performances*. CRC Press; 2020. doi:10.1201/9781003000327

2. Lu Y, Deshmukh S, Jones I, Chiu YL. Biodegradable magnesium alloys for orthopaedic applications. *Biomater Transl*. 2021;2(3):214-235. doi:10.12336/biomatertransl.2021.03.005

3. Bakhsheshi-Rad HR, Hamzah E, Ebrahimi-Kahrizsangi R, Daroonparvar M, Medraj M. Fabrication and characterization of hydrophobic microarc oxidation/poly-lactic acid duplex coating on biodegradable Mg–Ca alloy for corrosion protection. *Vacuum*. 2016;125:185-188. doi:10.1016/j.vacuum.2015.12.022

4. Li LH, Sankara Narayanan TSN, Kim YK, et al. Deposition of microarc oxidation–polycaprolactone duplex coating to improve the corrosion resistance of magnesium for biodegradable implants. *Thin Solid Films*. 2014;562:561-567. doi:10.1016/j.tsf.2014.04.004

PP07

Development of a method for obtaining blend degradable polysulfone/cellulose acetate membranes

Cezary WOJCIECHOWSKI*, Monika WASYŁECZKO, Andrzej CHWOJNOWSKI

Nalecz Institute of Biocybernetic and Biomedical Engineering, Polish Academy of Sciences, Trojdena 4 Str.02-109 Warsaw, Poland

* ***Corresponding author***. *E-mail address*: cwojciechowski@ibib.waw.pll

Keywords: capillary membranes; retention; degradation; hydrolysis; fouling

Motivation and Aim: A method for obtaining blend two-component capillary semi-permeable polysulfone(PSf)/cellulose acetate (CA) membranes was developed. These membranes should undergo partial degradation during operation (in an acidic or alkaline aqueous environment) through hydrolysis ester groups of CA. Slow degradation of CA fragments and their removal from the membrane structure will result in an increase in membrane porosity, which will lead to an increase in efficiency. The occurrence of membrane fouling, i.e. clogging of pores by filtered substances during membrane operation, will limit the efficiency of the process. If these two processes are in some balance, the flow through the membranes will not change and the process efficiency will not decrease over time. This will extend the operating life of the membranes, i.e. reduce the costs of their use.

Novelty: By using two different polymers in the PSf/CA membrane, one stable (PSf), acting as a durable scaffold, and the other (CA) decomposing during membrane operation, we obtain a membrane with increasing porosity and permeability, which does not degrade despite the loss of mass.

Methods: The membranes were obtained using spinning at the installation for obtaining capillary membranes using the wet phase inversion method by extruding the polymer solution through a capillary forming spinneret. The membranes were etched with sodium hydroxide (NaOH) solution using the flow method. Membrane properties, such as hydraulic permeability coefficient (UFC), retention factors, and membrane morphology (SEM images) before and after degradation, were evaluated. The degradation of the CA component in the membrane was assessed by comparing the mass of PCL before and after digestion.

Main results: The degree of CA removal from membranes after hydrolysis is almost complete. It is approximately 95%. We can conclude that the CA was effectively removed and played the role of a typical pores former, increasing the porosity of the membrane. All retention values after hydrolysis were lower than the retention values before hydrolysis for PSf/CA membranes The structure of membranes (SEM images) after NaOH etching becomes more porous and loose. The structure of the membrane changes significantly, numerous macropores are formed after the removal of CA. UFC of membranes increases by 30% after digestion.

Conclusion: A method was developed to obtain two-component blend semi-permeable PSf/CA membranes, where CA was used as a degradable polymer and a classic pores former, almost completely removed from the membrane structure in order to increase its porosity and permeability. SEM photos show a looser structure of the membranes and greater porosity after CA removal. The hydraulic permeability after hydrolysis increases by 30% due to the significant increase in porosity. The use of CA as a removable component in the PSf/CA membrane resulted in changes in the characteristics of the membrane, i.e. an increase in its porosity, a decrease in retention and an increase in membrane efficiency.

PP08

Electrospun UV-crosslinked polyvinylpyrrolidone fibres modified with microspheres for drug delivery systems

Aleksandra BARTKOWIAK[1*], Adam MIREK[1], Marcin GRZECZKOWICZ[1], Dorota LEWIŃSKA[1]

1 Nalecz Institute of Biocybernetics and Biomedical Engineering Polish Academy of Sciences,

Ks. Trojdena 4, 02-109 Warsaw, Poland

* ***Corresponding author***. *E-mail address*: abartkowiak@ibib.waw.pl

Keywords: Electrospinning, Microspheres, Drug delivery systems

Motivation and Aim: An unquestionable disadvantage of drug delivery systems based on electrospun nonwovens is their relatively low drug capacity [1]. Therefore, the aim of our research was to develop a new drug delivery system based on water-insoluble polyvinylpyrrolidone (PVP) fibres modified with polycaprolactone (PCL) and polyethersulfone (PES) microspheres. This approach could successfully increase the drug capacity of the system and eliminate the so-called burst effect.

Novelty: Modified electrospun mats were produced by pulsed suspension electrospinning of microspheres. The use of pulsed voltage in the electrospinning of microsphere suspensions has significantly improved process control [2].

Methods: Polycaprolactone and polyethersulfone microspheres were prepared using a method combining pulsed electrospinning and a wet phase inversion technique, which was developed in our laboratory. The microspheres produced were suspended in a benzophenone-enriched PVP solution and then spun using pulsed electrical voltage. The resulting fibre mats were collected on a drum collector and then cross-linked using UV light.

Main results: Our study showed that the equilibrium rhodamine concentration after 4 h of release from UV-crosslinked PVP mat is 0.0012 mg/ml, which is lower than the equilibrium rhodamine concentration released from fibres containing microspheres (0.0025 mg/ml - PCL, 0.0018 mg/ml - PES), clearly indicating that modification of fibres with microspheres increases the drug capacity of the whole system. Furthermore, the concentration of rhodamine released from the UV-crosslinked PVP mat after 24 h is about 0.1 mg/ml, while from the microsphere-modified fibres it is about 0.025-0.03 mg/ml, indicating a slower release when microspheres are added to the system. Additionally, in the case of the modified fibres, no undesirable burst effect was observed. Furthermore, the amount and type of microspheres used in the electrospun mats, as well as the longer crosslinking time, significantly affects their mechanical properties. It was reported that a small addition of PES microspheres increases the UV-crosslinked PVP mat's tensile strength by approximately 15%. Furthermore, based on degradation tests, it was found that electrospun UV-crosslinked PVP mats with benzophenone lead to water- and ethanol-insoluble fibres, which significantly broadens the application spectrum of such mats.

Conclusion: The microsphere-modified electrospun mat shows great potential as a drug delivery system.

References:

[1] C.A. Martínez-Pérez, Electrospinning: a promising technique for drug delivery systems, Rev. Adv. Mater. Sci., 59 (2020), pp. 441-454

[2] A. Mirek, P. Korycka, M. Grzeczkowicz, D. Lewińska, Polymer fibers electrospun using pulsed voltage, Mater. Des., 108106 (2019)

PP09

Combination of Cold Helium Plasma with Fluoride Varnish to Improve Enamel surface Protection

Sara FATHOLLAH[1,2*], Hossein ABBASI[2], Mohammad SADEGH AHMAD AKHOUNDI[3,4]

1 Nalecz Institute of Biocybernetics and Biomedical Engineering, Polish Academy of Sciences, Trojdena 4, 02-109 Warsaw, Poland
2 Department of Energy Engineering and Physics, Amirkabir University of Technology, P. O. Box, 15875-4413, Tehran, Iran
3 Department of Orthodontics, School of Dentistry, Tehran University of Medical Sciences, Tehran, Iran
4 Dental Research Center, Dentistry Research Institute, Tehran University of Medical Sciences, Tehran, Iran
* ***Corresponding author***. *E-mail address*: sfathollah@ibib.waw.pl

Keywords: cold atmospheric plasma, Bovine enamel, Fluoride varnish, Microhardness, SEM/EDX

Motivation and Aim: Tooth decay, an infectious disease, poses a significant global public health concern [1,2]. Fluoride is recognized as a critical intervention in reducing the incidence and severity of dental caries [3]. Tooth enamel resists erosion by absorbing fluoride and forming fluorapatite, indicating that increasing fluoride absorption is a preventative treatment [4]. In recent years, cold-atmospheric pressure plasma (CAP) has emerged as a method of altering surface properties, particularly adhesion [5,6]. Consequently, cold plasma at atmospheric pressure has the potential to modify surface electrical properties, thereby enhancing fluoride absorption and, by extension, tooth resistance to decay.

Novelty: A multitude of studies have demonstrated the superiority of fluoride varnish due to its user-friendly nature, particularly for young people, its time-saving properties, and the low likelihood of fluoride ingestion [7]. The mechanisms by which topical fluoride treatment exerts its effects include, firstly, the maintenance of fluoride concentration in saliva through regular use of fluoride toothpaste or analogous methods; and secondly, the facilitation of a reaction between fluoride and enamel-dentin, resulting in the formation of calcium fluoride (CaF2), which plays a pivotal role in preventing tooth decay. Consequently, enhancing the effectiveness and longevity of fluoride covering through optimal fluoride concentrations remains a significant endeavor for researchers in this domain [8,9]. This study pioneers the enhancement of fluoride uptake by helium cold atmospheric pressure plasma in the enamel layer and makes it more resistant to saliva dissolution. By integrating Fluoride with CAP, we are certain that the potential of cold plasma systems will soon establish them as therapeutic modalities in dentistry, as they develop in both directions to various extents.

Methods: A total of 91 freshly extracted bovine incisor teeth were meticulously prepared in accordance with established protocols. Following a four-day disinfection period with 0.1% chloramine, the soft tissues were meticulously removed, and the enamel surfaces were meticulously polished. The samples were then subjected to a thorough examination under a stereo microscope to ensure the absence of any defects. Subsequently, the samples were sectioned and embedded in acrylic resin. The specimens were then randomly divided into seven groups: three control groups (no treatment, fluoride varnish only, plasma only) and four experimental groups exposed to cold helium plasma before or after varnish application. Plasma exposure lasted two minutes. Surface morphology and elemental composition were analyzed via scanning electron microscopy (SEM) and energy-dispersive X-ray spectroscopy (EDX). Microhardness measurements were taken at three time points: immediately, 24 hours, and 48 hours after treatment. Statistical analysis was conducted using repeated-measures analysis of variance (ANOVA) and Bonferroni tests ($\alpha = 0.05$).

Main results: SEM analysis demonstrated that helium plasma treatment enhanced fluoride dispersion and reduced enamel imperfections. EDX results indicated a substantial increase in fluoride content (1.21% to 7.31%) and an augmented Ca/P ratio (1.95 to 2.39) after 48 hours of plasma treatment. Microhardness assessments revealed that the application of plasma both before and after fluoride varnish significantly increased enamel hardness. The combined treatment resulted in a 24% increase in Vickers hardness compared to the varnish-only group, suggesting enhanced resistance to degradation (figure 1.).

Conclusion: The integration of fluoride treatment with cold atmospheric plasma (CAP) shows promise in enhancing fluoride absorption, improving enamel restoration, and increasing caries resistance. This approach may contribute to more effective protective and therapeutic strategies by combining traditional techniques with CAP. Additionally, the findings highlight the potential for expanding non-invasive treatment options in dental care.

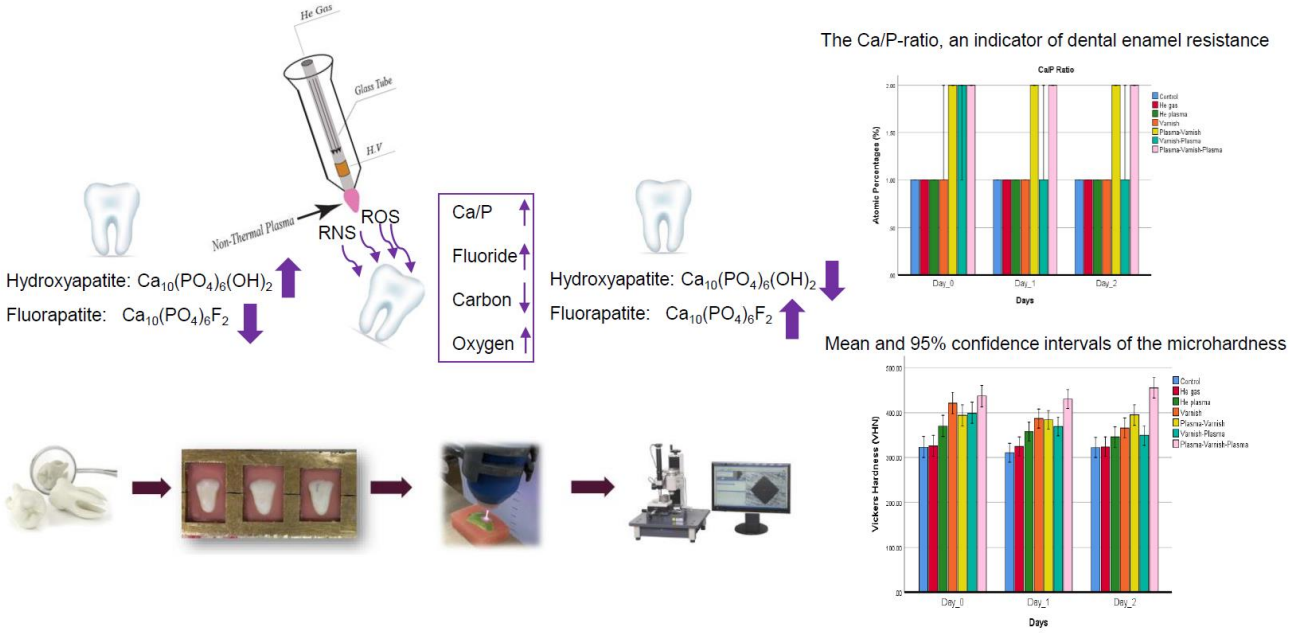

Figure 1. schematic of research and result

References:

[1] P. S. Casamassimo, H. Fields, D. J. McTigue, and A. J. Nowak, *Pediatric dentistry: infancy through adolescence*. Elsevier India, 2012.

[2] T. M. Karpiński and A. K. Szkaradkiewicz, "Microbiology of dental caries," *J Biol Earth Sci*, vol. 3, no. 1, pp. M21-4, 2013.

[3] M. Mansouri, M. Mohammadpour, A. Khademi, and M. Khoroushi, "A review of the systemic fluoride in preventive dentistry," pp. 498-506, 2014.

[5] F. L. Tabares and I. Junkar, "Cold plasma systems and their application in surface treatments for medicine," *Molecules*, vol. 26, no. 7, p. 1903, 2021.

[6] S. Reuter, T. Von Woedtke, and K.-D. Weltmann, "The kINPen—a review on physics and chemistry of the atmospheric pressure plasma jet and its applications," *Journal of Physics D: Applied Physics*, vol. 51, no. 23, p. 233001, 2018.

[7] P. E. Petersen, D. Bourgeois, H. Ogawa, S. Estupinan-Day, and C. Ndiaye, "The global burden of oral diseases and risks to oral health," *Bulletin of the world health organization*, vol. 83, pp. 661-669, 2005.

[8] J. Kalnina and R. Care, "Prevention of occlusal caries using a ozone, sealant and fluoride varnish in children," *Stomatologija*, 2016.

[9] D. T. Azevedo, J. J. Faraoni-Romano, J. d. R. Derceli, and R. G. Palma-Dibb, "Effect of Nd: YAG laser combined with fluoride on the prevention of primary tooth enamel demineralization," *Brazilian dental journal*, vol. 23, pp. 104-109, 2012.

PP10

Design and Experimental Research on a Self-Cleaning Endoscope Cover for the da Vinci Surgical Robot

Dominika SZUBERLA[1], Tadeusz PAŁKO[1], Wojciech ŚWIĘSZKOWSKI [2], Emilia CHOIŃSKA[2], Krzysztof Jakub PAŁKO[3]

1 Warsaw University of Technology, Faculty of Mechatronics, Institute of Metrology and Biomedical Engineering, A. Boboli 8 St., 02-525 Warsaw, Poland
2 Warsaw University of Technology, Faculty of Materials Engineering, Wołoska 141 St., 02-507 Warsaw, Poland
3 Nalecz Institute of Biocybernetics and Biomedical Engineering, Polish Academy of Sciences,
Ks. Trojdena 4 st., 02-109 Warsaw, Poland

d.szuberla17@gmail.com

Keywords: Self-cleaning, Endoscope cover, da Vinci surgical robot, Hydrophobic materials, Optical properties

Motivation and Aim: The use of the da Vinci surgical robot in minimally invasive procedures requires high optical clarity of the endoscopic camera. Contamination of the camera lens during surgery significantly affects the quality of visualization, potentially impacting surgical outcomes. Due to this fact, high water repellency became one of the key properties of, for example, self-cleaning materials [1].

One of the most important components of the console is the endoscope. In the da Vinci robotic system, a camera with zero-degree or thirty-degree optics (0° or 30°) is available. [2]

This research aims to design and experimentally evaluate self-cleaning endoscope covers using hydrophobic materials to prevent lens contamination and ensure consistent optical performance. This study explores the application of advanced hydrophobic materials, including PDMS, PMMA, polypropylene (PP), and polystyrene (PS), for endoscopic lens covers. The systematic evaluation of these materials' self-cleaning properties, transmission capabilities in the UV-VIS spectrum, and their modifications using plasma activation and silanization enhances their effectiveness in a surgical environment.

Methods: Two experimental approaches were investigated. The first involved testing hydrophobic polymer materials such as PDMS, PMMA, polypropylene (PP), and polystyrene (PS) to determine their suitability as endoscope covers. Their hydrophobic properties were measured using water contact angle analysis, while optical transparency was assessed using UV-VIS spectrophotometry. The second approach focused on surface modification techniques, including plasma activation and silanization, to enhance hydrophobicity. Scanning electron microscopy (SEM) and Fourier-transform infrared spectroscopy (FT-IR) were used to analyze surface morphology before and after treatment. Although this study focused on water repellency, future work will include the evaluation of body fluids commonly present in surgical environments such as blood, saline solutions, and acidic or protein-rich substances to better simulate real intraoperative conditions.

Main results:

- Hydrophobicity tests confirmed that PDMS, PMMA, PP, and PS exhibit significant water repellency, with enhanced performance after plasma treatment and silanization.
- UV-VIS analysis demonstrated high light transmission in the visible spectrum for all tested materials, ensuring minimal optical distortion.
- SEM analysis indicated that plasma activation did not introduce significant morphological changes to the materials.
- The application of 1H,1H,2H,2H-perfluorodecyltriethoxysilane further improved hydrophobic properties, confirming its potential use for self-cleaning endoscopic covers.

Based on a literature review, the most suitable sterilization methods for the tested materials appear to be ethylene oxide (EtO) sterilization and plasma sterilization. However, the effect of these processes on the hydrophobic and optical properties was not investigated in this study. This represents a limitation that should be addressed in future work.

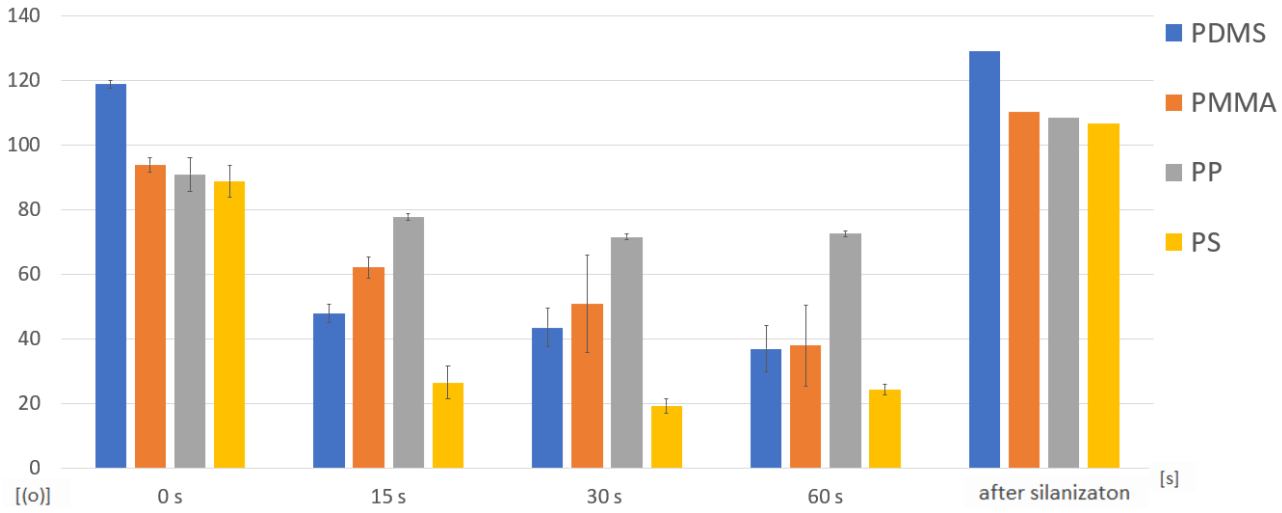

Figure 5. The graph shows the difference in hydrophobicity of the materials before (0 s) and after plasma treatment (15, 30, 60 s), as well as after the silanization process.

Conclusion: The research confirms that self-cleaning endoscope covers using hydrophobic materials can significantly reduce lens contamination and maintain optical clarity. The combination of plasma treatment and silanization enhances the hydrophobic properties of these materials, making them viable for application in the da Vinci surgical system. Future work will focus on further optimization of surface modifications and durability testing under surgical conditions.

References:

[1] M. Piłkowski, G. Morgiante, J. Myśliwiec, M. Kuchowicz, J. Marczak Environmental testing of hydrophobic fluorosilane-modified substrates April 2021 doi: 10.1016/j.rinma.2021.100064.

[2] D. Szuberla, R. Sosnowski, A. Grudziński, M. Nekanda-Trepka, T. Borkowski, P. Kania, J. Frey, Ł. Nyk, T. Jakubczyk, Surgeon Console of the da Vinci Robotic System

PP11

Electrospun PEDOT:PSS Nanofibers for Flexible Bioelectronics Applications

Izabela LEWANDOWSKA[1], Karolina CYSEWSKA[1*]

1 Faculty of Electronics, Telecommunications and Informatics, and Advanced Materials Centre, Gdansk University of Technology, ul. Narutowicza 11/12, 80-233 Gdańsk, Poland

* ***Corresponding author***. *E-mail address*: karolina.cysewska@pg.edu.pl

Keywords: flexible bioelectronics, conductive polymers, PEDOT:PSS, electrospinning

Motivation and Aim: Bioelectronics is evolving swiftly, integrating conductive materials like polymers, inks, and hydrogels to develop soft and stretchable devices. The rising demand for advanced medical solutions, fueled by new health challenges and an expanding patient population, is driving this sector's growth. A significant trend in bioelectronics is the move toward miniaturization and enhanced flexibility. PEDOT:PSS, a highly conductive and processable organic polymer, is attracting attention as a viable alternative to indium tin oxide (ITO) due to its superior mechanical properties and cost-effectiveness.

This study aims to develop a conductive mat using the polymer PEDOT:PSS via the electrospinning method. PEDOT:PSS (poly(3,4-ethylenedioxythiophene):poly(styrenesulfonate)) is known for its high stability, excellent electrical conductivity, and exceptional processability. To accomplish this, a conductive ink made from commercial PEDOT:PSS solution and poly(ethylene oxide) (PEO) will be formulated with optimized rheological properties to ensure effective electrospinning.

Novelty: This study introduces an innovative approach to fabricating highly conductive PEDOT:PSS nanofibers through electrospinning. Unlike traditional thin-film deposition methods, electrospinning allows for the creation of highly porous, interconnected nanostructures that enhance surface area and mechanical flexibility. Additionally, post-processing techniques involving ethylene glycol (EG) treatment have been explored to further improve electrical conductivity, distinguishing this work from existing studies. Furthermore, comparisons of electrochemical performance between electrospun PEDOT:PSS nanofibers, conventional PEDOT:PSS thin films, and platinum electrodes provide new insights into the material’s potential for bioelectronic applications, such as neural electrodes.

Methods: The electrospinning process for synthesizing PEDOT:PSS nanofibers was conducted under varying conditions. Solution parameters include PEDOT:PSS concentration, solution viscosity, and solvent type. Process parameters include flow rate, applied voltage, needle-to-collector distance, and needle diameter. Temperature and relative humidity are important environmental parameters. Several parameters were systematically adjusted, including PEDOT:PSS concentration, applied voltage, and collector rotational speed. Since these parameters are interdependent, precise optimization was essential for achieving the desired nanofiber properties.

The morphology of the obtained nanofibers was analyzed using scanning electron microscopy (SEM), offering detailed insights into their structure and uniformity. Electrical properties were

preliminarily evaluated through sheet resistance measurements with a simple multimeter. Furthermore, the effect of chemical post-treatment with ethylene glycol (EG) on the conductivity and morphology of the electrospun nanofibers was examined. Electrochemical performance was assessed by conducting comparative electrochemical measurements among electrospun PEDOT:PSS nanofibers, traditional PEDOT:PSS thin films, and platinum electrodes to evaluate their potential applications in bioelectronics. The measurements were carried out under simulated body conditions.

Main results: The optimization process enabled the development of a PEDOT:PSS-based conductive ink suitable for electrospinning, leading to the successful fabrication of conductive nanofibers. By carefully selecting solution, process, and environmental parameters, a uniform and flexible nanofiber mat with desirable electrical properties was produced. The introduction of ethylene glycol post-treatment significantly enhanced the conductivity of the nanofibers, demonstrating their potential for application in flexible bioelectronic devices.

Conclusion: The fabricated PEDOT:PSS nanofibers exhibit remarkable flexibility and conductivity, making them highly suitable for next-generation wearable bioelectronics. This study highlights the potential of electrospun PEDOT:PSS nanofibers in diverse bioelectronic applications, paving the way for developing advanced, flexible electronic devices.

Acknowledgements: This work was supported by National Science Centre (NCN), Poland: Sonata grant based on the decision 2021/43/D/ST7/01362.

References:

[1] B. Bessaire, M. Mathieu, V. Salles et al., „Synthesis of continuous conductive PEDOT: PSS nanofibers by electrospinning: A conformal coating for optoelectronics", ACS Appl. Mater. Interfaces, 2017, doi: 10.1021/acsami.6b13453.

[2] E. Verpoorten, G. Massaglia, C. F. Pirri, M. Quaglio, „Electrospun PEO/PEDOT:PSS nanofibers for wearable physiological flex sensors", Sensors, 2021, doi: 10.3390/S21124110/S1.

[3] K. Cysewska, S. Pawłowska, "A simple route of providing a soft interface for PEDOT:PSS film metallic electrodes without loss their electrical interface parameters", Electrochimica Acta, 2024, doi: 10.1016/j.electacta.2024.145115.

[4] M. Ahmadi Bonakdar, D. Rodrigue, "Electrospinning: Processes, Structures, and Materials", Macromol, 2024, doi: 10.3390/MACROMOL4010004.

PP12

Study on catalytic activity of lactate oxidase nanoflowers

Kamila SADOWSKA[1*], Abdelkader ZEBDA[2]

1 Nalecz Institute of Biocybernetics and Biomedical Engineering, Polish Academy of Sciences, Ks. Trojdena 4, 02-109 Warsaw, Poland

2 University of Grenoble Alpes, CNRS, INSERM, TIMC-IMAG UMR 5525, Grenoble, 38000, France

* ***Corresponding author***. *E-mail address*: ksadowska@ibib.waw.pl

Keywords: hybrid nanoflowers, lactate oxidase, H_2O_2 determination

Motivation and Aim: Biocatalytic medicine utilizes biocatalysts, such as enzymes, to trigger specific chemical reactions within the body for disease treatment or diagnosis. This strategy takes advantage of the exceptional ability of biocatalysts to facilitate complex chemical transformations with remarkable speed and specificity, enabling highly targeted therapeutic interventions. For example, in cancerous tumors with elevated lactate levels, lactate oxidase (LOx) has been proposed to convert lactate into hydrogen peroxide (H_2O_2), a compound capable of destroying cancer cells. Growing evidence indicates that reducing lactate in the tumor microenvironment can counteract immunosuppression and enhance immunotherapy, ultimately strengthening anti-tumor immune responses. As a result, lactate presents itself as a compelling target for cancer treatment. Lactate levels in tumor tissues range from 10 to 40 mM, necessitating high concentrations of LOx for effective depletion. [1] Moreover, the vulnerability of enzymes, particularly their limited lifespan and tendency to denature under physiological conditions, presents a significant challenge. Recently, a feasible approach for enzymes immobilization was developed basing on self-assembly of biomolecules in the presence of metal ions in the phosphate buffer [2]. The obtained hybrid, organic-inorganic flower-like structures show improved catalytic activity and stability. The aim of this study is to develop and characterize hybrid nanoflowers based on lactate oxidase through biomolecular self-assembly in the presence of metal ions, in order to create a stable and efficient biocatalyst for lactate oxidation in tumor microenvironments, thereby enhancing the therapeutic potential of biocatalytic medicine in cancer treatment.

Novelty: LOx-based hybrid nanoflowers were synthesized and characterized for the first time.

Methods: Hybrid nanoflowers were precipitated from LOx buffered solution (PBS, pH 7.4) by addition of Cu^{2+} or Mn^{2+} aqueous solution. Manufactured LOx nanoflowers were characterized by Fourier-transform infrared spectroscopy (FTIR), X-ray diffraction (XRD) and scanning electron microscopy (SEM). The catalytic activity of LOx nanoflowers was studied by colorimetric method, based on H_2O_2 determination.

Main results: In the first step the parameters of synthesis, as time, concentration and volume of PBS and ratio of reagents were studied. The obtained hybrid nanoflowers were composed of LOx, as organic part and copper or manganese phosphate, as inorganic part, as confirmed by FTIR and XRD, respectively. The average diameters were in the range of 10-20 μm. The studies demonstrated that immobilizing LOx in the form of hybrid nanoflowers with Mn^{2+} enhances

both its enzymatic activity and stability. Figure 1 presents the long term stability of LOx-manganese phosphate nanoflowers.

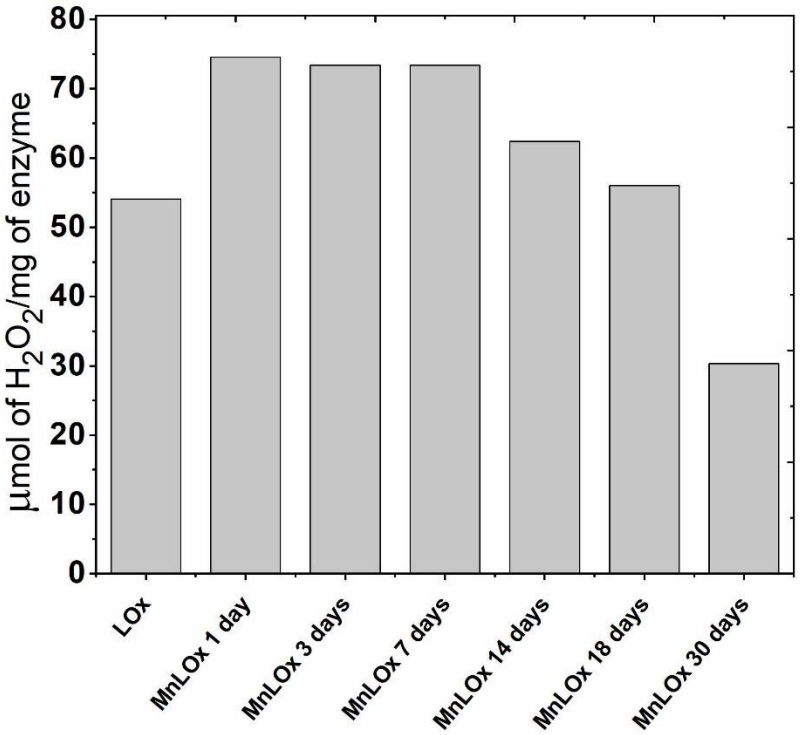

Figure 1. Long term activity of MnLOx in comparison to pristine enzyme

Conclusion: The designed nanoflowers have the potential to serve as an effective catalyst converting lactate present in tumor microenvironment to H_2O_2, which can destroy tumor cells. Hybrid nanoflowers, composed of non-toxic, biodegradable materials and synthesized through eco-friendly methods offers a great promise for biocatalytic medicine.

Acknowledgements: Project titled "Enzyme Based Metal Organic Frameworks for Cancer Treatment" supported by National Agency for Academic Exchange, BPN/BFR/2024/1/00025/U/00001.

References:

[1] Pérez-Tomás R, Pérez-Guillén I. Lactate in the Tumor Microenvironment: An Essential Molecule in Cancer Progression and Treatment. Cancers (Basel). 2020; 12(11):3244. doi: 10.3390/cancers12113244. PMID: 33153193; PMCID: PMC7693872.

[2] Ge J, Lei J, Zare RN. Protein–inorganic hybrid nanoflowers. Nat Nanotechnol. 2012;7(7):428–432. doi:10.1038/nnano.2012.80.

PP13

A novel *ds*DNA-based electrochemical biosensor for 6-mercaptopurine

Anna SOŁDATOWSKA*, Marcin URBANOWICZ, Kamila SADOWSKA, Dorota G. PIJANOWSKA

Nalecz Institute of Biocybernetics and Biomedical Engineering, Warsaw, Poland

* ***Corresponding author***. *E-mail address*: asoldatowska@ibib.waw.pl

Keywords: 6-mercaptopurine, electrochemical biosensor, DNA-drug interaction, short double-stranded DNA

Motivation and Aim: Accurate monitoring of drug concentrations in biological fluids is essential in pharmacological research and clinical practice to ensure both efficacy and safety in drug therapy. In the case of 6-mercaptopurine (6MP), the active metabolite of thiopurines, precise concentration assessment is particularly crucial due to its narrow therapeutic index, where the difference between an effective and toxic dose is minimal [1]. Thiopurines, including 6-MP, are widely used in the treatment of inflammatory bowel disease (IBD), autoimmune disorders, and certain types of cancer. However, their potential adverse effects necessitate careful monitoring throughout therapy. Current analytical tools remain insufficient for providing physicians with a fast and convenient means of optimizing treatment. Therefore, this study aims to develop a sensitive and reliable biosensing approach for 6-MP monitoring, facilitating more effective and personalized patient care.

Novelty: This research introduces the first-reported electrochemical biosensor based on drug-DNA interaction to the detection of 6-mercaptopurine. It utilizes a double-stranded (*ds*) DNA sequence (5'-GGCAGGACGGAG-3') that selectively interacts with 6MP, the development of which was reported in previous studies [2]. The integration of this DNA-based recognition element into an electrochemical platform offers a novel approach, providing a rapid, cost-effective, and user-friendly alternative to traditional analytical techniques.

Methods: Two types of biosensor designs were developed, each employing a different approach to bioreceptor immobilization on the electrode surface (Fig.1 A). The first design features a simple system utilizing screen-printed graphite electrodes (GSPEs) with an adsorbed *ds*DNA layer. The second modification also utilizes graphite electrodes but incorporates platinum nanoparticles, which, due to their electrocatalytic properties, significantly enhance the response of the biosensor. Subsequently, a linear linker – cysteamine (Cys) – was introduced onto the surface. The presence of terminal -NH_2 groups in cysteamine enabled the attachment of double-stranded DNA terminated with a -COOH group.

Main results: Voltammetric measurements confirmed the presence of DNA on electrodes surfaces as the oxidation signals of guanine and adenine are recorded. In the case of the latter signal, a significant decrease is observed after incubating the electrodes in 6-mercaptopurine solutions, indicating that analyte detection can occur indirectly by measuring this decrease. (Fig.1 B). The developed GSPPE/*ds*DNA and GSPE/Pt-Cys-*ds*DNA biosensors demonstrated a linear response within the nanomolar concentration range, from 200 to 1000 nM and from 2

to 75 nM respectively, aligning well with the concentrations typically found in different biological samples. The incorporation of platinum nanoparticles significantly improved the electrochemical signal, enhancing the sensor's sensitivity (Fig.1 C) – from 2.4 nA/nM for GSPE/*ds*DNA to 336.9 nA/nM.

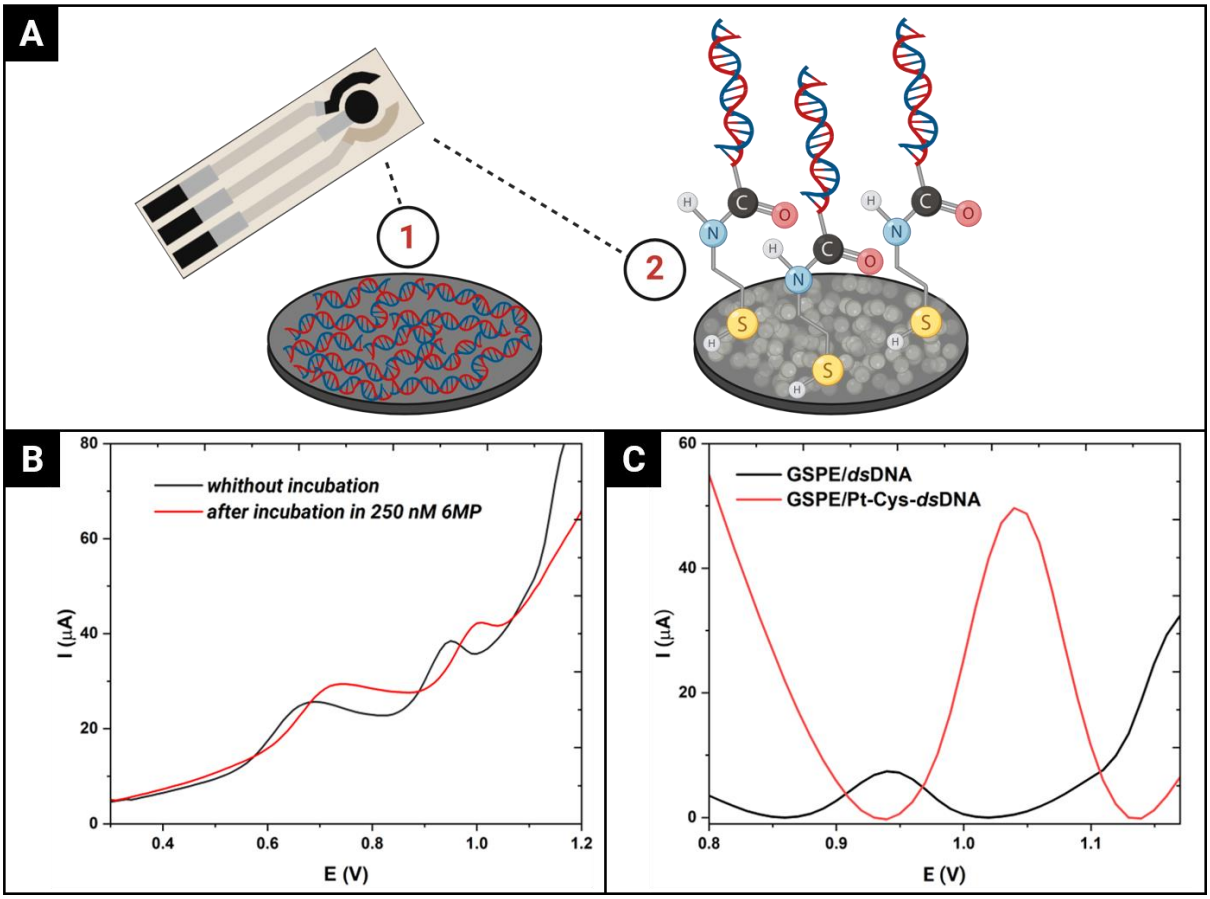

Figure 6. A) Two types of screen-printed graphite electrode modifications GSPPE/*ds*DNA and GSPE/Pt-Cys-*ds*DNA; Differential pulse voltammograms showing: **B)** change in adenine oxidation peak on GSPE/*ds*DNA, and **C)** difference in adenine oxidation peak on electrodes with different modifications.

Conclusions: This study describes the development of a new biosensor for the electrochemical detection of 6MP, an active metabolite of thiopurines, which is an important immunosuppressive drug. The presented novel bioanalytical tool provides a low-cost and simple alternative for the instrumental detection of 6-mercaptopurine.

Acknowledgements: The study was supported by the Polish National Science Center, Project 2019/35/O/ST5/01886

References:

1. Boekema M, Horjus–Talabur Horje CS, Roosenboom B, Roovers L, van Luin M. Therapeutic drug monitoring of thiopurines: Effect of reduced 6-thioguanine nucleotide target levels in inflammatory bowel disease patients. Br J Clin Pharmacol. 2022;88(8):3741-3748. doi:10.1111/bcp.15315

2. Sołdatowska A, Urbanowicz M, Urbanowicz M, Sadowska K, Pijanowska DG. Exploring DNA-6MP interactions to develop a receptor with selective binding properties. *Int J Biol Macromol*. 2025; 305. doi:10.1016/j.ijbiomac.2025.140910

PP14

Surface-Functionalized Electrodes via Plasma Treatment for Enhanced Detection of Pseudomonas Quinolone Signals

Sunil LUHAR[1*,] Kamila SADOWSKA[1]

[1]Nalecz Institute of Biocybernetics and Biomedical Engineering, Polish Academy of Sciences, Ks. Trojdena 4, 02-109 Warsaw, Poland

***Corresponding author**: E-mail address: sluhar@ibib.waw.pl, ksadowska@ibib.waw.pl*

Keywords: Plasma treatment, Quorum sensing, Biofilm detection, Electrochemical sensor

Motivation and Aim

Quorum sensing (QS) is a cell-to-cell communication process used by bacteria to regulate gene expression based on population density. Pseudomonas Quinolone Signal molecule (PQS) plays a crucial role in biofilm formation, virulence, and antibiotic resistance. Detecting PQS is essential for understanding bacterial behaviours and developing strategies to control biofilm-related infections. In this research we explore the use of oxygen plasma treatment to modify carbon-based screen-printed electrodes (SPEs) for improved PQS detection. Oxygen plasma introduces oxygen-containing functional groups that enhance surface wettability and electron transfer, enabling real-time PQS monitoring during the biofilm formation. This study aims to develop a more efficient electrochemical platform for studying bacterial communication and its broader implications in biomedical applications.

Novelty

The application of oxygen plasma in biosensing provides a simple, efficient, and scalable method to enhance electrode activity towards PQS molecules oxidation. Unlike traditional surface modification techniques, plasma treatment offers a clean, controllable, and reproducible approach for electrode functionalization, significantly improving sensor performance in control experiments. This study represents the first application of plasma-treated carbon-based electrodes for PQS detection, opening new possibilities for real-time monitoring of bacterial communication with enhanced sensitivity and reliability.

Methods

Oxygen plasma treatment was applied to carbon-based screen-printed SPEs to introduce oxygenated functional groups, enhancing surface hydrophilicity and facilitating PQS detection in control experiments. The impact of plasma treatment on electrode performance was evaluated using electrochemical impedance spectroscopy (EIS) by monitoring changes in charge transfer resistance before and after treatment. To assess molecular activity, cyclic voltammetry (CV) was used to analyze the electrochemical response of PQS at varying concentrations on plasma-treated and pristine electrodes. Surface modification and its effects on electron transfer were further characterized using EIS, ensuring reproducibility and consistency in biosensor performance.

Main Results

EIS confirmed an increase in electron transfer activity after plasma treatment, as indicated by a decrease in charge transfer resistance ***Fig 1 A)***. The detection of various PQS molecule concentrations was validated using CV, demonstrating enhanced electrochemical responses with plasma-treated electrodes. Additionally, pH studies were conducted to evaluate the stability and activity of PQS under different environmental conditions.

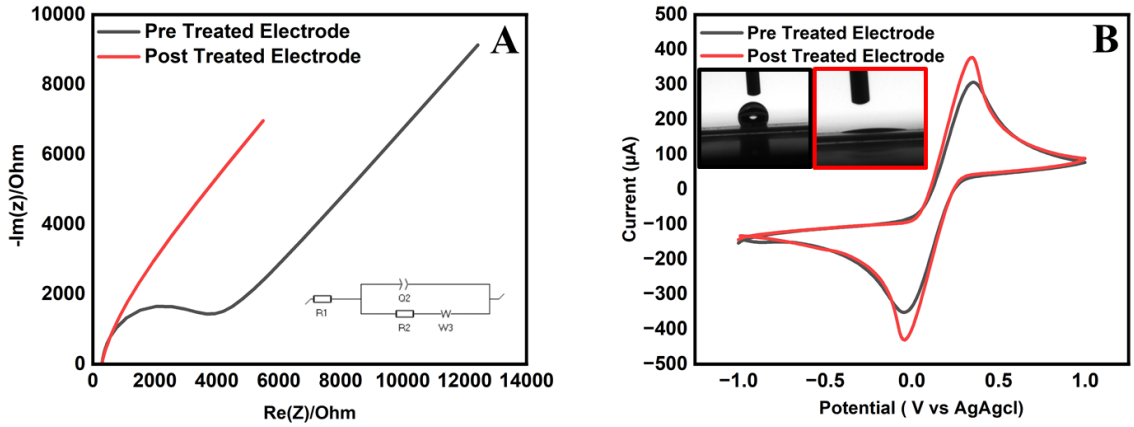

Figure 7. A) Impedance and B) cyclic voltammetry responses of pre and post treated screen printed electrode under 10mM equal concentrations of $K_3Fe(CN)_6$ and $K_4Fe(CN)_6$ [Inset: A) Randles circuit B) Contact angle measurement of pre and post treated electrode].

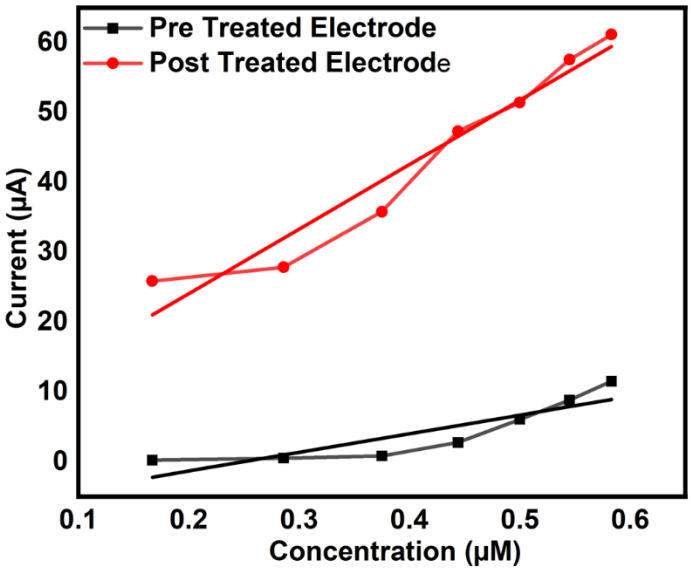

Figure 8. Calibration curves for PQS detection obtained by linear sweep voltammetry from –1.0 to +1.0 V at a scan rate of 50 mV s^{-1}. Standards were prepared by diluting PQS in an 80:20 (v/v) mixture of 0.1 M PBS (pH 7.4) and acetic acid. Peak currents (I_p) plotted versus PQS concentration (0.167–0.583 µM).

Surface modifications were further characterized using: Scanning electron microscopy (SEM) to visualise morphology of the electrode, Fourier-transform infrared spectroscopy (FTIR-ATR), X-ray photoelectron spectroscopy (XPS) to confirm the presence of functional groups introduced by plasma treatment Contact angle measurements to assess wettability improvements ***Fig. 1 B)***. The comparison between pre and post –treated electrodes reveals that plasma functionalization substantially enhances electroanalytical performance (***Fig.2).***

Untreated SPCEs display moderate sensitivity (26.64 $\mu A \cdot \mu M^{-1}$) and a relatively high detection limit (0.236 µM), indicative of sluggish electron transfer and limited surface activity toward PQS oxidation. In contrast, plasma-treated SPCEs exhibit over a threefold increase in sensitivity (92.20 $\mu A \cdot \mu M^{-1}$) alongside a twofold reduction in LOD (0.108 µM), reflecting dramatically improved charge-transfer kinetics and analyte adsorption. These improvements are attributable to the introduction of oxygenated functional groups (C–O, C=O) that enhance surface wettability—confirmed by a reduction in contact angle—and decrease charge-transfer resistance in EIS measurements ***Fig.1***. Moreover, the higher linearity (R^2 = 0.944 vs. 0.782) and stable positive intercept post-treatment indicate a more reliable baseline and consistent response. Collectively, these data underscore oxygen plasma treatment as a rapid, reproducible strategy to boost the sensitivity, detection threshold, and overall reliability of carbon SPEs for real-time PQS sensing applications

Conclusion

This study demonstrates that oxygen plasma treatment significantly improves the performance of carbon-based SPEs for PQS detection. Oxygen plasma treatment of carbon SPEs yields a dramatic

enhancement in PQS sensing performance: the water contact angle decreases from ~85° to ~35°, and electrochemical impedance spectroscopy shows a ~70% reduction in charge-transfer resistance. Linear sweep voltammetry calibration (–1.0 to +1.0 V at 50 mV s^{-1}, PQS in 80:20 0.1 M PBS/acetic acid) reveals that sensitivity increases from 26.64 $\mu A \cdot \mu M^{-1}$ (R^2 = 0.782, LOD = 0.236 μM) for untreated SPEs to 92.20 $\mu A \cdot \mu M^{-1}$ (R^2 = 0.944, LOD = 0.108 μM) after plasma functionalization. Surface analyses (SEM, FTIR-ATR, XPS) confirm the uniform incorporation of C–O and C=O groups, and pH stability tests (pH 6–8) show <10% variation in response. Together, these data demonstrate that oxygen plasma–treated carbon electrodes provide a scalable, reproducible platform with superior wettability, electron-transfer kinetics, and analytical figures of merit for real-time monitoring of PQS, with clear potential for applications in biomedical diagnostics and biofilm control.

Acknowledgements

Authors would like to acknowledge financial support from National Science Centre, project number 2023/50/E/ST5/00347.

References

1. Simanek KA, Schumacher ML, Mallery CP, Shen S, Li L, Paczkowski JE. Quorum-sensing synthase mutations re-calibrate PQS concentrations in clinical isolates of Pseudomonas aeruginosa to enhance pathogenesis. *Nat Commun*. 2023;14(1). doi:10.1038/s41467-023-43702-4

2. Nemade R, Cotts S, Berry V. Plasma treatment for enhanced microbe-electrode interfaces: A bio-electronic sink. *J Power Sources*. 2022;544. doi:10.1016/j.jpowsour.2022.231834

3. Khelifa F, Ershov S, Habibi Y, Snyders R, Dubois P. Free-Radical-Induced Grafting from Plasma Polymer Surfaces. *Chem Rev*. 2016;116(6). doi:10.1021/acs.chemrev.5b00634

PP15

Simultaneous recordings of vascular and neuronal responses using 3D printed head casts

Tilmann SANDER[1*], Urban MARHL[2], Pichaya TAPPAYUTHPIJARN[1], Piotr SAWOSZ[3], Paul ANDERS[1], Stanislaw WOJTKIEWICZ[3], Vojko JAZBINŠEK[2], Adam LIEBERT[3]

1 Physikalisch-Technische Bundesanstalt, Biosignals, Berlin, Germany

2 Institute of Mathematics, Physics and Mechanics, Ljubljana, Slovenia

3 Nalecz Institute of Biocybernetics and Biomedical Engineering, Warsaw, Poland

* ***Corresponding author***. *E-mail address*: Tilmann.sander-thoemmes@ptb.de

Keywords: functional near-infrared spectroscopy, magnetoencephalography, optically pumped magnetometers, individualized head cast, 3D printing

Motivation and Aim: Magnetoencephalography (MEG) is the complementary technique to electroencephalography (EEG) and yields additional information on electrophysiological brain activations. Combining functional near-infrared spectroscopy (fNIRS) with MEG to study vascular and neuronal responses synchronously has the potential for clinical applications such as, e.g., stroke monitoring. For this combination always fibre coupled fNIRS devices are required since photodiodes (lasers) and photodetectors on the head generate magnetic fields compromising MEG. The combination of fNIRS with Dewar based cryogenic sensor MEG was to the disadvantage of MEG. Placing fibres on the head increased the distance between active brain regions and magnetic field sensors and in turn the recorded magnetic field strength was substantially attenuated.

Novelty: Recently the combination has become easier due to a new type of MEG, which uses optically pumped magnetometers (OPM) to measure brain magnetic fields. OPMs are single sensors and can be placed in between optodes. To have a mechanically stable setup reducing movement artifacts, a 3D printed rigid head cast was developed, which holds both optodes and OPM sensors in place.

Methods: Starting with participants MRI a shell fitting the head is designed and the slots for OPMs and optodes are added. Then the structure is printed by additive manufacturing. We made head casts for 6 participants. For motor stimulation the grid was centered at C3 and for visual stimulation the grid covered the O1/O2 region. The CAD design and the experimental setup for one participant are shown in Fig. 1 for the O1/O2 region.

The motor task was self-paced finger opposition of the right hand and checkerboard inversion at 8 Hz was used for visual stimulation. Both had a duration of 8 or 16 s followed by a rest period and at least 35 repetitions. fNIRS was recorded with an in-house built continuous wave device operating at 750 nm and 850 nm, the OPMs were of a triaxial commercial type (quspin.com). Multi-region studies using a visuo-motor task were explored as well.

a) 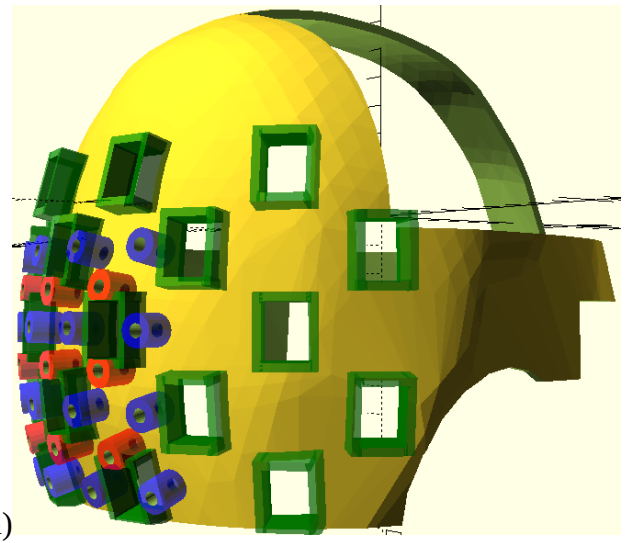 b) 

Fig. 1: a) CAD design made in openSCAD of head cast for the O1/O2 region. Green are the OPM slots, blue the fNIRS source optode slots, and red the fNIRS detector slots. b) Realization with a participant with inserted OPMs (black cubes with white stickers) and optodes (fibres in black sheath). One OPM sits on an extender to record background signals away from the brain. Below the head cast the neck support can be seen and the round structure to the left records the position of the OPMs (Halo, quspin.com).

Main results: To obtain clear activation signals from both modalities simultaneously for a participant proved to be a challenge both with respect to the stimulation and the experimental setup. The 8 s stimulation yields good MEG results, the 16 s stimulation yields better fNIRS results than 8 s. Hair degrading fNIRS light transmission cannot be moved away underneath the optodes inside the cast and MEG signal quality can be degraded by unavoidable movement artifacts, which are dependent on each participant. Nevertheless, vascular and neuronal responses were obtained for a third of the participants.

Conclusion: Using an individualized head cast is an effective way to combine fNIRS with OPM-MEG, but improved noise rejection for MEG and optimized optode slots are required. Another drawback is the availability and cost of MRI, but this will not be of concern in a clinical setting. Optical scanning technology might allow to get head surface data for the head cast. This is particularly useful if brain anatomy is not required for data analysis.

Acknowledgements: Supported by ARIS program P2-0348 and project N1-0283; by DFG project 505063244; and by NCN National Science Center Poland.

PP16

Continuous, Non-Invasive Intra-Abdominal Pressure Monitoring by Transient Radar Methodology

Salar TAYEBI[1], Ashkan ZARGHAMI[1], Ali POURKAZEMI[1], Manu L. N. G. MALBRAIN[2,3], Johan STIENS[1]

[1] Department of Electronics and Informatics, Vrije Universiteit Brussel, Brussels, Belgium

[2] First Department of Anaesthesiology and Intensive Therapy, Medical University of Lublin, Poland

[3] International Fluid Academy, Lovenjoel, Belgium

* ***Corresponding author***. *E-mail address*: salar.tayebi@vub.be

Keywords: Transient radar methodology, intra-abdominal pressure, patient monitoring, non-invasive

Motivation and Aim: The monitoring of physiological signals and vital signs have long been crucial areas of research, leading to the exploration and development of various techniques and technologies over years. In the context of non-invasive methodologies, application of microwave sensors in the healthcare domain has gained significant popularity. Reviewing relevant literature shows the surge in the number of publications reporting the application of microwave sensors in patient care including respiration and heart-rate screening, blood glucose monitoring, temperature assessment, skin tumour detection, breast cancer diagnosis, sleep stage monitoring, skin hydration measurement, and biological infection detection [1]. Intra-abdominal pressure (IAP) reflects the steady state pressure within the abdominal compartment and has been recognized as a new vital sign to monitor critically ill patients [2]. The current gold standard to measure IAP is an invasive approach through the bladder, which is not applicable to patients with pelvic masses. Moreover, it has a risk of infection and trauma of the urinary tract. Accordingly, in the previous decades, there has been a significant increase in studies focused on IAP measurement techniques. The aim of this study is to introduce the transient radar methodology (TRM) as a promising biomedical sensing approach and to investigate its robustness in continuous IAP and respiration monitoring in an in vitro model.

Novelty: TRM [3] is a relatively novel radar-based, time-domain measurement technique that is being investigated for continuous IAP monitoring. Although our previous feasibility study already showed the potential of this technique in IAP monitoring [4], no in-vitro validation of the TRM in continuous IAP monitoring is presented yet. In this study, the application of this methodology in continuous IAP monitoring (including respiration monitoring and, therefore, abdominal pressure variations assessment in real-time) is presented. This study contributes to the literature by complementing our previous findings in this domain.

Methods: A measurement sensor based on the concept of TRM has been designed and developed to radiate at 10 GHz. Subsequently, the measurement hardware has been used to monitor the IAP changes in an abdominal phantom, which represents the human abdominal compartment from the anatomical and electromagnetic points of view. IAP was changed 10 times in the range of 8 to 30 mmHg. At each IAP value, the reflection of the electromagnetic waves, in addition to the pressure readings by an intra-bladder, intra-gastric, and a pressure gauge (connected to the abdominal phantom) were recorded. The reflection of the electromagnetic radiations at 10 GHz (from the first round of measurements) was processed to

investigate how different signal features correlate with IAP and to find the most suitable signal features that can be used to monitor IAP, and to calibrate the TRM device. The remaining nine rounds of IAP measurement data were then used to study the accuracy, precision, and concordance of the TRM results in monitoring IAP by means of Bland-Altman, and concordance analysis. Error grid analysis was also carried out to assess the risk level for a wrong treatment strategy due to erroneous IAP measurements.

Main results: The results of this study revealed the applicability of this sensing approach to monitor IAP in a non-invasive and continuous manner. Bland-Altman analysis showed a total bias (mean difference between IAP results from TRM and the pressure gauge) of 0.12 mmHg and a precision of 2.03 mmHg. The percentage error was 23.56% with upper and lower limits of agreement of 4.10 and -3.86 mmHg, respectively. A concordance coefficient of 96% was also obtained for the TRM approach, showing its robustness in tracking IAP changes rather than determining the absolute IAP value. Lastly, the error-grid-analysis showed no medium to high risk error due to wrong IAP measurement by the TRM. Nevertheless, a low-risk of 9% was observed in the obtained results. An overview of the IAP results via each measurement method is shown in Figure 1.

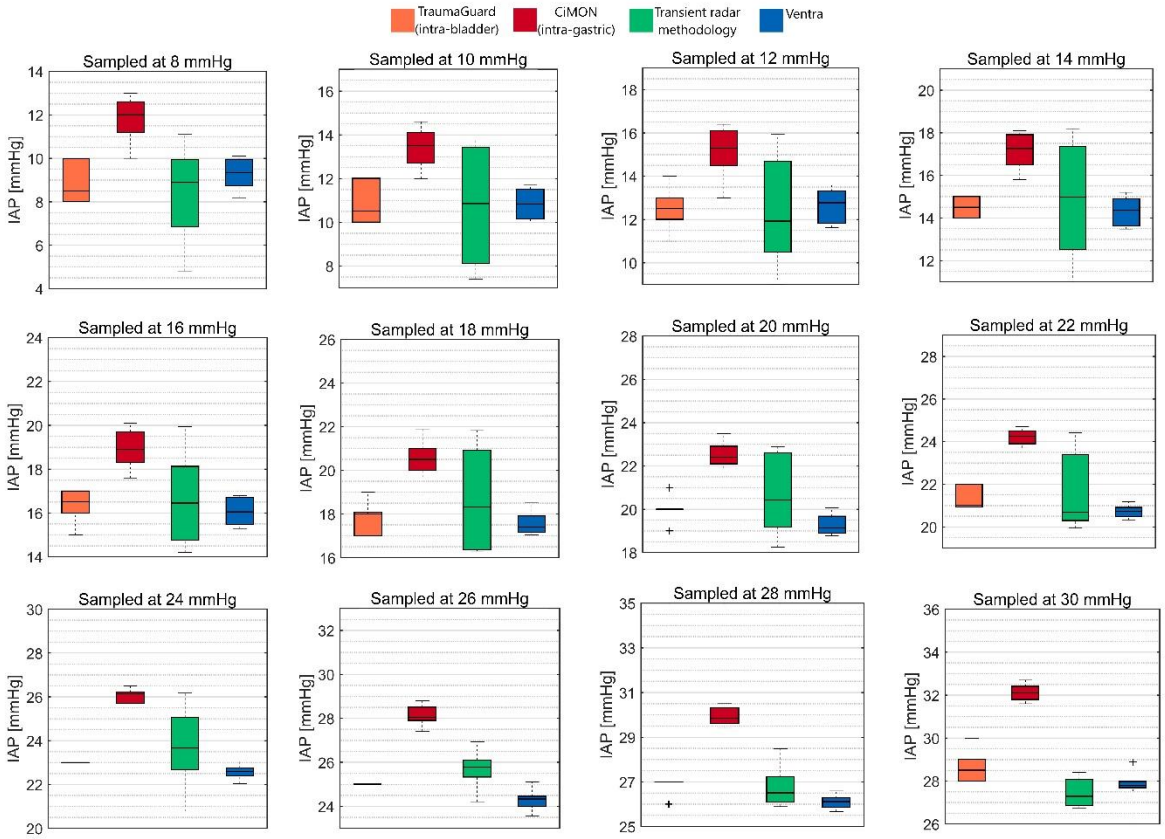

Figure 1. Boxplot of the IAP measurement via TRM, intra-bladder measurement method via TraumaGuard catheter, intra-gastric measurement method via CiMON nasogastric tube, and the pressure sensor of the abdominal phantom (Ventra) at 8 – 30 mmHg.

Conclusion: Application of TRM as a novel contact-free approach to patient monitoring seems promising. Nevertheless, further clinical validations should be done in the future.

Acknowledgements: The authors of the ETRO department acknowledge the “SB fellow at FWO” (“SB van het FWO”), Fonds Wetenschappelijk Onderzoek—Vlaanderen, Research Foundation—Flanders, project number: 1S51124N.

References:

[1] Gartshore A, Kidd M, Joshi LT. Applications of Microwave Energy in Medicine. *Biosensors (Basel)*. 2021;11(4):96. Published 2021 Mar 26. doi:10.3390/bios11040096.

[2] Carter BM, Howard C. A 6th Vital Sign--Potential Use of Nasogastric Tube for Intra-abdominal Pressure Monitoring Method to Detect Feeding Intolerance in Very Low Birth-Weight Preterm Infants (<1500 g). *Adv Neonatal Care*. 2015;15(3):176-181. doi:10.1097/ANC.0000000000000175.

[3] Pourkazemi A, Stiens JH, Becquaert M, Vandewal M. Transient radar method: novel illumination and blind electromagnetic/geometrical parameter extraction technique for multilayer structures. IEEE Trans Microw Theory Tech. 2017;65(6):2171-2184. doi:10.1109/TMTT.2017.2665633.

[4] Tayebi S, Pourkazemi A, Malbrain MLNG, Stiens J. Non-Invasive Intra-Abdominal Pressure Measurement by Means of Transient Radar Method: In Vitro Validation of a Novel Radar-Based Sensor. Sensors. 2021; 21(18):5999. https://doi.org/10.3390/s21185999

PP17

Direct printed potentiometric sensors for pH monitoring in body fluids

Marcin URBANOWICZ[*1], Marek DAWGUL[1], Agnieszka PAZIEWSKA-NOWAK[1], Kornelia BOBROWSKA[1], Anna SOŁDATOWSKA[1], Dorota G. PIJANOWSKA[1]

1 Nalecz Institute of Biocybernetics and Biomedical Engineering, Polish Academy of Sciences, Ks. Trojdena 4 St., 02-109 Warsaw, Poland

* ***Corresponding author***. *E-mail address*: murbanowicz@ibib.waw.pl

Keywords: pH sensor, direct printing, polyazulene, ion-selective electrode

Motivation and Aim: Monitoring of pH in body fluids is a basic parameter of paramount importance in clinical diagnostics and therapy, as pH variations can serve as early indicators of pathological changes, treatment efficacy, and potential complications following extensive surgical procedures. We present a novel, miniaturized potentiometric pH sensor developed using a cost-effective direct printing technology. The sensor is specifically designed for continuous measurements in flow conditions, making it particularly suitable for applications such as monitoring pH changes in various body fluids.

Novelty: The novelty of our work stems from the combination of cost-effective direct printing technology with the use of advanced electroconductive materials characterized by high hydrophobicity. This approach significantly enhances sensor stability by preventing the formation of an interfacial water layer. In our study, we compared the effects of 3 electroconductive polymers as ion-electron transducer layers on the response of a pH sensor. This study is the first to employ polyazulene as the transducing layer in potentiometric pH sensors. Moreover, the direct printing technique facilitates scalable production and provides flexibility in designing sensor geometry.

Methods: Three electroconducting polymers (ECP), polyazulene (pAz), poly(3,4-ethylenedioxythiophene) (pEDOT), and polypyrrole (pPy), were deposited onto glassy carbon (GC) electrodes. Modified electrodes were covered by 60 µL ion-selective membrane (ISM) mixture. The cocktail, composed of 0.5 wt.% potassium tetrakis(*p*-chlorophenyl)borate, 1 wt.% tridodecylamine, 65.5 wt.% bis-(2-ethylhexyl)-sebacate, and 33 wt.% polyvinyl chloride. Potentiometric measurement data were recorded using a 16-channel precision electrochemistry interface, EMF16 from Lawson Labs Inc. (Malvern, PA, USA). To achieve miniaturization, the pAz-based pH sensor fabrication process was adapted for electrodes manufactured using direct printing technology. The direct printing was processed using a programmable microdispensing robot (Nordson EDF PROPlus/PRO Series Automated Dispensing Systems). The basic structures of the electrode were fabricated on a nonconductive polyester foil, with consecutively deposited silver paste, carbon paste, and insulating layers.

Main results: A series of pH sensors were fabricated on GC substrates, each modified with a different electroconducting polymer. Comparison of calibration curves and metrological parameters shown Fig.1. and Table 1. Based on these results, pAz was selected as the best polymer and integrated into graphite sensors fabricated using direct printing technology. The printed pAz-based pH sensors maintained similar metrological parameters ($S = 55.4 \pm 0.1$

mV/decade, response time: 7 second) while offering significant miniaturization advantages. Selectivity tests confirmed that the direct printed pH sensors provided sufficient discrimination against interfering ions in biomedical applications, as the obtained selectivity coefficients are as follows log(K_{ij}^{pot}): -9.7 for Na^+, -8.3 for K^+, -7.2 for NH_4^+, -8.8 for both Ca^{2+} and Mg^{2+}. pH measurements in human blood plasma using the printed pH sensor (7.291 ± 0.003) closely matched those obtained with a commercial pH meter (7.301 ± 0.005). Our sensor, although simple in design, achieves metrological performance comparable to that of much more structurally complex sensors, such as those utilizing photo-induced grafting to simultaneously attach an ionophore-doped crosslinked poly(decyl methacrylate) membrane to both a surface of carbon electrode and inert polymeric electrode body material [1].

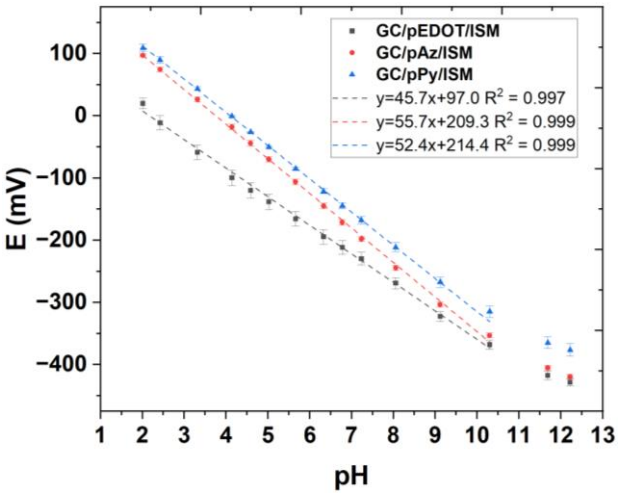

Fig.1. Comparison of calibration curves of pH sensors based on different ECP.

Table 1. Comparison of metrological parameters for pH sensors with various ECP-based transducing layers.

Electrocnductive polimer, ECP	**Contact angle of GC electrodes modified with ECP (°)**	**S (mV/pH)**	**pH linear range**	**$t_{95\%}$ (s)**
PAz	99±1	55.7±0.6	2-10	5
PPy	83±1	52.4±1.9	2-10	31
PEDOT	47±1	45.7±0.8	2-10	25

Conclusion: We developed a novel miniaturized potentiometric pH sensor using cost-effective direct printing and a hydrophobic polyazulene layer. The sensor shows high sensitivity, a wide linear range, excellent repeatability, and selectivity, with performance comparable to commercial pH electrodes in human plasma.

Acknowledgements: The studies were financially supported by the project KPOD.07.07-IW.07-0115/24 funded by the Medical Research Agency (ABM), Poland, and IBBE PAS statutory project 225.

References:

[1] Choi KR, Troudt BK, Bühlmann P. Ion-Selective Electrodes With Sensing Membranes Covalently Attached to Both the Inert Polymer Substrate and Conductive Carbon Contact. Angew Chemie - Int Ed. 2023;62(28). doi:10.1002/anie.202304674

[2] Urbanowicz M, Dawgul M, Pijanowska DG. Planarna mikroelektroda jonoselektywna oraz sposób jej wytwarzania. Patent application 2024:WIPO ST 10/C PL448894.

PP18

Radio Frequency Magnetic Field Detection for Magnetic Hyperthermia: Low-Cost, Lab-Friendly Hardware

Serhat Ilgaz YÖNER[1,2,6*],Alpay ÖZCAN[3,4,5,6]

1 Institute of Biomedical Engineering, Boğaziçi University, İstanbul, Türkiye

2 Department of Biomedical Equipment Technology, Junior College, Acıbadem Mehmet Ali Aydınlar University, İstanbul, Türkiye

3 Center for Targeted Therapy Technologies (CT3), Boğaziçi University, İstanbul, Türkiye

4 Electrical and Electronics Engineering Department, Boğaziçi University, İstanbul, Türkiye

5 Systems Science and Mathematics Laboratory, Boğaziçi University, İstanbul, Türkiye

6 Magnetic Medical Devices Laboratory, Boğaziçi University, İstanbul, Türkiye

* ***Corresponding author***. *E-mail address*: serhat.yoner@acibadem.edu.tr

Keywords: magnetic hyperthermia, radio frequency detection, low-cost instrumentation, magnetic field measurement, hardware development, real-time RF detection

Motivation and Aim: Magnetic Hyperthermia has emerged as a promising technique for targeted cancer therapy, utilizing radio frequency fields in the 30–300 kHz range to induce localized heating in magnetic nanoparticles accumulated at tumor sites [1, 2]. Despite its growing importance, the lack of commercially available radio frequency field measurement systems within this frequency range presents a significant barrier to experimental reproducibility, device calibration, magnetic performance assessment and system development in research laboratories. This work aims to address this critical gap by developing a basic, cost-effective, and lab-friendly radio frequency magnetic field detection system. The proposed setup comprises a sense coil paired with an intermediate amplifier board, designed to be compatible with standard laboratory oscilloscopes for the detection and analysis of weak magnetic signals during Magnetic Hyperthermia experiments.

Novelty: Unlike conventional magnetic field sensors or Gauss meters that are either not optimized for low radio frequencies or come with prohibitive costs and complex integration requirements [3], the proposed system offers a streamlined and economical alternative tailored specifically for Magnetic Hyperthermia research. The novelty lies in its minimalist yet effective design: a passive sensing coil combined with a configurable analog amplification stage. This modular system can be seamlessly integrated into standard oscilloscope-based setups without requiring specialized software, firmware, or proprietary interfaces. A key feature of the amplifier board is its continuously adjustable gain, allowing researchers to precisely match amplification to the signal amplitude and noise environment, making the system highly adaptable across various experimental conditions in preclinical Magnetic Hyperthermia studies.

Methods: A custom-designed electronic board was utilized to preprocess signals originating from a custom-made 1-turn sense coil with 6 mm coil diameter made from a 1.2 mm wire diameter, enabling the measurement of low magnetic fields within the 30-300 kHz frequency range. The board incorporates a power regulation stage, passive high-pass and low-pass filter stages to reduce unwanted noise and artifacts, and an LF411CN based amplification stage with continuously adjustable gain between 1 and 11 to enhance the signal amplitude. The refined signal can be outputted to any standard commercial oscilloscope system, facilitating the visualization and analysis of low-level magnetic field measurements in the low radio frequency spectrum. The system's performance was initially evaluated under an approximately 1.839 mT peak magnetic flux density, 100 kHz magnetic field frequency generated by a 20-turn, 44 mm diameter Helmholtz coil driven by a 4.5 A RMS current. Baseline noise measurements were also performed in the absence of any magnetic field. Additionally, signal-to-noise ratio calculations were conducted for the sense coil, and the prototyping cost of the custom-designed electronic board was calculated to assess its affordability for widespread laboratory use.

Main results: The system accurately measured a 1.867 mT peak, 100 kHz magnetic field, exhibiting a low measurement error of 1.52% for the magnetic flux density. The sense coil achieved a signal-to-noise ratio of 58.627 dB. The total material cost for producing a single prototype of the electronic board was approximately 19.59 USD, a globally relevant estimate for the core hardware of the low-budget magnetic field measurement system.

Conclusion: A low-cost radio frequency magnetic field detection system with integrated filtering for Magnetic Hyperthermia (30-300 kHz) was developed, combining a sense coil and an oscilloscope-compatible amplifier board. The prototype's low material cost (approximately 19.59 USD) provides an accessible solution for improved and refined measurements in preclinical research.

Acknowledgements: This project is funded by Boğaziçi University Research Fund Grant Number 19661.

References:

[1] Kafrouni L, Savadogo O. Recent Progress on Magnetic Nanoparticles for Magnetic Hyperthermia. Prog Biomater. 2016;5(3-4):147-160. doi:10.1007/s40204-016-0058-2.

[2] Rubia-Rodríguez I, Santana-Otero A, Spassov S, et al. Whither Magnetic Hyperthermia? A Tentative Roadmap. Materials (Basel). 2021;14(4):706. doi:10.3390/ma14040706

[3] Herrera-May AL, Aguilera-Cortés LA, García-Ramírez PJ, Manjarrez E. Resonant Magnetic Field Sensors Based on MEMS Technology. Sensors (Basel). 2009;9(10):7785-7813. doi:10.3390/s91007785

PP19

Advancing Sweat-Based Wearable Biosensors: Enzyme Stabilization and AI-Driven Correction for Long-Term Multi-Biomarker Monitoring

Abdelkader ZEBDA*, Chloé AYMARD, Pauline KIEFER

TIMC (Translational Innovation in Medicine and Complexity), UMR 5525 CNRS, UGA, INSERM,VetagroSup, Faculté de Médecine de Grenoble, Pavillon Taillefer, 38706 La Tronche*

Corresponding author: abdelkader.zebda@univ-grenoble-alpes.fr

Keywords: Biosensors, sweat, machine learning

Motivation and Aim: Continuous monitoring of physiological biomarkers is crucial for optimizing health, preventing disease, and enhancing athletic performance. Sweat-based wearable biosensors offer a promising, non-invasive alternative to traditional blood sampling. However, these devices face significant challenges, including enzymatic degradation, signal drift, and limited operational lifespan. The Olympic Health project addresses these limitations by integrating advanced enzyme stabilization strategies with AI-driven correction models, enabling multi-biomarker monitoring in sweat over extended periods.

Novelty: We developed electrochemical enzymatic biosensors for glucose, lactate, and uric acid using a dual immobilization method based on chitosan and glutaraldehyde. These sensors retained their activity for over four months under ambient conditions. We tested the biosensors with real samples and demonstrated their capacity to measure the concentrations of the three biomarkers. Comparing our results with gold standard methods, we found that our biosensors exhibited over 95% reliability.

Methods: To address sensor drift and improve long-term accuracy, we implemented Random Forest algorithms trained on impedance data. Using datasets generated from replicate biosensors, we performed two types of tests: i) Predictions on aging sensors to evaluate correction over time, ii) Predictions on new, unseen sensors to assess model robustness across manufacturing batches.

Main Results: Our models successfully reduced sensitivity drift from 200% to less than 25%, achieving over 85% prediction accuracy. These results highlight the effectiveness of our approach in maintaining the accuracy and reliability of sweat-based biosensors over extended periods.

Conclusion: These preliminary results demonstrate the potential of combining enzymatic biosensors with machine learning for reliable, long-term, non-invasive monitoring of sweat biomarkers in both medical and sports applications

References

[1] Tan S.Y., Sumner J., Wang Y., Yip A.W. (2024). A systematic review of the impacts of remote patient monitoring (RPM) interventions on safety, adherence, quality-of-life and cost-related outcomes. npj Digital Medicine, 7:192

[2] Baker L.B. et al. (2022). Sweat Biomarkers for Sports Science Applications. Sports Science Exchange, 35(226), 1–9.

[3] Chmayssem A., Shalayel I., Marinesco S., Zebda A. (2023). Investigation of GOx Stability in a Chitosan Matrix: Applications for Enzymatic Electrodes. Sensors, 23(1), 465.

PP20

Leveraging Pulse Wave Signal Properties for Coronary Artery Calcification Screening in CKD Patients

Urszula BIALONCZYK[1*], Leszek PSTRAS[1], Malgorzata DEBOWSKA[1], Lu DAI[2], Abdul Rashid QURESHI[3], Torkel B BRISMAR[4], Jonas RIPSWEDEN[4], Bengt LINDHOLM[3], Peter STENVINKEL[3], Jan POLESZCZUK[1]

[1] Nalecz Institute of Biocybernetics and Biomedical Engineering, Polish Academy of Sciences, Warsaw, Poland

[2] Aging Research Center, Department of Neurobiology, Care Sciences and Society, Karolinska Institutet and Stockholm University, Stockholm, Sweden

[3] Renal Medicine and Baxter Novum, Department of Clinical Science, Intervention and Technology, Karolinska Institutet, Stockholm, Sweden

[4] Unit of Radiology, Department of Clinical Sciences, Intervention and Technology, Karolinska Institutet

* ***Corresponding author***. *E-mail address*: ubialonczyk@ibib.waw.pl

Keywords: coronary artery calcium score, chronic kidney disease, pulse wave analysis

Motivation and Aim: Chronic kidney disease (CKD) patients are particularly susceptible to coronary atherosclerosis, which can be assessed using computed tomography (CT)-based coronary artery calcium (CAC) score [1]. However, such an expensive examination might not always be required or cost-effective. Therefore, a pre-screening tool is needed to help decide which patients should undergo a confirmatory CT scan.

Novelty: This study investigates a novel screening approach utilizing pulse wave analysis combined with machine learning models to identify CKD patients at high risk for coronary atherosclerosis.

Methods: We analyzed retrospective data from 124 CKD stage 5 patients who underwent kidney transplantation. Arterial pulse wave signals were collected by applanation tonometry using the SphygmoCor system (AtCor Medical, Sydney, Australia), and CAC scores were determined via CT scans. Machine learning models were developed using either pulse wave features or traditional risk factors (TRF) to detect high CAC scores (≥100 Agatston units) in four age groups.

Main results: The pulse wave-based model outperformed the TRF-based model in identifying high CAC scores, particularly among younger patients. Specifically, the pulse wave-based classifier showed superior balanced accuracy in all analyzed age groups and superior sensitivity in patients under 60 years old, especially in those under 50 years old (**Fig.1**). For all age groups combined, the overall balanced accuracy of the pulse wave-based model exceeded 80%, suggesting its potential as a reliable screening tool for detecting high risk of coronary atherosclerosis in CKD patients.

Conclusion: Pulse wave analysis combined with machine learning offers a promising, non-invasive method for preliminary CAC screening in CKD patients. This approach could enhance

early risk identification and improve clinical management, although further research is needed to validate and refine this method in larger, more diverse populations.

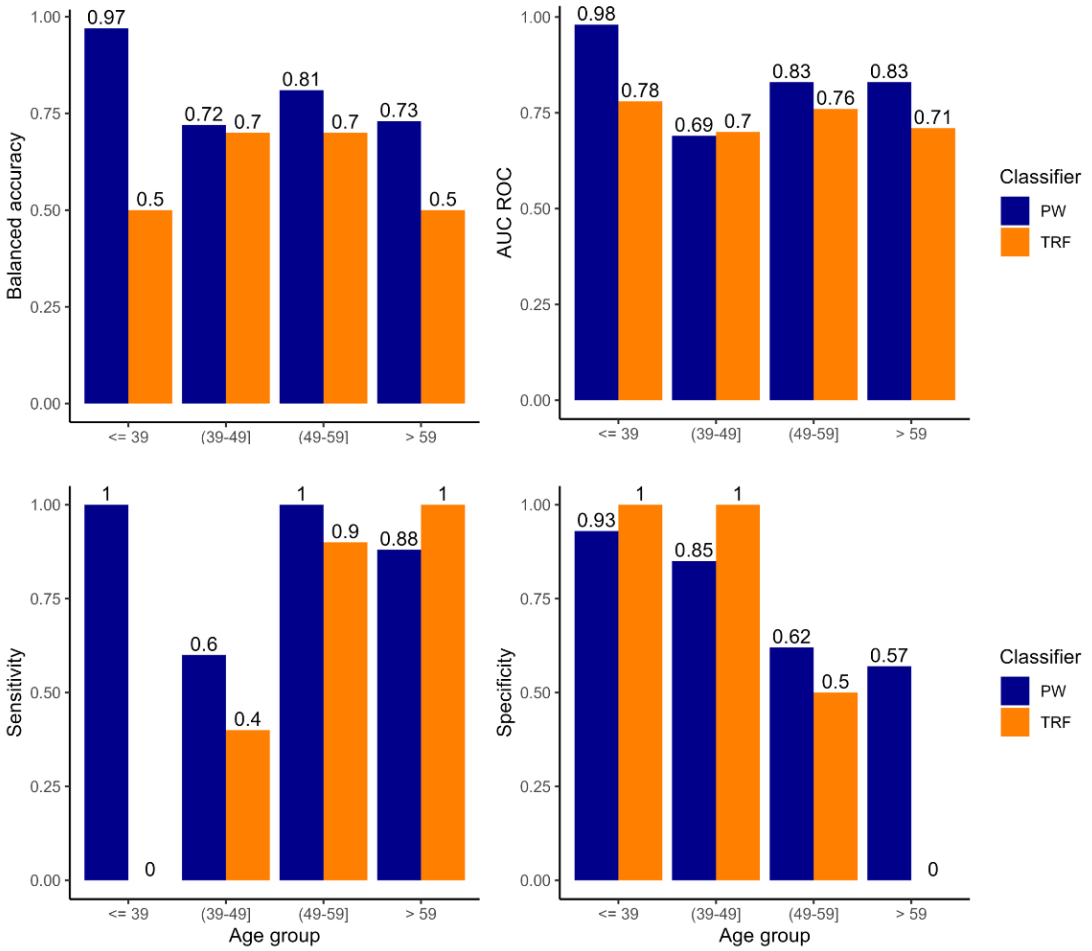

Fig. 1. Performance metrics of the two analyzed classifiers of coronary artery calcium scores across different age groups. AUC ROC – area under receiver operating characteristic curve; PW – pulse wave-based only classifier, TRF – classifier trained with traditional risk factors only.

Acknowledgements: This study was supported by the National Science Centre (Poland), grant No. 2018/31/D/ST7/03472.

References:

[1] Polonsky TS, McClelland RL, Jorgensen NW, Bild DE, Burke GL, Guerci AD, et al. Coronary artery calcium score and risk classification for coronary heart disease prediction. JAMA 2010;303. https://doi.org/10.1001/jama.2010.461

PP21

Attention U-Net for Retinal Blood Vessel Segmentation Using Various Color Space Models Channels

Patrycja KWIEK[1*], Małgorzata JAKUBOWSKA[1]

1 AGH University of Krakow, Faculty of Materials Science and Ceramics, Kraków, Poland

* ***Corresponding author***. *E-mail address*: pakwiek@agh.edu.pl

Keywords: image segmentation, attention U-net, color space models, retinal vessel segmentation

Motivation and Aim:

The length, width, tortuosity, branching patterns, and angles of retinal blood vessels are important in diagnosing, monitoring, and treating cardiovascular and ophthalmological diseases such as diabetes, hypertension, atherosclerosis, and vascular tumors.

Automatic vessel analysis facilitates screening of diabetic retinopathy and assessment of the relationship between vessel tortuosity and hypertensive retinopathy. It is also used to measure vessel diameters in diagnosing hypertension and supports laser surgery. Additionally, automatic generation of retinal maps and the identification of branching points enable image registration and creation of retinal mosaics. Moreover, the unique structure of the vessels makes them suitable as a biometric identification tool.

Novelty:

1. Using various color space models channels as an input for Attention U-Net for retinal blood vessel segmentation
2. Study of image illumination equalization on retinal blood vessel segmentation

Methods:

The study implemented the Attention U-Net, which demonstrated superior performance compared to the standard U-Net after initial testing. This architecture incorporates attention mechanisms, enabling it to focus on the most relevant areas of an image, making it particularly effective for medical image segmentation.

In this study, using Attention U-Net resulted in a higher Intersection over Union (IoU) value. The network consists of five encoder blocks with progressively increasing filters (32, 64, 128, 256, and 512) and five decoder blocks. Each convolutional block includes six layers: two convolutional layers, two batch normalization layers, and two activation layers, utilizing the ReLU activation function.

Additionally, various input conditions were examined to address illumination challenges in the images, with the original dataset being procured from the DRIVE Dataset [1]. For each input variation, the Attention U-Net was trained from scratch for 50 epochs.

Main results:

The results of the study showed that the segmentation accuracy depends on the channels used in a given color space. The best results were obtained for the image channels R (RGB) and U (YUV), and grayscale images, which achieved similar accuracy values. The maximum DICE coefficient for these three variants was about 0.91 (Tab. 1), which indicates their high efficiency in the segmentation process.

Tab. 1. DICE value for the test dataset of the designed Attention U-Net for retinal images represented in greyscale and channels R and U of the RGB and YUV color space models, respectively as an input

input	mean DICE	max DICE
greyscale	0.838	0.909
RGB: R	0.839	0.906
YUV: U	0.838	0.906

Conclusion:

This study highlights that there is no single best approach to retinal vessel segmentation. Numerous methods exist, each with its strengths and limitations. In this study, the impact of illumination equalization and the usage of various color space models were studied. In the end, the proposed method, presented above, achieves high-quality segmentation, benefiting various applications.

Funding:

Research project supported by the program „Excellence initiative – research university" for the AGH University of Krakow.

References:

[1] Staal JJ, Abramoff MD, Niemeijer M, Viergever MA, van Ginneken B. Ridge-based vessel segmentation in color images of the retina. IEEE Transactions on Medical Imaging. 2004;23(4):501-509.

[2] Sule OO. A Survey of Deep Learning for Retinal Blood Vessel Segmentation Methods: Taxonomy, Trends, Challenges and Future Directions. IEEE Access. 2022;10:38202-38236. doi:https://doi.org/10.1109/access.2022.3163247

PP22

Significance of stable feature selection in classifier performance assessment on high-dimensional genetic data

Tomasz ŁUKASZUK[1*], Jerzy KRAWCZUK[1]

1 Faculty of Computer Science, Bialystok University of Technology, Bialystok, Poland

* ***Corresponding author***. *E-mail address*: t.lukaszuk@pb.edu.pl

Keywords: Classification, Feature selection stability, Classifier evaluation

Motivation and Aim: With the rapid advancements in high-throughput technologies, gene expression data analysis has become a crucial tool in bioinformatics for identifying biomarkers and understanding gene regulation. Feature selection plays a key role in this process by reducing dimensionality while preserving meaningful biological information. However, while accuracy and the number of selected features are frequently reported in classifier evaluations, the stability of feature selection—reflecting its reproducibility and generalizability—is often overlooked. This study aims to address this gap by emphasizing the importance of feature selection stability in classifier evaluation.

Novelty: We introduces a novel methodology for generating dataset subsamples to assess stability, evaluates four classification models on high-dimensional gene expression datasets, and investigates the relationship between accuracy and feature selection stability. The ultimate goal is to propose a more comprehensive evaluation framework that integrates both stability and accuracy to enhance the reliability of gene expression-based classification models.

Methods: This study employs machine learning classifiers with embedded feature selection to analyze high-dimensional genetic data. We focuses on models that inherently perform feature selection, as they efficiently handle the challenge of high-dimensional gene expression data. The chosen models include classifiers using L1 regularization (Logistic Regression, Support Vector Machine, and Convex and Piecewise Linear (CPL) criterion function) and decision tree-based methods (Random Forest).

The feature selection stability is assessed to ensure the reproducibility of selected features across different training data samples. Two primary stability metrics are used: Lustgarten's measure and Nogueira's stability measure.

A novel cross-validation method, trains-p-diff, is introduced to systematically control dataset variability. This procedure ensures that each training set differs from others by precisely p objects, enabling controlled experiments on feature selection stability. It allows precise analysis of how small variations in training data impact stability and classification performance.

Main results: The study was conducted on four gene expression datasets (Breast, Prostate, Renal, Throat) from the CuMiDa database, characterized by a high number of features and two decision classes. The experiments used the trains-p-diff procedure, where classifiers were trained for different values of p (the number of differing objects between training sets), and key

metrics such as accuracy, feature selection stability, and the number of selected features were measured.

The harmonic mean of feature selection stability and test accuracy was introduced as a single measure of classifier quality. Since accuracy remained relatively consistent across classifiers, the results mainly reflect feature selection stability: LR > SVM > CPL > RF.

Conclusion: This study analyzed four classifiers with built-in feature selection—three using L1 regularization and one based on decision trees—across four high-dimensional gene expression datasets. Using the novel trains-p-diff cross-validation method, which ensures training sets differ by exactly p items, we evaluated feature selection stability under varying levels of data disturbance. Our key findings include: a) classification accuracy remained mostly unaffected by data disturbances, b) even minor dataset changes can significantly impact selected features.

Feature selection stability is essential in gene expression data analysis, aiding robust gene subset identification and improving classification model reliability.

\

PP23

Application of Artificial Intelligence in Psychiatric Neuroimaging: A Systematic Review

Ilona Karpiel[1] Ewelina Sobotnicka[1] and Ana Starcevic[2]

1 Łukasiewicz Research Network— Krakow Institute of Technology, ul. Zakopiańska 73, 30-418, Krakow, Poland

2 Laboratory for Multimodal Neuroimaging, Institute of Anatomy, Medical Faculty, University of Belgrade, 11000 Belgrade, Serbia

Ilona.karpiel@kit.lukasiewicz.gov.pl

Abstract. With the growing application of artificial intelligence (AI) in mental health research, there is an increasing need to evaluate its clinical utility in diagnosing, predicting, and treating psychiatric disorders. This systematic review examines the role of AI methods in individuals undergoing neuroimaging assessments (fMRI, MRI, EEG). A comprehensive literature search was conducted in the PubMed Medline database and Cochrane Library, following PRISMA 2020 guidelines. The final analysis included 20 studies published between January 2020 and January 2025. The findings indicate that deep learning models, particularly convolutional neural networks (CNNs), demonstrate higher accuracy in classifying psychiatric conditions such as autism spectrum disorder (ASD) and schizophrenia com- pared to traditional machine learning approaches. Moreover, AI is increasingly being explored for predicting treatment response, particularly in depression and bipolar disorder, by integrating neuroimaging with behavioral and physiological data. Despite promising results, data heterogeneity, lack of standardized validation protocols, and ethical concerns remain significant challenges for clinical implementation. This review highlights the strengths and limitations of AI applications in psychiatric neuroimaging and underscores the need for standardized methodologies, larger datasets, and ethical guidelines to ensure the reliability and clinical applicability of AI-driven diagnostic tools. These findings provide a foundation for future research aimed at optimizing AI integration into psychiatric practice.

Keywords: brain, AI, Machine learning, central nervous system disorders, clinical trials

PP24

The method of artificial membranes profile image construction for AI-based porosity evaluation tool

Jakub ŻAK[1*], Antonina PATER[1]*, Monika WASYŁECZKO[1], Natalia NAJUCH[2], Andrzej CHWOJNOWSKI[1], Anna KORZYŃSKA[1]

[1]Nałęcz Institute of Biocybernetics and Biomedical Engineering Polish Academy of Sciences, Warsaw, Poland

[2]Warsaw University of Technology, Warsaw, Poland

*_**Corresponding author**_. *E-mail address*: jzak@ibib.waw.pl or apater@ibib.waw.pl

Keywords: Semi-permeable membranes, Depth estimation, Synthetic data

Motivation and Aim: The performance and efficiency of semi-permeable membranes are critically dependent on their pore structure, which directly influences their ability to filter materials at the molecular level [1]. Traditional methods, such as measuring the mass removed during flushing, provide limited insights into the membrane's internal structure and do not adequately capture the complexity of pore depth and distribution. The gold standard for understanding these structures should be a form of 3D scanning (atomic force microscopy, interferometry), however this method is prohibitively expensive and time-consuming [2], particularly when repeated measurements are required. Additionally, manual analysis of cross-sections of membranes is both tedious and prone to errors [2]. Therefore, there is a clear need for an automated, high-throughput method to quantify pore structures. This research aims to address these challenges by exploring the usage of images synthesized according to the need.

Novelty: While depth estimation models have been successfully applied in various domains [3] including autonomous vehicle technology, their application to the study of semi-permeable membranes is [4] unprecedented. More specifically, the use of simulated data to replicate the intricate structures of membrane pores has not been explored previously in this context. This innovative approach could help bridge the gap between expensive 3D scanning methods and the need for extensive pore structure analysis.

Methods: To investigate the feasibility of this approach, we utilize a well-established 3D depth estimation model based on Keras tutorial. Model is commonly used as a base for depth estimation in large-scale images datasets such as: DIODE, Cityscapes. The model was chosen due to its relatively low complexity of architecture, so it can be studied deeply. These datasets, originally designed for autonomous vehicle applications, contain vast amounts of image data with ground truth depth maps, making them ideal for training depth estimation models. In this study, however, the model is tested on artificial images, which are synthesized to simulate pore-like structures. The synthetic data consists of ellipses with varying depths along the Z-axis, created using meshgrid equations and mathematical models for ellipse rotation. The complexity of the pore shapes is increased step-by-step to evaluate how different 3D depth estimation models handle this increasing complexity. By comparing the performance of that model on increasingly sophisticated synthetic datasets, we gain insights into their ability to generalize to real-world, microscopic data.

Main Results: Initial experiments with synthetic data have yielded promising results, showcasing the ability of 3D depth estimation models to capture the varying depths of pore-like structures.

Table 1. Average ± Standard Deviation of Mean Square Error (MSE) of Depth Estimation vs Actual Depth : Test results on 1000 test samples, similar to the training synthetic dataset.

Synthetic / Dataset	DIODE	+CityScapes	+Synthetic
One object in center	0.883 ± 0.019	0.758 ± 0.015	0.0009 ± 0.0003
Two object randomly placed	0.821 ± 0.039	0.720 ± 0.037	0.0013 ± 0.0006

As expected, the model trained on synthetic data with one object fared worse on two-object synthetic data. Compared to training on other datasets only, however, the model achieves very high performance in estimating the depth data. Interestingly, models trained on DIODE and +Cityscapes achieve better depth estimation on two-object synthetic data, suggesting that the more objects in the image, the better. As expected, model finetuned on CityScapes after training on DIODE reached lower MSE than model trained on DIODE only. However, the artificial data, while effective in testing model capabilities, does not fully replicate the challenges of working with real microscopic images, such as noise, irregularities in pore shape, and variations in membrane texture. The complexity of synthesized image content could be gradually increased to bridge the synthetic-to-real data gap as much as possible, but there may always be an unbridgeable gap left. However, decreasing the size of this gap should allow building a more comprehensive tool for depth estimation of porous membranes in the future.

Conclusion: The current study suggests that artificial data, in combination with robust 3D depth estimation models, can provide a useful foundation for automating the analysis of membrane pore structures. While synthetic datasets are not a perfect match for real-world microscopic images, they offer a viable starting point for model development and evaluation. Furthermore, the findings suggest that the transfer of learning from large-scale 3D depth datasets, such as DIODE and Cityscapes, could provide a pathway for further enhancement of these models. This work opens the door to the possibility of automating pore depth analysis, which could significantly reduce the time and cost associated with membrane porosity evaluation in both research and industrial applications.

References

[1] M. P. Nikolova and M. S. Chavali, "Recent advances in biomaterials for 3D scaffolds: A review," *Bioactive Materials*, vol. 4, p. 271–292, December 2019.

[2] H. Chamani, A. Rabbani, K. P. Russell, A. L. Zydney, E. D. Gomez, J. Hattrick-Simpers and J. R. Werber, "Data-science-based reconstruction of 3-D membrane pore structure using a single 2-D micrograph," *Journal of Membrane Science,* vol. 678, p. 121673, July 2023.

[3] S. K. Nayar and Y. Nakagawa, "Shape from focus," *IEEE Transactions on Pattern Analysis and Machine Intelligence,* vol. 16, p. 824–831, 1994.

[4] T. Houben, T. Huisman, M. Pisarenco, F. van der Sommen and P. H. N. de With, "Depth estimation from a single SEM image using pixel-wise fine-tuning with multimodal data," *Machine Vision and Applications,* vol. 33, July 2022.

PP25

Explainable estimation of blood volume pulse signals from video sequences using a combination of deep learning models and signal processing methods

Milena SOBOTKA, Kamil KOPRYK, Muhammad USMAN, Jacek RUMIŃSKI

Gdansk University of Technology, FETI, Department of Biomedical Engineering, Gdansk, 80-233, Poland

milena.sobotka@pg.edu.pl,

Abstract. This study evaluates the application of Gradient-weighted Class Activation Mapping (Grad-CAM) to identify key image regions for enhancing pulse wave estimation using traditional signal analysis methods. The approach assumes that Grad-CAM masking enables the selection of relevant image areas, improving the Signal to Noise Ratio (SNR). Experiments were conducted on the PURE dataset using the TS-CAN model and rPPG-Toolbox. Grad-CAM maps identified facial regions most influential for model prediction, allowing the exclusion of areas not contributing to accurate estimation. The study also explored different temporal window sizes and their impact on signal quality. Method evaluation included SNRraw , SNRmax, SNRsum, and Hjorth descriptors. Results confirmed that Grad-CAM masking enhances rPPG signal quality, enabling more precise heart rate estimation. Statistical analysis validated the significance of the findings, highlighting the potential of interpretable deep learning methods in signal analysis.

Keywords: blood volume pulse, remote photoplethysmography, signal processing, explainable AI

Rapid Fire Poster Presentations RF2
Medical Image Processing, Biomedical Signal Processing, Artificial Organs, Modeling Physiological Systems, Biomeasurements
Chairs: Aleksandrs Sisojevs (Latvia), Krzysztof Zieliński (Poland)
PP26–PP49

PP26

Deep Learning-Based Wound Segmentation Using a U-Net Architecture

Martinus BOOM

University of Coimbra, Department of Informatics Engineering, Coimbra, Portugal.

uc2024154464@student.uc.pt

Abstract

Inspired by the IFMBE Scientific Challenge Competition at NBC 2025, this work presents a deep learning approach for semantic wound segmentation employing a U-Net architecture. The approach focuses on segmenting three components within wound images: wound area, background, and scale marker. Preprocessing included grayscale conversion, resizing, and data augmentation on a dataset consisting of 371 training images and 80 validation images, each with associated 512×512 pixel masks. On the validation set, the model gets a weighted F1 score of 0.8327 using an encoder-decoder structure with skip connections. Post-processing Lanczos interpolation guarantees that output masks satisfy the criteria of the challenge. The best model achieved a test set F1 score of 0.7924, as reported by the challenge organizers.

Keywords: Wound Segmentation, U-Net, Deep Learning, Medical Imaging, Data Augmentation, Image Resizing

PP27

Unified Wound Detection and Segmentation Using YOLO: An Efficient Approach for Accurate Wound Measurement

Mahdi BAZARGANI[1], Mohammad JAVAD HEIDARI[1], Mehrdad ANVARI-FARD[1], Hamid SOLTANIAN-ZADEH[1,2]

1 School of Electrical and Computer Engineering, College of Engineering, University of Tehran, Tehran, Iran

2 School of Cognitive Sciences, Institute for Research in Fundamental Sciences (IPM), Tehran, Iran

mahdi.bazargani@ut.ac.ir, mj.heidary@ut.ac.ir,

mehrdad.anvari@ut.ac.ir, and hszadeh@ut.ac.ir

Abstract. Chronic wounds pose significant clinical and economic challenges globally, requiring accurate assessment for effective management. Traditional wound measurement methods suffer from subjectivity and inefficiency, while existing AI solutions often lack integration of scale markers crucial for size estimation. This study presents an automated wound segmentation system using YOLOv11 Nano, a unified architecture combining detection and segmentation with integrated scale marker analysis. Leveraging transfer learning on 2760 external images and fine-tuning with the IFMBE Challenge dataset (451 annotated images), our model achieved performance with a wound Dice score of 0.8728 and marker Dice score of 0.9475. The lightweight design demonstrated real time inference at 100 FPS (10 ms/image) on an NVIDIA RTX 3090 GPU – 15× faster than U-Net architectures. By unifying detection and segmentation in a single efficient framework, this approach enables clinical grade wound measurements critical for personal device users seeking precise, efficient solutions that bridge gaps in automated assessment systems

Keywords: Wound segmentation, IFMBE Challenge, YOLOv11 Nano, medical image analysis, real-time AI, diabetic foot ulcers

PP28

Optimizing the Hemodynamic Response Function in EEG-fMRI Analysis of Focal Epilepsy: A Single-Case Report

Nikodem HRYNIEWICZ[1*], Rafał ROLA[2], Ewa PIĄTKOWSKA - JANKO[1], Danuta RYGLEWICZ[2], Piotr BOGORODZKI[1],

1 Nałęcz Institute of Biocybernetics and Biomedical Engineering, Polish Academy of Sciences, Warsaw, Poland

2 Military Institute of Aviation Medicine, Warsaw, Poland

* ***Corresponding author***. *E-mail address*: nhryniewicz@ibib.waw.pl

Keywords: EEG-fMRI, Focal epilepsy, Hemodynamic Response Function, Epileptogenic zone

Motivation and Aim: EEG-fMRI method enables determination of potential epileptogenic zones by analyzing fMRI data based on interictal epileptiform discharges (IEDs) detected from the simultaneously recorded EEG signal [1]. Focal epilepsy often presents challenges in precisely localizing the epileptogenic zone, especially when using EEG-fMRI due to variability in hemodynamic response function (HRF) used in the analysis and the need for precise IEDs timing determination from the EEG signal. This study aims to demonstrate how HRF optimization, performed with a novel application, can impact source localization in a single patient with focal epilepsy, leading to clinically relevant changes in interpretation of the EEG-fMRI analysis results.

Novelty: This study utilizes a dedicated EEG-fMRI analysis application HOT (HRF Optimization Toolbox [2]), which allows for the optimization of HRF based on interictal epileptic discharges. In the presented case, the optimization of HRF in the analysis significantly changed the location of the epileptic focus, emphasizing the importance of individual HRF modeling in epilepsy diagnosis, especially considering the fact that the EEG-fMRI method can be used for preoperative planning in patients with epilepsy [3].

Methods: A patient (female, 39 YO, drug-resistant temporal epilepsy with complex partial seizures; hippocampal sclerosis) underwent 3 sessions of simultaneous EEG-fMRI acquisition (64-channel EEG Neuroscan SynampsRT, fMRI: GE Discovery MR750w, TR = 2.5 s, TE = 25 ms, voxel size 3 mm x 3 mm x 3 mm). fMRI data were preprocessed using SPM12, and EEG data were analyzed in CURRY7. An experienced neurologist manually detected interictal epileptiform discharges (IEDs) in EEG signal. The analysis of fMRI data based on 17 IEDs was performed with a general linear model (GLM) in SPM12 using the canonical HRF to create the regressor. HRF optimization was performed using the HOT application. Then, SPM reanalysis was performed using the optimized canonical HRF parameters in the GLM.

Main results: Before HRF optimization, EEG-fMRI analysis indicated a focus in an anatomically questionable location (right part of lingual gyrus). After optimization, the new location (right precentral gyrus – Figure 1) matched well with the neurologist's observations based on the patient's other modalities and semiology, suggesting that standard HRF assumptions may have contributed to the initial mislocalization. While the HOT toolbox has

been applied in a larger cohort, generally resulting in increased statistical power or broader activation patterns, the case presented here is distinctive in that HRF optimization led to a fundamental shift in the location of the identified epileptogenic zone. Thus, this single-case report was selected to illustrate a qualitatively different and clinically significant impact of the optimization process, emphasizing the potential benefit of patient-specific HRF modeling in select cases.

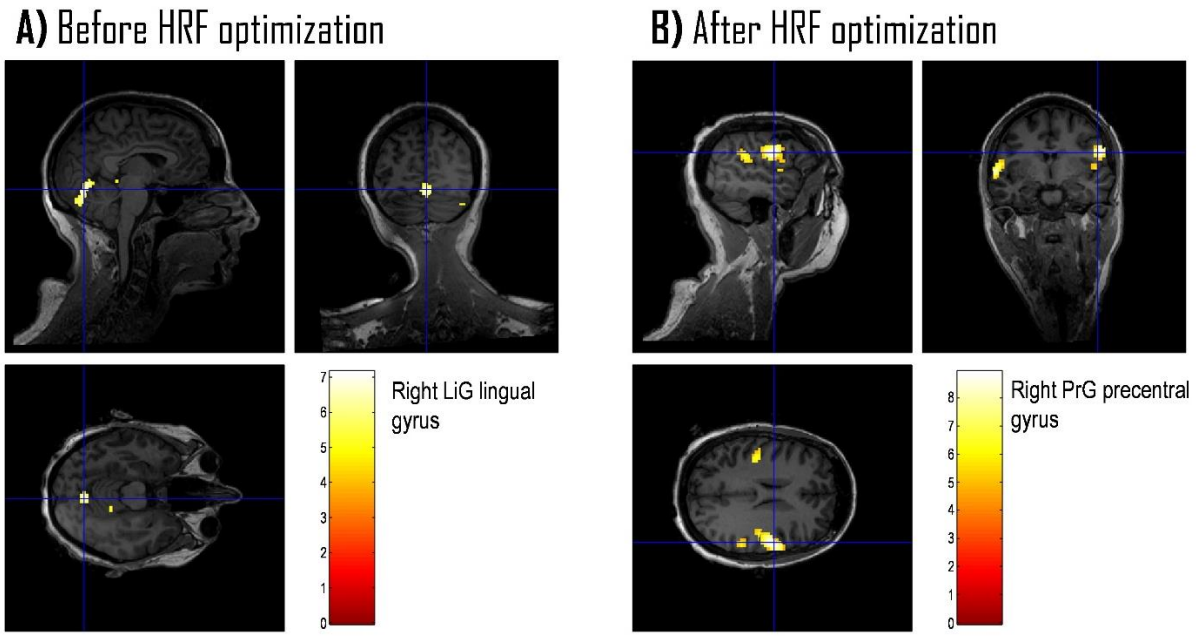

Conclusion: This case highlights the critical role of HRF optimization in EEG-fMRI for epilepsy diagnostics. The findings suggest that patient-specific HRF modeling can improve the accuracy of epileptogenic focus localization, potentially impacting clinical decision-making and treatment planning. Further research is ongoing, with the HOT toolbox being applied in a larger patient cohort to systematically assess its clinical utility and broader applicability in epilepsy diagnostics.

Acknowledgements: The study protocol was approved by an institutional ethics committee, and informed consent was obtained from the participant.

References:

[1] Ritter P, Villringer A. Simultaneous EEG-fMRI. Neurosci Biobehav Rev. 2006;30(6):823-838. doi:10.1016/j.neubiorev.2006.06.008

[2] Hryniewicz N. Studium hemodynamicznych modeli sygnału BOLD indukowanego padaczkowymi wyładowaniami międzynapadowymi. 2024, Rozprawa doktorska (PhD Thesis). https://www.ibib.waw.pl/images/ibib/grupy/Doktorat_2024_N_Hryniewicz.pdf

[3] Kowalczyk MA, Omidvarnia A, Abbott DF, Tailby C, Vaughan DN, Jackson GD. Clinical benefit of presurgical EEG-fMRI in difficult-to-localize focal epilepsy: A single-institution retrospective review. Epilepsia. 2020;61(1):49-60. doi:10.1111/epi.16399

PP29

Analyzing fractal measures in MRI: The role of Fractal Scale Variability Index and image filtering

Ewelina BEBAS[1*], Marta BOROWSKA[1,] Jolanta PAUK[1]

1 Bialystok University of Technology, Bialystok, Poland

* ***Corresponding author***. *E-mail address*: j.pauk@pb.edu.pl

Keywords: MRI filtering, fractal scale variability index, lung cancer.

Motivation and Aim: Fractal theory is a branch of mathematics focused on fractals - complex geometric structures characterized by self-similarity at different magnification scales. Fractals are widely used in science and technology, including physics, biology, geology, and computer graphics [1]. They effectively model irregular natural structures such as coastlines, clouds, mountain ranges, vegetation, and blood vessel systems. In recent years, fractal analysis has gained recognition in medical imaging, offering new possibilities for studying and interpreting complex biological structures [2]. This study aimed to analyze fractal measures in MRI images, focusing on the role of the newly proposed Fractal Scale Variability Index (FSVI) in the context of image filtering techniques. The evaluation was specifically targeted at differentiating between two types of non-small cell lung cancer (NSCLC) - adenocarcinoma (ADC) and squamous cell carcinoma (SCC).

Novelty: The innovative aspect of this study lies in the introduction of the Fractal Scale Variability Index as a new parameter for analyzing the variability of fractal structures at different scales in MRI images. Unlike traditional fractal measures such as the fractal dimension (FD) and lacunarity, which focus on characterizing the complexity and homogeneity of structures, FSVI offers insights into scale-dependent variations in the fractal properties of the image. This allows for a more nuanced understanding of the structural changes that occur at different scales within the tumor tissues, enhancing the analysis of complex biological structures in medical imaging.

Methods: The study involved experimental research using MRI data from 45 patients diagnosed with adenocarcinoma (ADC) and squamous cell carcinoma (SCC), meeting inclusion and exclusion criteria related to age, diagnosis, and scan feasibility. To assess structural complexity and texture, three fractal measures were employed: Fractal Dimension (FD), Lacunarity, and the newly proposed Fractal Scale Variability Index. The FSVI parameter was designed to quantify how the local distribution of fractal complexity varies across multiple spatial scales. It is defined as follows:

$$FSVI = \frac{s\sum(i \cdot H_i) - \sum i \sum H_i}{s\sum i^2 - (\sum i)^2}, \quad (1)$$

where: s is the number of scales (grid sizes) used in the box-counting method, i represents the scale index (i=1,2,...s), Hi is the estimated fractal entropy at scale i.

The FSVI captures the linear trend of entropy variability across scales, complementing the traditional multiscale fractal dimension by emphasizing changes in scale-dependent complexity rather than focusing solely on absolute fractal dimensions [3,4]. The number of scales used in

the analysis was empirically determined and set to five. Although the multiscale fractal dimension method is widely recognized, FSVI offers a distinct approach by highlighting entropy fluctuations across scales. This may improve the sensitivity of differentiating carcinoma types, particularly when combined with various image filtering techniques.

To evaluate the effect of preprocessing on fractal measures, each MRI image was processed using four filters: Normalization, Averaging, Laplacian Sharpening, and Gaussian Noise Addition. The impact of each filter on FD, Lacunarity, and FSVI was analyzed to determine their role in enhancing discrimination between ADC and SCC.

Main results: The results indicate that Fractal Dimension and lacunarity show significant differences between ADC and SCC under most filtering conditions, with SCC demonstrating higher complexity (FD) and lower homogeneity (lacunarity) compared to ADC. However, the Fractal Scale Variability Index remained relatively stable across the different filtering conditions, suggesting that scale-dependent variability does not significantly differentiate between ADC and SCC. This stability implies that FSVI may not be a reliable marker for distinguishing between these tumor types. Nonetheless, it may have potential applications in assessing structural variability in other areas of medical imaging.

Conclusion: Although FSVI does not differentiate between ADC and SCC, it offers a novel perspective on fractal variability across scales. Future research should investigate its potential applications in other areas of medical imaging where scale-dependent fractal changes may be significant. Additionally, the study underscores the impact of image filtering on fractal parameters, highlighting the importance of standardized processing techniques in fractal-based medical image analysis.

Acknowledgments: This work was supported by a grant from Bialystok University of Technology (grant No. WZ/WM-IIB/2/2024).

References:

[1] Chen, S.S., Keller J.M., Crownover R.M. On the calculation of fractal features from images, IEEE Transactions on Pattern Analysis and Machine Intelligence, 1993, 15, 10: 1087-1090.

[2] Borowska, M., Bebas E., Hladunski M., et al. Fractal dimension analysis of PET-MRI liver images for various ROI's sizes, Polish Conference on Biocybernetics and Biomedical Engineering, Springer, 2019.

[3] Ting J.Y.C, Wood A.T.A, Barnard A.S. Sphractal: Estimating the fractal dimension of surfaces computed from precise atomic coordinates via Box-Counting algorithm, Adv. Theory Simul, 7, 6, 2024. doi:10.1002/adts.202470013.

[4] Santos I.G., Faria F.R., et al. Fractal dimension, lacunarity, and cortical thickness in the mandible: Analyzing differences between healthy men and women with cone-beam computed tomography, Imaging Sci Dent 2023, 53: 153-159. doi: 10.5624/isd.20230042.

PP30

Assessing Blood-Brain Barrier impairments in non-enhancing multiple sclerosis lesions with perfusion MRI

Nikodem HRYNIEWICZ[1*], Piotr BOGORODZKI[1], Stefan GAŹDZIŃSKI[2], Ewa PIĄTKOWSKA-JANKO[1], Kamil LIPIŃSKI[1], Anna KARLIŃSKA[2], Paweł GRIEB[3], Mikołaj PAWLAK[4], Rafał ROLA[2], Danuta RYGLEWICZ[2], Iwona KURKOWSKA-JASTRZĘBSKA[5];

1 Nałęcz Institute of Biocybernetics and Biomedical Engineering, Polish Academy of Sciences, Warsaw, Poland
2 Military Institute of Aviation Medicine, Warsaw, Poland
3 Mossakowski Medical Research Centre, Polish Academy of Sciences, Warsaw, Poland
4 Poznan University of Medical Sciences, Poznań, Poland
5 Institute of Psychiatry and Neurology, Warsaw, Poland

* ***Corresponding author***. *E-mail address*: nhryniewicz@ibib.waw.pl

Keywords: Multiple sclerosis, Dynamic susceptibility contrast, Blood-brain barrier, Leakage

Motivation and Aim: The enhancement of T1-weighted (T1w) MRI images acquired after contrast administration in patients with multiple sclerosis (MS) is a well-established indicator of active inflammation and blood-brain barrier (BBB) disruption. However, the evaluation of possible inflammation in the lesions that do not enhance remains a challenge. Determination of the K2 parameter, characterizing the leakage effect in dynamic susceptibility contrast (DSC) curves, may serve as an additional marker to describe MS lesions. This study aims to assess the utility of the K2 parameter in detecting BBB impairments in non-enhancing MS lesions, providing insight into their inflammatory activity.

Novelty: This study introduces the use of the K2 parameter from DSC MRI as a potential biomarker for BBB disruption in non-enhancing MS lesions. Unlike conventional T1w contrast-enhanced imaging, which identifies only active inflammation, the K2 parameter may reveal subtle BBB permeability changes resulting from the extravasation of contrast agent, which shortens the T2* relaxation time and alters the signal curve in DSC MRI. This approach could improve the sensitivity of MS lesion characterization and offer a more comprehensive understanding of disease pathology.

Methods: Data were acquired using a 3T scanner with a DSC T2* sequence (3x3x4mm, TR = 1500ms, TE = 16.5ms). The K2 parameter was determined based on the relaxivity-time curves $\Delta R2*(t)$ derived from DSC data in lesions, according to the formula [1,2]:

$$\Delta R2^*(t) = K1 \cdot \overline{\Delta R}2^*(t) + K2 \cdot \int_0^t \overline{\Delta R}2^*(t')\,\mathrm{dt}'$$

where: $\Delta R2^*(t)-$ relaxivity-time curve, $K1$ – term reflecting uncontaminated perfusion, $\overline{\Delta R}2^*(t)$ – average signal from non-enhancing voxels, $K2$ – term reflecting leakage effect.

To validate the accuracy of the K2 parameter, measurements were taken from two imaging sessions 1.5 years apart in a MS patient (Patient A) with a low-grade tumor enhancing on T1w,

where a high K2 value was expected [3]. Additionally, K2 values were calculated for lesions in 36 datasets of patients without radiological evidence of T1w enhancements. All lesion ROIs were selected based on automatic segmentation using VolBrain. Other processing was carried out using in-house MATLAB scripts, based on SPM12, and included steps such as realignment, to ensure accurate spatial registration of the images..

Main results: For Patient A, the K2 values for the enhancing (tumor) area were 0.05 and 0.07, respectively—significantly higher than the mean K2 values of the MS lesions. A high K2 is characterized by the concentration curve not returning to baseline, indicating persistent leakage. Among the 36 patients without T1w enhancement, seven of them exhibited lesions with high K2 values (0.025 and higher), where the threshold was determined as the 95th percentile of the aggregated K2 distribution. Three of them (Patients B, C, and D), as presented in Figure 1, had lesions with K2 values of 0.032, 0.038, and 0.031, respectively, which may suggest subclinical inflammatory activity or blood-brain barrier (BBB) disruption. Notably, no correlation was found between the calculated K2 values and the signal intensity difference between T1-weighted post-contrast and pre-contrast images (T1+c − T1), indicating that K2 may capture BBB impairment beyond conventional imaging markers. No follow-up data were available for the seven patients with high K2 values, and further longitudinal monitoring is required to assess the clinical significance of these findings.

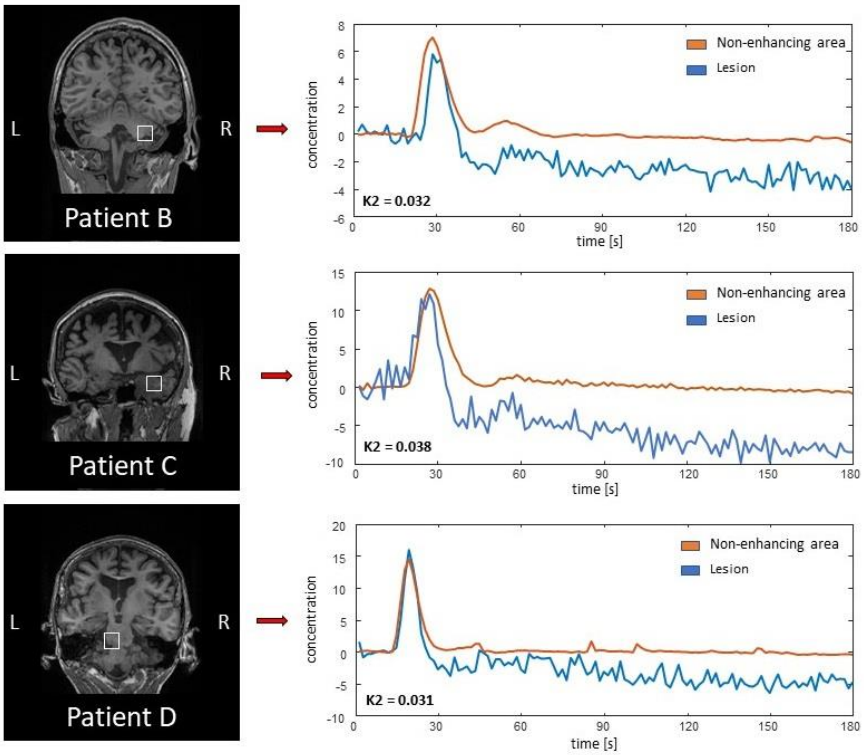

Conclusion: The elevated K2 values observed in the enhancing lesion of Patient A validate the utility of this parameter for detecting BBB impairments. Moreover, the high K2 values in non-enhancing lesions of seven other patients indicate that this method may uncover subclinical inflammation or BBB disruption not evident on standard T1w imaging. These findings suggest the potential of K2 as a complementary marker for more sensitive MS lesion assessment.

Acknowledgements: This study was supported by the Medical Research Agency of Poland, grant 2021/ABM/02/00002 – 00. The study protocol was approved by an institutional ethics committee, and informed consent was obtained from all participants. .

References:

[1] Boxerman JL, Schmainda KM, Weisskoff RM. Relative cerebral blood volume maps corrected for contrast agent extravasation significantly correlate with glioma tumor grade, whereas uncorrected maps do not. AJNR Am J Neuroradiol. 2006;27(4):859-867.

[2] Peruzzo D., Castellaro M., Dynamic Susceptibility Contrast (DSC) MRI toolbox (github.com/FAIR-Unipd/dsc-mri-toolbox).

[3] Withey SB, MacPherson L, Oates A, et al. Dynamic susceptibility-contrast magnetic resonance imaging with contrast agent leakage correction aids in predicting grade in pediatric brain tumours: a multicenter study. Pediatr Radiol. 2022;52(6):1134-1149. doi:10.1007/s00247-021-05266-7

PP31

Influence of the 3D printing infill, pattern and CT kV on the Hounsfield Units for biomedical applications

Nikolay DUKOV[1], Kristina BLIZNAKOVA[1], Yanka BANEVA[1,2], Zhivko BLIZNAKOV[1]

1 Medical University of Varna, Varna, Bulgaria

{ntdukov, kristina.bliznakova, yanka.baneva, zhivko.bliznakov}@mu-varna.bg

2 St. Marina University Hospital, Varna, Bulgaria

Abstract. Polylactic Acid (PLA) is a biodegradable thermoplastic polymer, commonly used with low-cost fused filament fabrication (FFF) 3D printers. Amongst the many biomedical applications of PLA, is the use in the Radiology field, where it is exploited for preparing physical phantoms. The aim of this study is to investigate the influence of 3D printing patterns on the Hounsfield Units (HU) of Computed Tomography (CT) scanned samples. For this study, we fabricated samples with two different infill patterns—cubic subdivision and quarter cubic—across a range of infill densities (10% to 100%). The samples were scanned at a CT facility using three different kV settings. Regions of interest (ROIs) were selected from the CT images of the scanned samples, and the corresponding HU were measured. The results demonstrated that both infill pat- tern and density significantly influence the HU values. Both patterns were found to be suited for representing lung tissue, while the Quarter Cubic pattern was appropriate for replicating the radiological properties of adipose tissue, as well. The kV settings had a slight effect on the HU measurements. These findings will be applied to the development of anthropomorphic phantoms for radiological applications.

Keywords: 3D printing, PLA, printing pattern and infill, Hounsfield units, physical phantoms

PP32

Morphological analysis of total hemoglobin concentration pulse waveform and its relationship with age

Marta HENDLER[1*], Arkadiusz ZIÓŁKOWSKI[1], Tomasz SOZAŃSKI[2], Magdalena KASPROWICZ[1]

[1] Department of Biomedical Engineering, Faculty of Fundamental Problems of Technology, Wroclaw University of Science and Technology, Wrocław, Poland

[2] Department of Preclinical Sciences, Pharmacology and Medical Diagnostics, Faculty of Medicine, Wroclaw University of Science and Technology, Wrocław, Poland

* ***Corresponding author***. *E-mail address*: marta.hendler@pwr.edu.pl

Keywords: functional near-infrared spectroscopy, hemoglobin concentration, morphological analysis, fNIRS-derived pulsatile signals

Motivation and Aim: With aging, the cerebrovascular system undergoes significant structural and functional changes that can impair the regulation of cerebral blood flow. These vascular alterations influence the morphology of cerebral blood flow oscillations in both macro- and microcirculation [1]. Functional near-infrared spectroscopy (fNIRS) is a noninvasive, portable, and user-friendly technique that enables real-time monitoring of pulsatile changes in blood oxygenation and volume within the cerebral cortex.

This study aims to investigate age-related changes in the morphology of total hemoglobin concentration (tHb) pulse waveforms in a healthy population. Additionally, sex-related differences in tHb pulse morphology were also studied.

Novelty: The morphological characteristics of fNIRS-derived pulse signals remain largely unexplored. This study is one of the first attempts to investigate the changes in the shape of tHb pulse waveform with aging.

Methods: The study was approved by the bioethical committee of the Lower Silesian Chamber of Physicians (approval number 03/PNDR/2024). Continuous records of high-resolution (81.4 Hz) changes in oxygenated and deoxygenated hemoglobin concentration (HbO, HbR) in a resting state were collected from 57 healthy volunteers in different age (range: 19-66, median: 28, IQR: 22-47 [years], males: 26) using continuous wave fNIRS device (NIRSport2, NIRx Medizintechnik GmbH, Berlin, Germany) configured with eight active channels in the frontal lobe area. Two representative, symmetrically-located channels from the forehead area were selected for the analysis based on the signal quality criterion. Total hemoglobin concentration (tHb) was calculated as a sample-to-sample sum of HbO and HbR. The tHb signal was automatically cut into single pulse waveforms using modified Scholkmann algorithm [2]. Median number of obtained pulse waveforms per subject was 398 (IQR: 317-461). Pulse waveforms were analyzed separately: each was detrended, linearly interpolated in X axis to a length of 200 samples, and normalized along the Y axis. A similarity of the tHb pulse to the triangle was measured using five indices presented in Fig. 1 [3]. Non-parametric tests were applied due to the rejection of the normality hypothesis for most of the analyzed indices based on the Shapiro-Wilk test. The differences in median values of analyzed parameters assessed on two sides of the head based on two selected fNIRS channels was verified using Wilcoxon test.

Correlations between the morphological variables and age were assessed using Spearman rank test (R_S). Interactions between age group (defined as I for individuals younger than 28 years and II otherwise - based on the median age value to ensure comparable number of volunteers in each group) and sex and their impact on morphological variables was tested using Scheirer-Ray-Hare test.

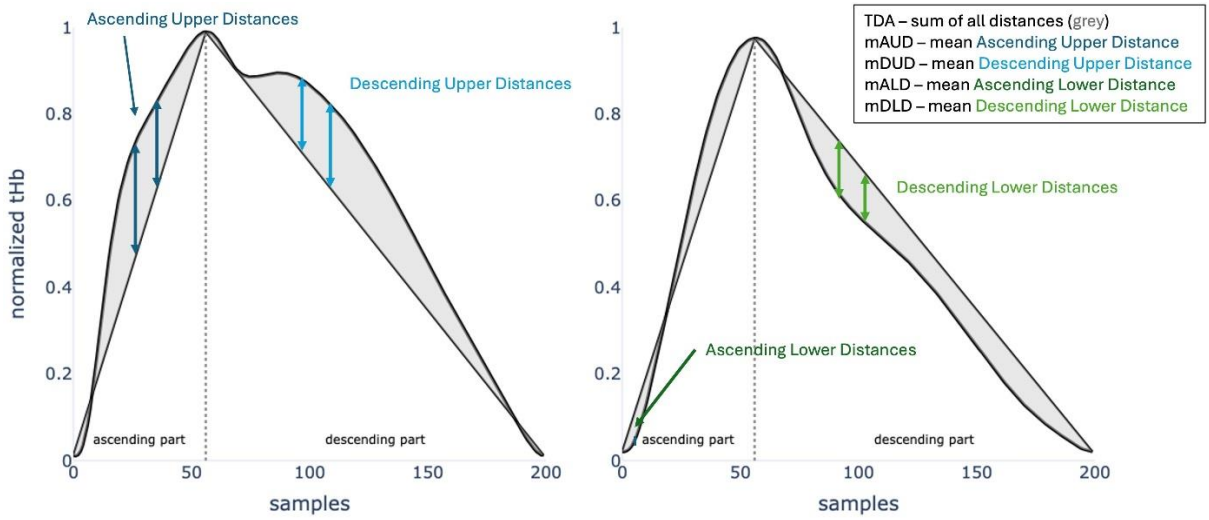

Fig. 1. Visualization of a triangle fitted into the total hemoglobin concentration (tHb) pulse waveform and triangle similarity indices in young (25 years) and old (55 years) volunteer.

Main results: There were no differences between the tested variables on the two sides of the head, hence all metrices were averaged sidewise. TDA was negatively correlated with age (R_S=-0.459, p<<0.01) indicating more triangle shape of tHb pulse with advanced age. Among four tested average to-triangle distances, only two metrices were correlated with age: mAUD (R_S=-0.626, p<<0.01) and mDUD (R_S=-0.283, p=0.03). Sex and age group have significant effect on TDA, mAUD and mDUD, and there is an interaction between these two factors (TDA: H_{sex}=5.01, p_{sex}=0.03; H_{age}=11.28, p_{age}<<0.01; $H_{sex\text{-}age}$=14.53, $p_{sex\text{-}age}$<<0.001; mAUD: H_{sex}=5.36, p_{sex}=0.02; H_{age}=21.72, p_{age}<<0.001; $H_{sex\text{-}age}$=8.00, $p_{sex\text{-}age}$<0.01; mDUD: H_{sex}=4.91, p_{sex}=0.03; H_{age}=4.73, page=0.03; $H_{sex\text{-}age}$=5.61, $p_{sex\text{-}age}$=0.02).

Conclusion: Aging causes a change in the morphology of tHb pulse waveform, making it more triangle-like. Sex is another factor differentiating the tHb pulse waveform similarity to the triangle, showing that the aged-induced changes are more pronounced in women.

Acknowledgements: The work was supported by the project Minigrants for doctoral students of the Wroclaw University of Science and Technology.

References:

1. Thorpe SG, Thibeault CM, Canac N, et al. Toward automated classification of pathological transcranial Doppler waveform morphology via spectral clustering. *PLoS ONE*. 2020;15(2):e0228642. doi:https://doi.org/10.1371/journal.pone.0228642
2. Bishop SM, Ercole A. Multi-Scale Peak and Trough Detection Optimised for Periodic and Quasi-Periodic Neuroscience Data. *Acta Neurochirurgica Supplement*. Published online 2018:189-195. doi:https://doi.org/10.1007/978-3-319-65798-1_39
3. Ziółkowski A, Kasprowicz M, Czosnyka M, Czosnyka Z. Brain blood flow pulse analysis may help to recognize individuals who suffer from hydrocephalus. *Acta Neurochirurgica*. 2023;165(12):4045-4054. doi:https://doi.org/10.1007/s00701-023-05839-5

PP33

Does functional brain stimulation change the brain tissue scattering?

Kamil LIPIŃSKI*, Neda MOGHARARI, Adam LIEBERT, Stanisław WOJTKIEWICZ

* ***Corresponding author***. *E-mail address*: klipinski@ibib.waw.pl

Keywords: fNIRS, tissues oxygenation, tissues optical properties, tissues scattering

Motivation and Aim: Time-Domain Near-Infrared Spectroscopy (TD-NIRS) is a non-invasive optical technique used to measure the optical properties of the biological tissues. It relies on near-infrared (NIR) picoseconds-short, pulsed light (typically in the range of 650–940 nm) to probe tissue and provides insights into its absorption and scattering properties [1]. These measurements allow for a separation of absorption and scattering properties of tissues, offering improved accuracy over the most common continuous-wave NIRS [2]. Functional brain stimulation, such as task-based motor cortex activation, induces localized hemodynamic changes, locally altering tissue optical properties [3–5]. While absorption(μ_a) changes related to oxygenated and deoxygenated haemoglobin are well-studied, the potential influence of scattering (μ_s') changes has not been thoroughly investigated.

This gap raises an important question: Does a functional brain stimulation significantly impact the scattering coefficient of the measured tissue, and should this effect be accounted for in NIRS data analysis? This study addresses this question combining in silico simulations with in vivo task-based experiments involving motor cortex activation.

Novelty: This study reveals that task-related motor cortex activation causes statistically significant changes in the activated tissue scattering μ_s', challenging the common assumption of constant scattering in functional NIRS research. We quantify the errors introduced by neglecting the scattering change — 4.8% for oxygenated, 182.8% for deoxygenated, and -29.7% for total haemoglobin concentrations. We emphasize the need to account for both absorption and scattering changes to address all physical phenomena in the fNIRS data interpretation.

Methods:

Stimulation Protocol: Twelve healthy adult volunteers were recruited (two females and ten males, aged 24-43 years, mean age 32.2 years), of which eleven were included in the analysis. A series of measurements was carried out to investigate the influence of cortical activation on optical properties. The experiment was divided into two phases (left- or right-hand motor stimulation). To activate the motor cortex, the subject firmly pressed a small soft ball (made of foam rubber) with their hand, repeating squeezes with the frequency of 2 Hz.

Crosstalk check: To estimate the magnitude of the mutual influence between absorption and scattering observed during parameter recovery from the measured distributions of time of flight of photons (DTOFs), a series of simulations was carried out. In silico data were generated with the in-house developed Monte Carlo code[6] to examine the parameters recovery crosstalk, between the absorption and scattering. The simulation involved generating 44 DTOFs with varying scattering and absorption parameters for each scenario, followed by adding Poisson noise. Simulations were carried out for the same magnitude of changes of the optical properties that were observed in the data from the in-vivo experiment, i.e. approximately 1%.

Testing method: DTOFs measured in vivo were used to recover optical properties using the moments method as shown in [7] and Curve fitting methods as shown in [8,9]. In further part

of this paper estimating optical properties from measurands ΔA and $\Delta\langle t\rangle$ will be referred as At and from $\Delta\langle t\rangle$ and ΔV as tV. Where ΔA, $\Delta\langle t\rangle$ and ΔV correspond to changes in 0th, 1st and 2nd centralized statistical moment (light intensity, mean time of flight and variance of distribution) of a DTOF.To check the potential error of neglecting changes in the scattering to the well established CW-NIRS measurements the following procedure was applied: We implemented a numerical procedure using the finite element method (FEM). The simulation was based on a standard slab model, where absorption and scattering properties at 690 nm and 830 nm were defined for both baseline and stimulus conditions. Two cases were considered: one where only absorption changed and another where both absorption and scattering varied, as inferred from in vivo experiments.A 3D mesh was generated, and light propagation was computed using time-resolved FEM simulations with appropriate boundary conditions. The time-domain reflectance (TPSF) was obtained for all conditions and processed to extract the first statistical moment, representing attenuation changes. These data were then used to estimate oxyhemoglobin and deoxyhemoglobin concentration changes based on differential attenuation at both wavelengths. Finally, the relative error between the two cases was computed for oxy-, deoxy-, and total hemoglobin concentrations, quantifying the bias introduced by ignoring scattering variations in CW-NIRS measurements.

Main results: Both, the μ_a and μ_s' are affected by the stimulation. The changes are not lower than 0.05% and 0.03% of initial value for μ_a and μ_s' respectively.

Table 5: Recovery of $\Delta\mu_s'$ during task period within the tested volunteers group

Datasource	Median [%]
Left hemisphere activation @690 nm	0.2217
Left hemisphere activation @830 nm	0.0901
Right hemisphere activation @690 nm	0.0948
Right hemisphere activation @830 nm	0.1457

Expected crosstalk is highest for tV and moments method. LMA and At method are significantly closer to "ground truth". Table 6 presents how much crosstalk is expected when optical properties change by 1 % as observed in vivo.

Table 6: Crosstalk detection/interference results for 1% change of optical properties as observed in vivo.

Value changing	crosstalk on	At	tV	LMA	Moments
μ_a by 1%	μ_s' [%]	-0.01	-0.23	0.06	-0.23
μ_s' by 1%	μ_a [%]	-0.04	0.24	0.02	0.24

As shown the recovered scattering is around one-fold of magnitude greater than the expected crosstalk. Additionally the error predicted with FEM simulated data suggests that assuming constant scattering during functional brain stimulation measured with a continuous wave NIRS can introduce the: 4.8 % in oxygenated, 182.8 % in deoxygenated and -29.7 % in total haemoglobin concentrations.

Conclusion: This study confirms that statistically significant changes (order of magnitude above the crosstalk) in μ_s' occur during task-related motor cortex activation. These findings emphasize the need to consider scattering changes, in addition to absorption, when interpreting functional NIRS experiments.

Experimental data suggests that assuming constant scattering during functional brain stimulation can introduce the following error to a continuous wave NIRS measurement: 4.8 % in oxygenated, 182.8 % in deoxygenated and -29.7 % in total haemoglobin concentrations.

Acknowledgements: Study was financed and conducted in Statuatory Topic 253 (ST253)

References:

1. W. Tosh and M. Patteril, "Cerebral oximetry," BJA Education **16**(12), 417–421 (2016).

2. A. Torricelli, D. Contini, A. Pifferi, M. Caffini, R. Re, L. Zucchelli, and L. Spinelli, "Time domain functional NIRS imaging for human brain mapping," NeuroImage **85**, 28–50 (2014).

3. C. Hirth, H. Obrig, K. Villringer, A. Thiel, J. Bernarding, W. Mühlnickel, H. Flor, U. Dirnagl, and A. Villringer, "Non-invasive functional mapping of the human motor cortex using near-infrared spectroscopy," Neuroreport **7**(12), 1977–1981 (1996).

4. D. R. Leff, F. Orihuela-Espina, C. E. Elwell, T. Athanasiou, D. T. Delpy, A. W. Darzi, and G.-Z. Yang, "Assessment of the cerebral cortex during motor task behaviours in adults: A systematic review of functional near infrared spectroscopy (fNIRS) studies," NeuroImage **54**(4), 2922–2936 (2011).

5. M. Mihara, I. Miyai, N. Hattori, M. Hatakenaka, H. Yagura, T. Kawano, M. Okibayashi, N. Danjo, A. Ishikawa, Y. Inoue, and K. Kubota, "Neurofeedback Using Real-Time Near-Infrared Spectroscopy Enhances Motor Imagery Related Cortical Activation," PLOS ONE **7**(3), e32234 (2012).

6. S. Wojtkiewicz and A. Liebert, "Parallel, multi-purpose Monte Carlo code for simulation of light propagation in segmented tissues," Biocybernetics and Biomedical Engineering **41**(4), 1303–1321 (2021).

7. A. Liebert, H. Wabnitz, D. Grosenick, M. Möller, R. Macdonald, and H. Rinneberg, "Evaluation of optical properties of highly scattering media by moments of distributions of times of flight of photons," Appl. Opt., AO **42**(28), 5785–5792 (2003).

8. A. Liemert and A. Kienle, "Light diffusion in N-layered turbid media: frequency and time domains," JBO **15**(2), 025002 (2010).

9. A. Sudakou, H. Wabnitz, A. Liemert, M. Wolf, and A. Liebert, "Two-layered blood-lipid phantom and method to determine absorption and oxygenation employing changes in moments of DTOFs," Biomed. Opt. Express, BOE **14**(7), 3506–3531 (2023).

PP34

Utilization of Instantaneous Frequency and Amplitude Obtained via EWT for Motor Imagery Classification

Patryk ZYCH[1*], Kacper FILIPEK[1], Adam PATALAS[1]

1 Institute of Mechanical Technology, Poznan University of Technology, Poznan, Poland

* ***Corresponding author***. *E-mail address*: zych.patryk@outlook.com

Keywords: Brain-computer interface, EEG, signal processing, EWT, HOS, LDA, SVM

Motivation and Aim: Brain-computer interfaces (BCIs) are becoming increasingly popular due to technological advancements. BCIs provide an alternative way to control end devices in situations where conventional control methods are not possible. As a result, they are particularly valuable for individuals with neurological disorders that impair limb functions, as well as for elderly, ill, or weakened patients recovering from illness or surgery. Based on existing knowledge of brain physiology, researchers have developed methods that utilize specific paradigms, such as event-related potentials (ERP) and event-related desynchronization/synchronization (ERD/ERS). These methods enable users to operate end devices using their brain potentials[1]. One of the applications of BCIs includes systems supporting rehabilitation, for example after a stroke. These systems rely on a non-invasive technique for recording brain activity called electroencephalography (EEG), which enables the delivery of feedback to patients via external devices or virtual reality (VR) triggered through motor imagery (MI) or motor execution (ME) attempts. Researchers believe that such a closed-loop system supports long-term motor rehabilitation by inducing appropriate neuroplastic changes. As this field is still under development, further research is essential to advance these technologies and better support individuals in need[2].

Novelty: The development of BCIs supporting patients during upper limb rehabilitation requires a system that meets critical demands: effectiveness in event recognition, reliability throughout the rehabilitation process, low latency for optimal immersion and neurofeedback, and also accessibility for different users. Due to physiological variability, particularly in individual brain signal patterns, a user-adaptive approach is optimal, achieved by training classifiers offline on acquired signal data prior to deployment. While traditional ERD/ERS for both motor execution (ME) and motor imagery (MI) uses bandpower features, this study investigates usage of higher order statistics (HOS) to improve MI detection in right- versus left-hand tasks.

Methods: The study utilized a dataset[3] comprising 52 subjects whose brain signals were recorded using an EEG with 64 electrodes arranged according to the international 10-10 system, at a sampling frequency of 512 Hz. In the experiment, participants performed five to six hand movement imagination trials, separated by 4-minute rest periods as needed. Before the actual experiment, each subject practiced four finger movement patterns: touching their index, middle, ring, and little fingers to the thumb within 3-second intervals. During the motor imagery (MI) task, participants were instructed to focus on kinesthetic rather than visual representation of the movements. The extracted features included mean absolute deviation (MAD), interquartile range (IQR), skewness (Sk), and kurtosis (Kt). The first step in signal processing included 60

Hz notch filtering. Then, using the empirical wavelet transform (EWT) method, the signal was decomposed into 10 modes (empirically determined), with hyperparameters optimized via brute-force method. Power spectrum analysis using Welch's method was employed to identify the most MI-sensitive mode, which was subsequently used for further processing. The Hilbert-Huang Transform (HHT) was then applied to extract instantaneous amplitude (IA) and instantaneous frequency (IF) features. The signal was subsequently segmented into 200 ms windows without overlap. From these, four higher order statistics (HOS) were computed and used as input features to train the two most commonly used classifiers in MI applications: linear discriminant analysis (LDA) and support vector machine (SVM). The dataset (consisting of 7026x512 samples for each subject) was split into training and test sets using 5-fold cross-validation with algorithm performance measured through accuracy (representing the ratio of correct assessments to all assessments) and F1 score (calculated as the harmonic mean of precision and recall scores).

Main results: Each classifier was individually trained for all 52 subjects, using the features previously described and extracted from each EEG channel. The LDA classifier achieved an average accuracy of 99.58% across all participants, with an equally high F1 score of 99.58%. The SVM classifier demonstrated slightly lower performance, yielding 96.64% accuracy and 96.56% F1 score, respectively. The classifiers achieved exceptionally high performance metrics, significantly outperforming the results reported by the original dataset authors, who reached a maximum accuracy of only 67.46% in their best-case scenario[4].

Conclusion: The study demonstrated that HOS features derived from IF and IA, extracted using EWT from EEG signals, can significantly enhance the classification of MI tasks. The exceptionally high classification accuracy achieved by both LDA and SVM classifiers across all 52 subjects suggests that used signal processing and feature extraction methods can be very effective in capturing MI-related brain activity patterns. The outcome allows for two possible interpretations. On one hand, the models may have overfit the training data—potentially acceptable in this context, as they were specifically tailored to individual users based on extensive subject-specific datasets. On the other hand, the outstanding results may genuinely reflect the classifiers' discriminative power, as the extracted HOS features appeared to enable nearly unambiguous separation between motor imagery tasks. Furthermore, the superior performance of LDA compared to SVM suggests potential linear separability in the feature space, which is consistent with the underlying assumptions of the LDA algorithm.

References:

1. Rao RPN. *Brain-Computer Interfacing: An Introduction*. Cambridge University Press; 2013.

2. Sieghartsleitner S, Sebastián-Romagosa M, Ortner R, Cho W, Guger C. Chapter 6 - BCIs for stroke rehabilitation. In: El-Baz AS, Suri JS, eds. *Brain-Computer Interfaces*. Advances in Neural Engineering. Academic Press; 2025:131-150.

3. Cho H, Ahn M, Ahn S, Moonyoung Kwon, Jun SC. Supporting data for "EEG datasets for motor imagery brain computer interface." Published online 2017:10 GB.

4. Cho H, Ahn M, Ahn S, Kwon M, Jun SC. EEG datasets for motor imagery brain–computer interface. *GigaScience*. 2017;6(7):gix034

PP35

Nonlinear analysis of ECG signals in arrythmia simulated by MPS450 Fluke and measured with ADS1298 AFE

Elzbieta RAUS-JARZABEK[1], Elzbieta OLEJARCZYK[1,2]

1 AGH University of Krakow, Al. Mickiewicza 30, Krakow 30-059, Poland

2 Nalecz Institute of Biocybernetics and Biomedical Engineering Polish Academy of Sciences, Trojdena 4 str., 02-109 Warsaw, Poland

eolejarczyk@agh.edu.pl

Abstract. Arrhythmia detection and classification are critical for early diagnosis and management of cardiac disorders. In this study, we performed a nonlinear analysis of ECG signals representing up to 35 types of arrhythmias generated by the MPS450 Fluke simulator. These signals were recorded with the ADS1298 analog front-end (AFE). Eight measures were analysed such as variance, Higuchi Fractal Dimension (HFD), Katz Fractal Dimension (KFD), Detrended Fluctuation Analysis (DFA), Sample Entropy (SampEn), Approximate Entropy (ApEn), and Multiscale Entropy (MSE). The impact of window size was tested also. These measures allowed to differentiate between a normal rhythm and 20 out of 35 arrythmias as well as between 73.7 % of pairs of different arrhythmias, highlighting their diagnostic potential. The best results were obtained for 30- second window. All fractal dimension measures (KFD, HFD and DFA) and ApEn were the most important features for arrythmias classification. This study demonstrates the efficacy of nonlinear ECG signal analysis in characterizing arrhythmias and emphasizes the importance of advanced simulation and acquisition systems like the MPS450 Fluke and ADS1298 for cardiac research and clinical applications, i.e. integration of an application based on nonlinear measures with wearable ECG devices for automated arrhythmia classification.

Keywords: ECG, arrythmia, nonlinear analysis, MPS450 Fluke simulator, ADS1298

PP36

Influence of Liner Material Poisson's Ratio on Contact Pressure Distribution in Transtibial Prosthetic Sockets: A Finite Element Analysis Study

Agata MROZEK-CZAJKOWSKA[1]

1 Poznan University of Technology, Poznan, Poland

Abstract. Additive manufacturing has significantly advanced the field of prosthetics, allowing for the production of highly customized prosthetic components. Among these, the prosthetic socket plays a critical role in securely attaching the residual limb to the prosthesis. The interface pressure between the residual limb and the prosthetic socket greatly impacts user comfort and quality of life. This study explores the influence of liner material Poisson's ratio on contact pressure distribution within transtibial prosthetic sockets using Finite Element Analysis (FEA). Auxetic metamaterials, characterized by a negative Poisson's ratio, exhibit unique mechanical properties that enhance adaptability and comfort in prosthetic applications. By analyzing the pressure distribution for various Poisson's ratio values, the study reveals that auxetic materials contribute to a more uniform pressure distribution, reducing peak stresses on the residual limb. The findings suggest that integrating auxetic materials into prosthetic socket design can significantly improve the comfort and performance of prosthetic users. Further re- search should investigate additional mechanical properties to optimize prosthetic liner materials further.

Keywords: Prosthetics, FEA, Auxetics.

PP37

Acid-base modelling in peritoneal dialysis

Mauro PIETRIBIASI[1,*], Joanna STACHOWSKA-PIETKA[1], Olof HEIMBURGER[2], Jacek WANIEWSKI[1], Bengt LINDHOLM[2]

1 Nalecz Institute of Biocybernetics and Biomedical Engineering, Polish Academy of Sciences, Warsaw, Poland.

2 Division of Renal Medicine, Baxter Novum, Department of Clinical Science Intervention and Technology. Karolinska Institutet, Solna, Sweden.

* ***Corresponding author***. *E-mail address*: mpietribiasi@ibib.waw.pl

Keywords: Peritoneal dialysis, acid-base equilibrium, mathematical modelling

Motivation and Aim: Chronic acidosis in chronic kidney patients undergoing peritoneal dialysis (PD) is treated with the addition of buffer bases to the dialysis fluid. Traditional lactate solutions (TL) presented several factors, like low pH, that were shown to reduce biocompatibility, which led to the development of mixed solutions like bicarbonate plus lactate (BL). Mathematical models can be used as testing bench to predict the outcomes of different dialysate solutions, or to individualize the prescription of dialysate acid-base composition. Current models used to explain transport in PD, such as the 3-pore model, might have limited application in describing the transport of bicarbonate, because of the complexity of the respiratory and chemical regulation mechanisms of the bicarbonate buffer system in the body. To address this issue, we integrated the 3-pore model with a comprehensive model of whole-body acid-base equilibrium, and applied it to describe PD dwells in patients using both TL and BL dialysis fluid solutions.

Novelty: Compared to hemodialysis, few models are available to explain the evolution of acid-base equilibrium in PD patients. To date, ours is the most comprehensive model ever applied to describe this type of data.

Methods: We analyzed data from collected in a previous study [1], describing 7 patients who each underwent two 4-hour dialysis exchanges: one with the BL solution (glucose 3.86%, bicarbonate 25 mmol/L, lactate 15 mmol/L) and one with the TL solution (glucose 3.86%, lactate 40 mmol/L) with radiolabeled albumin added to the dialysis fluid as a volume marker. Frequent peritoneal fluid samples and plasma samples were taken during each exchange; solutes concentrations in plasma and dialysate were assessed with laboratory assays and blood gas analysis.

The acid-base portion of the model was previously developed for hemodialysis [2] and adapted to PD. This model describes the transport of CO_2 and oxygen between body compartments representing the main circulation, lung capillaries, tissue cells and interstitial spaces. Changes to the equilibrium of buffers in body fluids, driven by PD, were calculated solving nonlinear systems of equations describing the blood acid-base biochemistry. The 3-pore model was used to describe the transport of bicarbonate, dissolved CO_2, lactate, and other major solutes in plasma, across the peritoneal membrane. Transport occurs through a mix of large, small, and ultra-small pores, with different degrees of permeability to each solute. Water transport is

determined by the osmotic gradient between plasma and peritoneal fluid, balanced by the hydrostatic and oncotic pressure gradients and peritoneal absorption.

For each patient in the study, the model was fitted to the clinical data by tuning several patient-specific parameters, the filtration coefficient of the peritoneal membrane (LpS), the fluid absorption rate, the percentage of ultrasmall pores (αUP), and the permeability-surface area product (PS) coefficients for each solute.

Main results: The model fitted dialysate data with an overall root mean squared error (RMSE) of 8.3 ± 1.4% for BL fluid and 8.4 ± 1.6% for TL, compared to the data. The estimated LpS and αUP were within the expected range, with relatively high values of absorption rates, compared to the physiological range, that did not significantly differ from the estimates obtained directly based on the volume marker concentration. The estimated values of PS were significantly different between the two fluids (Table 1). In BL, the predictions of the evolution of bicarbonate and CO_2 concentrations in plasma were accurate with a relative error of 3.9 ± 2.4% and 6.4 ± 3.9%, respectively, while the errors in TL were 4.9 ± 4.2% and 5.0 ± 2.7%, respectively ($p > 0.05$).

Table 1. Median values of permeability-surface area coefficients (PS, in mL/min) estimated by the model in the lactate-only solution (TL) and bicarbonate plus lactate solution (BL). *Wilcoxon test with $p < 0.05$ for BL vs TL.

	BL	**TL**
PS Glucose	12.84 [10.37; 13.41]	10.42 [9.26; 14.42]
PS Na	11 [7.15; 20.57]*	8.11 [4.03; 10.99]
PS Urea	24.59 [21.26; 28.86]	24.14 [20.03; 27.01]
PS Creatinine	10.96 [9.24; 19.72]	10.46 [9.16; 14.59]
PS Cl^-	15.54 [13.6; 20.99]*	8.75 [7.41; 18.39]
PS K^+	23.73 [16.8; 26.81]*	20.84 [15.72; 22.01]
PS P^-	6.04 [3.21; 7.36]	5.4 [3.5; 6.81]
PS Lactate	17.76 [16.83; 21.63]*	14.66 [13.96; 17.02]
PS Bicarbonate	22.17 [17.96; 28.28]	16.45 [13.12; 21.44]
PS CO_2	2.51 [2.51; 5.71]*	17.04 [11.2; 17.93]

Conclusion: After tuning the peritoneal transport parameters, the model fitted dialysate data with high accuracy, and the simulation of the acid-base equilibrium allowed to predict the evolution of bicarbonate and CO_2 levels in plasma during the PD dwell. However, the differences in the estimated PS values between the two dialysis fluids are perhaps indicative of some other mechanisms related to the transport of bicarbonate and lactate that are not described by the model.

References:

[1] Heimburger O, Mujais S. Buffer transport in peritoneal dialysis. Kidney Int Suppl. 2003 Dec;(88):S37-42. doi: 10.1046/j.1523-1755.2003.08804.x. PMID: 14870876.

[2] Pietribiasi M, Waniewski J, Leypoldt JK. Mathematical modelling of bicarbonate supplementation and acid-base chemistry in kidney failure patients on hemodialysis. PLoS One. 2023 Feb 24;18(2):e0282104. doi: 10.1371/journal.pone.0282104.

PP38

Modified kinetics of plasma electrolytes during hemodialysis after changing dialysate bicarbonate concentration

Malgorzata DEBOWSKA[1*], Monika WIELICZKO[2], Mauro PIETRIBIASI[1], Urszula BIALONCZYK[1], Jolanta MALYSZKO[2], John K. LEYPOLDT[1], Jacek WANIEWSKI[1]

1 Nalecz Institute of Biocybernetics and Biomedical Engineering, Polish Academy of Sciences, Warsaw, Poland

2 Department of Nephrology, Dialysis and Internal Disease, Medical University of Warsaw, Warsaw, Poland

* ***Corresponding author***. *E-mail address*: mdebowska@ibib.waw.pl

Keywords: acid-base, bicarbonate, dialysis fluid, electrolytes, hemodialysis

Motivation and Aim: The concentration of bicarbonate (Dbic) and some electrolytes (sodium, potassium, calcium) in dialysis fluid may be individually adjusted during hemodialysis session according to medical prescriptions. However, because of technical reasons, the concentration of other electrolytes in dialysis fluid may change, if Dbic is changed. We aimed at the assessment of the impact of modifications of Dbic on plasma electrolytes.

Novelty: Our study allowed for the quantification of the changes in plasma chloride and calcium following the change of Dbic, whereas the settings for concentrations of sodium, potassium and calcium in dialysis fluid were unchanged.

Methods: During two midweek, 4 hour long hemodialysis sessions in 25 anuric, prevalent hemodialysis patients the acid-base parameters and small electrolytes were measured using blood gas analyser (ABL90 Flex Plus, Radiometer, Denmark) at 0, 60, 120, 180 and 240 min of the session. During the first session (treatment A) Dbic was constant at 33.6±1.7 mmol/L during the whole session, while for the second week (treatment B) it was modified before and after 2 h of the session and was on average 30.8±2.3 mmol/L for the initial 2 hours and 34.0±2.5 mmol/L for the final 2 hours.

Main results: During treatments A and B plasma bicarbonate (Pbic), pCO2, pH and calcium increased during the sessions, whereas plasma potassium, sodium and chloride decreased. The time profiles of plasma sodium and potassium did not differ between Treatments A and B. Pbic was lower in treatment B than A at 60 and 120 min of dialysis; plasma chloride and calcium were higher at 60 and 120 min of dialysis in treatment B than A. The difference in Pbic between the treatments A and B assessed at 2 and 4 h of the session correlated positively, whereas the differences in plasma chloride and calcium assessed at 2 and 4 h correlated negatively, with the difference in Dbic between treatments B and A at 2 and 4 h of the session, respectively. For each percent of Dbic increase one may expect after 2 hours of hemodialysis -0.27 and -0.16% change in plasma chloride and calcium, respectively.

Conclusion: Modifications of dialysate bicarbonate may influence the concentrations of some other electrolytes in plasma, as chloride (following the modification of chloride concentration in dialysis fluid during its preparation) and calcium (probably because of the change in plasma pH).

Acknowledgements: This work was supported by the Polish National Science Center (grant number 2017/27/B/ST7/03029).

PP39

Patient-Specific Pulse Wave Propagation Modeling for Improving Vasopressor Therapy in Severe Traumatic Brain Injury Patients

Kamil WOLOS[1*], Leszek PSTRAS[1], Urszula BIALONCZYK[1], Malgorzata DEBOWSKA[1], Wojciech DABROWSKI[2], Dorota SIWICKA-GIEROBA[2], Jan POLESZCZUK[1]

1 Nalecz Institute of Biocybernetics and Biomedical Engineering, Warsaw, Poland

2 Medical University of Lublin, Lublin, Poland

* ***Corresponding author***. *E-mail address*: kwolos@ibib.waw.pl

Keywords: personalized modeling, pulse wave propagation, severe traumatic brain injury, vasopressor dosing

Motivation and Aim: Hypotension is a common complication in patients with severe traumatic brain injury (sTBI), requiring vasopressor therapy to maintain adequate organ perfusion pressure[1]. Currently, vasopressor management relies on a trial-and-error approach, highlighting the need to improve dosing strategies[1,2]. In this study, we explored the potential of personalized pulse wave propagation modeling to predict the direction of the next norepinephrine (NE) dose change (or lack thereof).

Novelty: To our knowledge, this is the first study utilizing personalized pulse wave propagation modeling to predict the direction of NE dose changes.

Methods: We performed a longitudinal study on 25 sTBI patients in an intensive care unit. Arterial pulse waves were recorded non-invasively from wrists and ankles using the oscillometric method (AngE, SOT Medical, Austria) and then fitted by a 0-1D model of arterial blood flow dynamics describing pulsatile changes in blood pressure and arterial cross-sectional area along the arterial tree The model was fitted to data by adjusting selected model parameters, including arterial stiffness, maximal left-ventricular elastance, left atrial pressure, and the scaling factor of the resistances of small arteries and arterioles. These patient-specific cardiovascular parameters, along with the parameters obtained directly from the oscillometric device (e.g. the duration of the upslope of the recorded pulse waveforms) were then used in a statistical model to predict whether the next NE dose will be 1) increased, or 2) decreased or unchanged. This binary classification, combining no change in NE dose with a dose reduction, was adopted for the sake of simplicity of the predictive model and because, from a clinical perspective, it seems particularly important to predict the potential need to increase the vasopressor dose (to avoid hypotensive episodes).

Main results: The cardiovascular model demonstrated a good fit to the recorded pulse waves, with coefficients of determination (R^2) around 0.9 and a mean difference of 0.1 ± 1.0 mmHg between the measured and model-estimated mean arterial pressure ($R^2 = 0.99$). Apart from a few cases, no clear correlation was observed between the model-derived cardiovascular parameters and NE dose at the time of pulse wave recording. However, the statistical model predicting the NE dose changes achieved a balanced accuracy of 0.85 when trained on the full dataset and 0.76 with the leave-one-out cross-validation, with 8 misclassifications out of 77 observations.

Conclusion: The proposed framework allowed predicting the direction of NE dose adjustments over the next 24 hours with satisfactory accuracy despite the known inter-patient variability in the hemodynamic response to NE[3].

Acknowledgements: This study was supported by National Science Centre (Poland), grant No. 2018/31/D/ST7/03472.

References:

1. Sookplung P, Siriussawakul A, Malakouti A, et al. Vasopressor Use and Effect on Blood Pressure After Severe Adult Traumatic Brain Injury. *Neurocrit Care*. 2011;15(1):46-54. doi:10.1007/s12028-010-9448-9

2. Rossaint R, Afshari A, Bouillon B, et al. The European guideline on management of major bleeding and coagulopathy following trauma: sixth edition. *Crit Care*. 2023;27(1):80. doi:10.1186/s13054-023-04327-7

3. Johnston AJ, Steiner LA, O'Connell M, Chatfield DA, Gupta AK, Menon DK. Pharmacokinetics and pharmacodynamics of dopamine and norepinephrine in critically ill head-injured patients. *Intensive Care Med*. 2004;30(1):45-50. doi:10.1007/s00134-003-2032-4

PP40

Markov Model Simulation of Nicotine Addiction and the Effectiveness of Nicotine Replacement Therapy (NRT)

Joanna CHWAŁ[1,2,3], Arkadiusz BANASIK[1*], Radosław DZIK[1], Ewaryst TKACZ[1]

1 Academy of Silesia, Department of Clinical Engineering, Katowice, Poland;

2 Joint Doctoral School, Silesian University of Technology, Gliwice, Poland;

3 Silesian University of Technology, Faculty of Biomedical Engineering, Department of Medical Informatics and Artificial Intelligence, Gliwice, Poland.

* ***Corresponding author***. *E-mail address*: *arkadiusz.banasik@akademiaslaska.pl*

Keywords: Nicotine Addiction, Markov Model, Smoking Cessation, Nicotine Replacement Therapy (NRT)

Motivation and Aim: Nicotine addiction remains a major threat to public health, and both tobacco and electronic cigarettes can lead to long-term dependence. This study employs a Markov model to simulate the dynamics of nicotine addiction, comparing the progression of addiction among users of traditional cigarettes and e-cigarettes across three distinct intervention scenarios: no intervention, nicotine gum therapy, and nicotine patch therapy. In order to provide important insights into public health measures, the goal here is to quantify addiction patterns and cessation probability.

Novelty: This study expands on previous research [1,2] by explicitly differentiating addiction dynamics between e-cigarettes and traditional cigarettes. The model enhances accuracy by using real-world transition probabilities and incorporates nicotine gum and patches to evaluate their distinct impacts on addiction duration. By utilizing the latest epidemiological data, it provides a more precise depiction of nicotine addiction trends and cessation success rates.

Methods: A Markov model was developed with five states: No Contact, First Try, Experimenting, Addiction, and Cessation. Transition probabilities P_{ij} were derived from recent epidemiological studies [3] and structured in a transition matrix T, where each element P_{ij} represents the probability of transitioning from state i to state j over a one-year period. The system evolves according to the equation: $S_{t+1} = S_t \cdot t$, where S_t is the state distribution at time t, and T is the transition matrix. The simulation was conducted over a 20-year period, comparing traditional cigarette and e-cigarette users under three conditions: no therapy, nicotine gum (6.56% effectiveness), and nicotine patches (13.83% effectiveness) [4]. Studies on nicotine metabolism suggest that replacement therapies significantly alter addiction dynamics by stabilizing nicotine levels [5]. The expected time spent in each state was analyzed using Markov chain methods, emphasizing addiction and cessation states.

Main results: The simulation results indicate that e-cigarette users spend less time in addiction compared to traditional cigarette users. The implementation of NRT significantly reduces the duration of addiction, with nicotine patches demonstrating a higher effectiveness rate than nicotine gum. Without therapy, traditional cigarette users remain addicted for an average of 57.65 years, whereas e-cigarette users average 27.77 years in the addicted state. With nicotine

patches, the addiction duration decreases to 46.48 years for cigarette users and 21.46 years for e-cigarette users. These findings underscore the potential benefit of NRT in reducing addiction duration and enhancing smoking cessation rates (Figure 1).

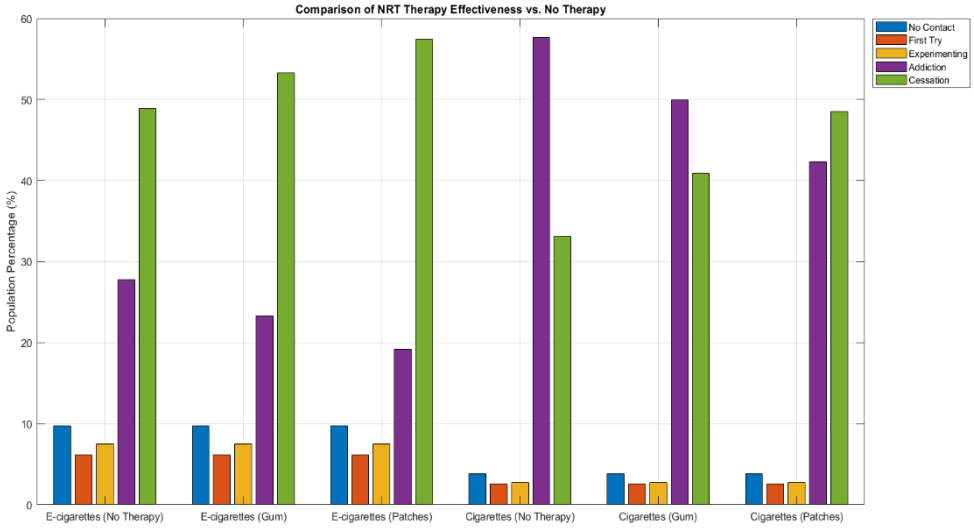

Figure 1. Simulation Results for Different Interventions

Conclusion: E-cigarettes can help smokers quit more effectively than regular cigarettes but still carry an addiction risk. Nicotine patches outperformed gums in terms of length of addiction and quit rates, making them a good option for smoking cessation programs. These findings are in line with previous studies, indicating that NRTs should be integrated with smoking cessation strategies for best efficacy. Future research should look at the long-term health effects of e-cigarettes as a harm reduction tool (but also their potential health effects), as well as the importance of behavioral support in combination with NRT.

References:

1. Nikose Y, Madhu PP, Reche A, Agarwal P, Jidewar N, Sayyed M, Chhabra KG. Markov model: Quantifying outlook towards success of tobacco cessation counseling. *J Family Med Prim Care*. 2022;11(8):4263-4266. doi:10.4103/jfmpc.jfmpc_2096_21.
2. Yeh HW, Ellerbeck EF, Mahnken JD. Simultaneous evaluation of abstinence and relapse using a Markov chain model in smokers enrolled in a two-year randomized trial. *BMC Med Res Methodol*. 2012;12:95. doi:10.1186/1471-2288-12-95.
3. Lopez-Quintero C, Pérez de los Cobos J, Hasin DS, Okuda M, Wang S, Grant BF, Blanco C. Probability and predictors of transition from first use to dependence on nicotine, alcohol, cannabis, and cocaine: Results of the National Epidemiologic Survey on Alcohol and Related Conditions (NESARC). *Drug Alcohol Depend*. 2011;115(1-2):120-130. doi:10.1016/j.drugalcdep.2010.11.004.
4. Sivasankari T, Sankaran A, Murugappan S, Subramanyam V, Subramanian B, Reddy RCJ, Vandana S. Comparative evaluation of the efficacy of nicotine chewing gum and nicotine patches as nicotine replacement therapy using salivary cotinine levels as a biochemical validation measure. *Indian J Psychiatry*. 2023;65(6):635-640. doi:10.4103/indianjpsychiatry.indianjpsychiatry_291_23.
5. Sandhu A, Hosseini SA, Saadabadi A. Nicotine Replacement Therapy. [Updated 2023 Nov 12]. In: StatPearls [Internet]. Treasure Island (FL): StatPearls Publishing; 2025 Jan-. Available from: https://www.ncbi.nlm.nih.gov/books/NBK493148/

PP41

Spontaneous Breathing and Mechanical Power Management: Toward Safer Ventilation Practices

Tomasz URBANKOWSKI[1*], Krzysztof ZIELIŃSKI[1] , Maciej KOZARSKI[1], Barbara STANKIEWICZ[1], Krzysztof Jakub PAŁKO[1], Raman PASLEDNI[1], Marek DAROWSKI[1]

1 Nalecz Institute of Biocybernetics and Biomedical Engineering, Polish Academy of Sciences, Warsaw, Poland

* ***Corresponding author***. *E-mail address*: tomasz.urbankowski@gmail.com

Keywords: Spontaneous breathing, mechanical power, ventilator-induced lung injury, patient-ventilator synchronization, lung-protective ventilation

Motivation and Aim: Spontaneous breathing during mechanical ventilation offers benefits such as improved ventilation-perfusion matching and preservation of diaphragm function. However, it also introduces risks, including patient self-inflicted lung injury (P-SILI) and ventilator-patient asynchrony. Non-invasive ventilation (NIV) is commonly employed in conditions like chronic obstructive pulmonary disease (COPD) exacerbations, heart failure, and sleep apnea, allowing patients to maintain spontaneous respiration. Nevertheless, emerging evidence suggests that NIV may also contribute to ventilator-induced lung injury (VILI), a phenomenon traditionally associated with invasive ventilation.

This study addresses the underexplored issue of managing mechanical ventilation with preserved spontaneous breathing by proposing strategies that balance its physiological benefits with the need to reduce the risk of ventilator-induced lung injury (VILI). It focuses on minimizing mechanical power and improving patient-ventilator synchronization to promote safer and more effective ventilation practices.

Novelty: This work aims to introduce novel strategies for mechanical power management during mechanical ventilation with preserved spontaneous breathing. It explores ventilation strategies, monitoring techniques, their impact on mechanical power, and potential methods to mitigate mechanical power. By proposing a structured approach to safe mechanical ventilation, this research aims to stimulate new discussions within the biomedical engineering community and contribute to the development of lung-protective ventilation techniques.

Methods: The research approach combines an in-depth review of current practices with simulation studies using a physical respiratory system model. The simulator replicates spontaneous breathing under mechanical ventilation, allowing adjustable parameters such as respiratory rate (10–30 breaths per minute), tidal volume (300–800 mL), and inspiratory effort profiles. Simulated patient efforts include normal, increased, and asynchronous patterns to realistically model clinical variability.

Preliminary experiments focus on adapting inspiratory pressure and flow to stabilize respiratory power during inspiration. While simulation studies offer valuable initial insights, limitations include potential discrepancies between simulated and real patient responses due to biological variability and complex pathophysiology, which will be addressed in future experimental validation phases.

Main results: Preliminary study proved that it is possible to reduce peak inspiratory power up to 30% through adaptation of inspiratory pressure/flow to stabilize respiratory power during an inspiration phase.

Currently, the research is progressing toward developing an advanced experimental setup with a physical simulator capable of dynamically replicating various spontaneous breathing patterns. This platform will support further investigation into strategies that enhance patient-ventilator synchronization and minimize mechanical power.

The expected outcomes of this study include:

- **Identification of key ventilation parameters** minimizing the risk of VILI in spontaneously breathing patients.
- **Development of a real-time mechanical power monitoring approach**, potentially contributing to safer ventilation with preserved spontaneous breathing.
- **Establishing a groundwork for future experimental research**, supporting the development of clinical guidelines for lung-protective ventilation with preserved spontaneous breathing.

Conclusion: This study highlights the role of spontaneous breathing during mechanical ventilation while minimizing mechanical power and preventing patient-ventilator asynchrony. The intention is to propose strategies that harness the physiological benefits of spontaneous breaths, including improved diaphragm function and better ventilation-perfusion matching, while ensuring a high standard of safety in clinical practice. Future research will focus on experimental validation and potentially obtaining evidence to propose clinical guidelines that effectively balance spontaneous breathing with protective ventilation strategies.

Acknowledgements: This research was fully funded by the National Science Centre, Poland, under Grant No. 2023/50/A/ST7/00498

References:

[1] Yoshida T, Fujino Y, Amato MBP, Kavanagh BP. Fifty years of Research in ARDS. Spontaneous Breathing during Mechanical Ventilation. Risks, Mechanisms, and Management. Am J Respir Crit Care Med. 2017;195(8):985-992. doi:10.1164/rccm.201604-0748CP

[2] Thille AW, Rodriguez P, Cabello B, Lellouche F, Brochard L. Patient-ventilator asynchrony during assisted mechanical ventilation. Intensive Care Med. 2006;32(10):1515-1522. doi:10.1007/s00134-006-0301-8

[3] Mauri T, Cambiaghi B, Spinelli E, Langer T, Grasselli G. Spontaneous breathing: a double-edged sword to handle with care. Ann Transl Med. 2017;5(14):292-292. doi:10.21037/atm.2017.06.55

[4] Bertoni M, Spadaro S, Goligher EC. Monitoring Patient Respiratory Effort During Mechanical Ventilation: Lung and Diaphragm-Protective Ventilation. Crit Care. 2020;24(1):106. doi:10.1186/s13054-020-2777-y

[5] Albani F, Pisani L, Ciabatti G, et al. Flow Index: a novel, non-invasive, continuous, quantitative method to evaluate patient inspiratory effort during pressure support ventilation. Crit Care. 2021;25(1):196. doi:10.1186/s13054-021-03624-3

PP42

The influence of the ventilation methods on respiratory variables – model studies

Raman PASLEDNI[1*], Maciej KOZARSKI[1], Krzysztof ZIELIŃSKI[1], Barbara STANKIEWICZ[1], Krzysztof Jakub PAŁKO[1], Tomasz URBANKOWSKI[1], Marek DAROWSKI[1]

1 Nalecz Institute of Biocybernetics and Biomedical Engineering, Polish Academy of Sciences, Ks. Trojdena 4, 02109 Warsaw, Poland

* ***Corresponding author***. *E-mail address*: rpasledni@ibib.waw.pl

Keywords: mechanical ventilation, mechanical power, pressure and flow adaptation

Motivation and Aim: During mechanical ventilation, it is essential to regulate inspiratory pressure, air flow and ventilation power to minimize the risk of lung damage [1-3]. Modern lung ventilators are sophisticated devices designed to automatically supply inspiratory gas to a patient's lungs. Newer ventilation modes, such as Adaptive Support Ventilation (ASV) and Intelligent-ASV [4, 5], are considered the first ventilator systems to utilize targeting solutions, automatically determining the optimal ventilation frequency to minimize the patient's work of breathing. But these ventilation modes have their drawbacks:

- ***Potential for Excessive Mechanical Power*** – ASV adjusts tidal volume and respiratory rate automatically, but in certain cases, it may generate excessive mechanical power, leading to lung overdistension and ventilator-induced lung injury (VILI), especially in patients with reduced lung compliance.
- ***High Inspiratory Flow*** – ASV tends to deliver relatively high inspiratory flows to meet its target minute ventilation. This can create rapid lung inflation, potentially increasing the risk of volutrauma or barotrauma [6].
- ***Limited Adaptation in Severe Lung Conditions*** – In conditions like **ARDS** (Acute Respiratory Distress Syndrome), where lung mechanics are highly heterogeneous [7], ASV may not always optimize flow patterns effectively, leading to uneven lung ventilation.
- ***Inconsistent Response to Sudden Changes*** – ASV relies on real-time monitoring and algorithm-based adjustments, but it may lag in responding to sudden changes in lung mechanics, such as airway collapse or secretion buildup, potentially causing inappropriate ventilatory support [8].

To address these limitations, in the present study we adjusted inspiratory pressure and flow patterns to minimize mechanical ventilation power.

Novelty: In this study, we were able to adjust the inspiratory pressure and flow to minimize the power of mechanical ventilation.

Methods: To validate the proposed concept of adapting inspiratory pressure and flow to stabilize respiratory power during the inspiration phase, studies were conducted using a system comprising a servo ventilator (*Siemens-Elema 900B*) and a physical lung model (*SmartLung 2000*). The mechanical parameters of the test lung, including compliance (C) [$mL \cdot mbar^{-1}$] and flow resistance (R) [$mbar \cdot s \cdot L^{-1}$] in series, were progressively adjusted to simulate healthy, obstructive, and resistive lung conditions. Before simulations, the test lung was assessed to establish the range of its compliance linear characteristics.

Main results: For high airway resistance (R=21.74 mbar·s·L^{-1}) and high lung compliance (C=75 mL·$mbar^{-1}$), the smallest reduction in power was observed (7.75%), while the largest reduction occurred for R=0.54 mbar·s·L^{-1}, C=25 mL·$mbar^{-1}$ (29.98%).

For resistances of 3.52 mbar·s·L^{-1} and 21.74 mbar·s·L^{-1}, the greatest reduction in power was observed at C = 60 mL·$mbar^{-1}$, with values of 22.78% and 13.01%, respectively.

Conclusion: The optimized ventilation produced varying effects depending on the respiratory system's mechanical properties. Specifically: 1) The most significant reduction in peak power occurred under conditions of low resistance and low compliance (R=0.54 mbar·s·L^{-1}, C=25 mL·$mbar^{-1}$), suggesting that optimization is particularly effective in reducing ventilatory power in stiff lungs and promotes a more uniform distribution of power throughout inspiration. 2) Conversely, the smallest impact was observed with high resistance and high compliance (R=21.74 mbar·s·L^{-1}, C=75 mL·$mbar^{-1}$), indicating that in more compliant lungs, the advantages of dynamically regulating flow and pressure are less pronounced.

Acknowledgements: This research was funded in whole by National Science Centre, Poland, Grant number 2023/50/A/ST7/00498.

References:

[1] Silva PL, Ball L, Rocco PRM, Pelosi P. Power to mechanical power to minimize ventilator-induced lung injury? *ICMx*. 2019;7(S1):38. doi:10.1186/s40635-019-0243-4

[2] Serpa Neto A, Deliberato RO, Johnson AEW, et al. Mechanical power of ventilation is associated with mortality in critically ill patients: an analysis of patients in two observational cohorts. *Intensive Care Med*. 2018;44(11):1914-1922. doi:10.1007/s00134-018-5375-6

[3] Marini JJ, Rocco PRM. Which component of mechanical power is most important in causing VILI? *Crit Care*. 2020;24(1):39, s13054-020-2747-4. doi:10.1186/s13054-020-2747-4

[4] Becher T, Adelmeier A, Frerichs I, Weiler N, Schädler D. Adaptive mechanical ventilation with automated minimization of mechanical power—a pilot randomized cross-over study. *Crit Care*. 2019;23(1):338. doi:10.1186/s13054-019-2610-7

[5] Bialais E, Wittebole X, Vignaux L, Roeseler J, Wysocki M, Meyer J, Reychler G, Novotni D, Sottiaux T, Laterre PF, Hantson P. Closed-loop ventilation mode (IntelliVent®-ASV) in intensive care unit: a randomized trial. Minerva Anestesiol. 2016 Jun;82(6):657-68.

[6] Yang SH, Wu CP, Huang YCT, Peng CK. The Effects of Automatic Inspiratory Rise Time and Flow Termination on Operation of Closed-Loop Ventilation. *Respir Care*. 2023;68(5):669-675. doi:10.4187/respcare.10475

[7] Santos RS, Maia LDA, Oliveira MV, et al. Biologic Impact of Mechanical Power at High and Low Tidal Volumes in Experimental Mild Acute Respiratory Distress Syndrome. *Anesthesiology*. 2018;128(6):1193-1206. doi:10.1097/ALN.0000000000002143.

[8] Reddy H, Dillard TA. A failure of adaptive servo-ventilation to correct central apneas in Cheyne-Stokes breathing. *J Clin Sleep Med*. 2012;8(1):103-106. Published 2012 Feb 15. doi:10.5664/jcsm.1674

PP43

Model-based investigation of the effect of multi-site arterial occlusion by cuffs on the distribution of blood flow in the arterial tree

Kamil WOLOS[1], Leszek PSTRAS[1], Malgorzata DEBOWSKA[1], Jan POLESZCZUK[1,*]

1 Nalecz Institute of Biocybernetics and Biomedical Engineering, Polish Academy of Sciences, Warsaw, Poland

* ***Corresponding author***. *E-mail address*: jpoleszczuk@ibib.waw.pl

Keywords: oscillometric blood pressure measurement, arterial occlusion, blood flow redistribution

Motivation and Aim: While traditional oscillometric blood pressure measurements are performed using a single arm cuff, there exist devices that utilize simultaneous multi-limb measurements to enhance diagnostic capabilities by determining a variety of vascular and hemodynamic parameters. However, concurrent occlusion of multiple arteries raises questions about its impact on hemodynamics, particularly in vulnerable patients with impaired cardiovascular regulatory mechanisms. We set out to investigate this potential impact using mathematical modeling.

Novelty: To our knowledge, this is the first study of the impact of multi-site arterial occlusion caused by oscillometric cuff-based measurements on the distribution of blood flow in the arterial tree and hemodynamic parameters.

Methods: We extended a 0-1D pulse wave propagation model to simulate the effects of cuff inflation on arms and legs [1, 2]. Specifically, we examined the impact of complete arterial occlusion by the cuffs on blood pressure and flow at different locations in the circulatory system (assuming no cardiovascular regulation). The simulations included various cuff configurations on four limbs, including cuffs placed on all four limbs (wrists and ankles).

Main results: When applying a uniform 150 mmHg cuff pressure on all four limbs (30 mmHg above the assumed systolic pressure), our simulations showed an increase in mean arterial pressure (MAP) of about 10% in the ascending aorta, carotid artery, and abdominal aorta. Moreover, we observed an approximately 11% increase in mean carotid blood flow compared to baseline value. In contrast, applying the same cuff pressure at only one site (right wrist) resulted in a significantly smaller MAP increase of 2.6%, with a 2.9% increase in mean blood flow in the carotid artery.

Conclusion: This *in silico* study provides preliminary evidence suggesting that multi-limb oscillometric blood pressure measurements may induce measurable hemodynamic alterations if not counteracted rapidly and effectively by cardiovascular regulatory mechanisms. This might be of great importance for patients with impaired baroreflex mechanisms or vascular autoregulation, such as traumatic brain injury patients.

Acknowledgements: The study was supported by the National Science Centre (Poland), grant No. 2018/31/D/ST7/03472.

References:

[1] K. Wołos, L. Pstras, M. Debowska, W. Dabrowski, D. Siwicka-Gieroba, and J. Poleszczuk, "Non-invasive assessment of stroke volume and cardiovascular parameters based on peripheral pressure waveform," PLOS Comput. Biol., vol. 20, no. 4, p. e1012013, Apr. 2024, doi: 10.1371/journal.pcbi.1012013.

[2] G. Drzewiecki, R. Hood, and H. Apple, "Theory of the oscillometric maximum and the systolic and diastolic detection ratios," Ann. Biomed. Eng., vol. 22, no. 1, pp. 88–96, 1994, doi: 10.1007/BF02368225.

PP44

Ornithine - a marker for metabolic liver disease

Elżbieta REMISZEWSKA[1]*, Marcin GRZECZKOWICZ[1], Dorota G. PIJANOWSKA[1]

1 Nalecz Institute of Biocybernetics and Biomedical Engineering, Polish Academy of Sciences, Ks. Trojdena 4, 02-109 Warsaw, Poland

* ***Corresponding author***. *E-mail address*: eremiszewska@ibib.waw.pl

Keywords: ornithine, enzymatic microreactor, luminescence, absorption

Motivation and Aim: L-ornithine is a non-building protein α-amino acid. It is a substrate in several biochemical reactions: urea cycle, polyamines synthesis, and glutamate and proline metabolism. It is, therefore, an interesting analyte for determination in biological samples, as it allows the functionality of a selected metabolic pathway to be assessed, particularly the urea cycle[1,2]. The range of determination of ornithine in body fluids is 0.75±0.005 mM in plasma, 75±5 mM/mol creatinine in urine, or 0.006-0.011 mM in CSF[3]. In addition, it can be determined in biological systems in vitro, i.e., in liver-derived cell cultures[4]. Sato et al.[5] presented a flow injection analysis (FIA) type system using an oxygen electrode was described there, obtaining a linear range between 0.05 and 3 mM ornithine. This study aims to determine ornithine using our own developed microfluidic system with the enzymatic flow-through microreactor and optical detection based on the absorption and luminescence measurements.

Novelty: A novel microfluidic system with an enzymatic microreactor and optical detection for determining ornithine is presented. This system is designed for multimodal absorption and luminescence measurements proceed independently. The advantage of the proposed system is that either a single measurement or quasi-continuous monitoring can be performed. In addition, it reduces the cost of using the immobilized enzyme and reagents for small-volume samples.

Methods: The study used the enzymatic oxidation of ornithine by the enzyme lysine oxidase (LyOx) to the products 2-keto-5-aminovaleric acid (KV), hydrogen peroxide (H_2O_2) and ammonium ions (NH_4^+) (Fig. 1).

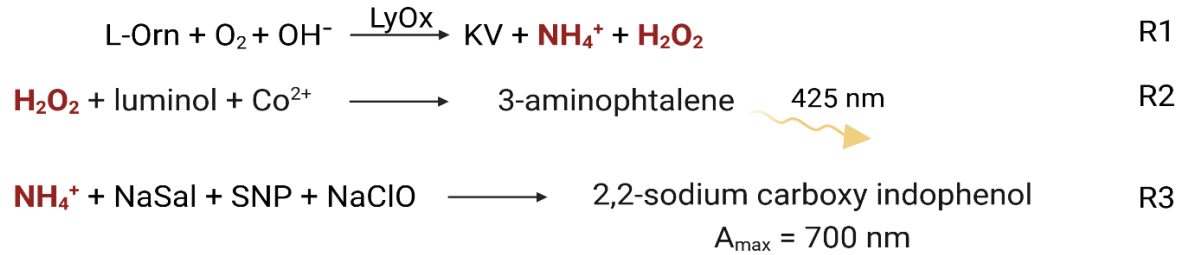

Fig.1 Scheme of reactions.

Two different optical detection methods were used: luminescence and absorption, with products of ornithine enzymatic oxidation (R1) as the substrate. Subsequently, the product hydrogen peroxide reacts with luminol and, in the presence of cobalt ions, gives 3-amino-phthalene, a product that emits light at 425 nm (R2). The measurement has been optimised under flow conditions. In the first phase, the voltage of the luminescence detector was selected for the optimum response signal of the system. In the microfluidic system reaction time depends on flow rate. For luminescence measurements, rates of 50 µL/min was selected. However, in the

second reaction, ammonium ions react with sodium salicylate (NaSal), sodium hypochlorite (NaClO) in the presence of sodium nitroprusside (SNP) to give the coloured product indophenol salt (R3). All measurements were performed in phosphate buffer solutions.

Main results: The absorbance maximum is observed at 700 nm. In the absorption measurement, the pH and temperature of the oxidation reaction were optimised. The flow rate for this reaction was chosen to be 9 µL/min. In the first stage of the study, all three reactions were optimised. In the ornithine oxidation reaction, the optimum pH and temperature were selected to obtain the best possible efficiency of the lysine oxidase enzyme. The best results were obtained for reactions performed at pH 8 and temperature above 30°C. The sample volume was chosen as small as 3 µl. For absorption measurements, reaction (R3) occurs more slowly than for luminescence (R2). Next, a flow rate was optimised for each detection technique and selected as a 9 µL/min and 50 µL/min for the absorption and luminescence, respectively. Exemplary calibration curves for the absorption and luminescence measuring system obtained for the 25th measurement day are shown in Fig. 2. As can be seen, compared to absorbance, luminescence-based measurements can be used to detect ornithine in a concentration range a decade lower.

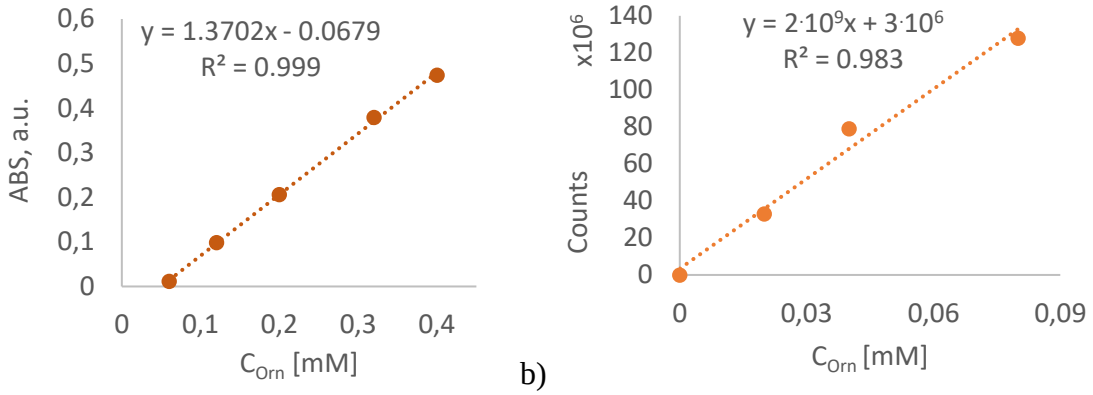

a) b)

Fig. 2. Exemplary calibration curves for ornithine concentrations in absorption mode for the flow rate of 9 µL/min (a) and luminescence - for the flow rate of 50 µL/min (b).

Conclusion: The results showed that the linear response of the microfluidic system range from 0.004 to 0.08 mM for luminescence measurements and from 0.06 to 0.4 mM for absorption measurements. The obtained ranges of quantification allow to determine ornithine in biological samples using these methods. Higher sensitivity was obtained for luminescence. Measurements were carried out for samples of low volume - 3 µL. In the next stage of research, ornithine will be determined in biological samples using both developed methods.

Acknowledgements: Research partially financed by the National Science Centre within Miniatura 6 project no. DEC-2022/06/X/ST7/01078

References:

1. Sivashanmugam M, et al., Ornithine and its role in metabolic diseases: An appraisal. *Biomed Pharmacother*. 2017;86:185-194. doi:10.1016/j.biopha.2016.12.024
2. Kennelly PJ, et al., Weil PA. *Harper's Illustrated Biochemistry*. McGraw Hill/Medical; 2022.
3. Przyrembel H. Disorders of Ornithine, Lysine and Tryptophan. In: Blau N, et al., eds. *Physician's Guide to the Laboratory Diagnosis of Metabolic Diseases*. Springer Berlin Heidelberg; 2003:277-299.
4. Pluta KD, et al., Genetically modified C3A cells with restored urea cycle for improved bioartificial liver. *Biocybernetics and Biomedical Engineering*. 2020;40(1):378-387. doi:10.1016/j.bbe.2019.12.006
5. Sato N, et al., Development of a bienzyme reactor sensor system for the determination of ornithine. *Analytica Chimica Acta*. 2002;456:219-226.

PP45

Serum NMR-based lipidomics of patients with morbid obesity

Beata TOCZYLOWSKA[1*], Piotr KALINOWSKI[2], Elzbieta ZIEMINSKA[3], Paulina DUDA[1], Michał GRĄT[2]

1 Nałęcz Institute of Biocybernetics and Biomedical Engineering PAS, PAS, Warsaw, Poland

2 Department of General, Transplant and Liver Surgery, Medical University of Warsaw, Poland

3 Mossakowski Medical Research Institute, PAS, Warsaw. Poland

* ***Corresponding author***. *E-mail address*: beata.toczylowska@ibib.waw.pl

Keywords: lipidomic, morbid obesity, NMR spectroscopy

Motivation and Aim: Obesity, according to the World Health Organization (WHO), is defined as an excessive accumulation of fat that may pose health risks and disrupt the body's energy balance system [1]. It is characterized by an abnormal or excessive accumulation of fat mass that can impair health and lead to serious cardiometabolic complications. The global prevalence of childhood and adolescent obesity is increasing, with projections suggesting that by 2030, more than 250 million people will be affected. While environmental changes significantly contribute to this increase, genetic factors also play a crucial role, with studies indicating heritability rates as high as 67%. Researchers have long studied lipid metabolism to better understand its chemical diversity and functionality [2].

Novelty: In our study, we aimed to evaluate differences in the lipidome between individuals with morbid obesity and those with normal body weight. The purpose of this study was to identify patients who would respond well to bariatric surgery.

Methods: Serum samples were obtained from blood clots collected after overnight fasting and were frozen at -23°C until NMR analysis. The hydrophobic compounds were prepared using a modified Bligh and Dyer method, following the procedure described in our previous publication [3]. All nuclear magnetic resonance (NMR) spectra were recorded at 25°C using an Avance III HD 500 MHz spectrometer with a one-pulse sequence. Vendor software was employed to apply a line broadening of 0.3, as well as baseline and phase correction, to each spectrum. NMR signals were identified using our own reference database, the Human Metabolome Database, and relevant literature [3, 4]. Metabolite quantities are expressed as signal magnitudes corresponding to compound concentrations, with spectra normalized to chloroform signals prior to statistical analysis. For NMR data selection, we used a custom-written application (IBBE PAS). For the statistical analysis, we selected 27 functional group/compound signals from the lipid extracts. For the statistical analysis of lipid data, one-way ANOVA with Holm–Sidak or Dunn's correction and multivariate statistical analysis, orthogonal partial least squares discriminant analysis (OPLS–DA), were used. Model validation was performed using a jackknifing test. The quality of the models was assessed on the basis of the goodness of fit (R^2) and predictive ability (Q^2), where the theoretical maximum is 1 for a perfect prediction. To be considered significant, an OPLS component must have R^2 and Q^2 values significantly greater than zero, with values of 0.5 or higher generally regarded as good. Before constructing the model, mean-centering and Pareto scaling were applied. All analyses were conducted using SIMCA-P 18.0 software. The most important compounds for classification were identified using the variable importance for projection (VIP) score.

Main results: Univariate statistical analysis comparing the bariatric patient group to the control group revealed significant differences only in triacylglyceride levels (187%, p = 0.019) and pelargonic acid levels (72%, p = 0.013). When comparing metabolic profiles between controls and patients, OPLS-DA allows the construction of a valid model (p < 0.001, CV-ANOVA) consisting of three components: one predictive component and two orthogonal components (Fig. 1). The model demonstrated a good fit to the data (R^2 = 0.625) and good predictive ability (Q^2 = 0.542). The most important metabolites/functional groups with VIP>1 are arachidonic acid; cholesterol esters; pelargonic acid; complex NMR signal of lauric, myristic, palmitic, arachidonic, alfa-linolenic and oleic acids; complex NMR signal of pelargonic, arachidonic, oleic and palmitoleic acids; complex NMR signal of lauric and palmitic acids; complex NMR signal of dodecanonic, palmitic, arachidonic, palmitoleic and oleic acids; and complex NMR signal of cholesterol and cholesterol esters.

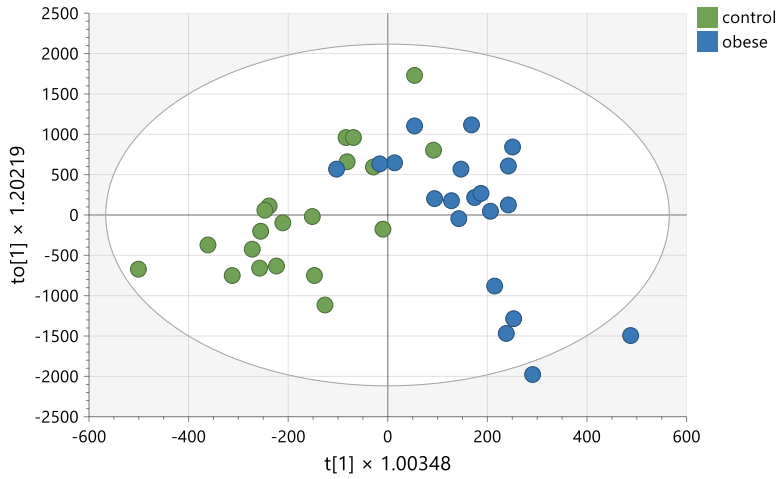

Fig. 1 Score plot of the OPLS-DA model for serum hydrophobic compounds. t [1] on the x-axis represents the between-class variation in the predictive component. to [1] – on the y-axis represents within-class variation in the first orthogonal component. The ellipse represents the Hotelling T2 with a 95% confidence interval.

Conclusion: Metabolomics is a high-throughput detection method that provides insights into disease states by reflecting the overall biochemical phenotype. This approach allows for the examination of changes in endogenous metabolites on a macroscopic scale following exposure to biological stimuli. By analyzing metabolic profiles, researchers can identify disease-related metabolites and elucidate their metabolic pathways [5].

References:

[1] H.Y. Jeong, Y.S. Moon, K.K. Cho, omega-6 and omega-3 Polyunsaturated Fatty Acids: Inflammation, Obesity and Foods of Animal Resources, Food Sci Anim Resour, 44 (2024) 988-1010.
[2] Y. Huang, K. Sulek, S.E. Stinson, L.A. Holm, M. Kim, K. Trost, K. Hooshmand, M.A.V. Lund, C.E. Fonvig, H.B. Juel, T. Nielsen, L. Angquist, P. Rossing, M. Thiele, A. Krag, J.C. Holm, C. Legido-Quigley, T. Hansen, Lipid profiling identifies modifiable signatures of cardiometabolic risk in children and adolescents with obesity, Nat Med, DOI 10.1038/s41591-024-03279-x(2024).
[3] B. Toczylowska, E. Zieminska, M. Michalowska, M. Chalimoniuk, U. Fiszer, Changes in the metabolic profiles of the serum and putamen in Parkinson's disease patients - In vitro and in vivo NMR spectroscopy studies, Brain Res, 1748 (2020) 147118.
[4] B. Toczylowska, E. Zieminska, A. Podlecka-Pietowska, A. Ruszczynska, M. Chalimoniuk, Serum metabolic profiles and metal levels of patients with multiple sclerosis and patients with neuromyelitis optica spectrum disorders - NMR spectroscopy and ICP-MS studies, Mult Scler Relat Disord, 60 (2022) 103672.
[5] P.Q. Sun, W.M. Dong, Y.F. Yuan, Q. Cao, X.Y. Chen, L.L. Guo, Y.Y. Jiang, Targeted metabolomics study of fatty-acid metabolism in lean metabolic-associated fatty liver disease patients, World J Gastroenterol, 30 (2024) 3290-3303.

PP46

Post-exercise Heart Rate Recovery in male soccer players under 13 years old

Magdalena MIKIELEWICZ[1*], Jakub S. GĄSIOR[2*], Kacper KORZENIEWSKI[1], Robert MAKUCH[3], Marcel MŁYŃCZAK[1]

[1] Faculty of Mechatronics, Institute of Metrology and Biomedical Engineering, Warsaw University of Technology, Warsaw, Poland
[2] Department of Pediatric Cardiology and General Pediatrics, Medical University of Warsaw, Warsaw, Poland
[3] Department of Physical Education, Kazimierz Pulaski University of Technology and Humanities in Radom, Radom, Poland

* ***Corresponding author***. *E-mail address*: magdalena.ladogorska.dokt@pw.edu.pl

Keywords: Post-exercise recovery, Heart Rate Recovery (HRR), Young Male Soccer Players, VO_2max, YoYo Intermittent Recovery Test

Motivation and Aim: The objective of this study was to conduct a comprehensive analysis of the recovery phase patterns among young male soccer players, focusing on their heart rate recovery (HRR) after the exercise. By examining the relationship between HRR and VO_2max (maximum rate of oxygen consumption) estimation, the study aimed to provide insights into the recovery processes and aerobic fitness levels of young athletes.

Novelty: The recovery phase after the exercise is not well documented in the literature, particularly for young athletes. While recovery strategies for adult athletes have been widely studied [1, 2], there is a noticeable gap in research including young athletes, especially those under 13 years old. This study addresses that gap by focusing on young soccer players, an age group for which recovery protocols are less well understood.

Methods: A group of 30 young male soccer players, aged 10 to 12 years (age 11.62 ± 0.41 [years], height 152.46 ± 8.15 [cm], weight 42.05 ± 8.56 [kg], BMI 17.97 ± 2.48 [kg/m^2]), performed the YoYo Intermittent Recovery Test (YoYo IR1) to assess their recovery response and estimate their VO_2max value [3]. RR intervals (time between corresponding R waves in a ECG curve) were measured using Polar Team2 [4]. Heart rate was calculated at various time points during the cooldown phase (10, 20, 30, 60, 120, 180, 240, and 300 seconds) [1] as a percentage of the maximal heart rate (HRmax) achieved during the test. To analyze HRR patterns, a linear regression model was applied to the data, with the equation $y = ax + b$ fitted to the obtained graphs. The correlation between the YoYo VO_2max estimation and HR values at each time point was examined using Spearman correlation, along with the variables 'a' and 'b' from the regression equation.

Main results: In this population, no significant correlations were found between the YoYo-estimated VO_2max and heart rate recovery (HRR) values at any of the measured time points. The p-values for each interval were as follows: 10s – 0.79, 20s – 0.74, 30s – 0.84, 60s – 0.53, 120s – 0.16, 180s – 0.27, 240s – 0.1, and 300s – 0.33. Additionally, the parameters ‘a’ and ‘b’ from the regression equation had p-values of 0.23 and 0.99, respectively. However, due to the lack of established VO_2max norms for athletes under the age of 13 [5, 6], differential criteria could not be applied for comparison. The subjects were categorized based on the median

VO_2max value which was found to be 42.1 $mL \cdot kg^{-1} \cdot min^{-1}$. The boxplots presenting the values for those groups are shown on Figure 1. The 'above median' group demonstrated a lower median %HRmax across almost all time points, not including 60 s. No significant differences between the groups were identified, which probably may be affected by high variance and limited amount of data used in the study. To enhance the study, a larger sample size could be used to better account for maturation differences and ensure more accurate stratification according to developmental maturation parameters.

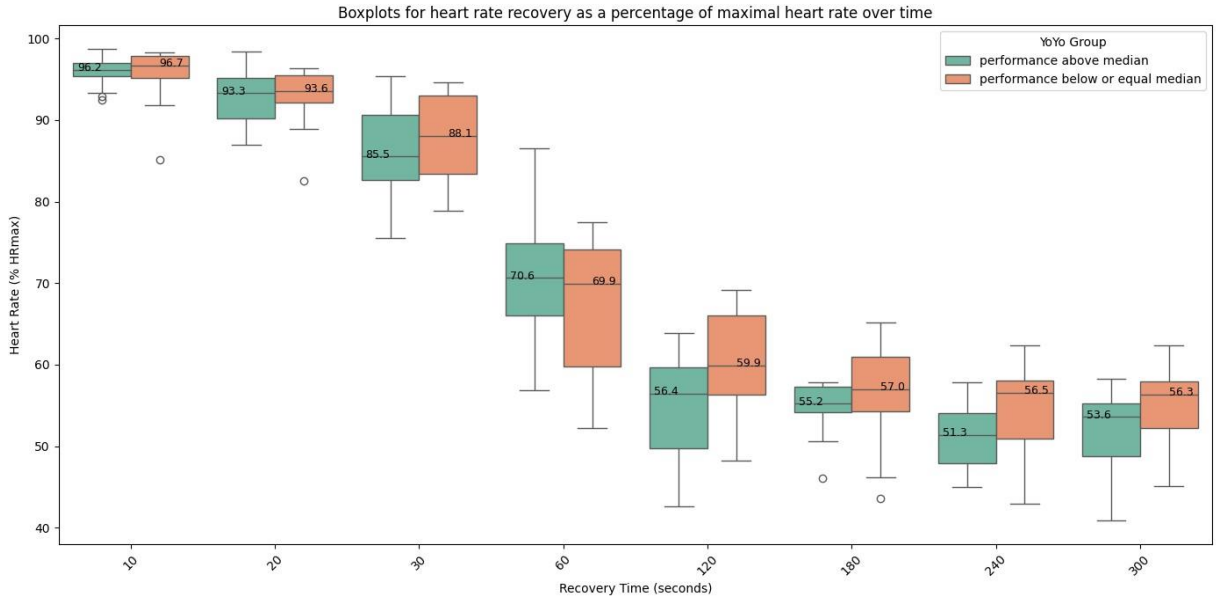

Figure 9 – Boxplots presenting heart rate recovery differences between soccer players.

Conclusion: The findings of this study provide a valuable starting point for understanding the heart rate recovery dynamics in young male soccer players. While no significant correlations were observed between YoYo VO_2max and HR recovery values, expanding the sample size and considering other factors such as maturation could significantly influence the results. Another thing worth considering is fitting other types of functions to the chart. Establishing VO_2max norms for athletes under 13 years old will also be crucial for more robust comparisons and conclusions in future studies.

References:

[1] Watson AM, Brickson SL, Prawda ER, Sanfilippo JL. Short-Term Heart Rate Recovery is Related to Aerobic Fitness in Elite Intermittent Sport Athletes. *J Strength Cond Res*. 2017;31(4):1055-1061. doi:10.1519/JSC.0000000000001567

[2] Hung CH, Clemente FM, Bezerra P, et al. Post-Exercise Recovery of Ultra-Short-Term Heart Rate Variability after Yo-Yo Intermittent Recovery Test and Repeated Sprint Ability Test. *Int J Environ Res Public Health*. 2020;17(11):4070. Published 2020 Jun 7. doi:10.3390/ijerph17114070

[3] Bangsbo J, Iaia FM, Krustrup P. The Yo-Yo intermittent recovery test: a useful tool for evaluation of physical performance in intermittent sports. *Sports Med*. 2008;38(1):37-51. doi:10.2165/00007256-200838010-00004

[4] Polar_Team2_sw_help_English.pdf. Accessed March 1, 2025. https://support.polar.com/e_manuals/Team2/Polar_Team2_sw_help_English.pdf

[5] Shvartz E, Reibold RC : Aerobic fitness norms for males and females aged 6 to 75 years : a review. Aviat Space Environ Med; 61 :3-11, 1990.

[6] Klusiewicz A, Starczewski M, Ładyga M, et al. Reference values of maximal oxygen uptake for polish rowers. *J Hum Kinet*. 2014;44:121-127. Published 2014 Dec 30. doi:10.2478/hukin-2014-0117

PP47

Novel approach to ventilation therapy of neonates with congenital diaphragmatic hernia

Barbara STANKIEWICZ[1*], Krzysztof Jakub PAŁKO[1], Magdalena MIERZEWSKA-SCHMIDT[2], Dariusz MADAJCZAK[3], Marcin MICHNIKOWSKI[1], Maciej KOZARSKI[1], Marek DAROWSKI[1]

1 Polish Academy of Sciences, Nalecz Institute of Biocybernetics and Biomedical Engineering, Department of Modeling and Supporting Internal Organ Functions, Warsaw, Poland

2 Medical University of Warsaw, Department of Pediatric Anaesthesiology and Intensive Therapy, Warsaw, Poland

3 Medical University of Warsaw, Department of Neonatology and Rare Diseases, Warsaw, Poland

* ***Corresponding author***. *E-mail address*: bstankiewicz@ibib.waw.pl.

Keywords: neonates, congenital diaphragmatic hernia, mechanical ventilation, ventilation inhomogeneity, ventilator-induced lung injury

Motivation and Aim: Mechanical ventilation is a crucial therapy for neonates with congenital diaphragmatic hernia (CDH). These neonates are extremely susceptible to ventilator-induced lung injury (VILI) because of ventilation inhomogeneity (VI) and lung hypoplasia. Their ventilation is difficult as the VI degree is highly variable in CDH patients. Due to that, we aim to develop a non-invasive bedside method of VI assessment that could help physicians choose optimal personalised ventilator settings for a given patient.

Novelty: We propose an individual approach to the ventilation of CDH infants, based on the new method of VI-degree assessment by a ratio of time constants of the contralateral and ipsilateral lung (T_1/T_2). Currently, there are no clinical methods of VI-degree evaluation that could be used to find individual optimal ventilation parameters of a patient. We expect this new approach will increase ventilation effectiveness and decrease the VILI risk.

Methods: We hypothesize that the parameters of personalized ventilation therapy can be specified by the application of regression models describing ventilation variables (PIP – peak inspiratory pressure, MAP – mean airway pressure, WOBvt – work of breathing done by ventilator) as a function of the mechanical properties of the respiratory system (including VI-degree) and ventilator settings (RR – respiratory rate, I:E – inspiration to expiration time ratio, V_T – tidal volume). We utilised the respiratory data of five CDH patients ventilated on conventional mode to design and conduct a series of laboratory simulations of mechanical ventilation using a hybrid (numerical-physical) respiratory simulator and a ventilator. The simulation results created the database needed to build regression models.

Main results: We found non-linear regression models of ventilatory parameters (PIP, MAP, WOB_{vt}) as a function of the T_1/T_2 index (VI-degree), respiratory system compliance (C_{rs}) and resistance (R_{rs}) and ventilator settings (RR, I:E, V_T), well matched with clinical data ($R^2>0.95$, $P<0.01$). They enable us to estimate optimal ventilation parameters (PIP, MAP, WOB_{vt}) adjusted to individual VI-degree and the resistive-elastic properties of lungs.

Conclusion: Although a bigger sample size of clinical cases is necessary to prove our study hypothesis, we believe, that the diagnostic-therapeutic method, we are working on, may help to improve ventilation therapy of CDH neonates.

PP48

Portable NIRS Device for Real-Time Cerebral Oxygenation Monitoring in Aerospace Applications

Michał KACPRZAK[1*], Piotr SAWOSZ[1] , Anna GEREGA[1], Aleh SUDAKOU[1], Kamil LIPIŃSKI[1], Stanisław WOJTKIEWICZ[1], Krzysztof KOWALCZUK[2], Łukasz DZIUDA[2] , Adam LIEBERT[1,]

1 Nalecz Institute of Biocybernetics and Biomedical Engineering PAS, Warsaw, Poland

2 Military Institute of Aviation Medicine, Warsaw, Poland

* ***Corresponding author***. *E-mail address*: mkacprzak@ibib.waw.pl

Keywords: NIRS, wearable biosensors, cerebral oxygenation

Motivation and Aim: Near-infrared spectroscopy (NIRS) is a non-invasive optical technique used to monitor tissue oxygenation by measuring changes in oxygenated and deoxygenated hemoglobin. With advancements in technology, portable NIRS devices have emerged, enabling real-time monitoring of cerebral oxygenation in various settings, including clinical, sports, and aerospace applications [1,2]. Monitoring cerebral oxygenation in pilots during high-G maneuvers is critical for preventing cognitive impairment and loss of consciousness [3,4]. This study presents a compact, 8-channel, portable near-infrared spectroscopy (NIRS) device designed for real-time monitoring of cerebral oxygenation under extreme flight conditions. The device is tailored for aerospace applications, ensuring stability and accuracy even in high-G environments.

Novelty: The proposed NIRS system integrates Lock-In detection technology, minimizing ambient light and motion artifacts. Unlike existing commercial solutions, it is specifically engineered for aviation research, offering real-time, multi-channel monitoring with a lightweight and wearable design. This enhances its applicability in military and civilian aerospace environments.

Methods: The NIRS device consists of a host unit and two sensor modules placed on the forehead. It utilizes two wavelengths (730 nm and 850 nm) and features four-channel measurements per hemisphere. Validation was conducted in real-life scenarios, including daily activities, and it is ready for tests during flight simulations, and high-G human centrifuge measurements. The system transmits real-time data via Bluetooth Low Energy (BLE) or Wi-Fi. The built-in battery provides up to 8 hours of continuous operation and is rechargeable via a USB-C port.

Main results: The device demonstrated stable and accurate measurements of oxygenated (HbO) and deoxygenated (HbR) hemoglobin levels during various tasks. In cognitive and physical activities, significant variations in prefrontal cortex activation were observed. During tasks, such as selecting a medication in a pharmacy or choosing products in a grocery store, increased activation of the prefrontal cortex is observed (Fig.1.). This is reflected in a rise in oxygenated hemoglobin (HbO) and a reduction in deoxygenated hemoglobin (HbR), indicating heightened mental engagement during decision-making.

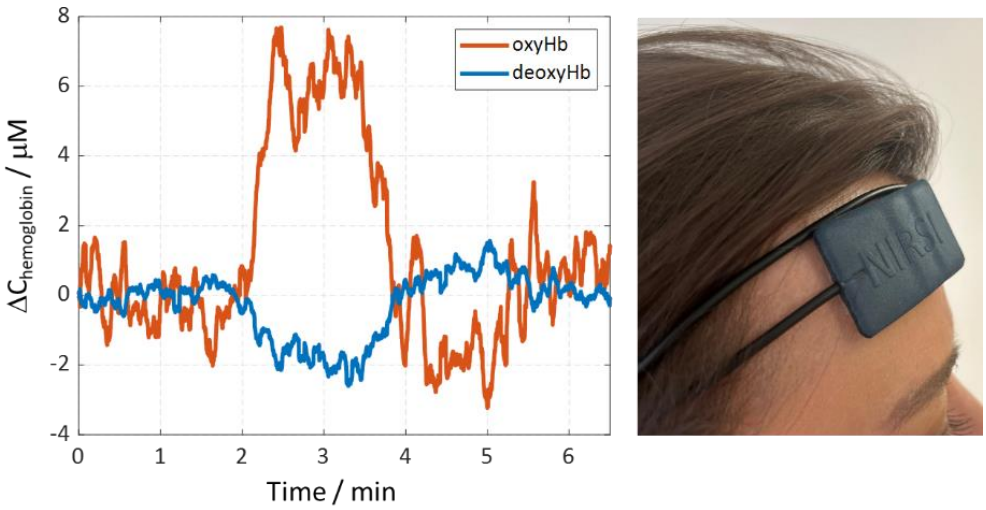

Fig.1. Example of measured hemoglobin concentration changes during daily activities and sensor modules placed on the forehead

Conclusion: The developed portable NIRS system provides a reliable tool for real-time cerebral oxygenation monitoring in daily activities. It's compact size, motion artifact reduction, and real-time data transmission make it well-suited for aerospace applications. Future studies will focus on expanding its use in flight simulations and operational pilot training.

Acknowledgements: This study was funded by the Polish National Center for Research and Development (DOB-BIO-12-05-001-2022) and the Nalecz Institute of Biocybernetics and Biomedical Engineering PAS (ST253/2025).

References:

[1] Pellicer A, Bravo Mdel C. Near-infrared spectroscopy: a methodology-focused review. Semin Fetal Neonatal Med. 2011;16: 42-9

[2] Chen C, Ma Z, Liu Z, Zhou L, Wang G, Li Y, et al. An Energy-Efficient Wearable Functional Near-infrared Spectroscopy System Employing Dual-level Adaptive Sampling Technique. IEEE Trans Biomed Circuits Syst. 2022;16:119-28

[3] Dziuda L, Krej M, Smietanowski M, Sobotnicki A, Sobiech M, Kwasny P, et al. Development and evaluation of a novel system for inducing orthostatic challenge by tilt tests and lower body negative pressure. Sci Rep. 2018;8:7793.

[4] Gerega, A., Wojtkiewicz, S., Sawosz, P. et al. Assessment of the brain ischemia during orthostatic stress and lower body negative pressure in air force pilots by near-infrared spectroscopy, Biomed. Opt. Express 11, 1043-1060 (2020).

PP49

Seroma prevention with hypertonic irrigation in breast reconstructions: A double-blind trial – the SHIELD trial

Marcin EKMAN[1*], Paulina CICHON[1], Kamil DRUCIS[1], Magdalena GRACZYK[2], Piotr WOŹNIACKI[1], Jarosław KOBIELA[1]

1 Department of Surgical Oncology, Transplant Surgery and General Surgery, Medical University of Gdańsk, Mariana Smoluchowskiego 17, 80-214, Gdańsk, Poland

2 Department of Plastic Surgery, Medical University of Gdańsk, Mariana Smoluchowskiego 17, 80-214, Gdańsk, Poland

* ***Corresponding author***. *E-mail address*: eq@gumed.edu.pl

Keywords: Seroma, Breast reconstruction, Hypertonic saline irrigation

Motivation and Aim: Seroma formation is one of the most common complications following implant-based breast reconstruction, significantly impacting wound healing, infection risk, and patient quality of life. Current preventive strategies, including prolonged drainage and tissue adhesives, provide inconsistent results. Intraoperative hypertonic saline irrigation (HSI) has shown promising outcomes in abdominal surgery, yet its efficacy in breast surgery remains unverified. This study aims to evaluate the effectiveness of HSI in reducing postoperative seroma formation following mastectomy with immediate implant-based reconstruction.

Novelty: This is the first randomized, double-blind clinical trial investigating the role of intraoperative hypertonic saline irrigation in breast reconstruction surgery. The study introduces a novel approach to seroma prevention, leveraging osmotic and sclerotherapy-like effects to minimize postoperative fluid accumulation.

Methods: A total of 80 female patients undergoing mastectomy with immediate reconstruction (implant or expander) will be randomly assigned (1:1) to either the experimental group (HSI with 10% NaCl) or the control group (standard saline irrigation with 0.9% NaCl). Randomization will be stratified by surgical technique and axillary dissection status. The blinded intervention involves placing a saline-soaked surgical drape in the surgical cavity for 4 minutes before wound closure. Seroma volume will be measured via drain output over the first 72 postoperative hours. Secondary endpoints include the number of aspirations, complication rates, reoperation frequency, and cost analysis.

Main results: The primary outcome is the total seroma volume collected within 72 hours postoperatively. Secondary outcomes include the incidence of wound complications, unplanned reoperations, and healthcare costs associated with seroma management. Statistical analyses will employ t-tests and multivariate regression models to adjust for confounding variables.

Conclusion: This study aims to establish whether HSI is a viable, low-cost, and effective method for seroma prevention in breast reconstruction surgery. If successful, it may lead to a paradigm shift in surgical protocols, improving patient outcomes and reducing healthcare burdens.

Acknowledgements: Acknowledgements and References are optional.

References:

[1] Seth, A. K. & Sisco, M. Prepectoral Breast Reconstruction. Plast. Reconstr. Surg. 155, 213e (2025).
[2] Meshkin, D. H., Firriolo, J. M., Karp, N. S. & Salibian, A. A. Management of complications following implant-based breast reconstruction: a narrative review. Ann. Transl. Med. 11, 416 (2023).
[3] Al-Hilli, Z. & Wilkerson, A. Breast Surgery: Management of Postoperative Complications Following Operations for Breast Cancer. Surg. Clin. North Am. 101, 845–863 (2021).
[4] Srivastava, V., Basu, S. & Shukla, V. K. Seroma Formation after Breast Cancer Surgery: What We Have Learned in the Last Two Decades. J. Breast Cancer 15, 373–380 (2012).
[5] Gül, D. K. The role of saline irrigation of subcutaneous tissue in preventing surgical site complications during cesarean section: A prospective randomized controlled trial. J. Surg. Med. 5, 8–11 (2021).
[6] Mueller, T. C. et al. Intra-operative wound irrigation to reduce surgical site infections after abdominal surgery: a systematic review and meta-analysis. Langenbecks Arch. Surg. 400, 167–181 (2015).
[7] Zamkowski, M. & Śmietański, M. Efficacy of intraoperative hypertonic saline irrigation in seroma prevention after abdominal wall reconstruction procedures - a pilot cohort study. ANZ J. Surg. 93, 1594–1598 (2023).
[8] Seretis, K., Goulis, D., Demiri, E. C. & Lykoudis, E. G. Prevention of Seroma Formation Following Abdominoplasty: A Systematic Review and Meta-Analysis. Aesthet. Surg. J. 37, 316–323 (2017).
[9] Throckmorton, A. D. et al. Sclerotherapy for the treatment of postmastectomy seroma. Am. J. Surg. 196, 541–544 (2008).

Organizers:

IFMBE

IBIB PAN

PTIB

MCB

PAN
POLISH ACADEMY OF SCIENCES
Committee of Biocybernetics and Biomedical Engineer

Sponsors:

LABSOFT
NANOTECHNOLOGY EXPERTS

The conference is co-financed from the state budget, allocated by the Minister of Science under the Excellent Science II Programme
Contract No. KONF/SP/0624/2024/02

Doskonała Nauka

Minister of Science
Republic of Poland

Honorary Patronage
Professor Marek Konarzewski
President of the Polish Academy of Science

Endorsing Organizations:

European Alliance for
EAMBES
Medical and Biological Engineering & Science

PAN
POLISH ACADEMY OF SCIENCES

https://www.nbc2025.ibib.waw.pl